Immunstimulatorische und immunregulierende Wirkungen von Nanopartikeln und Umweltschadstoffen auf das Darm-assoziierte Immunsystem

Inaugural-Dissertation

Zur Erlangung des Doktorgrades der
Mathematisch-Naturwissenschaftlichen Fakultät
der Heinrich-Heine-Universität Düsseldorf

vorgelegt von

Meike Winter

aus Wuppertal

Düsseldorf, Juni 2010

Aus dem Institut für umweltmedizinische Forschung
an der Heinrich-Heine-Universität Düsseldorf

Gedruckt mit der Genehmigung der Mathematisch-Naturwissenschaftlichen Fakultät der Heinrich-Heine-Universität Düsseldorf

Referentin: Prof. Dr. rer. nat. Irmgard Förster
Koreferent: Prof. Dr. rer. nat. Peter Proksch

Tag der mündichen Prüfung: 02.07.2010

Meinen Eltern und
Pauline gewidmet

Inhaltsverzeichnis

Abkürzungsverzeichnis

AhR	Arylhydrocarbon Rezeptor
AhRR	AhR Repressor
AM	Alveolare Makrophagen
APC	Antigen präsentierende Zelle
Arnt	AhR nuclear translocator
ASC	apoptosis-associated speck-like protein containing a caspase recruitment domain
Atg16L1	Autophagy-related 16-like 1
bHLH-PAS	basic helix-loop-helix Per-Arnt-Sim
cAMP	cyclic Adenosine Monophosphat
CED	chronisch entzündliche Darmerkrankung
CU	Colitis ulcerosa
Cyp1A1	Cytochrom P450 1A1
DC	dendritische Zelle
DRE	dioxinresponsives Element
DSS	Dextran Sulfat Sodium
EAE	experimental autoimmune encephalomyelitis
eGFP	enhanced green flourescent protein
FAE	Follikel-assoziiertes Epithel
FICZ	6-Formylindol[3,2-b]carbazol
Foxo	forkhead box O
HA	Hämagglutinin
HNF-4α	hepatocyte nuclear factor-4α
IARC	International Agency for Research on Cancer
Ig	Immunglobulin
IL	Interleukin
ILF	isolierte lymphoide Follikel
IFN	Interferon
iNOS	Inducible nitric oxide synthase
IRF	Interferon-regulator-factor
KM-DC	Knochenmark-abgeleitete DC
KP	Kryptopatches
Lin	lineage marker

LPS	Lipopolysaccharid
LDL	Low Density Lipoprotein
LK	Lymphknoten
LP	Lamina Propria
LRR	Leucin rich repeat
MC	Morbus Crohn
3-MC	3-Methylcholanthren
MHC	Major histocompatibility complex
mLK	mesenteriale Lymphknoten
MP	Mikropartikel
MSU	Mononatriumurat
NF-κB	nuclear factor kappa-light-chain-enhancer of activated B cells
NLR	NOD-like Rezeptor
NLRP3	NOD-like receptor family, pyrin domain containing 3
NK-Zellen	Natürliche Killer Zellen
NP	Nanopartikel
OVA	Ovalbumin
PLGA	Polylactic-co-glycolic acid
pLK	peripherer Lymphknoten
PP	Peyer'sche Plaques
PRR	Pattern recognition receptor
ROS	reaktive Sauerstoffspezies
SeP	Selenoprotein P
TCDD	2,3,7,8-Tetrachlorodibenzo-P-Dioxin
TGFβ	Transforming growth factor β
Th-Zellen	T Helfer-Zellen
TIR	Toll/IL-1 Rezeptor
TLR	Toll-like receptor
TNFα	Tumornekrosefaktor-α
Treg-Zellen	regulatorische T-Zellen

Zusammenfassung

In der vorliegenden Arbeit wurde der Einfluss von Umweltfaktoren auf die Homöostase des intestinalen Immunsystems und die Pathogenese entzündlicher Darmerkrankungen durchgeführt.

Nanopartikel (NP) sind per Definition Partikel mit einem Durchmesser ≤ 100 nm. Es ist bekannt, dass NP andere Eigenschaften aufweisen als größere Partikel der gleichen Substanz. Seit einigen Jahren finden NP auch in der Nahrungsmittelproduktion zunehmend größere Verwendung, obwohl nur wenige Studien über die Folgen einer oralen Aufnahme von NP verfügbar sind. In der hier vorgelegten Dissertation wurde der Einfluss von NP aus der Nahrung auf das Immunsystem des Darms, sowie auf die genomische Stabilität in murinen Modellen für entzündliche Darmerkrankungen untersucht. In zwei unabhängigen Modellen für akute Darmentzündungen konnte gezeigt werden, dass nach oraler Applikation von SiO_2-NP die mukosale Entzündung verstärkt war, was mit einer erhöhten Produktion inflammatorischer Zytokine einherging. In einem Modell für chronische Colitis konnte in SiO_2-NP-behandelten Mäusen ebenfalls eine erhöhte Produktion inflammatorischer Mediatoren, sowie eine erhöhte Frequenz vermutlich regulatorischer $Gr1^+$-Zellen in den mesenterialen Lymphknoten (mLK) detektiert werden. Zusätzlich war in SiO_2-NP-gefütterten Tieren eine erhöhte Anzahl oxidativer Läsionen in Epithelzellen des Colon nachweisbar. Darüber hinaus konnten in *in vitro* Experimenten dendritische Zellen (DC) als mögliche Zielpopulation für NP im Immunsystem des Darms identifiziert werden. SiO_2- wie auch TiO_2-NP waren in der Lage das NLRP3-Inflammasom in DC zu aktivieren und somit die Sekretion von proinflammatorischen Zytokinen wie IL-1β zu induzieren. Zusammengenommen lassen diese Ergebnisse vermuten, dass SiO_2-NP, die über die Nahrung in den Gastrointestinaltrakt gelangen, bevorzugt in entzündete Bereiche der Mukosa aufgenommen werden, wo sie von Zellen des angeborenen Immunsystems phagozytiert werden und durch Aktivierung des NLRP3-Inflammasoms zur einer verstärkten Sekretion proinflammatorischer Zytokine beitragen.

Des Weiteren wurde die Funktion des Arylhydrocarbon Rezeptors (AhR) im Immunsystem des Darms untersucht. Der AhR ist ein ligandeninduzierter Transkriptionsfaktor, der als Rezeptor für Dioxin beschrieben wurde, aber auch endogene Liganden, sowie sekundäre Pflanzeninhaltsstoffe aus der Nahrung, wie z.B. Flavonoide binden kann. Es ist bekannt, dass der AhR neben der Induktion des Fremdstoffmetabolismus auch eine Funktion in der Regulation des Immunsystems hat. In einem negativen Rückkopplungsmechanismus induziert er die Expression des AhR-Repressors (AhRR), welcher wiederum die Transkription des AhR reprimiert. In der hier vorgelegten Arbeit konnte ein spezifisches Expressionsmuster des AhR und des AhRR in Immunzellen des Darms gezeigt werden, was eine Rolle der AhR/AhRR-regulierten Genexpression bei der Aufrechterhaltung der immunologischen Homöostase im Darm impliziert. Damit übereinstimmend konnte gezeigt werden, dass eine Aktivierung des AhR mit Dioxin zu einer gestörten Ausbildung von Toleranz gegen oral applizierte Antigene führt.

Reaktive Sauerstoff- und Stickstoff-Metabolite spielen eine entscheidende Rolle in der Pathogenese entzündlicher Darmerkrankungen. Durch antioxidative Enzyme wie dem Selenoprotein P (SeP) wirkt der Körper einer Gewebe- und DNA-Schädigung durch diese Metabolite entgegen. In der hier vorgelegten Arbeit konnte gezeigt werden, dass SeP in Epithelzellen des Darms exprimiert ist, aber im Verlauf einer chronischen Darmentzündung herunterreguliert wird. Dieser Mechanismus trägt wahrscheinlich zur Pathogenese chronischer Darmentzündungen und möglicherweise auch zur Colitis-assoziierten Kanzerogenese bei.

1. Einleitung

1.1. Das Immunsystem

Das Immunsystem hat die Aufgabe, uns vor Pathogenen zu schützen, sowie die Ausbreitung körpereigener, entarteter Zellen zu verhindern.
Als Barriere zur Außenwelt verhindern Epithelien das Eindringen von Bakterien, Viren, Pilzen und Parasiten. Wenn es Erregern dennoch gelingt, diese erste Hürde zu überwinden und in den Körper zu gelangen, so stehen spezialisierte Zellen des angeborenen Immunsystems bereit, um eine Infektion zu verhindern oder einzudämmen, sowie eine pathogenspezifische adaptive Immunreaktion zu induzieren. Das angeborene Immunsystem ist der phylogenetisch ältere Teil unseres Immunsystems und verfügt über eine begrenzte Anzahl von Mustererkennungs-Rezeptoren, die konservierte Strukturen von Pathogenen erkennen. Die wichtigsten Effektorzellen des angeborenen Immunsystems sind phagozytierende Zellen, die nach Rezeptorbindung die eingedrungenen Erreger aufnehmen und vernichten, sowie natürliche Killer-Zellen (NK-Zellen), die z.B. anhand einer veränderten Expression körpereigener Major histocompatibility complex (MHC) Moleküle der Klasse I (MHC-I), virusinfizierte Zellen erkennen und zerstören können. Auch stellen Phagozyten das Bindeglied zwischen angeborener und adaptiver Immunität dar. Sie können Informationen über Eigenschaften des eingedrungenen Erregers an Lymphozyten übermitteln und so antigenspezifisch die zellulären und humoralen Komponenten des adaptiven Immunsystems aktivieren, welche mit hoher Spezifität gegen den eingedrungenen Erregertyp wirken können. Durch somatische Rekombination bei der Ausbildung des Rezeptorrepertoires im Knochenmark bzw. im Thymus entsteht eine Vielzahl von spezifischen Antigen-Rezeptoren, so dass die Wahrscheinlichkeit sehr hoch ist, dass Antigene eines Pathogens von einem passenden Rezeptor gebunden werden können. Um zu verhindern, dass B- bzw. T-Zellen mit einer Spezifität gegen endogene Strukturen aus den primären lymphatischen Organen in die Peripherie gelangen, werden autoreaktive Lymphozyten durch einen negativen Selektionsprozess aus dem Zellpool eliminiert.

1.2. Das Immunsystem des Darms

Der menschliche Darm enthält mit einer Dichte von ca. 10^{12} Organismen pro ml Darminhalt mindestens 400 verschiedene Arten von Kommensalen, die für die Verwertung der Nahrung dringend notwendig sind (1; 2). Diese potentiell inflammatorischen Mikroorganismen stellen jedoch eine akute Bedrohung dar, wenn sie in die Mukosa des Darms gelangen. Die Hauptaufgabe des Darm-assoziierten Immunsystems besteht demnach darin zwischen pathogenen und harmlosen Mikroorganismen zu unterscheiden. Außerdem muss verhindert werden, dass eine Immunreaktion gegen die Darmflora oder Nahrungsbestandteile ausgebildet wird, sowie dass luminale Bakterien in die Mukosa gelangen. Parallel müssen die Zellen des Darm-assoziierten Immunsystems in der Lage sein, Pathogene zu erkennen und effektiv zu eliminieren. Der Darm ist das größte lymphatische Gewebe des Körpers, dessen Immunzellen teilweise in einer lockeren Ansammlung von Zellen in der Lamina propria (LP) oder assoziiert mit dem Epithel, welches die Barriere zwischen Darmlumen und Mukosa bildet, vorliegen. Es gibt jedoch auch eine Vielzahl organisierter Strukturen, wie die mesenterialen Lymphknoten (mLK), Peyer'sche Plaques (PP), isolierte lymphoide Follikel (ILF), sowie Kryptopatches (KP), die eine spezifische Funktion bei der Induktion von lokalen Immunreaktionen bzw. der Aufrechterhaltung der Homöostase, sowie der Bildung von Immunzellen im Darm übernehmen (3).

PP sind sekundäre Lymphorgane, welche in der Maus über die gesamte Länge des Dünndarms verteilt vorliegen, während sie im Menschen vor allem im Ileum zu finden sind (3). Sie bestehen aus mehreren B-Zell-Follikeln zwischen denen die T-Zell-Regionen lokalisiert sind. Zum Lumen hin werden PP von dem Follikel-assoziierten Epithel (FAE) begrenzt, welches spezialisierte Epithelzellen, die sogenannten M-Zellen, enthält. Diese transportieren Antigene aus dem Lumen in die subepitheliale Domregion der PP; dort werden die Antigene von DC aufgenommen, welche dann in die interfollikulären T-Zellregionen der PP oder in die mLK einwandern und eine entsprechende Immunreaktion initiieren (4). Außerdem findet in B-Zellen, die in den Follikeln der PP lokalisiert sind, der Klassenwechsel zu Immunglobulin (Ig) A statt, welches gegen luminale Antigene gerichtet ist und in das Darmlumen sekretiert wird (5). IgA-exprimierende B-Zellen in den PP sind klonal verwand mit IgA-exprimierenden Plasmazellen in der LP. Die orale Verabreichung nicht-mikrobieller Antigene führt in den PP der Maus zu einer Th_2-Antwort, die durch die Produktion von Interleukin (IL)-4, IL-5 und Tumor growth factor β (TGFβ) charakterisiert ist (3). Ein großer Anteil der $CD3^+$ T-Zellen in den PP haben einen regulatorischen Phänotyp und sind in der Lage via IL-10 T-Zell Proliferation *in vitro* zu inhibieren. *In vivo* führt dieser Mechanismus zu einer systemischen Unempfindlichkeit gegenüber dem verabreichten

Antigen. Dieser Prozess wird als orale Toleranz bezeichnet (6). Allerdings wird die Rolle der PP in diesem Zusammenhang kontrovers diskutiert, da sowohl zwischen den gängigen Mausstämmen, als auch zwischen Maus und Mensch große Diskrepanzen aufgezeigt wurden (7). Im Vergleich zu Maus PP werden in den PP des Menschen vorwiegend Th_1-Immunantworten induziert, was mit der Problematik korreliert, dass im Menschen nur schwer Toleranz gegen oral aufgenommene Antigen hervorgerufen werden kann (7). Eine gestörte Induktion der oralen Toleranz gegenüber luminalen Antigenen wird als eine mögliche Ursache diskutiert, die zur Ausbildung entzündlicher Darmerkrankungen beitragen kann.

KP sind als primäre Lymphgewebe beschrieben, die sowohl im Dünndarm, als auch im Colon an der Basis der epithelialen Krypten lokalisiert sind und aus einer Ansammlung von etwa 1000 Zellen bestehen. KP setzen sich vor allem aus linage-marker negativen (lin^-)$c\text{-}kit^+$ Zellen, dendritischen Zellen (DC) und Stromazellen zusammen und enthalten weniger als 2% reife B- bzw. T-Lymphozyten. Die Funktion dieser Zellaggregate ist bis heute nicht vollständig geklärt, es gibt jedoch Hinweise, dass dort eine extrathymische Differenzierung von αβ und γδ T-Zellen stattfindet (8; 9). Außerdem wird eine Rolle für $lin^-c\text{-}kit^+$ Zellen bei der Organisation lymphoider Strukturen diskutiert. So könnten KP als Vorläufer der ILF fungieren (3; 8). ILF sind kleine induzierbare Zellaggregate, die sowohl im Dünndarm, als auch im Colon zu finden sind und strukturell gesehen eine hohe Ähnlichkeit mit PP aufweisen. Sie bestehen zu 70% aus B-Zellen und zu je ca. 10% aus T-Zellen und DC und werden wie die PP von einem FAE begrenzt. Auch findet in den B-Zellen der ILF ebenso wie in den B-Zellen der PP der Klassenwechsel zu IgA statt, welches als negativer Regulator fungiert und die Bildung zusätzlicher ILF inhibiert bzw. die Regression der vorhandenen ILF steuert (10). Einerseits werden in ILF eher anti-inflammatorische Immunreaktionen induziert, während andererseits eine Rolle für ILF bei chronisch entzündlichen Darmerkrankungen (CED) beschrieben wurde. So ist in Patienten mit Morbus Crohn (MC) eine erhöhte Anzahl isolierter Follikel zu finden, die eine mögliche Rolle bei der Initiation von unkontrollierten Immunreaktionen in CED spielen könnten (11).

Die mLK sind die größten Lymphknoten (LK) im Körper und entwickeln sich in der Maus zwischen Tag 10.5 und 15.5 der Embryogenese. Wenn der Darm einer hohen Konzentration an Antigen ausgesetzt ist, findet die Präsentation der Antigene in zahlreichen Zelltypen, sowohl in der Mukosa, als auch in den mLK statt. Bei einer geringen Menge, wird das Antigen vor allem in den mLK präsentiert, wo vornehmlich eine Th_2-Antwort induziert wird (12). MLK sind essentiell daran beteiligt, dass die Penetration von luminalen Darmbakterien in die Mukosa limitiert und eine systemische Infektion verhindert wird. Allerdings wurde in murinen Modellen für CED eine dysregulierte Immunreaktion nicht nur in den PP und ILF, sondern auch in mLK gezeigt (13).

Die Erhaltung der Homöostase im Darm wird durch ein komplexes Netzwerk aus zellulären und humoralen Faktoren aufrechterhalten, wobei die einzelnen Faktoren sich gegenseitig regulieren. Dadurch ist das Gesamtsystem relativ stabil. Wenn jedoch ein Schlüsselregulator in diesem System fehlt, oder einen Defekt aufweist, kann es zu einer gestörten Regulation der Homöostase kommen, die z.B. in der Ausbildung von Nahrungsmittelallergien oder chronischen Darmentzündungen resultieren kann.

1.3. Rolle von DC im Immunsystem des Darms

DC stellen das Bindeglied zwischen angeborener und adaptiver Immunität dar. In der Peripherie liegen DC als unreife Zellen vor, deren Aufgabe es ist, kontinuierlich Material aus ihrer näheren Umgebung aufzunehmen. Erhält eine unreife DC ein Gefahrensignal, z.B. durch Kontakt mit einem Pathogen, so reift sie aus und wandert in die drainierenden LK ein. Dort präsentiert sie die prozessierten Antigene im Kontext mit kostimulatorischen Molekülen und induziert so die Differenzierung und Proliferation von spezifischen T-Zellen (14). Abhängig von der Art des Pathogens wird die Differenzierung unterschiedlicher T-Zelltypen (T Helfer (Th) Zellen, regulatorische T (Treg) Zellen und zytotoxische T-Zellen) induziert. Man unterscheidet die Gruppe der $CD4^+$ Th-Zellen grob in Th_1-Zellen, die Interferon (IFN)γ produzieren und eine zelluläre proinflammatorische Immunantwort vermitteln; Th_2-Zellen, die vor allem IL-4 produzieren und deren Hauptaufgabe in der Induktion einer humoralen Immunantwort besteht; sowie Th_{17}-Zellen, die IL-17 sekretieren und ebenfalls eine proinflammatorische Funktion haben. Treg-Zellen hingegen supprimieren Effektor T-Zellen und schützen den Körper so vor einer überschießenden Immunreaktion (15). Neben den reifen DC migrieren aber auch immer einige unreife DC, die nur eine geringe Anzahl an kostimulatorischen Molekülen auf ihrer Oberfläche exprimieren, in die Lymphorgane ein. In Abwesenheit von kostimulatorischen Signalen werden durch Bindung des T-Zell-Rezeptors an MHC Moleküle der Klasse II (MHC-II) auf der Oberfläche von DC, Treg-Zellen induziert. Dieser Prozess spielt eine wichtige Rolle bei der Induktion von Toleranz gegenüber körpereigenen Antigenen (14).

DC stellen eine extrem plastische Gruppe von Zellen dar, die von ihrer Umgebung geprägt werden, um spezifische Aufgaben zu erfüllen. Im Darm gibt es eine Vielzahl von Subtypen, denen jeweils distinkte Funktionen zugewiesen werden. Inwiefern die komplizierte Unterscheidung anhand von Oberflächenmolekülen und Funktion in einzelne Subpopulationen als Paradigma gesehen werden kann, ist jedoch fraglich. Vielmehr scheint es so, als wären die verschiedenen DC Typen in der Lage ihren Phänotyp, abhängig vom

umgebenden Milieu zu verändern, so dass eine eindeutige Klassifizierung der Zellen nicht immer möglich erscheint (16-18).

DC kommen in allen Bereichen des Darms vor. Sie sind in der LP des Dünn- und Dickdarms, in PP in ILF, in KP sowie in den mLK zu finden. Die DC der LP werden anhand ihrer Expression von CD103, dem Rezeptor für E-cadherin unterschieden. $CD103^+$ DC sind in der Lage die de novo Differenzierung von $Foxp3^+$ Treg-Zellen zu induzieren. Dieser Prozess ist abhängig von Retinsäure und TGFβ bzw. von Indoleamin-2,3-Dioxygenase (19; 20). Eine weitere Subpopulation von DC wird anhand ihrer Expression des Toll like receptor (TLR)5 definiert. TLR5 bindet Flagellin und erkennt somit motile Mikroorganismen. Diese DC Population ist in der Lage die Differenzierung von Th_{17}-Zellen, sowie den Klassenwechsel zu IgA in B-Zellen zu induzieren (21). Neben den $TLR5^+$ DC ist eine weitere Population von DC beschrieben, die den Fractalkine/Neurotactin Rezeptor CX_3CR_1, sowie CD70 exprimiert. Diese DC-Population kann die Differenzierung von naiven T-Zellen zu Th_{17}-Zellen in Abhängigkeit von ATP aber TLR-unabhängig hervorrufen (22). Auch sind $CX_3CR_1^+$ DC in der Lage aktiv Antigene im Darmlumen aufnehmen, indem sie mit ihren dendritischen Ausläufern das Epithel durchdringen (23; 24). Insgesamt sind die Funktionen der einzelnen DC-Populationen im Darm und ihre Rolle bei der Induktion von oraler Toleranz jedoch nicht in allen Einzelheiten verstanden.

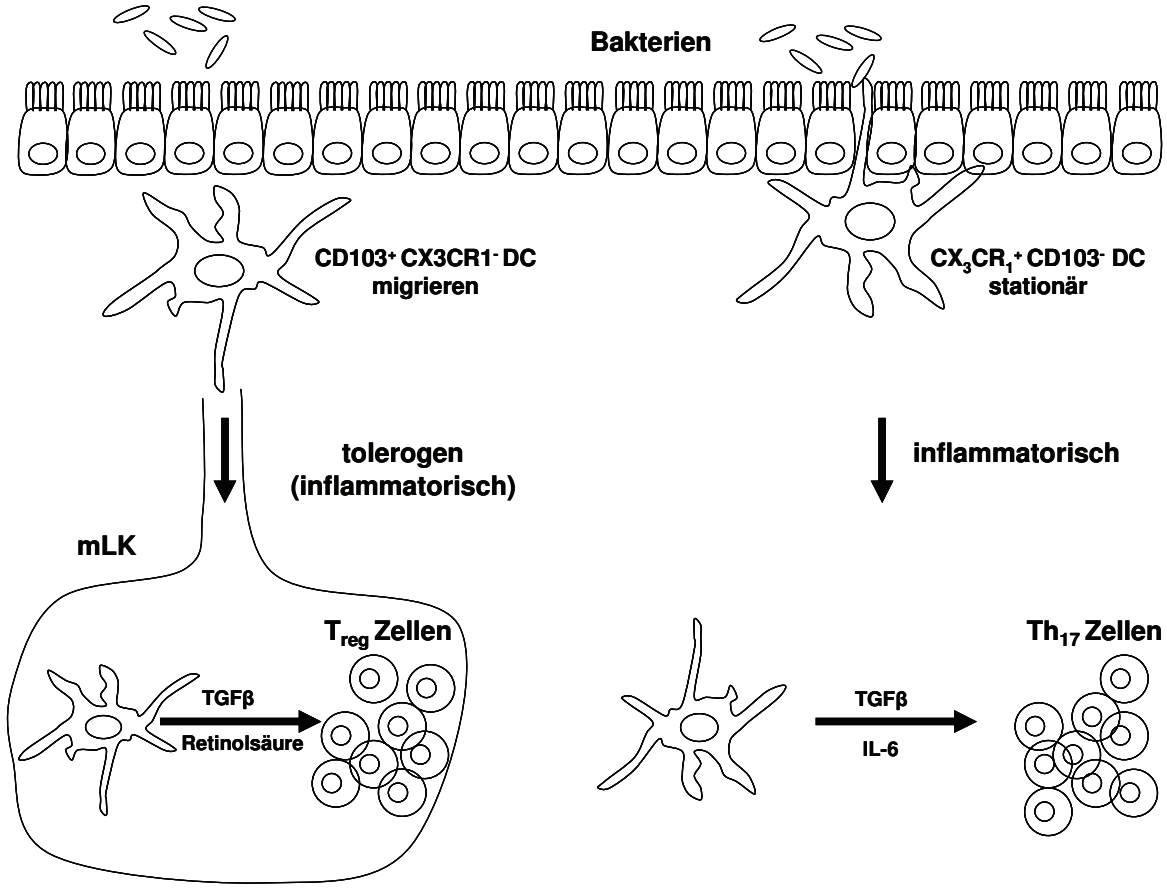

Abbildung 1. Rolle CD103+ und CX3CR1+ DC bei der Aufrechterhaltung der Homöostase im Darm. In der LP werden DC anhand ihrer Expression von CD103 und CX3CR1 unterschieden. CD103+ CX3CR1- DC sind in der LP lokalisiert und in der Lage nach Antigenkontakt in die mLK einzuwandern und die de novo Differenzierung von Treg-Zellen zu induzieren. Diese Zellen spielen eine entscheidende Rolle bei der Aufrechterhaltung der Homöostase im Darm. CD103- CX3CR1+ DC können ihrerseits die Tight junctions zwischen Epithelzellen durchbrechen und dendritische Ausläufer in das Lumen des Darms stecken, wo sie Antigene aufnehmen. Ihre Aufgabe besteht in der Induktion von Immunreaktionen gegen luminale Antigene durch Induktion von Th17-Zellen, um ein Eindringen von Mikroorganismen in die Darmmukosa zu beschränken.

1.4. Aktivierungsmechanismen von DC

Die Aktivierung von DC erfolgt nach Erkennung von Bestandteilen von Pathogenen, Bindung von inflammatorischen Mediatoren, nach Kontakt mit Allergenen und Fremdstoffen wie z.B. Partikeln oder auch endogenen Gefahrsignalen, die aus infizierten oder nekrotischen Zellen freigesetzt werden. Zu diesem Zweck exprimieren DC eine komplexes Repertoire an Rezeptoren, die beispielsweise konservierte Molekülstrukturen von Pathogenen erkennen. Diese sogenannten Pattern recoginition receptors (PRR) können anhand ihrer Funktion und

ihrer Ligandenspezifität unterschieden werden. Beispiele für PRR, die Pathogenstrukturen erkennen, aber keine Signale weiterleiten, sind die C-reaktiven Proteine oder Lektine des Komplementsystems, welche z.B. Mikroorganismen opsonisieren und so für Phagozyten erkennbar machen oder Phagozytoserezeptoren, die die Aufnahme von Mikroorganismen vermitteln. Zur Gruppe der PRR, die nach Ligandenbindung selbst Signale weiterleiten können und so zur Aktivierung der Zellen, sowie zur Produktion proinflammatorischer Mediatoren führen können, gehören die TLR. TLR sind membranständige Rezeptoren, die konservierte Pathogenstrukturen erkennen (25). Im Menschen sind 10 und in der Maus 12 TLR beschrieben. TLR haben eine extrazelluläre, Leucin-reiche Domäne, die für die Ligandenbindung entscheidend ist, sowie eine intrazelluläre Region, die sogenannte Toll/IL-1 Rezeptor (TIR) Domäne, welche für die Signalweiterleitung essentiell ist. TLR erkennen verschiedene Substanzgruppen. So wird z.B. Lipopolysaccharid (LPS), ein Bestandteil der Zellwände gram-negativer Bakterien von TLR4 zusammen mit dem TLR4-assoziierten löslichen Faktor MD-2 erkannt. Flagellin, ein Protein aus bakteriellen Geißeln, wird von TLR5 detektiert. Bakterielle und virale DNA, die eine hohe Frequenz unmethylierter CpG-Motive aufweist, wird von TLR9 gebunden, während virale RNA von den TLR3, 7 und 8 (nur im Menschen) erkannt wird (26). Ligandenbindung an TLR führt zu einer Aktivierung von Transkriptionsfaktoren wie dem nuclear factor kappa-light-chain-enhancer of activated B cells (NF-κB) oder dem Interferon-regulator-factor (IRF). Es gibt jedoch Unterschiede in den Signalwegen, die zu einem TLR-spezifischen individuellen Aktivierungsmuster führen. Diese Unterschiede sind zurückzuführen auf alternative Adaptermoleküle, die an die intrazelluläre TIR-Domäne der TLR rekrutiert werden. Das Adapterprotein MyD88 ist an der Signaltransduktion aller TLR, außer TLR3 beteiligt und ist essentiell notwendig für die Induktion inflammatorischer Zytokine wie IL-6 und IL12p40. TLR3 und TLR4 können MyD88-unabhängig über das Adaptermolekül TRIF die Transkription von IFNβ aktivieren. Alternativ erkennen intrazelluläre PRR wie die RNA-Helikasen RIG-1 und Mda5 doppelsträngige RNA und führen über Aktivierung von NF-κB zur Transkription inflammatorischer Zytokine und Typ I IFN (26).

Als eine weitere Gruppe intrazellulärer PRR sind NOD-Rezeptoren beschrieben, die vor allem in Epithelzellen, aber auch in Immunzellen, an der Erkennung von bakteriellen Peptiden beteiligt sind. Via NF-κB induzieren sie die Expression inflammatorischer Zytokine. Mutationen im NOD2 Gen im Bereich der Leucin-rich-repeat (LRR) Region, die zum Verlust der Bakterien-Erkennung führen, sind mit MC assoziiert. Diese Korrelation beruht wahrscheinlich auf einer gestörten Toleranzinduktion gegen luminale Kommensalen (27).

IL-1β und IL-18 sind proinflammatorische Zytokine, welche als Proform nach TLR-Aktivierung im Zytosol translatiert werden. Um als aktivierte Form sekretiert werden zu können, muss

proIL-1β von der Cystein-Protease Caspase-1 gespalten werden, die ihrerseits zuvor unter bestimmten Bedingungen in Multiproteinkomplexen, die als Inflammasom beschrieben sind, durch autoproteolytische Spaltung aktiviert werden muss. NOD-like Rezeptoren (NLR) sind intrazelluläre, LRR-enthaltende Proteine, die als Strukturproteine im Inflammasom fungieren und eine Rolle bei der Erkennung von endogenen Gefahrsignalen und bakteriellen Bestandteilen, sowie bei der Rekrutierung und Aktivierung der Caspase1 spielen (27-29). Man unterscheidet verschiedene Arten von Inflammasomen. Das wohl am besten beschriebene NOD-like receptor family, pyrin domain containing 3 (NLRP3)-Inflammasom, setzt sich aus den Proteinen NLRP3, apoptosis-associated speck-like protein containing a caspase recruitment domain (ASC), Cardinal und der Pro-Caspase1 zusammen. Wie die Aktivierung von NLR auf molekularer Ebene stattfindet, ist bisher nur unvollständig verstanden. Einige Gefahrsignale wurden jedoch bereits identifiziert. So führt der Abfall der K+ Konzentration in der Zelle durch Bindung von extrazellulärem ATP an den Purinrezeptor P2X7 zur spontanen Bildung von Inflammasomen (30; 31). Neben diesen Faktoren können auch Kristalle das Inflammasom aktivieren. Harnsäure, als Endprodukt des zellulären Purin-Metabolismus kristallisiert im Na+-reichen Extrazellulärraum zu Mononatriumurat (MSU) aus. MSU wirkt als Adjuvanz, indem es das NLRP3-Inflammasom aktiviert, während eine Aktivierung von Antigen präsentierenden Zellen (APC) über TLR durch MSU nicht beschrieben ist (32). Eine Überproduktion von Harnsäure ist mit vielen inflammatorischen Krankheiten assoziiert. So findet man große Mengen an Harnsäure im Blut von Gicht-Patienten. Gicht ist eine inflammatorische Krankheit, in der Harnsäurekristalle starke Entzündungsreaktionen in Gelenken und dem umgebenden Gewebe auslösen, wobei dieser Prozess ebenfalls Inflammasom-abhängig zu sein scheint (33). Alum ist das weitverbreitetste Adjuvanz, das im Menschen angewendet wird. Seine aktivierende Wirkung ist ebenfalls auf die Induktion des NLRP3-Inflammasoms zurückzuführen (32; 34; 35). Neben Alum können auch Siliziumdioxid Kristalle (Quartz) und Asbest das NLRP3-Inflammasom aktivieren (36-38). Alum wird seit vielen Jahren als Adjuvanz bei Vakzinierungen eingesetzt. In neueren Studien wird untersucht, ob neuartige Partikel in ähnlicher Weise das Inflammasom aktivieren können und möglicherweise eine Alternative zur herkömmlichen Vakzinierungsstrategie bieten können. So wurde gezeigt, dass LPS-beschichtete Polylactic-co-glycolic acid (PLGA) Nanopartikel (NP), die zusätzlich mit bestimmten Antigenen beladen waren, das Inflammasom aktivieren und eine Immunantwort gegen das verabreichte Antigen induzieren können (39). Auch die inflammatorischen Symptome in der Lunge nach Inhalation von Quartz sind abhängig vom NLRP3-Inflammasom (36). Hornung et al. haben einen Wirkmechanismus postuliert, wonach Quarzkristalle in Lysosomen aufgenommen werden, die daraufhin lysieren. Die lysosomale Protease Kathepsin B gelangt so in das Zytoplasma

und führt direkt oder indirekt zur Aktivierung des NLRP3-Inflammasoms (38). Die Bildung reaktiver Sauerstoffspezies (ROS) in Zellen, die mit Inflammasomaktivatoren behandelt wurden, kann ebenfalls zur Aktivierung des Inflammasoms führen (40). Wie jedoch genau das NLRP3-Inflammasom durch Kathepsin B oder ROS auf molekularer Ebene aktiviert wird, ist derzeit noch unklar und bedarf weiterer Studien.

Neben den hier beschriebenen NOD-like Rezeptoren scheinen auch NOD-Rezeptoren neben der Aktivierung von NF-κB eine Rolle bei der Aktivierung des Inflammasom zu spielen. So sind Monozyten aus MC Patienten, die eine funktionale Mutation im NOD2 Gen haben, nicht in der Lage nach Stimulation mit bakteriellen Zellwandproteinen IL-1β zu produzieren (41).

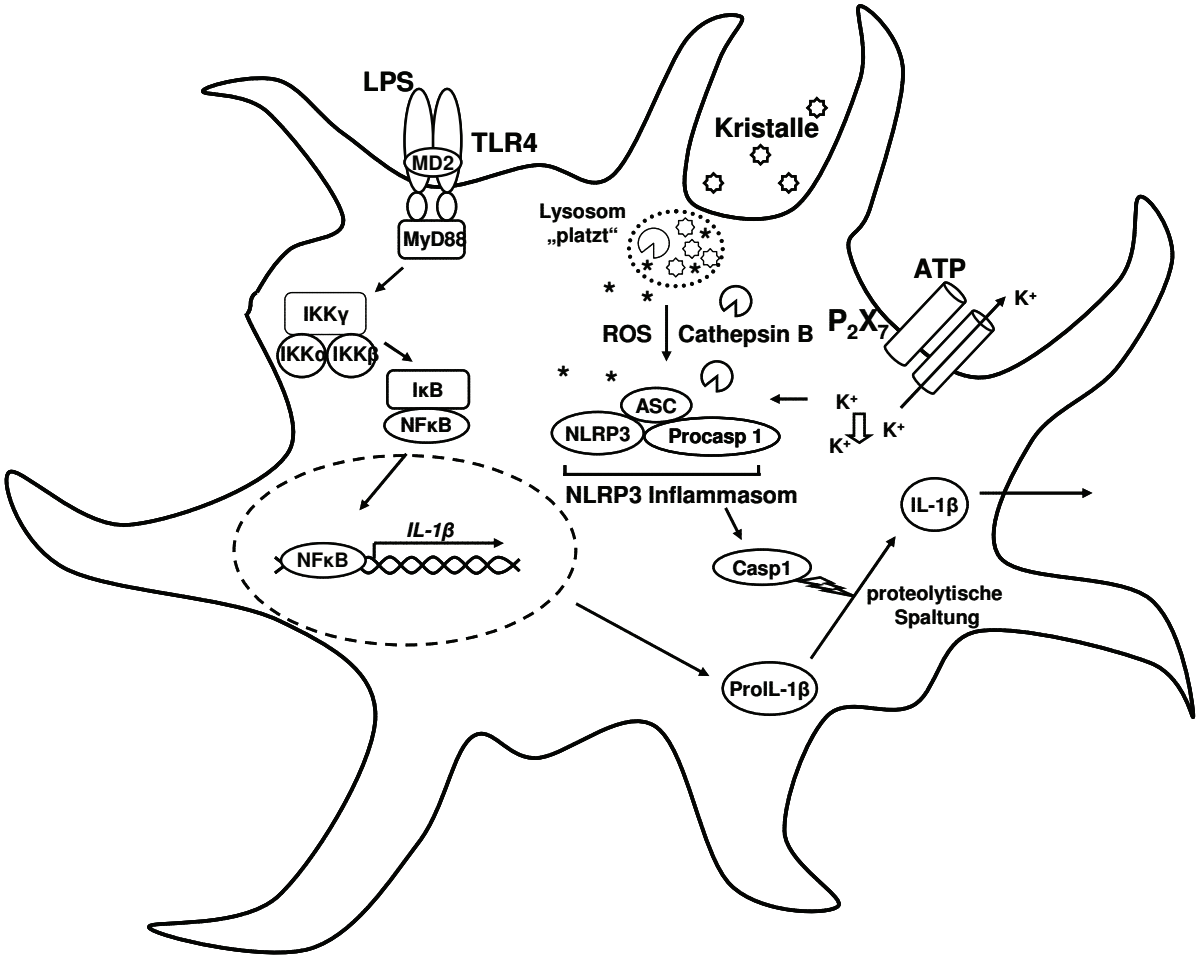

Abbildung 2. Vereinfachte Darstellung der Aktivierungsmechanismen des NLRP3-Inflammasoms in APC. Die Aktivierung des NLRP3-Inflammsoms erfolgt über 2 sukzessiv geschaltete Signale. Das erste Signal stellt die Bindung eines Liganden an TLR dar. Über die NF-κB Signalkaskade wird so die Expression von proIL-1β induziert, welches von der Caspase1 gespalten werden muss, um als aktive Form aus der Zelle sekretiert werden zu können. Die Caspase1 liegt ihrerseits als Zymogen in der Zelle vor und muss in einem Multiproteinkomplex, dem Inflammasom gespalten werden. Die Autoaktivierung der proCaspase1 erfolgt in Assoziation mit NLRP3, welches wiederum zuvor durch ein Gefahrensignal in der Zelle aktiviert werden muss. Als 2. Signal kann z.B. die Bindung von ATP an den Rezeptor P_2X_7 fungieren, wodurch ein Kalium Ionen Kanal geöffnet wird

und K^+ aus der Zelle strömt. Der Abfall der intrazellulären K^+-Konzentration führt zur Aktivierung des NLRP3-Inflammasoms, wobei der genaue Mechanismus jedoch noch ungeklärt ist. Kristalle, wie z.B. MSU, welches nach Freiwerden von Harnsäure aus sterbenden Zellen entsteht, sowie Asbest und Quarz können ebenfalls als 2. Signal das NLRP3-Inflammasom aktivieren. Nach Aufnahme in die Zelle, kommt es zum „Platzen" der Lysosomen, die ihren Inhalt aus Enzymen und Kristallen, sowie ROS in das Zytosol entleeren. Als ein kritischer Faktor, der zur Aktivierung des NLRP3 führt, wurde die Protease Kathepsin B beschrieben. Inwiefern ROS zur Aktivierung des NLRP3-Inflammasoms beiträgt, ist noch nicht abschließend geklärt.

1.5. Der Arylhydrocarbon Rezeptor (AhR) und seine Rolle im Immunsystem

Der AhR ist ein Transkriptionsfaktor, der zur Familie der basic helix-loop-helix Per-Arnt-Sim (bHLH-PAS) Familie gehört. In Abwesenheit von Liganden liegt er, an Chaperonproteine gebunden, im Zytoplasma der Zelle vor. Nach Ligandenbindung transloziert er in den Nukleus, wo die Chaperone abdissoziieren und dimerisiert mit dem AhR nuclear translocator (Arnt). Das AhR/Arnt Heterodimer bindet wiederum an dioxinresponsive Elemente (DRE) und induziert die Expression einer Vielzahl von Genen. Seit einiger Zeit sind jedoch weitere Bindungspartner wie z.B. der Östrogenrezeptor identifiziert worden (42). Eine wichtige Rolle spielt die AhR-induzierte Genexpression in der Leber, wo sie zur Metabolisierung von Fremdstoffen beiträgt. Das bekannteste Zielgen des AhR ist wohl das Cytochrom P450 1A1 (Cyp1A1), welches als Phase 1 Enzym die Metabolisierung von polyzyklischen aromatischen Kohlenwasserstoffen katalysiert (43). Ein weiteres Zielgen ist der AhR Repressor (AhRR), welcher ebenfalls zur Familie der bHLH-PAS Transkriptionsfaktoren gehört (44). Im Gegensatz zum AhR fehlt ihm jedoch die transaktivierende Domäne, so dass er nach Dimerisierung mit Arnt und Bindung an DRE nicht die Expression von Genen induziert, sondern den Promotor für den AhR blockiert. Neben der Suppression von AhR-Zielgenen reprimiert der AhRR auch die Expression des *ahr* selbst in einem negativen Rückkopplungsmechanismus (44). Neben halogenierten aromatischen Kohlenwasserstoffen wie z.B. 2,3,7,8-Tetrachlorodibenzo-P-Dioxin (TCDD), die über kontaminierte Lebenmittel aufgenommen werden, können auch pflanzliche Stoffe wie Flavonoide und Catechine den AhR aktivieren (45). Außer der Funktion im Fremdstoffmetabolisims hat der AhR auch eine physiologische Funktion, die jedoch noch näher untersucht werden muss. In der letzten Zeit wurden bereits zahlreiche endogene Liganden wie cyclic Adenosine Monophosphat (cAMP), Low Density Lipoprotein (LDL), Bilirubin und ein Photoprodukt des Tryptophans 6 Formylindolo[3,2-b]Carbazole (FICZ), beschrieben (46-49). Neben der Aufgabe des AhR, die Transkription metabolisierender Enzyme in Hepatozyten zu induzieren, spielt der AhR auch eine Rolle im Immunsystems.

Eine Exposition mit TCDD oder konstitutive Aktivierung des AhR führt langfristig zu einer Störung des Immunsystems, die sich in einer ausgeprägten Immunsuppression, wahrscheinlich bedingt durch eine gestörte T-Zell Entwicklung im Thymus, sowie eine Störung bei der Antigenpräsentation durch APC, manifestiert (50).
Auch konnte gezeigt werden, dass in AhR-defizienten Mäusen die Differenzierung von Th_{17}-Zellen gestört ist. Th_{17}-Zellen, die eine wichtige Rolle bei der Rekrutierung und Aktivierung von neutrophilen Granulozyten spielen, aber auch mit einer Anzahl von Autoimmunerkrankungen in Verbindung gebracht werden, exprimieren in hohem Maße den AhR (51). Es wurde gezeigt, dass Th_{17}-Zellen aus AhR-defizienten Mäusen nicht in der Lage sind, *in vitro* nach Stimulation mit IL-23, IL-22 zu exprimieren. Umgekehrt induziert die Stimulation von Th_{17}-Zellen mit AhR-Liganden die Expression von IL-22 *in vitro* (52). Dieser Effekt könnte eine Erklärung für die verstärkende Wirkung von AhR-Liganden auf die Pathogenese Th_{17}-abhängiger Erkrankungen, wie z.B. im murinen Modell für Multiple Sklerose, experimental autoimmune encephalomyelitis (EAE), gezeigt werden konnte, bieten (51; 53). *In vitro* Experimente ergeben darüber hinaus, dass auch der Anteil von IL-22-sekretierenden Th_{17}-Zellen, durch Stimulation mit AhR-Liganden gesteigert werden kann. Th_{17}-Zellen spielen auch im Darm eine wichtige Rolle und tragen essentiell zur Pathogenese von CED bei. In Anbetracht der Tatsache, dass die Zellen des Darms täglich mit starken AhR-Liganden aus der Nahrung exponiert sind, stellt sich die Frage, inwiefern AhR-Signaltransduktion zur Aufrechterhaltung bzw. Störung der Homöostase im Darm beitragen kann.

1.6. Ursachen und Pathogenese von CED

Mit einer Prävalenz von 10,2 - 33,6 / 100.000 Einwohner sind Colitis ulcerosa (CU) und MC (54) die beiden häufigsten Formen von CED in Mitteleuropa. CED Patienten stehen unter einem starken Leidensdruck, da zu den Symptomen Erbrechen, Durchfall, sowie starke abdominale Schmerzen zählen. CED ist eine schubweise auftretende Erkrankung, wobei CU und MC oft nur schwer voneinander abzugrenzen sind. Die Entzündung in CU ist aber auf das Colon beschränkt, während bei MC der gesamte Intestinaltrakt betroffen sein kann. Symptomatisch bei MC sind transmurale, fokale Entzündungsherde mit einer Infiltration von neutrophilen Granulozyten, sowie mononukleären Zellen, während bei UC die Entzündungsreaktion eher oberflächlich ist und ein durchgängiges Areal betrifft. Eine symptomatische Behandlung erfolgt mit immunsupprimierenden Medikamenten wie Tumornekrosefaktor (TNF)-α-Inhibitoren, Mesalamin und Steroiden. Im schlimmsten Fall

kann eine chirurgische Sektion von Darmsegmenten oder eine temporäre oder permanente Colostomie oder Ileostomie notwendig werden. Auch haben CED-Patienten ein erhöhtes Risiko an Darmkrebs zu erkranken (55).

Die grundlegenden Ereignisse, die zur Entstehung von CED beitragen, sind nur unzureichend bekannt, es gibt jedoch sowohl Hinweise auf genetische Prädispositionenen, wie auch auf eine Beteiligung von exogenen Faktoren. Beispielsweise korreliert eine erhöhte Aufnahme von mehrfach ungesättigten Fettsäuren mit einem erhöhten Risiko für CED (54). Die meisten epidemiologischen Studien, die den Einfluss von Nahrungsinhaltstoffen untersuchen, haben allerdings nur eine geringe Aussagekraft, weshalb keine abschließende Aussage über die Bedeutung der Ernährung in diesem Zusammenhang getroffen werden kann. Die Prävalenz von CED weist ein starkes Nord-Süd-Gefälle auf, mit einer deutlich stärkeren Prävalenz in Nordeuropa und Nordamerika, wobei weniger ethnische Unterschiede, als vielmehr die hygienischen Standards in den jeweiligen Ländern von Bedeutung zu sein scheinen. So könnte die Limitierung der Exposition mit Antigenen in unserer sehr auf Hygiene bedachten Gesellschaft dazu führen, dass die funktionelle Ausreifung des Immunsystems im frühen Kindesalter nur unzureichend stattfindet. Die fehlende Induktion von Toleranz gegen spezielle Antigene könnte bewirken, dass ein wiederholter Kontakt mit diesen Antigenen im späteren Leben zu einer Überreaktion des Darm-assoziierten Immunsystems führt, die sich z.B. in Allergien oder auch CED manifestieren könnte (56). Ein weiterer wichtiger Faktor ist die Darmflora selbst. Die Besiedlung mit Kommensalen findet ebenfalls erst nach der Geburt statt, in der Zeit, in der orale Toleranz etabliert wird; so werden adverse Effekte einer Kaiserschnittgeburt im Vergleich zur natürlichen Geburt und Flaschenfütterung im Vergleich zum Stillen diskutiert. Auch wurden psychologische Faktoren wie z.B. Stress mit der Entstehung von CED in Verbindung gebracht (54).

Den Hauptrisikofaktor für CED stellt jedoch eindeutig das Vorkommen von CED in der eigenen Familie dar. Ein eineiiger Zwilling hat ein 37%iges Risiko MC, bzw. ein 10%iges Risko CU zu entwickeln, wenn der andere Zwilling bereits erkrankt ist. Es gibt jedoch nicht nur ein einzelnes Gen, das für CED prädisponiert, sondern eine Vielzahl, wobei die meisten mit dem Immunsystem assoziiert sind. HLA DRB*0103 ist ein wichtiges Prädispositionsgen für CU, während NOD2 ausschließlich mit MC assoziiert ist, wobei vor allem der Funktionsverlust zu einer Überproduktion von proinflammatorischen Zytokinen nach TLR-Stimulation führt. Aber auch Mutationen, die mit einer verstärkten Aktivität von NOD2 einhergehen, welche in einer erhöhten Aktivierung des Inflammasoms und demnach einer erhöhten Sekretion von IL-1β resultieren, sind beschrieben (27).

Das Zusammenspiel dieser Vielzahl an genetischen und exogenen Faktoren, sowie die Tatsache, dass aller Wahrscheinlichkeit nach zahlreiche Faktoren noch nicht einmal bekannt sind, gestalten die Entwicklung einer ursächlichen Therapie schwierig.

1.7. Murine Modelle zur Untersuchung von CED

Transgene Tiermodelle sind von großem Nutzen, um die Mechanismen, die der Entstehung von CED zugrunde liegen, zu verstehen. Es sind bereits einige murine Modelle beschrieben, die spontan eine Entzündung der Darmmukosa ausprägenbilden. So entwickeln IL-10 defiziente Mäuse, sowie Mäuse, in denen selektiv in allen eosinophilen Granulozyten und Makrophagen der Transkriptionsfaktor Stat3 deletiert ist, eine Entzündung im Colon, die unter anderem auf eine gestörte negative Regulierung von Immunzellen über den IL-10-Rezeptor zurückzuführen ist (57; 58). Auch sind Mausmodelle mit verschiedenen NOD2 Mutationen verfügbar (59). In dieser Arbeit wurden zwei murine Modelle zur induzierbaren Darmentzündung untersucht, die im Folgenden näher beschrieben werden.

VILLIN-HA Modell:
Das VILLIN-HA Modell für CED beruht auf einer Immunreaktion von T-Zellen auf ein Autoantigen, welches als Transgen ausschließlich in Enterozyten des Darms exprimiert wird. VILLIN-HA-transgene Mäuse exprimieren das A/PR8/34 Hämagglutinin (HA) unter dem Villin-Promoter, der spezifisch in Epithelzellen des Darms aktiv ist (60). Durch einen adoptiven Transfer von transgenen $CD8^+$ T-Zellen wird eine Immunreaktion gegen die HA-exprimierenden Enterozyten induziert (61). Diese transgenen T-Zellen besitzen einen T-Zellrezeptor, der spezifisch an ein H-$2K^d$ restringiertes HA-Peptid bindet (CL4-TCR) (62). VILLIN-HA transgene Mäuse entwickeln etwa 5 Tage nach T-Zell Transfer eine Entzündung der Mukosa im Dünndarm, die durch eine starke Infiltration mit Lymphozyten, Plasmazellen und APC gekennzeichnet ist. Das Modell ermöglicht eine Untersuchung der adaptiven Immunreaktionen im Zusammenhang mit CED, da es eine fehlerhafte Selektion von autoreaktiven T-Zellen nachstellt. Durch einen Cotransfer von HA-spezifischen Treg-Zellen und HA-spezifischen $CD8^+$ T-Zellen kann die Entzündung signifikant reduziert werden, was auf ein gestörtes Verhältnis zwischen regulatorisch- und inflammatorisch-wirkenden T-Zellen in diesem Modell hindeutet (61). Das Modell eignet sich außerdem, Effekte von Nahrungsmittelbestandteilen auf T-Zell-abhängige Entzündungsmechanismen bei CED zu untersuchen.

Dextran Sulfat Sodium (DSS)-induzierte Colitis:

Die Applikation von 2% DSS über das Trinkwasser führt innerhalb von 6 Tagen zu einer starken akuten Entzündung der Colonmukosa in C57BL/6 Mäusen. Dabei führt das DSS zur Zerstörung der Integrität des Darmepithels, so dass Mikroorganismen aus dem Lumen in die Mukosa eindringen können, wo sie vor allem Phagozyten des angeborenen Immunsystems aktivieren. In der vorliegenden Arbeit wurde das ursprüngliche Protokoll von Okayasu et al. mit leichten Modifikationen genutzt (63). Die Colitis manifestiert sich etwa an Tag 6 und ist gekennzeichnet durch starken Gewichtsverlust der Tiere, sowie das Auftreten von blutigem Durchfall. Makrophagen scheinen eine große Rolle in der Pathologie der DSS-induzierten Colitis zu spielen, während T-Zellen wohl nur eine untergeordnete Rolle zukommt, da auch in T-Zell-defizienten Mäusen eine Colitis durch orale Gabe von DSS ausgelöst werden kann (64). In Abbildung 3 ist das Protokoll zur Induktion einer chronischen DSS-induzierten Colitis skizziert.

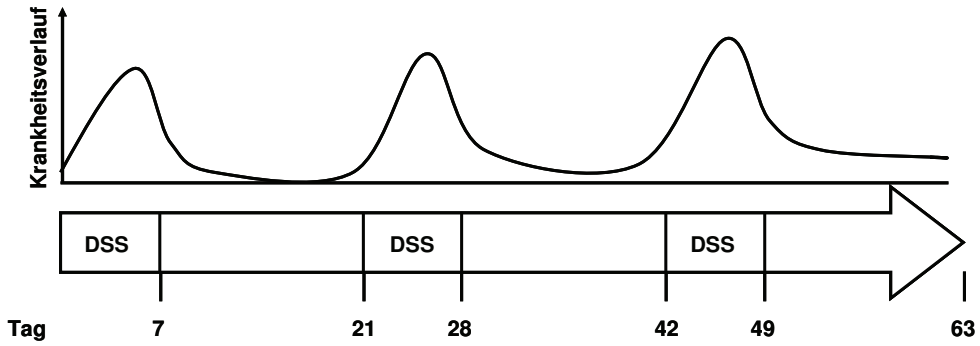

Abbildung 3. Chronisches DSS Modell der Colitis. Die Induktion einer chronischen Colitis in C57BL/6 Mäusen erfolgt in 3 Intervallen. Während eines Zyklus erhalten die Mäuse für eine Woche 2% DSS im Trinkwasser, gefolgt von zwei Wochen mit normalem Trinkwasser. Während jeder Behandlung verlieren die Tiere bis zu 20% ihres Ausgangsgewichts und entwickeln blutigen Durchfall, sowie eine starke akute Entzündung der Mukosa des Colons. Im Laufe der Behandlung chronifizieren die Symptome. An Tag 63 zeigen die Tiere eine gemäßigte, chronische Entzündung des Colon und weichen Kot, während das Gewicht sich wieder normalisiert.

1.8. DC als zentrale Akteure in der Entstehung von CED

Die exakte Rolle von DC bei der Entstehung chronisch entzündlicher Darmerkrankungen ist noch nicht geklärt; es gibt jedoch zahlreiche Studien, die DC in unterschiedlichen murinen Colitismodellen untersuchen und eine Beteiligung von DC an der Pathogenese von CED

eindeutig belegen. Auch sind eine Reihe von Prädispositionsfaktoren bekannt, unter anderem auch NOD2, welches eine Rolle bei der Aktivierung von DC spielt (27).

Wurden DC in einem Modell zur konstitutiven Ablation $CD11c^+$ Zellen während einer DSS-induzierten Colitis deletiert, waren die Symptome der Colitis gemildert. Im Gegensatz hierzu bewirkte die Abwesenheit von DC vor Induktion der Colitis eine Verschlechterung der Symptome. Wenn die Mäuse jedoch vor der Induktion einer DSS-Colitis mit GpG (TLR9-Ligand) behandelt wurden, so hatte dies eine protektive Wirkung (65). Diese Studie lässt eine duale Funktion von DC während der Induktion und Pathogenese von CED erkennen. In der Entstehungsphase von CED scheinen DC demnach regulativ zu wirken, wahrscheinlich durch Initiation der Differenzierung von naiven T-Zellen zu T_{reg}-Zellen, während sie im Verlauf eine pathogene Rolle einnehmen.

Th_{17} Zellen sind als entscheidener Pathogenitätsfaktor für CED identifiziert worden (66). Es wurde beschrieben, dass DC zur Pathogenese von MC beitragen, indem sie in den mLK die Differenzierung von Th_1- und Th_{17}-Zellen induzieren (67). Zusätzlich stellen DC im terminalen Ileum die Quelle von p40 dar, einer Untereinheit der Zytokine IL-12 und IL-23. IL-23 ist in der Maus für die Erhaltung und die Proliferation und im Menschen für die Entstehung von Th_{17}-Zellen essentiell (68). Die Expression von p40 wird durch Aktivierung von NOD2 in DC induziert. Die häufigste Mutation im *NOD2*-Gen, die in CED Patienten vorkommt, ist jedoch eine Funktionsverlust-Mutation, so dass NOD2 scheinbar eher eine protektive als eine pathogene Wirkung zukommt (27). Neben NOD2 wurden auch Gene, die eine Rolle bei der Autophagie in DC und anderen Zelltypen spielen, wie das *Autophagy-related 16-like 1 (Atg16L1)*, als Prädispositionsfaktoren für CED identifiziert (69). Autophagie ist ein Mechanismus, der die Prozessierung zelleigener aber auch phagozytierter Proteine in einem spezialisierten Organell, dem sogenannten Autophagosom beschreibt. In Atg16L1-defizienten Makrophagen war nach LPS Gabe die Sekretion von IL-1β erhöht. Es ist allerdings nicht klar, inwiefern dieser Effekt auch in DC eine Rolle spielt (70). Weitere Indizien für eine Beteiligung von DC an pathogenen oder protektiven Prozessen in CED liefern Untersuchungen, die in CED erkrankten Patienten durchgeführt wurden. So werden myeloide und plasmazytoide DC aus dem Blut zu den Entzündungsherden im Darm rekrutiert. Dies erfolgt via CCL20-CCR6 und MAdCAM-1-α4β7 Wechselwirkung (71). In Darmläsionen von MC-Patienten findet sich eine erhöhte Anzahl an DC, die eine gesteigerte Expression von TLR und costimulatorischen Molekülen auf ihrer Zelloberfläche aufweisen (72). Auch sind DC als Quelle von TNFα in MC beschrieben und die Behandlung mit TNFα-Inhibitoren führt zu einer verminderten Aktivierung der mukosalen DC von MC-Patienten (73).

Zusammenfassend kann gesagt werden, dass die Rolle, die DC bei der Pathogenese von CED spielen, noch nicht abschließend verstanden ist. Eine Vielzahl an Indizien spricht sowohl für eine protektive, als auch für eine pathogene Rolle von DC bei der Entstehung und Pathogenese von CED, wobei die genauen Mechanismen jedoch in weiteren Studien aufgeklärt werden müssen.

1.9. Adverse Effekte von Partikeln am Beispiel der Lunge

In neuerer Zeit hat die Industrie den Nutzen sehr kleiner Partikeln entdeckt, deren Eigenschaften sich vollkommen von denen herkömmlich genutzter größerer Partikel unterscheiden können. NP sind als Partikel mit einem Durchmesser von 1 - 100 nm definiert. Im Nanogrößenbereich wird die Oberfläche des Partikels im Verhältnis zu seiner Masse besonders wichtig und bestimmt entscheidend seine Eigenschaften, während die Oberflächeneigenschaften bei größeren Partikeln eine untergeordnete Rolle spielen (74). Neben SiO_2-NP werden auch andere Substanzen wie TiO_2 in großem Maßstab als NP produziert. SiO_2-NP haben Eigenschaften, die z.B. die Viskosität einer Rezeptur positiv verändern können. Auch finden SiO_2-NP Anwendung im Bereich der Mikroelektronik, während TiO_2-NP als Photokatalysatoren in verschiedenen Anwendungsbereichen genutzt werden. Ihre antibakteriellen Eigenschaften, die auf einer photokatalytischen Produktion von ROS beruhen, macht man sich z.B. bei der Beschichtung von Oberflächen zu Nutze (75). Es gibt zahllose weitere Anwendungsbereiche für TiO_2- und SiO_2-NP in der Elektronik-, Kosmetik-, Lebensmittel- und Textilindustrie. Die Risikobewertung dieser neuartigen Partikel ist jedoch bei Weitem nicht abgeschlossen. Sowohl in *in vitro* als auch in *in vivo* Studien konnte bereits früh eine starke Abhängigkeit der Reaktivität eines Partikels von seiner Oberfläche gezeigt werden (76).

Es ist lange bekannt, dass die Inhalation von Quarzstäuben zu einer Reihe pathologischer Veränderungen der Lunge führen kann. Die bekannteste Folge einer chronischen Exposition mit Quarzstäuben ist als Silikose beschrieben. Silikose ist vor allem eine Berufserkrankung von Bergleuten, die mit SiO_2-haltigen Feinstäuben exponiert waren. Die Akkumulation von Quarz in der Lunge führt zur Entstehung einer chronischen Entzündung, die nach einer Latenzzeit von bis zu 40 Jahren zur Versteifung der Lungenflügel durch Kollagen-Neubildung führt und im Endstadium das Ersticken des Patienten zur Folge hat. Außerdem, kann die chronische Entzündung des Lungengewebes auch zur Entstehung von Lungenkrebs führen (77). Im Normalfall werden Partikel durch gezielte Bewegungen des Flimmerepithels aus der Lunge transportiert und verschluckt. Erreichen die Partikel jedoch die Alveolaren, so werden

sie von alveolaren Makrophagen (AM) phagozytiert, die daraufhin aktiviert werden und zu den drainierenden LK wandern, um dort T-Zellen ihre Antigene zu präsentieren und eine adaptive Immunantwort zu induzieren. Quarz kann jedoch nicht in den Vakuolen der AM abgebaut werden und führt zu einer Daueraktivierung der Zellen (78). Wenn diese hyperaktivierten Zellen im Interstitialraum verbleiben, können sie zur Pathogenese der Silikose beitragen. Quarz-aktivierte AM sekretieren inflammatorische Mediatoren, darunter IL-1β, welches wiederum Immunzellen aktiviert und zur Gewebezerstörung beiträgt. In *in vitro* Studien konnte gezeigt werden, dass Quarz sowohl in Makrophagen, als auch in DC die Aktivierung des NLRP3-Inflammasoms über Cathepsin B induziert (38). Damit übereinstimmend, ist die Pathogenese der Silikose eng mit der Aktivierung des NLRP3-Inflammsoms verknüpft (36). SiO_2 kommt in mehreren kristallinen Formen aber nur in einer amorphen Form vor. Während kristallines SiO_2 im Jahr 1997 von der International Agency for Research on Cancer (IARC) als humanes Karzinogen der Klasse 1 klassifiziert wurde, wurde amorphes SiO_2 lange für inert gehalten und ist von der IARC als nicht krebserregend eingestuft. Starke adverse Effekte konnten nur nach Inhalation von SiO_2-Kristallen, nicht aber nach Inhalation von amorphem SiO_2-Partikeln beobachtet werden (79). In den vergangenen Jahren hat sich jedoch der Blick auf diese Partikel verändert, da in einigen Untersuchungen adverse Effekte von SiO_2-NP aufgedeckt wurden. Sowohl TiO_2- als auch SiO_2-NP können im Tiermodell eine starke Entzündung hervorrufen, die zur Entstehung einer Fibrose beiträgt (80-82). Amorphe SiO_2-NP zeigten nach Inhalation im Mausmodell fibrinogene Effekte und eine starke Entzündungsreaktion, die mit einer Produktion proinflammatorischer Zytokine wie IL-1β einherging. Anders als nach Inhalation von kristallinem SiO_2 waren diese Effekte jedoch transient, was wahrscheinlich auf die unterschiedlichen Löslichkeitseigenschaften der beiden Partikel zurückzuführen ist (80; 81). Anhand von Inhalationsstudien im Rattenmodell konnte gezeigt werden, dass TiO_2-NP zu einer vermehrten Deposition von Kollagen in der Lunge führen, sowie eine erhöhte Bildungsrate von Lungentumoren induzieren, im Vergleich zu größeren TiO_2-Partikeln (83). Neben diesen Effekten können TiO_2-NP auch als Adjuvanz während der Sensibilisierung gegen Atemwegsallergene wirken (84). Neben ihren potentiell toxischen und immunogenen Eigenschaften sind sie aufgrund ihrer geringen Größe in der Lage, Zellmembranen zu passieren und sich so im gesamten Organismus zu verteilen. Die Gefahr, die sich daraus ergibt, ist bisher nicht abschätzbar.

1.10. Relevanz von NP in der Nahrung und mögliche Konsequenzen für die Homöostase des intestinalen Immunsystems

TiO_2 (E171) und SiO_2 (E551) sind Substanzen, die schon lange in unserer Nahrung enthalten sind. TiO_2-Partikel finden als weißer Lebensmittelfarbstoff in zahlreichen Nahrungsmitteln und Medikamenten Anwendung, während SiO_2-Partikel das Verkleben einzelner Bestandteile in einer Mixtur verhindern und z.B. die Fließeigenschaften von zähen Flüssigkeiten erhöhen. Beide Zusätze gelten als unbedenklich. Die veränderten Eigenschaften von SiO_2- und TiO_2-NP sind jedoch ebenfalls für die Lebensmittelproduktion interessant, so dass mittlerweile bereits geschätzt 150-600 Lebensmittel mit Nanozusatzstoffen vermarktet werden. Da es keine Deklarationspflicht für NP gibt, ist es für den Verbraucher beinahe unmöglich nachzuvollziehen, in welchen Produkten Nanomaterialien enthalten sind. Über adverse Effekte einer erhöhten Aufnahme von NP ist demnach so gut wie nichts bekannt. In einigen Tiermodellen wurde allerdings bereits eine größenabhängige Aufnahme von Partikeln in die Mukosa des Darms nachgewiesen. Vor allem Partikel mit einem Durchmesser im unteren Nanobereich werden über den Darm aufgenommen und verteilen sich besonders schnell in alle Organe des Körpers. In BALB/c Mäusen konnten Goldpartikel mit primären Durchmessern von 4 – 28 nm nach oraler Applikation im Blut, im Gehirn, in der Lunge, im Herzen, in den Nieren, in der Leber, in der Milz und dem Gastrointestinaltrakt nachgewiesen werden, während sich Goldpartikel mit einem primären Durchmesser von 58 nm fast ausschließlich in Gewebe des Gastrointestinaltraktes, aber auch im Gehirn wiederfanden (85). In Kombination mit aktuellen Erkenntnissen zu den zytotoxischen und immunstimulierenden Eigenschaften von NP, implizieren diese Daten eine potentielle Gefährdung durch eine orale Aufnahme von NP, nicht nur für die Homöostase des Darms.
Während bereits die Aufnahme von NP in gesunden Individuen Bedenken aufkommen lässt, stellt sich des Weiteren die Frage, welche Effekte NP aus der Nahrung in Patienten mit einer Vorschädigung der Darmintegrität z.B. durch CED haben können. In einer Multi-Center-Studie wurde der Einfluss einer Mikropartikel (MP)-reichen Ernährung in 83 Patienten mit aktivem MC untersucht. Es konnte jedoch kein positiver Effekt einer Exklusion von MP-reichen Lebensmitteln auf den Verlauf der Krankheit beobachtet werden (86). In *ex vivo* Analysen konnte gezeigt werden, dass die Inkubation von Colon-Biopsien aus MC Patienten mit TiO_2-MP mit einem Durchmesser von 200 nm zusammen mit LPS die Expression von IL-1β im Vergleich zu einer Stimulation ausschließlich mit LPS stark erhöhte (87). Einer aktuelleren Studie zu Folge, führt die orale Aufnahme von TiO_2-NP in C57BL/6 Mäusen zu einer Akkumulation von DNA-Schäden in Zellen des hämatopoetischen Systems (88). Im Gegensatz zu einer Aufnahme von TiO_2-NP sind für die Aufnahme amorpher SiO_2-NP nur wenige Daten verfügbar.

Zusammengenommen gibt es zahlreiche Indizien für adverse Effekte, die durch die orale Aufnahme von NP hervorgerufen werden können, so dass eine systematische und auch mechanistische Untersuchung der durch orale Aufnahme von NP hervorgerufenen Effekte dringend benötigt wird.

1.11. Zielsetzung der Dissertation

In der vorgelegten Arbeit „Immunstimulatorische und immunregulierende Wirkungen von Nanopartikeln und Umweltschadstoffen auf das Darm-assoziierte Immunsystem“ sollte der Einfluss exogener Faktoren aus der Nahrung auf die Homöostase des Darms untersucht werden mit einem speziellem Fokus auf NP. Dabei wurden zwei Schwerpunkte gesetzt:

- Untersuchung des Einflusses von NP aus der Nahrung auf die Entstehung und Pathogenese von CED im Tiermodell.

- Analyse des Einflusses von NP aus der Nahrung auf die Aktivierung von DC und Aufklärung des zugrunde liegenden Mechanismus.

2. Ergebnisse

2.1. Manuskripte als Erstautor

Im Folgenden werden die Ergebnisse der im Anhang A angefügten Manuskripte als Erstautor zusammengefasst und im Zusammenhang dargestellt, wobei die Ergebnisse der Manuskripte die Zielsetzung der beiden Arbeitsteile wieder spiegeln.

2.1.1. Oral uptake of amorphous SiO_2 nanoparticles exacerbates experimental inflammatory bowel disease

Meike Winter, Katrin Schumann, Hans-Anton Lehr, Kirsten Gerloff, Roel P.F. Schins, Jan Buer, Astrid M. Westendorf*, and Irmgard Förster*
*equal contribution

Manuskript in Vorbereitung

NP sind ein Teil unserer Umwelt. In vielen Produkten des täglichen Bedarfs, wie in Kleidung, in Kosmetik und auch in der Nahrung, finden sich Partikel mit einem Durchmesser von weniger als 0,1 µm. In der hier beschriebenen Studie wurde der Einfluss von amorphen SiO_2-NP mit einem primären Durchmesser von 14 nm auf die Entstehung und Pathogenese von CED im Tiermodell untersucht. Partikel, die für diese Studie genutzt wurden, haben identische Merkmale wie SiO_2-NP, die bereits in der Nahrungsmittelproduktion vor allem Gewürzmischungen zugesetzt werden, um diese vor dem Verkleben zu schützen (www.evonik.com). Um mögliche adverse Effekte der Aufnahme dieser SiO_2-NP zu untersuchen, erhielten Mäuse in drei unabhängigen Modellen für CED Zuchtfutter, welchem 0,1% SiO_2-NP beigemischt war (SiO_2-Futter). VILLIN-HA transgene Mäuse exprimieren ein Peptid des viralen Hämagglutinins (HA) in Assoziation mit MHC-I, spezifisch in den Enterozyten des Darms. Ein adoptiver Transfer von transgenen HA-spezifischen $CD8^+$ T-Zellen führt in diesen Mäusen zu einer Entzündung der Mukosa des Dünndarms (61). Wurde den Tieren eine Woche vor Transfer und während der Induktion der Entzündungsreaktion SiO_2-Futter verabreicht, so war der Gewichtsverlust signifikant stärker im Vergleich zu Mäusen, die Futter erhalten hatten, dem keine Partikel beigemischt waren (Placebofutter). Auch war in den SiO_2-gefütterten Tieren eine stärkere Entzündungsreaktion in der Mukosa zu beobachten. Zusätzlich zu diesen Parametern wurde die Expression des Aktivierungsmarkers CD69 auf $CD8^+$ T-Zellen in den mLK der Empfängertiere und deren Proliferation nach Restimulation mit einem HA Peptid *in vitro* analysiert. Sowohl die Expression von CD69, als auch die Proliferation der $CD8^+$ T-Zellen war in den mLK der erkrankten, SiO_2-gefütterten Mäuse höher als in Placebo-gefütterten Tieren. Die Untersuchung der Zytokinproduktion in der Darmmukosa ergab ebenfalls eine eindeutig erhöhte Produktion von IL-10, TNFα und IFNγ in den SiO_2-gefütterten VILLIN-HA Mäusen im Vergleich zu Placebo-gefütterten Tieren. Ähnliche adverse Effekte der oralen Aufnahme von SiO_2-NP konnten in einem T-Zell-unabhängigen Modell für akute Colitis beobachtet werden. In C57BL/6 Mäusen wurde über 6 Tage mit 2% DSS im Trinkwasser eine akute

Darmentzündung induziert. Während dieser Phase erhielten die Tiere normales Zuchtfutter, um Adsorptionseffekte des DSS zu vermeiden. 18 Tage vor Induktion der Colitis, sowie für 2 Tage im Anschluss an die DSS-Behandlung, erhielten die Mäuse SiO_2- oder Placebofutter und normales Trinkwasser. Während DSS/Placebo-gefütterte Tiere von Tag 7 bis Tag 8 bereits eine Verbesserung der Symptome zeigten, war die Colitis in DSS/SiO_2-behandelten Mäuse an Tag 8 unverändert stark. Auch wiesen DSS/SiO_2-gefütterte Mäuse eine reduzierte Colonlänge auf, was auf eine stärkere Entzündung der Schleimhaut des Colons, im Vergleich zu DSS/Placebo-behandelten Tieren hindeutet. Die Analyse der Zytokinproduktion in mLK ergab eine eindeutig erhöhte Produktion von TNFα in DSS/SiO_2-gefütterten Mäusen. Da CED eine typischerweise chronische Erkrankung darstellt, wurde in drei Zyklen mit jeweils einer Woche DSS, gefolgt von 2 Wochen mit normalem Trinkwasser in C57BL/6 Mäusen eine chronische Entzündung in der Mukosa des Colons induziert. Um den Einfluss von SiO_2-NP in diesem Modell zu untersuchen, erhielten die Tiere für zwei Wochen vor der ersten DSS-Behandlung und jeweils in den 2 Wochen nach DSS-Applikation, SiO_2-Futter oder Placebofutter ad libidum. Gewichtsabnahme, sowie Länge des Colons, die mit dem Schweregrad der Colitis korrelieren, waren in beiden Gruppen unverändert. Eine Analyse der mLK ergab jedoch einen signifikanten Unterschied in der zellulären Zusammensetzung der mLK der DSS/SiO_2- im Vergleich zu DSS/Placebo-gefütterten Mäusen. Es konnte gezeigt werden, dass die Gesamtzellzahl und vor allem der Anteil $Gr1^+$ Zellen in den mLK von SiO_2-gefütterten Mäusen, im Vergleich zu den mLK DSS/Placebo-gefütterter Tiere signifikant erhöht war. Analysen der Zytokinsekretion in der Mukosa des Colons ergaben eine starke Erhöhung des proinflammatorischen Zytokins IFNγ, sowie der Inducible nitric oxide synthase (iNOS) in SiO_2-gefütterten Mäusen, während die Expression von IL-1β nur leicht erhöht und die Expression von IL-17 in beiden DSS-behandelten Gruppen unverändert zur Kontrollgruppe war. In allen drei Modellen (HA-VILLIN, akute und chronische DSS-induzierte Colitis) hatten SiO_2-NP keinerlei immunstimulierende Wirkung in Kontrollmäusen, in denen keine Entzündung induziert worden war.

Zusammengenommen konnte in dieser Arbeit in 3 unabhängigen Modellen für entzündliche Darmerkrankungen eindeutig gezeigt werden, dass die orale Aufnahme von amorphen SiO_2-NP zu einer Verstärkung der Symptome führt. Daraus lässt sich eine potentielle Gefährdung durch SiO_2-NP für Patienten ableiten, die unter CED leiden.

2.1.2. Activation of the inflammasome by amorphous silica and TiO_2 nanoparticles in murine dendritic cells

Meike Winter, Hans-Dietmar Beer, Veit Hornung, Roel P.F. Schins, and Irmgard Förster

Eingereicht bei Nanotoxicology, in Revision

DC des Gastrointestinaltraktes spielen eine entscheidende Rolle bei der Induktion von Toleranz gegenüber luminalen Mikroorganismen und Antigenen aus der Nahrung und sind so an der Aufrechterhaltung der Immunhomöostase im Darm beteiligt. In verschiedenen Studien wurde bereits eine Rolle für DC bei der Manifestierung von CED beschrieben. Amorphe SiO_2-Partikel mit einem primären Durchmesser von 14 nm sind bereits im großen Maßstab in verschiedenen Nahrungsmitteln enthalten, während für TiO_2-NP nur wenige Informationen vorliegen, da es keine Deklarationspflicht für NP in Nahrungsmitteln gibt. SiO_2-NP werden als Trennmittel z.B. in Konfekt oder als Rieselhilfe in Gewürzmischungen und Salz eingesetzt, während TiO_2-Partikel als weißer Lebensmittelfarbstoff genutzt werden. Die beiden hier getesteten NP (TiO_2 und SiO_2) wirken potentiell immunogen und rufen nach Inhalation in der Lunge akute und chronische Entzündungsreaktionen hervor. Das NP aus der Nahrung in der Lage sind, die Homöostase im Darm zu beeinflussen, wurde bereits in der unter 2.1.1 beschriebenen Arbeit gezeigt. Aus diesem Grund wurde in der vorliegenden Arbeit der Einfluss von TiO_2- und SiO_2-NP auf den Reifungsstatus von DC, als mögliche Zielzellen von NP im Darm untersucht. Hierzu wurden Knochenmark-abgeleitete DC (KM-DC) für 18 Stunden mit TiO_2-NP und -MP, sowie amorphen SiO_2-NP und kristallinen SiO_2-Partikeln (Quarz) inkubiert und der Reifungsstatus der Zellen anhand der Expression von MHC-II und den kostimulatorischen Molekülen CD80 und CD86 analysiert. Die getesteten Partikel hatten keinen nennenswerten Einfluss auf die Viabilität der Zellen mit Ausnahme von SiO_2-NP und in geringerem Maße Quarz. Kultivierung mit TiO_2- und SiO_2-NP, sowie mit Quarz führte zu einer stärkeren Ausreifung der Zellen, gemessen an einer starken Hochregulation der Oberflächenmoleküle MHC-II und CD80/CD86 im Vergleich zu den unbehandelten Kontrollen. TiO_2-MP hatten so gut wie keinen Einfluss auf den Reifungsstatus der KM-DC. Neben der Expression stimulatorischer Moleküle wurde als zusätzlicher Marker für Aktivierung die Sekretion von IL-1β von Partikel-behandelten KM-DC analysiert. Nach Vorstimulation der Zellen mit LPS, welches die Transkription der Proform von IL-1β (Pro-IL-1β) induziert, wurden die Zellen mit Partikeln inkubiert und nach 18 Stunden wurde die aktive Form von IL-1β im Überstand quantifiziert. Pro-IL-1β muss von der Protease Caspase1 proteolytisch gespalten werden, um sekretiert werden zu können. Ihrerseits liegt die

Caspase1 in der unstimulierten Zelle als Zymogen vor, welches nach Aktivierung intrazellulärer Rezeptoren wie NLRP3 autokatalytisch gespalten wird. Der Proteinkomplex in dem Caspase1, NLRP3 und weitere Adapter- und Strukturproteine vorliegen, wird als Inflammasom bezeichnet. Es wurden bereits mehrere Aktivatoren des Inflammasom identifiziert, darunter kristalline Partikel wie Quarz, aber auch zelluläre Mediatoren wie ROS oder ATP. In dieser Arbeit konnte gezeigt werden, dass SiO_2-NP im gleichen Maße wie Quarz, sowie in geringerem Maße auch TiO_2-NP die Sekretion von aktivem IL-1β induzieren können. Dieser Effekt war abhängig von Caspase1 und NLRP3, wie in Experimenten mit KM-DC aus Mäusen, die für das jeweilige Protein defizient waren, gezeigt werden konnte. Auch war die Aktivierung des NLRP3-Inflammasoms abhängig von der Aufnahme der Partikel in die Zelle. Wurde die β-Aktin-abhängige Aufnahme der Partikel mit Cytochalasin-D blockiert, konnte keine erhöhte Menge an IL-1β im Überstand Partikel-aktivierter Zellen gemessen werden. Im Gegensatz hierzu hatten TiO_2-MP keinen Einfluss auf die Prozessierung von IL-1β. Um einen möglichen Wirkmechanismus zu postulieren, der zur Inflammasom-Aktivierung durch die hier getesteten NP führt, wurden ROS-Messungen durchgeführt. Diese ergaben, dass ausschließlich TiO_2-NP, nicht aber TiO_2-MP, SiO_2-NP oder Quarz die Bildung von ROS in DC induzieren. Möglicherweise führen TiO_2- und SiO_2-NP über unterschiedliche Wege zur Aktivierung des NLRP3-Inflammasoms.

In dieser Arbeit konnte erstmalig gezeigt werden, dass TiO_2- und SiO_2-NP in DC das NLRP3-Inflammasom aktivieren. Da die Aktivierung des NLRP3-Inflammasoms mit zahlreichen Erkrankungen wie Morbus Alzheimer, Gicht oder CED assoziiert ist, sollte eine erneute Risikobewertung diese Nanomaterialien in Betracht gezogen werden.

2.2. Manuskripte als Koautor

Im Folgenden werden die Ergebnisse der im Anhang B angefügten Manuskripte im Kontext des Promotionsprojektes dargestellt. Um ein besseres Verständnis über den Einfluss exogener Faktoren auf das Darm-assoziierte Immunsystem mit besonderem Fokus auf ihrer Rolle bei der Dysregulation während der Entstehung und Pathogenese chronischer Darmerkrankungen zu gewinnen, wurden in den, in diesem Kapitel zusammengefassten Projekten, folgende Fragestellungen bearbeitet: Einfluss von SiO_2-NP auf die Genom-Integrität von Darmepithelzellen; Rolle des AhR bei der Induktion von oraler Toleranz; Expression des AhRR, als wichtiger Regulator des AhR im Darm-assoziierten Immunsystem; Rolle des Selenoprotein P (SeP) in der Pathogenese von CED.

2.2.1. In vitro and in vivo investigation on the effect of amorphous silica on DNA damage in the inflamed intestine

Kirsten Gerloff, **Meike Winter**, Agnes W. Boots, Damian van Berlo, J Kolling, Cathrin Albrecht, Irmgard Förster, and Roel P.F. Schins

Manuskript in Vorbereitung

Amorphe SiO_2-NP sind bereits in mehreren Lebensmitteln enthalten. Mögliche Gefahren, die sich aus der oralen Aufnahme ergeben, sind jedoch nur unzureichend untersucht. Vor allem in Kleinkindern oder Patienten mit einer bereits etablierten Darmerkrankung könnte die Aufnahme von SiO_2-NP nachteilige Effekte hervorrufen. In der hier zusammengefassten Arbeit wurde der Einfluss von SiO_2-NP auf die DNA-Integrität in einem *in vitro* Coinkubations-Modell und *in vivo* im murinen DSS-induzierten Colitismodell untersucht. Die mukosale Entzündung bei CED ist gekennzeichnet von einem starken Influx aktivierter neutrophiler Granulozyten, die durch eine erhöhte ROS-Produktion möglicherweise zur Colitis-assoziierten Kanzerogenese beitragen. Um potentielle oxidative DNA-Schäden in Darmepithelzellen, hervorgerufen durch neutrophile Granzulozyten zu simulieren, wurden neutrophile Granulozyten zusammen mit Caco-2-Zellen (eine Epithelzelllinie) kultiviert. Zusätzlich wurde der Einfluss von SiO_2-NP in diesem Szenario untersucht. Wie bereits in einer vorherigen Studie gezeigt werden konnte (89), induzieren SiO_2-NP eine signifikante DNA-Schädigung in Caco-2-Zellen, im Vergleich zu unbehandelten Zellen, wobei in der hier beschriebenen Studie zwar eine erhöhte Anzahl an Doppelstrangbrüchen, jedoch keine oxidativen Läsionen nachgewiesen werden konnten. Ähnliche Effekte zeigte die Cokultivierung von Caco-2-Zellen mit aktivierten neutrophilen Granulozyten, welche sowohl Doppelstrangbrüche, als auch oxidative Läsionen in den Epithelzellen hervorriefen. Wurden Caco-2-Zellen und neutrophile Granulozyten zusätzlich mit SiO_2-NP behandelt, so waren weniger DNA-Schäden in den Epithelzellen messbar. Ein möglicher Erklärungsansatz für dieses Ergebnis ist, dass das Verhältnis von Partikeln zu Zelle in der Cokultur, aufgrund einer erhöhten absoluten Zellzahl, geringer war. Auch führten SiO_2-NP nicht zu einer Aktivierung der neutrophilen Granulozyten. Weder im chronischen noch im akuten DSS-induzierten Colitismodell in der Maus, zeigte eine orale Applikation von SiO_2-NP einen erhöhten Anteil an DNA-Strangbrüchen. Allerdings konnte im chronischen Colitismodell eine eindeutige Erhöhung oxidativer Läsionen im Colonepithel DSS-, sowie SiO_2-NP-behandelter Mäuse beobachtet werden. Die Tiere, die sowohl DSS, als auch SiO_2-NP erhalten hatten, zeigten im Vergleich eine weniger starke oxidative DNA-Schädigung. Dieser Effekt beruht

möglicherweise auf der erhöhten Induktion von DNA-Reperaturmechanismen, hervorgerufen durch eine verstärkte Entzündung in diesen Tieren. Insgesamt kann man von einem geringen Gefahrpotential einer oralen Aufnahme von SiO_2-NP über Nahrungsmittel ausgehen, was die hier untersuchten Endpunkte betrifft. Mögliche Langzeiteffekte auf die DNA-Integrität können jedoch nicht ausgeschlossen werden.

Die Autorin der Dissertation führte die Experimente im Tiermodell durch. Durch kurzzeitige Applikation von DSS wurde eine akute Entzündung der Darmmukosa induziert, während die Mäuse im chronischen Modell in drei Intervallen DSS erhielten. Der Einfluss von SiO_2-NP auf Entzündungsmechanismen in CED wurde bereits im Manuskript, welches unter 2.1.1. zusammengefasst ist, untersucht. Die hier beschriebene Studie stellt eine Ergänzung zu den bereits gezeigten Effekten dar und beleuchtet den Aspekt der Colitis-induzierten Kanzerogenese.

2.2.2. 2,3,7,8-Tetrachlorodibenzo-p-dioxin impairs stable establishment of oral tolerance in mice

Stephanie Chmill, Stefanie Kadow, **Meike Winter**, Heike Weighardt, and Charlotte Esser

Eingereicht bei Toxicological Sciences, in Revision

Die Aktivierung des AhR durch TCDD führt zu einer systemischen Immunsuppression, die sowohl adaptive, als auch angeborene Immunmechanismen betrifft. Es wurde bereits gezeigt, dass nach TCDD-Applikation die humorale Immunantwort gegen das Modellantigen OVA reduziert ist. Neben Dioxin sind auch zahlreiche sekundäre Pflanzeninhaltsstoffe wie Flavonoide und Indole als Liganden des AhR in der Nahrung enthalten, welche im Darm zu einer Aktivierung dieses Signalweges führen können. Die Wirkung der unterschiedlichen Liganden ist allerdings nicht einheitlich und muss für jeden einzelnen Wirkstoff getestet werden. In der vorgelegten Arbeit wurde die AhR-Expression in den Zelltypen des Darm-assoziierten Immunsystems via quantitativer PCR analysiert. Im unstimulierten Zustand konnten *ahr* Transkripte, sowohl in den mLK, als auch in der LP des Dünndarms detektiert werden, während in den PP kaum *ahr* mRNA nachgewiesen werden konnte. Auf zellulärer Ebene exprimierten vor allem intraepitheliale $CD8\alpha\alpha^+$ $TCR\gamma\delta^+$ T-Zellen, die für die Aufrechterhaltung der epithelialen Integrität zuständig sind, sowie eine Rolle bei der Immunüberwachung des Darms spielen, den AhR. In $CD103^+$ DC, die eine regulatorische

Funktion bei der Aufrechterhaltung der Homöostase im Darm innehaben, waren kaum *ahr* Transkripte messbar. Nach oraler Gabe von TCDD konnte im Dünndarm in abnehmender Stärke von proximal nach distal, in den mLK, den PP und der intraepithelialen Zellfraktion die Expression des AhR Zielgens *cyp1a1* induziert werden. Im Gegensatz hierzu wurde in den $CD103^+$ DC keine Hochregulation von *cyp1a1* nach TCDD gemessen. Allerdings konnte in dieser Zellpopulation eine starke Induktion des AhRR nach TCDD nachgewiesen werden, welcher die Expression des AhR in diesem Zelltyp möglicherweise reprimiert. Um den Einfluss einer Aktivierung des AhR-Signalweges auf die Homöostase im Darm zu untersuchen, wurde C57BL/6 Mäusen TCDD peroral verabreicht, woraufhin durch mehrmaliges Füttern Toleranz gegen das Modellallergen Ovalbumin (OVA) induziert wurde. Im Anschluss wurden die Tiere mit OVA und einem Adjuvanz restimuliert und OVA-spezifische, sowie Gesamt-IgG1-Spiegel im Serum gemessen. Nach TCDD-Gabe und einmaliger Sensibilisierung mit OVA, war die Menge von IgG1 im Serum signifikant reduziert. Dieser immunsupprimierende Effekt konnte jedoch durch einmalige Restimulation aufgehoben werden. Nach Toleranzinduktion gegen OVA war nach der ersten Sensibilisierung, sowie nach der ersten und zweiten Restimulation der IgG1-Spiegel in den TCDD-vorbehandelten Mäusen und in Mäusen, die kein TCDD erhalten hatten, im Serum auf Hintergrundniveau reduziert. Nach der dritten Restimulation jedoch war der IgG1-Gehalt in den TCDD-vorbehandelten Mäusen wieder auf demselben Niveau wie in den Mäusen, die ohne vorhergehende Toleranzinduktion sensibilisiert und restimuliert worden waren. Ein ähnlicher Effekt konnte auch für den IgA-Gehalt in den Fäzes beobachtet werden. Zusammenfassend konnte gezeigt werden, dass der AhR in Immunzellen des Darms exprimiert wird und TCDD die stabile Induktion von oraler Toleranz gegen das Modellallergen OVA im Mausmodell verhindert.

Die Autorin der Dissertation führte zusammen mit der Erstautorin des Manuskripts die Isolation der einzelnen Zellpopulationen aus dem Darm durch. Die hier dargestellte Arbeit trägt dazu bei, Mechanismen aufzuklären, inwiefern exogene Faktoren, die mit der Nahrung aufgenommen werden, die Homöostase des Darms stören und somit potentiell zur Entstehung oder zur Manifestation inflammatorischer Erkrankungen des Darms beitragen können.

2.2.3. Cell-type specific expression of the aryl hydrocarbon receptor repressor in immune cells of barrier organs and regulation by Toll-like Receptor ligands

Heike Weighardt, Olga Brandstätter, Stephanie Zwicker, **Meike Winter**, Thomas Haarmann-Stemmann, Markus Korkowski, Charlotte Esser, Joseph Abel, and Irmgard Förster

Manuskript in Vorbereitung

Um die Rolle des AhR-Signalweges im Zusammenhang mit Immunreaktionen besser zu verstehen, wurde eine knock-in Maus generiert, in welcher eine enhanced green flourescent protein (eGFP)-Kassette in das zweite Exon des *ahrr-Lokus* intergriert wurde. Um die Expression einer verkürzten Form des AhRR zu vermeiden, wurde zusätzlich das dritte Exon deletiert. Die heterozygote Expression des eGFP erlaubt die Detektion AhRR-exprimierender Zellen *in vitro* und *in vivo*, während die homozygote Expression zusätzlich eine Untersuchung der Funktion des AhRR ermöglicht, da diese Tiere AhRR-defizient sind. Der AhRR ist ein Zielgen des AhR und wirkt seinerseits supprimierend auf die Transkription des *ahr* Gens. Die Promotor-Region des AhRR enthält neben DREs auch eine Bindestelle für den Transkriptionsfaktor NF-κB, der als zentrale Schaltstelle während der Aktivierung von Immunzellen die Transkription vieler proinflammatorischer Gene steuert. Mit Hilfe der AhRR-Reporter-Mäuse wurde in dieser Arbeit die Expression des AhRR in verschiedenen Organen, sowie auf Einzelzellebene untersucht. Insgesamt war die Expression in homozygoten Tieren stärker als in heterozygoten Mäusen, was auf eine Autoregulation durch Suppression der AhR-Expression hindeutet. In der Haut konnte eine konstitutive Expression des AhRR in Langerhanszellen und Keratinozyten der Epidermis, sowie in dermalen DC und Fibroblasten der Dermis nachgewiesen werden. Die Untersuchung der immunologischen Zellpopulationen des Darms ergab eine starke Expression des AhRR in den DC der LP. Eine besonders starke Expression konnte in $CD103^+$ DC nachgewiesen werden, was mit den Beobachtungen der unter 2.2.2 diskutierten Arbeit übereinstimmt. In den mLK sowie in PP und in peripheren LK (pLK) war ebenfalls eine Population AhRR exprimierender DC detektierbar. In T-Zellen war der AhRR ausschließlich in der LP des Darms und in einem geringeren Prozentsatz der $CD8^+$ T-Zellen in den PP zu finden. Durch Gabe des AhR-Liganden 3-Methylcholanthren (3-MC) konnte die Expression des AhRR in den DC aller untersuchten Organe mit Ausnahme der Milz gesteigert werden. Stimulation von KM-DC mit den TLR-Liganden LPS, GpG und P3Cys *in vitro*, induzierte ebenfalls die Expression des AhRR. Dieser Prozess war unabhängig vom AhR-Signalweg, da die Induktion des AhRR mit TLR-Liganden auch in

Anwesenheit des AhR-Inhibitors 3-Methoxy-4-nitroflavon möglich war. Dagegen führte die Inkubation von KM-DC mit 3-MC nicht zu einer Hochregulation des AhRR, woraus geschlossen werden kann, dass die Induktion des AhRR in KM-DC nicht über den AhR-Signalweg läuft, sondern möglicherweise ebenfalls NF-κB reguliert ist. Dieser Befund legt eine Rolle für AhR-AhRR-regulierte Transkription in der Aufrechterhaltung der Homöostase des Darms Nahe, da intestinale Immunzellen, die sowohl AhR (siehe 2.2.2), als auch AhRR Expression aufweisen, in engem Kontakt mit den Mikroorganismen des Darmlumens stehen.

Die Autorin der Dissertation führte in Zusammenarbeit mit Olga Brandstätter die FACS Analysen der aus Darm und LK isolierten Zellpopulationen durch. Die hier beschriebene Arbeit deckt ein Zusammenspiel zwischen Mechanismen des angeborenen Immunsystems und der Induktion des AhR-AhRR-Signalweges in DC auf. Inwiefern dieser Mechanismus eine Rolle bei der Modulation von Immunreaktionen spielt, muss in weiteren funktionellen Untersuchungen der AhR und AhRR-defizienten Mäuse untersucht werden.

2.2.4. Down-regulation of selenoprotein P expression by proinflammatory cytokines in intestinal epithelial cells and in ulcerative colitis

Bodo Speckmann, Antonio Pinto, **Meike Winter**, Irmgard Förster, Helmut Sies, and Holger Steinbrenner

Eingereicht bei Free Radical Biology and Medicine, in Revision

Bei Entzündungsreaktionen kommt es zu einer vermehrten Produktion von ROS und NO, welche eine wichtige Rolle bei der Beseitigung von Bakterien durch Makrophagen und Granulozyten spielen. Durch die Produktion von ROS und NO besteht aber auch die Gefahr einer Schädigung körpereigener Strukturen wie Lipidmembranen, Proteinen oder DNA, so dass der Körper antioxidative Enzyme produziert, um eine größere Gewebeschädigung zu verhindern. Die Phospholipid Hydroperoxid Glutathion Peroxidase und Peroxinitrit Reduktase Selenoprotein P (SeP) ist vor allem in der Leber, der Niere und im Darm exprimiert. Die Hauptaufgabe des SeP liegt in der Versorgung der Gewebe mit Selen, welches als Selenocystein im katalytischen Zentrum der Oxidoreduktase gebunden vorliegt. Eine weitere Funktion des SeP ist der Schutz von Plasmamembranen vor Oxidation und Nitrierung. In dieser Arbeit wurde die Regulation des SeP in Caco-2-Zellen, sowie die Expression von SeP und iNOS im Darm von CED-Patienten und im Colon DSS-behandelter Mäuse untersucht.

SeP wird während der Differenzierung der Caco-2-Zellen in Kultur hochreguliert. Außerdem korrelierte die Expression von SeP mit der Expression des Transkriptionsfaktors hepatocyte nuclear factor-4α (HNF-4α) und eine Bindung von HNF-4α an die Promotorregion von *sep* konnte nachweisen werden. Stimulation von Caco-2-Zellen mit den Zytokinen IL-1β, IFNγ und TNFα resultierte in einer Hochregulation von iNOS und einer parallelen Herunterregulation von SeP. Die Herunterregulation von SeP konnte durch Inhibition der iNOS komplett aufgehoben werden, was auf eine negative Regulation der SeP-Expression durch iNOS hindeutet. Patienten, die an Colitis ulcerosa leiden, haben aufgrund der chronischen Darmentzündung ein höheres Risiko in ihrem Leben Colon-Karzinome zu entwickeln. Ein Hauptfaktor in der Kanzerogenese in Colitis-Patienten stellt eine oxidative DNA-Schädigung durch ROS und reaktive Stickstoffmetabolite (RNS) dar. In dieser Arbeit konnte gezeigt werden, dass SeP in Darmbiopsien von Colitis-Patienten im Vergleich zu Biopsien aus Kontroll-Patienten herunterreguliert war. Gleichzeitig konnte eine erhöhte Produktion von iNOS nachgewiesen werden. In einem murinen Modell der chronischen Colitis wurde in C57BL/6 Mäusen durch mehrmalige Gabe von 2% DSS eine chronische Entzündung des Colon induziert. Auch im Colongewebe der Tiere war im Vergleich zu unbehandelten Mäusen iNOS stark hochreguliert, während parallel die Expression von SeP herunterreguliert war. Diese Herunterregulation von SeP, zusammen mit einer erhöhten Produktion von RNS, könnte das Fortschreiten der Erkrankung beschleunigen und zu der Entwicklung von Colon-Tumoren beitragen. Die genaue Rolle für SeP während der Pathogenese von CED muss in weiteren Studien aufgeklärt werden. Zusammengefasst konnte SeP als Differenzierungsmarker von Enterozyten und als negatives Akute-Phase-Protein im Darm identifiziert werden.

Die Autorin der Dissertation führte das gesamte Experiment zur Expressionsanalyse von SeP und iNOS im Colongewebe von Mäusen mit DSS-induzierter, chronischer Colitis durch. Dazu wurden Mäuse über einen Zeitraum von zwei Monaten in drei Intervallen mit DSS behandelt. Die Tiere wurden über den gesamten Verlauf des Experiments jeden zweiten Tag untersucht. Nach dem Experiment wurden die Tiere getötet und die Expression von SeP und iNOS mittels qPCR analysiert.

3. Diskussion

3.1. Einfluss von NP aus der Nahrung auf Effektormechanismen des Darm-assoziierten Immunsystems

NP sind definiert als Partikel mit einem Durchmesser von weniger als 0,1 µm. In diesen Größenordnungen ist die Reaktivität eines Partikels vor allem abhängig von seinen Oberflächeneigenschaften. Aus diesem Grund können sich sehr kleine Partikel vollkommen anders verhalten als größere Partikel der gleichen Substanz. In jüngster Vergangenheit finden NP auch in der Nahrungsmittelproduktion Verwendung (90). In den unter 2.1.1, 2.1.2 und 2.2.1 beschriebenen Studien wurde der Einfluss von NP, die in der Nahrungsmittelindustrie eingesetzt werden, auf das Immunsystem des Darms, bzw. auf Zellen, die eine entscheidende Rolle bei der Aufrechterhaltung der Homöostase im Darm spielen, untersucht.

CED ist eine weit verbreitete Krankheit, bei der eine Dysregulation des Darm-assoziierten Immunsystems vorliegt. Neben einer starken genetischen Komponente, spielen auch exogene Substanzen, die über die Nahrung aufgenommen werden, eine wichtige Rolle bei der Entstehung und Manifestation von Erkrankungen des Gastrointestinaltraktes. Auch kann die Aufnahme bestimmter Lebensmittel-Antigene Unverträglichkeitsreaktionen oder Allergien hervorrufen, bei denen das Darm-assoziierte Immunsystem ähnliche Störungen aufweist wie bei CED (91). Da CED mit einer besonders hohen Prävalenz in Industrie-Ländern auftritt, liegt die Vermutung nahe, dass Lebensweise und Ernährung möglicherweise zur Entstehung der Krankheit beitragen können. Ein Merkmal unserer Gesellschaft ist die oft zu Fett-haltige und Zucker-reiche Ernährung, die für metabolische Erkrankungen wie Diabetes oder Krankheiten des Herz-Kreislauf-Systems verantwortlich sind. In mehreren unabhängigen epidemiologischen Erhebungen konnte jedoch keine eindeutige Korrelation zwischen CED und der Ernährungsweise hergestellt werden (54). In unserer Nahrung ist zusätzlich eine Vielzahl anorganischer Partikel enthalten. Vor allem Fertigprodukte und Süßwaren enthalten große Mengen an Partikeln, deren Durchmesser zumeist im µm-Bereich liegt. Auch können Partikel aus der Lunge in den Darmtrakt gelangen. Aufgrund der hohen Feinstaubbelastung in Städten, ist die Bevölkerung einer großen Anzahl Partikel unterschiedlicher Zusammensetzung und Größe über die Luft ausgesetzt. Diese Partikel werden eingeatmet und können einerseits in der Lunge Erkrankungen wie z.B. Asthma auslösen, aber auch

durch gerichtete Cilienbewegung aus der Lunge in den Gastrointestinaltrakt gelangen. In einer Studie von Lomer et al. wurde der Zusammenhang zwischen einer MP-reduzierten Ernährung und dem Schweregrad von MC untersucht. Patienten, die für 4 Monate eine spezielle MP-reduzierte Diät erhalten hatten, zeigten eine Verbesserung der Symptome, während Patienten, die eine normale Partikel-haltige Diät erhalten hatten, unverändert starke Symptome aufwiesen (92). In einer größeren Folgestudie konnte dieser Effekt jedoch nicht reproduziert werden (93). In beiden Untersuchungen wurde aber nicht zwischen NP- und MP-enthaltenden Nahrungsmitteln unterschieden und die Wirkung von NP in der Nahrung in Zusammenhang mit CED ist bis heute noch vollkommen ungeklärt. In der vorliegenden Arbeit wurde erstmals der Einfluss von NP aus der Nahrung auf die Entstehung und Pathogenese von CED und auf die genomische Stabilität in intestinalen Epithelzellen in murinen Modellen für intestinale Entzündung analysiert. Zusätzlich wurde in mechanistischen Untersuchungen die Wirkungsweise von NP in murinen DC, die eine wichtige Rolle bei der Aufrechterhaltung der Homöostase im Darm spielen, untersucht. Durch adoptiven Transfer transgener HA-spezifischer $CD8^+$ T-Zellen in VILLIN-HA-Mäuse wurde eine Autoimmunreaktion gegen intestinale Epithelzellen induziert, was zu einer mukosalen Entzündung in diesen Tieren führte. Die Tiere erhielten vor und während der Induktion der Entzündung Futter, welches mit 0,1% SiO_2-NP supplementiert war, oder Placebo-Futter. Anschließend wurde der Schweregrad der Erkrankung, sowie das Ausmaß der Entzündungsreaktion bewertet. SiO_2-gefütterte VILLIN-HA-Mäuse zeigten eine signifikant verstärkte Enzündungsreaktion in der Mukosa des Dünndarms, sowie eine erhöhte Produktion von IL-10, TNFα und IFNγ im Darm, im Vergleich zu Placebo-gefütterten Tieren. Außerdem wiesen $CD8^+$ T-Zellen in den mLK SiO_2-gefütterter Mäuse, im Vergleich zu Placebo-gefütterten Tieren einen aktivierteren Phänotyp, gemessen anhand der Oberflächen-Expression von CD69, sowie ihrer proliferativen Aktivität nach Restimulation mit einem HA-Peptid *in vitro*, auf. SiO_2-NP hatten weder in diesem noch in einem anderen Experiment einen Einfluss auf die gemessenen Parameter in Kontroll-Tieren, in denen keine Enzündung induziert worden war. Diese Ergebnisse legen nahe, dass SiO_2-NP vor allem im Verlauf einer bereits etablierten Enzündungsreaktion synergistisch mit anderen Entzündungsmediatoren wirken können, während sie in gesunden Individuen mit einem intakten Epithel keine offensichtlichen, schädigenden Effekte hervorrufen. In vorherigen Untersuchungen konnte bereits gezeigt werden, dass NP bevorzugt in entzündeten Bereichen der Darm-Mukosa aufgenommen werden. Dieser Effekt ist vor allem auf eine erhöhte Sekretion von wasserunlöslichem Mukus, sowie einer Akkumulation von Immunzellen in der entzündeten LP, die aktiv Partikel aufnehmen können, zurückzuführen (6). Diese Eigenschaft wird sich zu Nutze gemacht, um immunsupprimierende Wirkstoffe zur

Behandlung von CED mit NP als Transportmittel lokal zu applizieren und so systemische Nebenwirkungen zu minimieren (94; 95). Die hier vorgelegte Studie impliziert jedoch eindeutig, dass SiO_2-NP im Darm immunogen wirken, und zu einer Verstärkung von Entzündungsreaktionen in experimenteller Colitis führen können. Für PLGA-NP, die zur Therapie von CED, eingesetzt werden, wurde *in vitro* bereits gezeigt, dass sie ebenso wie die, in der vorliegenden Arbeit analysierten SiO_2-NP das NLRP3-Inflammasom aktivieren (39), so dass Partikel-spezifische Nebenwirkungen bei der Behandlung nicht ausgeschlossen werden können. In weiteren Studien sollte demnach der Nutzen des therapeutischen Einsatzes von NP zur Behandlung inflammatorischer Erkrankungen sogfältig gegen potentielle Gefahren abgewogen werden.

In der vorgelegten Studie, wurde in einem weiteren Modell für akute CED, C57BL/6 Mäusen für 6 Tage 2% DSS im Trinkwasser verabreicht. DSS führt zu einer Schädigung des Darmepithels, so dass Mikroorganismen aus dem Darmlumen in die Mukosa eindringen, wo sie zur Induktion einer starken Entzündung beitragen. Parallel wurde in einer aktuellen Studie gezeigt, dass das Modell der DSS-induzierten Colitis abhängig von der Aktivierung des NLRP3-Inflammasoms ist (96; 97). Bauer et al. konnten zeigen, dass NLRP3-defiziente Tiere weitestgehend resistent gegen Colitis, ausgelöst durch DSS, sind. Bereits in früheren Untersuchungen wurde die Caspase1, die als Bestandteil des Inflammasoms die Proformen von IL-1β und IL-18 spaltet, als wichtiger Faktor während der Entstehung von CED beschrieben (97). Als Zielpopulation der DSS-vermittelten Effekte wurden Makrophagen identifiziert, in denen DSS zur direkten Aktivierung des NLRP3-Inflammasom führte (96). In der unter 2.1.2 zusammengefassten Arbeit konnte analog gezeigt werden, dass sowohl SiO_2- als auch TiO_2-NP in KM-DC das NLRP3-Inflammasoms aktivieren. Da DC eine Schlüsselrolle bei der Entstehung von CED einnehmen (65), postulieren wir eine mögliche NLRP3-Inflammasom-Aktivierung in intestinalen DC durch SiO_2-NP, die zur Modulierung der Entzündungsreaktion beitragen könnte. In weiteren Experimenten, die unter 2.1.1 beschrieben wurden, zeigten die Tiere eine verzögerte Regeneration der Symptome von CED, gemessen anhand der Gewichtszunahme, sowie der Konsistenz des Stuhls und des Vorhandenseins von Blut in den Fäzes im Vergleich zu DSS/Placebo-behandelten Mäusen, wenn sie vor Induktion einer akuten Colitis mit DSS, sowie im Anschluss an die DSS-Behandlung SiO_2-Futter erhalten hatten. Zusätzlich war die Colonlänge in DSS/SiO_2-behandelten im Vergleich zu DSS/Placebo-behandelten Tieren reduziert und die Produktion des proinflammatorischen Zytokins TNFα in mLK erhöht. Eine mögliche Erklärung für diese Effekte ist, dass SiO_2-NP effektiv an entzündete Stellen in der Mukosa des Darms binden, wo sie von Makrophagen und DC aufgenommen werden.

Anhand unserer *in vitro* Untersuchungen, die unter 2.1.2 zusammengefasst sind und Untersuchungen anderer Arbeitsgruppen konnte gezeigt werden, dass SiO_2-NP in Makrophagen, DC und intestinalen Epithelzellen zytotoxisch wirken. SiO_2-NP-induzierte Zytotoxizität war in Makrophagen und Epithelzellen, nicht aber in DC, mit einer erhöhten Produktion von ROS verbunden (89; 98) (98). ROS wiederum wird als ein Mechanismus der Aktivierung des NLRP3-Inflammasoms diskutiert (40). Da wir in SiO_2-behandelten KM-DC keine gesteigerte ROS-Produktion messen konnten, gehen wir von einem alternativen Mechanismus zur Aktivierung des Inflammasoms durch SiO_2-NP aus. Hornung et al. haben einen Mechanismus postuliert, wonach Quarz und Harnsäure-Kristalle die Lyse von Lysosomen in Makrophagen herbeiführen können. Die Freisetzung von Cathepsin B aus den Lysosomen führt zur Aktivierung des NLRP3-Inflammasoms über einen bisher ungeklärten Mechanismus. Ebenso sind weitere Untersuchungen notwendig, um den molekularen Mechanismus der hier untersuchten, oder anderer NP zur Aktivierung des NLRP3-Inflammasoms in DC aufzuklären. Die Eigenschaft von SiO_2-NP, in verschiedenen Zelltypen direkt oder indirekt das Inflammasom zu aktivieren, und somit zur Sekretion von prozessiertem IL-1β und IL-18 beizutragen, könnte eine mögliche Erklärung für die verstärkten Symptome in DSS/SiO_2-behandelten Mäusen sein. So wurden in der Mukosa von Patienten mit CED in der aktiven Phase erhöhte Mengen von IL-1β gemessen (99; 100). Die Aufnahme von SiO_2-NP könnte demnach nicht nur in Patienten mit einer bereits bestehenden CED eine proinflammatorische Wirkung haben, sondern möglicherweise auch in Menschen mit einer Inflammasom-assoziierten genetischen Prädisposition den Ausbruch der Krankheit beschleunigen. Dieser Theorie stehen jedoch 2 aktuelle Studien entgegen, die einen schützenden Effekt des NLRP3-Inflammasoms in DSS- und 2,4,6Trinitrobenzolsulfonsäure (TNBS)-induzierter Colitis und Colitis-assoziierter Colon-Kanzerogenese postulieren. Mäuse, die für verschiedene Proteine des Inflammasoms wie NLRP3 oder Caspase1 defizient waren, zeigten in diesen Studien signifikant verstärkte Symptome der Colitis (101; 102). Worauf die starke Diskrepanz zwischen diesen aktuellen Studien beruht, ist unklar. Eine mögliche Erklärung könnten Unterschiede in der Zusammensetzung der Darmflora der Tiere, aufgrund von Unterschieden in der Tierhaltung bieten. Zusätzlich wurde in einigen Studien von einer protektiven Wirkung von IL-1β in CED berichtet. Applikation von IL-1β führte im CED-Modell im Kaninchen zu einer Verbesserung der Symptome in Abhängigkeit von ProstaglandinE2 (103). Die Bedeutung von IL-1β und somit auch des NLRP3-Inflammasoms ist aufgrund der widersprüchlichen Ergebnisse noch nicht zu bewerten.

Unabhängig von einer Induktion des Inflammasoms, könnte die SiO_2-NP-induzierte Verstärkung der Symptome im DSS-Modell, wie auch im VILLIN-HA-Modell für CED, auf

einer Aktivierung des NF-κB-Signalwegs beruhen. NF-κB wird nach Ligandenbindung an TLR, oder durch proinflammatorische Zytokine wie TNFα im Zytosol phosphoryliert, transloziert in den Nucleus und induziert die Expression von proinflammatorischen Faktoren, unter anderem auch von IL-6 und IL-12, die ihrerseits zur Differenzierung von Effektor-Lymphozyten und somit zur Produktion proinflammatorischer Zytokine wie IFNγ beitragen können. Aber auch die Expression von pro-IL-1β und NLRP3 muss in einem ersten Schritt NF-κB-abhängig induziert werden, bevor das Inflammasom auf weitere Signale, wie extrazelluläres ATP oder Partikel hin, aktiviert werden kann. Wenn SiO_2-NP oral aufgenommen werden, durchwandern sie den Darm, der mit einer hohen Dichte an Mikroorganismen besiedelt ist. Die Wahrscheinlichkeit ist demnach sehr hoch, dass Bestandteile von Bakterien wie z.B. LPS an die Oberfläche der Partikel adsorbiert und so in die Mukosa eingeschleust werden, wo sie an TLR binden können. In einer *ex vivo* Studie konnte gezeigt werden, dass LPS, welches an TiO_2-NP gebunden war, in Colon-Biopsien aus CED-Patienten die Produktion von IL-1β induzieren konnte. LPS und Partikel jeweils alleine verabreicht, führten nur zu einer schwachen Induktion von IL-1β, während Partikel und LPS zusammen eine starken, synergistischen Effekt hatten (87). Anhand der aktuellen Datenlage zur Bedeutung des NLRP3-Inflammasoms in Zusammenhang mit CED, kann demnach nicht abgeschätzt werden, über welche Mechanismen die Verstärkung der akuten Colitis durch SiO_2-NP induziert wird. Auf der Basis meiner eigenen Ergebnisse postuliere ich jedoch, dass dem NLRP3-Inflammasom eine Rolle in der proinflammatorischen Wirkung von SiO_2-NP in CED zukommt. Dieser Hypothese soll in zukünftigen Untersuchungen nachgegangen werden.

Sowohl MC, als auch CU sind schubweise auftretende, chronische Erkrankungen des Darms. Um den Einfluss von SiO_2-NP in einem murinen Modell für chronische Colitis zu untersuchen, wurden Mäuse in drei Intervallen über einen Gesamtzeitraum von 10 Wochen mit DSS behandelt. Wenn die Tiere vor, zwischen und nach den DSS-Behandlungen mit SiO_2-NP gefüttert wurden, waren die absoluten Zellzahlen in den mLK im Vergleich zu DSS/Placebo-behandelten Tieren stark erhöht, wobei vor allem eine $Gr1^+/CD11b^+$ Zellpopulation signifikant erhöht war. Eine Population unreifer DC und Monozyten-Vorläuferzellen, die die gleichen Marker exprimiert, und eine immunsupprimierende Funktion hat, wurde bereits in murinen Tumor-Modellen identifiziert (104; 105). IL-1β spielt eine ambivalente Rolle bei Tumorerkrankungen. Einerseits führt IL-1β zu einer erhöhten Angiogenese und Metastasierungsrate, verbunden mit einer schlechten Prognose für den Patienten, andererseits kann IL-1β auch Anti-Tumor-Immunität induzieren (106). Auch sind Polymorphismen im IL-1β Lokus mit einem erhöhten Risiko, an Brustkrebs zu erkranken, assoziiert (107). In einer Studie konnte gezeigt werden, dass IL-1β, welches von

Tumorzellen sekretiert wurde, die Akkumulation einer Population $Gr1^+/CD11b^+$ myeloider Suppressor Zellen (MSC) im Blut und in der Milz der Tiere induzierte. Diese Zellen waren in der Lage T-Zell-Proliferation zu inhibieren, was ein beschleunigtes Tumor-Wachstum und eine erhöhte Metastasierungsrate der Tumore zu Folge hatte (105). Wurden in unserem Colitis-Modell, VILLIN-HA transgene Mäuse wiederholt mit $CD8^+$ HA-spezifischen T-Zellen transferiert, so entwickelten die Tiere nur eine sehr schwache Entzündung im Vergleich zu einer einmaligen T-Zell-Transplantation. In dieser Studie von Haile et al. konnte eine stark erhöhte Population von MSC im Darm und in der Milz von VILLIN-HA-Mäusen, die mehrfach HA-spezifische T-Zellen erhalten hatten, nachgewiesen werden. Wurden transgene T-Zellen zur Induktion von Colitis und MSC cotransferiert, war die Entzündungsreaktion in der intestinalen Mukosa ebenfalls supprimiert (108). Wahrscheinlich dienen MSC demnach der Regulation von Immunreaktionen, um den Organismus vor Gewebe-Schäden zu schützen. Eine erhöhte Frequenz von MSC wurde jedoch nicht in einem DSS-abhängigen Modell für chronische Colitis beobachtet (108). Wir vermuten dennoch, dass es sich bei den $Gr1^+/CD11b^+$ Zellen in den mLK DSS/SiO_2-behandelter Mäuse um MSC handelt und spekulieren, dass die Diskrepanz zwischen unserer und der Studie von Haile et al. möglicherweise durch Unterschiede in der Darmflora der Tiere zu erklären ist, sowie durch Unterschiede in den genutzten Konzentrationen von DSS. Übereinstimmend mit dieser Theorie war im Colon-Gewebe chronisch DSS/SiO_2-behandelter Tiere eine stark erhöhte Menge an IL-1β nachweisbar, welches bereits als Induktor von MSC beschrieben wurde (104; 105). Zusätzlich führte die Verabreichung von SiO_2-Futter in DSS-behandelten Mäusen zu einer erhöhten Produktion von IFNγ und iNOS im Colon, verglichen mit DSS/Placebo-behandelten Tieren. Im DSS-induzierten, chronischen Modell für Colitis scheinen SiO_2-NP demnach zu einer Verstärkung der mukosalen Entzündung durch Induktion proinflammatorischer Mediatoren zu führen, die parallel durch eine möglicherweise IL-1β-abhängige Induktion von MSC, eingedämmt wird. Da MSC immunsupprimierend und somit im Tumor-Modell Tumor-promovierend wirken, stellt sich die Frage, inwiefern SiO_2-NP durch Induktion von MSC langfristig zur Colitis-assoziierten Kanzerogenese im DSS-Modell beitragen können. Auch wird in zukünftigen Studien zu klären sein, ob die Induktion von MSC durch SiO_2-NP-induzierte Aktivierung des NLRP3-Inflammasoms und einer damit verbundenen, erhöhten Sekretion von IL-1β bedingt ist.

Genotoxizität von SiO_2-NP in Epithelzellen in vivo und in vitro

Neben den beschriebenen immunogenen Effekten, wurde der direkte Einfluss von SiO_2-NP auf die Colitis-induzierte Kanzerogenese in der unter 2.2.1 zusammengefassten Arbeit

untersucht. In einer Cokultur von humanen Caco-2 Epithelzellen und humanen primären neutrophilen Granulozyten wurde der Effekt von reaktiven Metaboliten der neutrophilen Granulozyten auf die genomische Stabilität der Caco-2 Zellen analysiert. Um die Bedeutung von SiO_2-NP in diesem Zusammenhang zu analysieren, wurden die Zellen zusätzlich mit SiO_2-NP behandelt. Aktivierte neutrophile Granulozyten führten zu einer Induktion oxidativer Läsionen und Doppelstrangbrüchen in der DNA von Caco-2 Zellen. Ebenso waren SiO_2-NP in der Lage, wie bereits in einer vorherigen Studie gezeigt (89), DNA-Schäden in Caco-2 Zellen zu induzieren. SiO_2-NP hatten jedoch keinen Einfluss auf den Aktivierungszustand von neutrophilen Granulozyten. Auch führte die Inkubation mit SiO_2-NP von neutrophilen Granulozyten und Caco-2 Zellen zusammen, nicht zu einer weiteren Erhöhung der DNA-Schäden, sondern eher zu einer Verringerung der DNA-Schädigung in Caco-2 Zellen. Dieser Effekt kann möglicherweise darauf zurückgeführt werden, dass die neutrophilen Granulozyten SiO_2-Partikel phagozytieren, und sich so weniger Partikel frei in der Kultur befanden. Zusätzlich wurde in dem bereits oben diskutierten DSS-induzierten Modell für Colitis die DNA-Integrität in Colon-Epithelzellen und im gesamten Colon-Gewebe untersucht. In Einzelzellen des Gesamt-Colon-Gewebes der Experimentalgruppen im Vergleich zur unbehandelten Kontrolle, konnten keine vermehrten DNA-Doppelstrangbrüche nachgewiesen werden. Vielmehr war der Anteil an DNA-Doppelsträngbrüchen sowohl in Tieren, die nur SiO_2-NP erhalten hatten, als auch in DSS/Placebo-behandelten und DSS/SiO_2-gefütterten Mäusen reduziert. Dieser Effekt impliziert eine Hochregulation von DNA-Reparatur-Mechanismen, möglicherweise ausgelöst durch Enzündungsreaktionen, wobei diese Hypothese erst in weiteren Untersuchungen auf die Probe gestellt werden muss. Immunhistologische Analysen ergaben allerdings eine klare Induktion oxidativer Läsionen in der DNA der Epithelzellen SiO_2-behandelter Mäuse, sowie DSS-behandelter Tiere. DSS/SiO_2-behandelte Mäusen wiesen eine weniger starke DNA-Schädigung im Vergleich mit SiO_2- bzw. DSS-behandelten Tieren auf. Dieser Effekt ist möglicherweise ebenfalls auf eine verstärkte Expression von DNA-Reparatur-Enzymen, ausgelöst durch eine stärkere Immunreaktion in den DSS/SiO_2-behandelten Tieren zurückzuführen. Die Diskrepanz zwischen dem Nachweis oxidativer Läsionen im Epithel des Colon und der reduzierten Menge an Doppelstrangbrüchen im Gesamt-Colon-Gewebe rührt wahrscheinlich daher, dass aufgrund der Anwesenheit einer Vielzahl unterschiedlicher Zelltypen im Colon die DNA-Schäden der Colonepithelzellen stark verdünnt waren und der Comet-Assay nicht sensitiv genug ist, DNA-Schäden in so einer kleinen Population zu detektieren. Im DSS-vermittelten, akuten Modell für Colitis, konnte ebenfalls keine erhöhte DNA-Schädigung von DSS/SiO_2-behandelten Mäusen im Vergleich zu DSS/Placebo-gefütterten Tieren gemessen werden.

Die Mechanismen, die in Colitis-Patienten zur Kanzerogenese beitragen, sind bisher noch nicht vollständig entschlüsselt. Es konnte jedoch gezeigt werden, dass die Wahrscheinlichkeit, an Colon-Karzinomen zu erkranken, mit der Dauer der Erkrankung, sowie mit der Stärke der Entzündung korreliert (55). Auch wenn in unserer Studie zur Untersuchung der genomischen Stabilität in chronischer und akuter DSS-induzierter Colitis keine schädlichen Effekte von SiO_2-NP nachgewiesen werden konnten, könnte die Aufnahme von SiO_2-NP über die Nahrung auf lange Sicht indirekt, durch eine Verstärkung der Entzündung in CED zur Manifestation von Colon-Karzinomen beitragen.
Neben den hier diskutierten lokalen Effekten einer oralen Aufnahme von NP, müssen in zukünftigen Studien auch mögliche systemische Effekte einer oralen Aufnahme von SiO_2-NP untersucht werden. In einer Studie von Hillyer et al. konnte 2001 bereits gezeigt werden, dass Gold-NP nach oraler Applikation unter anderem in Gehirn, Lunge, Leber, Blut, Nieren und Milz akkumulieren, während Trouiller et al. nach oraler Aufnahme von TiO_2-NP signifikante DNA-Schäden und Mutagenese in Blut und Knochenmark beobachteten (88). Auch werden NP mit der Entstehung neurodegenerativer Krankheiten in Verbindung gebracht, während gleichzeitig neuartige Strategien entwickelt werden, mit Hilfe von NP-Polymeren Wirkstoffe über die Blut-Hirn-Schranke, zur Behandlung neurologischer Erkrankungen, zu schleusen (109; 110). Einerseits eröffnen neuartige Therapien, die NP zur gezielten Applikation von Wirkstoffen in bestimmte Gewebe nutzen, neue Möglichkeiten Krankheiten zu behandeln und dabei das Auftreten systemischer Nebenwirkungen zu minimieren, andererseits zeigen NP sowohl *in vitro*, als auch *in vivo* toxische und inflammatorische Eigenschaften, die zu adversen Effekten im Verlauf einer Therapie mit NP oder durch orale Aufnahme von NP in der Nahrung führen könnten. Unser Verständnis zur Wirkungsweise oral aufgenommener NP ist auf die Ergebnisse weniger Studien beschränkt. Um das Risiko von NP in der Nahrung oder in medizinischen Applikationen für die Gesundheit der Bevölkerung einschätzen zu können, sind weitere Untersuchungen demnach dringend notwendig.

3.2. Rolle des AhR-AhRR-Signalwegs im Darm-assoziierten Immunsystem

Der AhR wurde erstmal identifiziert als Rezeptor für polyzyklische halogenierte Kohlenwasserstoffe. Die Aktivierung des AhR führt zur Induktion von Fremdstoff-metabolisierenden Enzymen unter anderem in der Leber. In einem negativen Rückkopplungsmechanismus induziert der AhR auch die Expression des AhRR, welcher wiederum die Transkription des AhR inhibiert. In neuester Zeit sind jedoch neben der

Funktion des AhR/AhRR-Systems, die Transkription von Enzymen des Fremdstoffmetabolismus zu regulieren, weitere Funktionen in der Regulation von Immunantworten beschrieben worden. Es wurde gezeigt, dass in AhR-defizienten Mäusen ein Defekt in der Induktion von Th_{17}-Antworten vorliegt (52), während nach Stimulierung des AhR mit TCDD eine systemische Immunsuppression beobachtet wurde (51; 111). In den unter 2.2.2 und 2.2.3 beschriebenen Publikationen wurde das Expressionsmuster des AhR, sowie des AhRR in Zellen des Darm-assoziierten Immunsytems untersucht. Außerdem konnte erstmalig gezeigt werden, dass der AhR eine wichtige Rolle bei der stabilen Induktion oraler Toleranz spielt. In der unter 2.2.2 beschriebenen Arbeit wurde die Transkription des AhR in Immunzellen des Darms mittels quantitativer PCR untersucht. Das Expressionsmuster des AhRR wurde, wie unter 2.2.3 erläutert, in einem neuen transgenen AhRR-Reporter Modell analysiert, in welchem die cDNA des eGFP im Locus des *ahrr*-Gens exprimiert wird. Der AhR ist in den mLK, im Dünndarm und in den PP konstitutiv exprimiert. Auf Einzelzellebene konnte vor allem in intraepithelialen CD8ααTCRγδ-T-Zellen und Epithelzellen AhR-Expression nachgewiesen werden, während in $CD103^+$ DC kaum AhR-Transkript detektiert werden konnte. Dafür war in diesen Zellen der AhRR besonders hoch exprimiert, was auf eine Suppression der Expression des AhR durch den AhRR in diesen Zellen hindeutet, während die Expression des AhRR in intraepithelialen CD8ααTCRγδ-T-Zellen und Epithelzellen des Dünndarms unterhalb der Nachweisgrenze lag. Mit Hilfe der AhRR-Reporter-Mäuse konnte eine starke Expression des AhRR in DC der LP, PP und mLK nachgewiesen werden, wobei $CD103^+$ DC den AhRR in besonders hohem Maß exprimierten. Bemerkenswerterweise nahm die Expressionsintensität mit zunehmender Entfernung von der Darmmukosa graduell ab. Dieser Befund deutet auf eine Stimulation der Expression des AhRR durch luminale Stimuli wie z.B. Nahrungsinhaltsstoffe wie Flavonoide oder Tryptophan-Metabolite oder aber mikrobielle Faktoren der Darmflora hin. Zusätzlich konnte in den Reporter-Mäusen eine starke Expression des AhRR in $CD4^+$ und $CD8^+$ T-Zellen der LP und in $CD8^+$ T-Zellen der PP nachgewiesen werden, während weder in der Milz, noch in LK Expression des AhRR in T-Zellen detektierbar war. Weder in Leber, noch in Lunge konnte eine Expression des AhRR beobachtet werden. Insgesamt kann man zusammenfassen, dass der AhR und der AhRR in den untersuchten Zelltypen weitestgehend invers exprimiert sind. Das Zelltyp-spezifische Muster der AhR/AhRR-Expression im Darm, deutet auf eine mögliche Funktion des AhR in der Regulation von Immunantworten gegen luminale Antigene hin. So wurde bereits eine Rolle für das AhR/AhRR-System in der Regulation angeborener Immunmechanismen beschrieben. AhR-defiziente Mäuse zeigen eine Hypersensitivität gegenüber LPS-induzierter Sepsis. Dies könnte darauf zurückzuführen sein, dass Knochenmark-abgeleitete Makrophagen aus AhR-defizienten Mäusen erhöhte

Mengen von pro-inflammatorischen Zytokinen wie IL-1β nach LPS-Stimulation produzieren (112). Auch führt die Aktivierung des AhR in T-Zellen abhängig von der Art des Liganden entweder zu einer verstärkten Differenzierung von Th_{17}-Zellen oder zu einer Induktion von Treg-Zellen und kann so entweder proinflammtorisch oder regulatorisch auf die Pathogenese von Autoimmunerkrankungen wirken (113). Zusätzlich wurde eine Rolle für den AhR/AhRR-Signalweg in der Modulation des Gleichgewichts zwischen Th_1- und Th_2-Immunantworten beschrieben (114). Einen weiteren Hinweis auf eine Funktion des AhR/AhRR-Systems in der Regulation des Immunsystems bietet unser Ergebnis, dass sowohl *in vitro*, als auch *in vivo* die Stimulation mit TLR-Liganden zu einer Heraufregulierung des AhRR in DC führte. Dieses Ergebnis deutet auf eine Rolle des AhRR in der frühen Phase der Induktion von Immunantworten in Zellen des angeborenen Immunsystems hin. Des Weiteren konnten wir zeigen, dass die Aktivierung des AhR mit TCDD zu einer Störung der oralen Toleranzinduktion gegen OVA führte. Dieser Effekt war assoziiert mit einer erhöhten Frequenz von IL-6 produzierenden DC und von Th_{17}-Zellen in den mLK. Das Ergebnis ist von größtem Interesse, da möglicherweise auch AhR-Liganden aus der Nahrung zu einer Störung der Induktion von Toleranz gegenüber Umweltantigenen führen und so zur Entstehung von CED beitragen könnten. In zukünftigen Studien sollte daher der Effekt von weiteren Liganden des AhR aus der Nahrung auf die Toleranzinduktion gegen orale Antigene, untersucht werden. Auch muss die Rolle des AhR/AhRR Systems bei der Aufrechterhaltung der Homöostase des Darms, sowie bei der Entstehung von CED und bei Infektionen analysiert werden. Besonders wichtig ist hierbei die Evaluation von AhR-Agonisten wie z.B. Flavonoiden, die bereits in hohen Dosen in Tablettenform zur Supplementierung der Ernährung erhältlich sind.

3.3. Regulation von SeP in der Pathogenese von CED

Oxidativer Stress spielt eine wichtige Rolle in der Pathogenese von CED (115), wobei oxidative Gewebeschäden im Darm von CED Patienten auf einer erhöhten Produktion von ROS und RNS, sowie einer Störung antioxidativer Mechanismen beruhen (116). Als wichtigste Quelle von NO wurden in Patienten mit CED, sowie in Tiermodellen, intestinale Epithelzellen identifiziert, in denen die Expression von iNOS hochreguliert war (117; 118). Als Konsequenz einer erhöhten Produktion reaktiver Metabolite, akkumulieren im Verlauf von CED DNA-Mutationen in Colon-Epithelzellen, die zur Entstehung von Darmkrebs führen können. Zur Beschränkung von ROS- und RNS-induzierten Gewebe- und DNA-Schäden, verfügt der Organismus über antioxidative Mechanismen, die oftmals abhängig von Mikro-

Nährstoffen, wie z.B. Vitamin C, Flavonoiden und Selen, sind (119). Die antioxidativen Eigenschaften von Selen beruhen vor allem auf Selenoproteinen wie dem SeP, die als Oxidoreduktasen ein Selonocystein im katalytischen Zentrum aufweisen. Um die Regulation von SeP in Epithelzellen des Darms zu untersuchen, wurde die Expression der RNA in Caco-2 Zellen im Verlauf der Differenzierung analysiert. Es konnte erstmals gezeigt werden, dass die Transkription von SeP in Caco-2 Zellen durch den Transkriptionsfaktor HNF-4α induziert wird. HNF-4α wird vor allem in der Leber, im Darm und in den β-Zellen des Pankreas exprimiert und trägt bekanntermaßen zur Expression von SeP in Hepatozyten bei. In CED wurde bereits eine dysregulierte Transkription von HNF-4α beschrieben (120), wobei der schädigende Effekt einer verringerten Transkription von HNF-4α vor allem auf eine reduzierte Expression von SeP zurückzuführen war, wie auch in der hier diskutierten Studie gezeigt werden konnte. Als weiterer Transkriptionsfaktor, der zur Expression von SeP in Caco-2 Zellen beiträgt, wurde der Transkriptionsfaktor Foxo1a in der vorliegenden Studie identifiziert. Analog zur verringerten Expression von HNF-4α, zeigen Foxo3- (ein Foxo1a-Homolog) und Foxo4-defiziente Mäuse verstärkte Gewebeschäden und Entzündung in experimenteller Colitis. In Übereinstimmung hiermit weisen auch Patienten mit UC eine reduzierte Expression von Foxo4 auf (121; 122). SeP scheint die Funktion zuzukommen, extrazelluläre Proteine und Zellmembranen gegen Oxidation zu schützen (123). Auch wurde beschrieben, dass SeP mit Endothelzellen in einer pH-abhängigen Weise assoziiert und so möglicherweise zum Schutz der Zelle vor oxidativen Schäden beiträgt (124). Wir stellen die Hypothese auf, dass SeP von intestinalen Epithelzellen in das Darmlumen sekretiert wird, wo es aufgrund eines geringeren pH-Wertes immobilisiert wird und zum Schutz der gastrointestinalen Mukosa beiträgt.

Es ist bekannt, dass Stimulation mit proinflammatorischen Zytokinen zu einer Reduktion der SeP-Transkription in der Leber-Zelllinie HepG2 führt (125), was auf eine Reduktion der SeP-Sekretion in der Leber während einer systemischen Entzündungsreaktion hindeutet. In Übereinstimmung hiermit ist auch die Menge an SeP im Plasma von Patienten mit einem septischen Schock und in LPS-stimulierten Mäusen reduziert (126; 127), was möglicherweise auf die Bindung von SeP an Endothelzellen, oder auf eine verringerte SeP-Biosynthese in der Leber zurückzuführen ist.

In der hier diskutierten Studie wurde sowohl in Patienten mit UC, als auch in experimenteller Colitis im Mausmodell eine reduzierte Expression von SeP in Darmgewebe, einhergehend mit einer verstärkten Expression von iNOS gefunden. Bekanntermaßen ist die Expression von iNOS im Gewebe von CED-Patienten heraufreguliert und scheint eine zentrale Funktion in der Progression der Erkrankung auszuüben (128). Stimulation von Caco-2 Zellen mit pro-inflammatorischen Zytokinen, resultierte in einer Induktion der Transkription von iNOS

zusammen mit einer Inhibition der SeP-Expression, was anhand einer herabgesetzten Aktivität des SeP Promotors verifiziert werden konnte. Die reduzierte Transkription von SeP war teilweise abhängig von iNOS, was mit Hilfe von iNOS-Inhibitoren nachgewiesen werden konnte. Diese Konstellation der invers regulierten Expression von SeP und iNOS ist ebenfalls für Tumore der Prostata beschrieben und deutet auf eine Bedeutung oxidativer Metabolite bei der Kanzerogenese in diesem Organ hin (129). Die Untersuchung der Rolle von SeP im Darm, könnte zu einem verbesserten Verständnis der grundlegenden Ereignisse in der Entwicklung von CED und Colitis-assoziierter Kanzerogenese führen und den Weg für neue Therapieansätze ebnen.

4. Referenzliste

1. Shi HN, Walker A. Bacterial colonization and the development of intestinal defences. Can J Gastroenterol 2004;18:493-500.

2. Kelly D, Conway S, Aminov R. Commensal gut bacteria: mechanisms of immune modulation. Trends Immunol 2005;26:326-333.

3. Newberry RD, Lorenz RG. Organizing a mucosal defense. Immunol Rev 2005;206:6-21.

4. Garrett WS, Gordon JI, Glimcher LH. Homeostasis and inflammation in the intestine. Cell 2010;140:859-870.

5. Brandtzaeg P. Mucosal immunity: induction, dissemination, and effector functions. Scand J Immunol 2009;70:505-515.

6. Tsuji NM, Mizumachi K, Kurisaki J. Interleukin-10-secreting Peyer's patch cells are responsible for active suppression in low-dose oral tolerance. Immunology 2001;103:458-464.

7. Nagata S, McKenzie C, Pender SL, Bajaj-Elliott M, Fairclough PD, Walker-Smith JA, Monteleone G, MacDonald TT. Human Peyer's patch T cells are sensitized to dietary antigen and display a Th cell type 1 cytokine profile. J Immunol 2000;165:5315-5321.

8. Eberl G, Sawa S. Opening the crypt: current facts and hypotheses on the function of cryptopatches. Trends Immunol 2010;31:50-55.

9. Rocha B. The extrathymic T-cell differentiation in the murine gut. Immunol Rev 2007;215:166-177.

10. Hamada H, Hiroi T, Nishiyama Y, Takahashi H, Masunaga Y, Hachimura S, Kaminogawa S, Takahashi-Iwanaga H, Iwanaga T, Kiyono H, Yamamoto H, Ishikawa H. Identification of multiple isolated lymphoid follicles on the antimesenteric wall of the mouse small intestine. J Immunol 2002;168:57-64.

11. Yeung MM, Melgar S, Baranov V, Oberg A, Danielsson A, Hammarstrom S, Hammarstrom ML. Characterisation of mucosal lymphoid aggregates in ulcerative colitis: immune cell phenotype and TcR-gammadelta expression. Gut 2000;47:215-227.

12. Kunkel D, Kirchhoff D, Nishikawa S, Radbruch A, Scheffold A. Visualization of peptide presentation following oral application of antigen in normal and Peyer's patches-deficient mice. Eur J Immunol 2003;33:1292-1301.

13. Macpherson AJ, Uhr T. Induction of protective IgA by intestinal dendritic cells carrying commensal bacteria. Science 2004;303:1662-1665.

14. Steinman RM. Dendritic cells: understanding immunogenicity. Eur J Immunol 2007;37 Suppl 1:S53-S60.

15. Bluestone JA, Mackay CR, O'Shea JJ, Stockinger B. The functional plasticity of T cell subsets. Nat Rev Immunol 2009;9:811-816.

16. Rimoldi M, Chieppa M, Salucci V, Avogadri F, Sonzogni A, Sampietro GM, Nespoli A, Viale G, Allavena P, Rescigno M. Intestinal immune homeostasis is regulated by the crosstalk between epithelial cells and dendritic cells. Nat Immunol 2005;6:507-514.

17. Bogunovic M, Ginhoux F, Helft J, Shang L, Hashimoto D, Greter M, Liu K, Jakubzick C, Ingersoll MA, Leboeuf M, Stanley ER, Nussenzweig M, Lira SA, Randolph GJ, Merad M. Origin of the lamina propria dendritic cell network. Immunity 2009;31:513-525.

18. Varol C, Vallon-Eberhard A, Elinav E, Aychek T, Shapira Y, Luche H, Fehling HJ, Hardt WD, Shakhar G, Jung S. Intestinal lamina propria dendritic cell subsets have different origin and functions. Immunity 2009;31:502-512.

19. Matteoli G, Mazzini E, Iliev ID, Mileti E, Fallarino F, Puccetti P, Chieppa M, Rescigno M. Gut CD103+ dendritic cells express indoleamine 2,3-dioxygenase which influences T regulatory/T effector cell balance and oral tolerance induction. Gut 2010;59:595-604.

20. Sun CM, Hall JA, Blank RB, Bouladoux N, Oukka M, Mora JR, Belkaid Y. Small intestine lamina propria dendritic cells promote de novo generation of Foxp3 T reg cells via retinoic acid. J Exp Med 2007;204:1775-1785.

21. Uematsu S, Fujimoto K, Jang MH, Yang BG, Jung YJ, Nishiyama M, Sato S, Tsujimura T, Yamamoto M, Yokota Y, Kiyono H, Miyasaka M, Ishii KJ, Akira S. Regulation of humoral and cellular gut immunity by lamina propria dendritic cells expressing Toll-like receptor 5. Nat Immunol 2008;9:769-776.

22. Atarashi K, Nishimura J, Shima T, Umesaki Y, Yamamoto M, Onoue M, Yagita H, Ishii N, Evans R, Honda K, Takeda K. ATP drives lamina propria T(H)17 cell differentiation. Nature 2008;455:808-812.

23. Rescigno M, Urbano M, Valzasina B, Francolini M, Rotta G, Bonasio R, Granucci F, Kraehenbuhl JP, Ricciardi-Castagnoli P. Dendritic cells express tight junction proteins and penetrate gut epithelial monolayers to sample bacteria. Nat Immunol 2001;2:361-367.

24. Schulz O, Jaensson E, Persson EK, Liu X, Worbs T, Agace WW, Pabst O. Intestinal CD103+, but not CX3CR1+, antigen sampling cells migrate in lymph and serve classical dendritic cell functions. J Exp Med 2009;206:3101-3114.

25. Akira S, Takeda K, Kaisho T. Toll-like receptors: critical proteins linking innate and acquired immunity. Nat Immunol 2001;2:675-680.

26. Kaisho T, Akira S. Toll-like receptor function and signaling. J Allergy Clin Immunol 2006;117:979-987.

27. Vignal C, Singer E, Peyrin-Biroulet L, Desreumaux P, Chamaillard M. How NOD2 mutations predispose to Crohn's disease? Microbes Infect 2007;9:658-663.

28. Schroder K, Tschopp J. The inflammasomes. Cell 2010;140:821-832.

29. Sirard JC, Vignal C, Dessein R, Chamaillard M. Nod-like receptors: cytosolic watchdogs for immunity against pathogens. PLoS Pathog 2007;3:e152.

30. Pelegrin P, Surprenant A. Pannexin-1 mediates large pore formation and interleukin-1beta release by the ATP-gated P2X7 receptor. EMBO J 2006;25:5071-5082.

31. Petrilli V, Papin S, Dostert C, Mayor A, Martinon F, Tschopp J. Activation of the NALP3 inflammasome is triggered by low intracellular potassium concentration. Cell Death Differ 2007;14:1583-1589.

32. Kool M, Petrilli V, De Smedt T, Rolaz A, Hammad H, van Nimwegen M, Bergen IM, Castillo R, Lambrecht BN, Tschopp J. Cutting edge: alum adjuvant stimulates inflammatory dendritic cells through activation of the NALP3 inflammasome. J Immunol 2008;181:3755-3759.

33. Cronstein BN, Terkeltaub R. The inflammatory process of gout and its treatment. Arthritis Res Ther 2006;8 Suppl 1:S3.

34. Eisenbarth SC, Colegio OR, O'Connor W, Sutterwala FS, Flavell RA. Crucial role for the Nalp3 inflammasome in the immunostimulatory properties of aluminium adjuvants. Nature 2008;453:1122-1126.

35. Li H, Willingham SB, Ting JP, Re F. Cutting edge: inflammasome activation by alum and alum's adjuvant effect are mediated by NLRP3. J Immunol 2008;181:17-21.

36. Cassel SL, Eisenbarth SC, Iyer SS, Sadler JJ, Colegio OR, Tephly LA, Carter AB, Rothman PB, Flavell RA, Sutterwala FS. The Nalp3 inflammasome is essential for the development of silicosis. Proc Natl Acad Sci U S A 2008;105:9035-9040.

37. Dostert C, Petrilli V, Van Bruggen R, Steele C, Mossman BT, Tschopp J. Innate immune activation through Nalp3 inflammasome sensing of asbestos and silica. Science 2008;320:674-677.

38. Hornung V, Bauernfeind F, Halle A, Samstad EO, Kono H, Rock KL, Fitzgerald KA, Latz E. Silica crystals and aluminum salts activate the NALP3 inflammasome through phagosomal destabilization. Nat Immunol 2008;9:847-856.

39. Dementó SL, Eisenbarth SC, Foellmer HG, Platt C, Caplan MJ, Mark SW, Mellman I, Ledizet M, Fikrig E, Flavell RA, Fahmy TM. Inflammasome-activating nanoparticles as modular systems for optimizing vaccine efficacy. Vaccine 2009;27:3013-3021.

40. Tschopp J, Schroder K. NLRP3 inflammasome activation: The convergence of multiple signalling pathways on ROS production? Nat Rev Immunol 2010;10:210-215.

41. Ferwerda G, Kramer M, de Jong D, Piccini A, Joosten LA, Devesaginer I, Girardin SE, Adema GJ, van der Meer JW, Kullberg BJ, Rubartelli A, Netea MG. Engagement of NOD2 has a dual effect on proIL-1beta mRNA transcription and secretion of bioactive IL-1beta. Eur J Immunol 2008;38:184-191.

42. Beischlag TV, Perdew GH. ER alpha-AHR-ARNT protein-protein interactions mediate estradiol-dependent transrepression of dioxin-inducible gene transcription. J Biol Chem 2005;280:21607-21611.

43. Beischlag TV, Luis MJ, Hollingshead BD, Perdew GH. The aryl hydrocarbon receptor complex and the control of gene expression. Crit Rev Eukaryot Gene Expr 2008;18:207-250.

44. Baba T, Mimura J, Gradin K, Kuroiwa A, Watanabe T, Matsuda Y, Inazawa J, Sogawa K, Fujii-Kuriyama Y. Structure and expression of the Ah receptor repressor gene. J Biol Chem 2001;276:33101-33110.

45. Moon YJ, Wang X, Morris ME. Dietary flavonoids: effects on xenobiotic and carcinogen metabolism. Toxicol In Vitro 2006;20:187-210.

46. McMillan BJ, Bradfield CA. The aryl hydrocarbon receptor is activated by modified low-density lipoprotein. Proc Natl Acad Sci U S A 2007;104:1412-1417.

47. Oberg M, Bergander L, Hakansson H, Rannug U, Rannug A. Identification of the tryptophan photoproduct 6-formylindolo[3,2-b]carbazole, in cell culture medium, as a factor that controls the background aryl hydrocarbon receptor activity. Toxicol Sci 2005;85:935-943.

48. Oesch-Bartlomowicz B, Oesch F. Role of cAMP in mediating AHR signaling. Biochem Pharmacol 2009;77:627-641.

49. Wincent E, Amini N, Luecke S, Glatt H, Bergman J, Crescenzi C, Rannug A, Rannug U. The suggested physiologic aryl hydrocarbon receptor activator and cytochrome P4501 substrate 6-formylindolo[3,2-b]carbazole is present in humans. J Biol Chem 2009;284:2690-2696.

50. Kerkvliet NI. Recent advances in understanding the mechanisms of TCDD immunotoxicity. Int Immunopharmacol 2002;2:277-291.

51. Esser C, Rannug A, Stockinger B. The aryl hydrocarbon receptor in immunity. Trends Immunol 2009;30:447-454.

52. Veldhoen M, Hirota K, Christensen J, O'Garra A, Stockinger B. Natural agonists for aryl hydrocarbon receptor in culture medium are essential for optimal differentiation of Th17 T cells. J Exp Med 2009;206:43-49.

53. Becher B, Bechmann I, Greter M. Antigen presentation in autoimmunity and CNS inflammation: how T lymphocytes recognize the brain. J Mol Med 2006;84:532-543.

54. Baumgart DC, Carding SR. Inflammatory bowel disease: cause and immunobiology. Lancet 2007;369:1627-1640.

55. Xie J, Itzkowitz SH. Cancer in inflammatory bowel disease. World J Gastroenterol 2008;14:378-389.

56. Okada H, Kuhn C, Feillet H, Bach JF. The 'hygiene hypothesis' for autoimmune and allergic diseases: an update. Clin Exp Immunol 2010;160:1-9.

57. Farmer MA, Sundberg JP, Bristol IJ, Churchill GA, Li R, Elson CO, Leiter EH. A major quantitative trait locus on chromosome 3 controls colitis severity in IL-10-deficient mice. Proc Natl Acad Sci U S A 2001;98:13820-13825.

58. Takeda K, Clausen BE, Kaisho T, Tsujimura T, Terada N, Forster I, Akira S. Enhanced Th1 activity and development of chronic enterocolitis in mice devoid of Stat3 in macrophages and neutrophils. Immunity 1999;10:39-49.

59. Sollid LM, Johansen FE. Animal models of inflammatory bowel disease at the dawn of the new genetics era. PLoS Med 2008;5:e198.

60. Westendorf AM, Templin M, Geffers R, Deppenmeier S, Gruber AD, Probst-Kepper M, Hansen W, Liblau RS, Gunzer F, Bruder D, Buer J. CD4+ T cell mediated intestinal immunity: chronic inflammation versus immune regulation. Gut 2005;54:60-69.

61. Westendorf AM, Fleissner D, Deppenmeier S, Gruber AD, Bruder D, Hansen W, Liblau R, Buer J. Autoimmune-mediated intestinal inflammation-impact and regulation of antigen-specific CD8+ T cells. Gastroenterology 2006;131:510-524.

62. Morgan DJ, Liblau R, Scott B, Fleck S, McDevitt HO, Sarvetnick N, Lo D, Sherman LA. CD8(+) T cell-mediated spontaneous diabetes in neonatal mice. J Immunol 1996;157:978-983.

63. Okayasu I, Hatakeyama S, Yamada M, Ohkusa T, Inagaki Y, Nakaya R. A novel method in the induction of reliable experimental acute and chronic ulcerative colitis in mice. Gastroenterology 1990;98:694-702.

64. Axelsson LG, Landstrom E, Goldschmidt TJ, Gronberg A, Bylund-Fellenius AC. Dextran sulfate sodium (DSS) induced experimental colitis in immunodeficient mice: effects in CD4(+) -cell depleted, athymic and NK-cell depleted SCID mice. Inflamm Res 1996;45:181-191.

65. Abe K, Nguyen KP, Fine SD, Mo JH, Shen C, Shenouda S, Corr M, Jung S, Lee J, Eckmann L, Raz E. Conventional dendritic cells regulate the outcome of colonic inflammation independently of T cells. Proc Natl Acad Sci U S A 2007;104:17022-17027.

66. Sarra M, Pallone F, MacDonald TT, Monteleone G. IL-23/IL-17 axis in IBD. Inflamm Bowel Dis 2010.

67. Sakuraba A, Sato T, Kamada N, Kitazume M, Sugita A, Hibi T. Th1/Th17 immune response is induced by mesenteric lymph node dendritic cells in Crohn's disease. Gastroenterology 2009;137:1736-1745.

68. Becker C, Wirtz S, Blessing M, Pirhonen J, Strand D, Bechthold O, Frick J, Galle PR, Autenrieth I, Neurath MF. Constitutive p40 promoter activation and IL-23 production in the terminal ileum mediated by dendritic cells. J Clin Invest 2003;112:693-706.

69. Amre DK, Mack DR, Morgan K, Krupoves A, Costea I, Lambrette P, Grimard G, Dong J, Feguery H, Bucionis V, Deslandres C, Levy E, Seidman EG. Autophagy gene ATG16L1 but not IRGM is associated with Crohn's disease in Canadian children. Inflamm Bowel Dis 2009;15:501-507.

70. Saitoh T, Fujita N, Jang MH, Uematsu S, Yang BG, Satoh T, Omori H, Noda T, Yamamoto N, Komatsu M, Tanaka K, Kawai T, Tsujimura T, Takeuchi O, Yoshimori T, Akira S. Loss of the autophagy protein Atg16L1 enhances endotoxin-induced IL-1beta production. Nature 2008;456:264-268.

71. Souza HS, Elia CC, Spencer J, MacDonald TT. Expression of lymphocyte-endothelial receptor-ligand pairs, alpha4beta7/MAdCAM-1 and OX40/OX40 ligand in the colon and jejunum of patients with inflammatory bowel disease. Gut 1999;45:856-863.

72. Niess JH. Role of mucosal dendritic cells in inflammatory bowel disease. World J Gastroenterol 2008;14:5138-5148.

73. de Baey A, Mende I, Baretton G, Greiner A, Hartl WH, Baeuerle PA, Diepolder HM. A subset of human dendritic cells in the T cell area of mucosa-associated lymphoid tissue with a high potential to produce TNF-alpha. J Immunol 2003;170:5089-5094.

74. Oberdorster G, Oberdorster E, Oberdorster J. Nanotoxicology: an emerging discipline evolving from studies of ultrafine particles. Environ Health Perspect 2005;113:823-839.

75. Fu G, Vary PS, Lin CT. Anatase TiO2 nanocomposites for antimicrobial coatings. J Phys Chem B 2005;109:8889-8898.

76. Oberdorster G, Ferin J, Lehnert BE. Correlation between particle size, in vivo particle persistence, and lung injury. Environ Health Perspect 1994;102 Suppl 5:173-179.

77. Tauler J, Mulshine JL. Lung cancer and inflammation: interaction of chemokines and hnRNPs. Curr Opin Pharmacol 2009;9:384-388.

78. Hamilton RF, Jr., Thakur SA, Holian A. Silica binding and toxicity in alveolar macrophages. Free Radic Biol Med 2008;44:1246-1258.

79. Merget R, Bauer T, Kupper HU, Philippou S, Bauer HD, Breitstadt R, Bruening T. Health hazards due to the inhalation of amorphous silica. Arch Toxicol 2002;75:625-634.

80. Cho WS, Choi M, Han BS, Cho M, Oh J, Park K, Kim SJ, Kim SH, Jeong J. Inflammatory mediators induced by intratracheal instillation of ultrafine amorphous silica particles. Toxicol Lett 2007;175:24-33.

81. Choi M, Cho WS, Han BS, Cho M, Kim SY, Yi JY, Ahn B, Kim SH, Jeong J. Transient pulmonary fibrogenic effect induced by intratracheal instillation of ultrafine amorphous silica in A/J mice. Toxicol Lett 2008;182:97-101.

82. Sager TM, Kommineni C, Castranova V. Pulmonary response to intratracheal instillation of ultrafine versus fine titanium dioxide: role of particle surface area. Part Fibre Toxicol 2008;5:17.

83. Knaapen AM, Borm PJ, Albrecht C, Schins RP. Inhaled particles and lung cancer. Part A: Mechanisms. Int J Cancer 2004;109:799-809.

84. de Haar C, Hassing I, Bol M, Bleumink R, Pieters R. Ultrafine but not fine particulate matter causes airway inflammation and allergic airway sensitization to co-administered antigen in mice. Clin Exp Allergy 2006;36:1469-1479.

85. Hillyer JF, Albrecht RM. Gastrointestinal persorption and tissue distribution of differently sized colloidal gold nanoparticles. J Pharm Sci 2001;90:1927-1936.

86. Lomer MC, Thompson RP, Powell JJ. Fine and ultrafine particles of the diet: influence on the mucosal immune response and association with Crohn's disease. Proc Nutr Soc 2002;61:123-130.

87. Powell JJ, Harvey RS, Ashwood P, Wolstencroft R, Gershwin ME, Thompson RP. Immune potentiation of ultrafine dietary particles in normal subjects and patients with inflammatory bowel disease. J Autoimmun 2000;14:99-105.

88. Trouiller B, Reliene R, Westbrook A, Solaimani P, Schiestl RH. Titanium dioxide nanoparticles induce DNA damage and genetic instability in vivo in mice. Cancer Res 2009;69:8784-8789.

89. Gerloff K, Albrecht C, Boots AW, Förster I, Schins RPF. Cytotoxicity and oxidative DNA damage by nanoparticles in human intestinal Caco-2 cells. Nanotoxicology 2009;3:355-364.

90. Chaudhry Q, Scotter M, Blackburn J, Ross B, Boxall A, Castle L, Aitken R, Watkins R. Applications and implications of nanotechnologies for the food sector. Food Addit Contam Part A Chem Anal Control Expo Risk Assess 2008;25:241-258.

91. Prescott SL. Role of dietary immunomodulatory factors in the development of immune tolerance. Nestle Nutr Workshop Ser Pediatr Program 2009;64:185-194.

92. Lomer MC, Harvey RS, Evans SM, Thompson RP, Powell JJ. Efficacy and tolerability of a low microparticle diet in a double blind, randomized, pilot study in Crohn's disease. Eur J Gastroenterol Hepatol 2001;13:101-106.

93. Lomer MC, Grainger SL, Ede R, Catterall AP, Greenfield SM, Cowan RE, Vicary FR, Jenkins AP, Fidler H, Harvey RS, Ellis R, McNair A, Ainley CC, Thompson RP, Powell JJ. Lack of efficacy of a reduced microparticle diet in a multi-centred trial of patients with active Crohn's disease. Eur J Gastroenterol Hepatol 2005;17:377-384.

94. Lamprecht A, Schafer U, Lehr CM. Size-dependent bioadhesion of micro- and nanoparticulate carriers to the inflamed colonic mucosa. Pharm Res 2001;18:788-793.

95. Lamprecht A, Yamamoto H, Takeuchi H, Kawashima Y. Nanoparticles enhance therapeutic efficiency by selectively increased local drug dose in experimental colitis in rats. J Pharmacol Exp Ther 2005;315:196-202.

96. Bauer C, Duewell P, Mayer C, Lehr HA, Fitzgerald KA, Dauer M, Tschopp J, Endres S, Latz E, Schnurr M. Colitis induced in mice with dextran sulfate sodium (DSS) is mediated by the NLRP3 inflammasome. Gut 2010.

97. Siegmund B. Interleukin-1beta converting enzyme (caspase-1) in intestinal inflammation. Biochem Pharmacol 2002;64:1-8.

98. Park EJ, Park K. Oxidative stress and pro-inflammatory responses induced by silica nanoparticles in vivo and in vitro. Toxicol Lett 2009;184:18-25.

99. Nishiyama T, Mitsuyama K, Toyonaga A, Sasaki E, Tanikawa K. Colonic mucosal interleukin 1 receptor antagonist in inflammatory bowel disease. Digestion 1994;55:368-373.

100. Olson AD, Ayass M, Chensue S. Tumor necrosis factor and IL-1 beta expression in pediatric patients with inflammatory bowel disease. J Pediatr Gastroenterol Nutr 1993;16:241-246.

101. Allen IC, TeKippe EM, Woodford RM, Uronis JM, Holl EK, Rogers AB, Herfarth HH, Jobin C, Ting JP. The NLRP3 inflammasome functions as a negative regulator of tumorigenesis during colitis-associated cancer. J Exp Med 2010;207:1045-1056.

102. Zaki MH, Boyd KL, Vogel P, Kastan MB, Lamkanfi M, Kanneganti TD. The NLRP3 inflammasome protects against loss of epithelial integrity and mortality during experimental colitis. Immunity 2010;32:379-391.

103. Cominelli F, Nast CC, Llerena R, Dinarello CA, Zipser RD. Interleukin 1 suppresses inflammation in rabbit colitis. Mediation by endogenous prostaglandins. J Clin Invest 1990;85:582-586.

104. Bunt SK, Sinha P, Clements VK, Leips J, Ostrand-Rosenberg S. Inflammation induces myeloid-derived suppressor cells that facilitate tumor progression. J Immunol 2006;176:284-290.

105. Song X, Krelin Y, Dvorkin T, Bjorkdahl O, Segal S, Dinarello CA, Voronov E, Apte RN. CD11b+/Gr-1+ immature myeloid cells mediate suppression of T cells in mice bearing tumors of IL-1beta-secreting cells. J Immunol 2005;175:8200-8208.

106. Apte RN, Voronov E. Interleukin-1--a major pleiotropic cytokine in tumor-host interactions. Semin Cancer Biol 2002;12:277-290.

107. Liu X, Wang Z, Yu J, Lei G, Wang S. Three polymorphisms in interleukin-1beta gene and risk for breast cancer: a meta-analysis. Breast Cancer Res Treat 2010.

108. Haile LA, von Wasielewski R, Gamrekelashvili J, Kruger C, Bachmann O, Westendorf AM, Buer J, Liblau R, Manns MP, Korangy F, Greten TF. Myeloid-derived suppressor cells in inflammatory bowel disease: a new immunoregulatory pathway. Gastroenterology 2008;135:871-81, 881.

109. Modi G, Pillay V, Choonara YE. Advances in the treatment of neurodegenerative disorders employing nanotechnology. Ann N Y Acad Sci 2010;1184:154-172.

110. Oberdorster G, Elder A, Rinderknecht A. Nanoparticles and the brain: cause for concern? J Nanosci Nanotechnol 2009;9:4996-5007.

111. Vos JG, Moore JA, Zinkl JG. Effect of 2,3,7,8-tetrachlorodibenzo-p-dioxin on the immune system of laboratory animals. Environ Health Perspect 1973;5:149-162.

112. Sekine H, Mimura J, Oshima M, Okawa H, Kanno J, Igarashi K, Gonzalez FJ, Ikuta T, Kawajiri K, Fujii-Kuriyama Y. Hypersensitivity of aryl hydrocarbon receptor-deficient mice to lipopolysaccharide-induced septic shock. Mol Cell Biol 2009;29:6391-6400.

113. Quintana FJ, Basso AS, Iglesias AH, Korn T, Farez MF, Bettelli E, Caccamo M, Oukka M, Weiner HL. Control of T(reg) and T(H)17 cell differentiation by the aryl hydrocarbon receptor. Nature 2008;453:65-71.

114. Negishi T, Kato Y, Ooneda O, Mimura J, Takada T, Mochizuki H, Yamamoto M, Fujii-Kuriyama Y, Furusako S. Effects of aryl hydrocarbon receptor signaling on the modulation of TH1/TH2 balance. J Immunol 2005;175:7348-7356.

115. Grisham MB. Oxidants and free radicals in inflammatory bowel disease. Lancet 1994;344:859-861.

116. Kruidenier L, Kuiper I, Lamers CB, Verspaget HW. Intestinal oxidative damage in inflammatory bowel disease: semi-quantification, localization, and association with mucosal antioxidants. J Pathol 2003;201:28-36.

117. Singer II, Kawka DW, Scott S, Weidner JR, Mumford RA, Riehl TE, Stenson WF. Expression of inducible nitric oxide synthase and nitrotyrosine in colonic epithelium in inflammatory bowel disease. Gastroenterology 1996;111:871-885.

118. Tepperman BL, Brown JF, Whittle BJ. Nitric oxide synthase induction and intestinal epithelial cell viability in rats. Am J Physiol 1993;265:G214-G218.

119. Sies H. Strategies of antioxidant defense. Eur J Biochem 1993;215:213-219.

120. Ahn SH, Shah YM, Inoue J, Morimura K, Kim I, Yim S, Lambert G, Kurotani R, Nagashima K, Gonzalez FJ, Inoue Y. Hepatocyte nuclear factor 4alpha in the intestinal epithelial cells protects against inflammatory bowel disease. Inflamm Bowel Dis 2008;14:908-920.

121. Snoeks L, Weber CR, Wasland K, Turner JR, Vainder C, Qi W, Savkovic SD. Tumor suppressor FOXO3 participates in the regulation of intestinal inflammation. Lab Invest 2009;89:1053-1062.

122. Zhou W, Cao Q, Peng Y, Zhang QJ, Castrillon DH, DePinho RA, Liu ZP. FoxO4 inhibits NF-kappaB and protects mice against colonic injury and inflammation. Gastroenterology 2009;137:1403-1414.

123. Saito Y, Hayashi T, Tanaka A, Watanabe Y, Suzuki M, Saito E, Takahashi K. Selenoprotein P in human plasma as an extracellular phospholipid hydroperoxide glutathione peroxidase. Isolation and enzymatic characterization of human selenoprotein p. J Biol Chem 1999;274:2866-2871.

124. Steinbrenner H, Sies H. Protection against reactive oxygen species by selenoproteins. Biochim Biophys Acta 2009;1790:1478-1485.

125. Dreher I, Jakobs TC, Kohrle J. Cloning and characterization of the human selenoprotein P promoter. Response of selenoprotein P expression to cytokines in liver cells. J Biol Chem 1997;272:29364-29371.

126. Forceville X, Mostert V, Pierantoni A, Vitoux D, Le Toumelin P, Plouvier E, Dehoux M, Thuillier F, Combes A. Selenoprotein P, rather than glutathione peroxidase, as a potential marker of septic shock and related syndromes. Eur Surg Res 2009;43:338-347.

127. Renko K, Hofmann PJ, Stoedter M, Hollenbach B, Behrends T, Kohrle J, Schweizer U, Schomburg L. Down-regulation of the hepatic selenoprotein biosynthesis machinery impairs selenium metabolism during the acute phase response in mice. FASEB J 2009;23:1758-1765.

128. Rachmilewitz D, Stamler JS, Bachwich D, Karmeli F, Ackerman Z, Podolsky DK. Enhanced colonic nitric oxide generation and nitric oxide synthase activity in ulcerative colitis and Crohn's disease. Gut 1995;36:718-723.

129. Klotz T, Bloch W, Volberg C, Engelmann U, Addicks K. Selective expression of inducible nitric oxide synthase in human prostate carcinoma. Cancer 1998;82:1897-1903.

5. Manuskripte

Im Folgenden sind die, in dieser Arbeit diskutierten Manuskripte der Autorin angehängt.

Amorphous SiO_2 nanoparticles exacerbate symptoms in murine models of inflammatory bowel disease

Meike Winter, Katrin Schumann, Hans-Anton Lehr, Kirsten Gerloff, Jan Buer, Astrid M Westendorf* and Irmgard Förster*
*equal contribution

Abstract

Background: Amorphous, fumed SiO_2 nanoparticles (NP) are used as novel food supplements, although their biological effects upon oral uptake are largely unknown.

Aims: We investigated the effects of ingestion of SiO_2 NP in the context of 3 distinct murine models of inflammatory bowel disease (IBD).

Methods: Inflammation of the intestinal mucosa was induced either by adoptive transfer of HA-specific $CD8^+$ T cells into VILLIN-HA transgenic mice, or by administration of dextran sulfate sodium (DSS) to C57BL/6 mice. During treatment, mice received either SiO_2 NP-containing or placebo-chow. Subsequently, disease severity was assessed.

Results: VILLIN-HA mice, which had been induced to develop IBD in the small intestine by T cell transfer, showed a more severe mucosal inflammation, a higher production of inflammatory cytokines and an enhanced number of activated T cells, when they had received SiO_2 NP, in comparison to placebo-treated mice. In an acute model of DSS-induced colitis, SiO_2 NP-treated mice possessed reduced body-weight and enhanced inflammatory cytokine production, when compared to placebo-treated mice. Furthermore, SiO_2 NP-treatment resulted in enhanced absolute cell numbers in the mesenteric lymph nodes, with elevated levels of $Gr1^+$ cells and elevated production of inflammatory cytokines in a chronic model of DSS-induced colitis.

Conclusions: SiO_2 NP exacerbate symptoms of IBD and severely enhance mucosal inflammation in murine models of colitis. Therefore, we conclude that SiO_2 NP are not inert and need to be given further attention to estimate their potential health risk for humans.

Introduction:

Inflammatory bowel disease (IBD) is a chronic, relapsing and remitting inflammatory condition of the intestinal mucosa. The mechanisms, which cause IBD are still incompletely understood. It is known, however, that genetic predisposition, environmental factors, and symbiotic interactions with luminal commensals all contribute to the pathogenesis of this disease. The highest prevalence of Crohn's disease (CD) and ulcerative colitis (UC), the two major forms of IBD, is seen in Northern Europe and North America, whereas the incidence is lower in Southern Europe, Asia and most developing countries. This difference may be explained by ethnical differences but also by differences in food consumption, environmental factors, and hygiene standards. In developed countries, high sanitation standards might lead to an impaired maturation of the intestinal immune system due to a lack of antigen exposure, which could result in dysregulated mucosal immune responses in later life[1,2]. In addition, dietary factors like unsaturated fatty acids might participate in disease establishment[3]. Nevertheless, genetic predisposition clearly is the highest risk factor for IBD. About 35 gene loci associated with CD have been identified so far[4], with most of these genes relating to innate or adaptive immune mechanisms[5]. The best characterized genetic predisposition for IBD are mutations of the nucleotide-binding oligomerisation domain protein (NOD)2, which is encoded by *CARD15*[6,35,36]. NOD2 is a member of the nucleotide-binding domain and leucine-rich repeat-containing (NLR) family, comprising various intracellular pattern recognition receptors. It induces either activation of NF-κB or Caspase-1 upon stimulation with bacterial peptidogylycan components (PGN), resulting in expression of inflammatory cytokines[7]. There is evidence that loss of function mutations of *CARD15* result in hyperactive Toll-like receptor 2 (TLR2) mediated NF-κB signaling[8], whereas gain of function mutations of *CARD15* may result in increased IL-1β secretion via receptor interacting protein 2 (RIP2)[9]. It has been proposed that NOD2 is involved in Caspase-1 activation by interacting with NLR family, pyrin domain containing (NLRP)1 or NLRP3 in inflammasomes. In Western Countries synthetic NP with a diameter of less than 100 nm are increasingly used in industry for various applications, including paints, electronics, cosmetics and food production. Because of their small size, the physico-chemical properties of NP may differ from the same material with larger particle size. However, little is known about potential health hazards caused by NPs within the gastrointestinal tract[37]. Furthermore, it is not known exactly, how many products, containing NP are really on the market, because presently there is no obligation for declaration of these products. SiO_2 in its amorphous form is generally considered to be biologically inert and is frequently used as an anti-caking agent in spices, ketchup or sweets. In its larger, crystalline form, SiO_2 (silica) was shown to be a major activator of the NLRP3 inflammasome and to

cause silicosis in the lung following inhalation[8]. Recently, we showed that amorphous SiO_2 NP with a primary diameter of 14 nm, can activate the NLRP3 inflammasome in dendritic cells (DC) *in vitro*[10]. Additionally, it was reported, that instillation of the same SiO_2 NP induces severe inflammation in the lungs of mice, which is associated with strong IL-1β and IFN-γ production[11,12]. Since ingested NP are taken up efficiently into the gut mucosa, as was shown for gold particles with a mean diameter of 4 - 58 nm[13], we were concerned about possible adverse effects of oral uptake of SiO_2 NP in patients with an ongoing intestinal inflammation. In the present study, we therefore aimed to analyze the effects of amorphous SiO_2 NP on the pathology of IBD. We analyzed oral uptake of SiO_2 NP in 3 distinct murine models of intestinal inflammation. To evaluate the effects of SiO_2 NP on the innate arm of the intestinal immune system during inflammation, we used the well-studied dextrane sulfate sodium (DSS) model of colitis[14], which was recently shown to be strongly influenced by NLRP3 inflammasome activation[15,39-42]. Regarding adaptive immune mechanisms during IBD, we also assessed ingestion of SiO_2 NP in an autoimmune model of IBD, which is based on recognition of autoantigens on intestinal enterocytes by $CD8^+$ T cells[16].

Materials and Methods

Mice

C57BL/6 mice were originally purchased from Harlan-Winkelmann (Germany) and bred at the IUF animal facility under specific pathogen free conditions. VILLIN-HA mice express the A/PR8/34 haemagglutinin (HA) from influenza virus A under the control of the enterocyte-specific villin promoter[43]. CL4-TCR transgenic mice express an α/β-TCR that recognizes an epitope of the HA protein presented by MHC class I (the H-$2K^d$: HA512-520 complex). All mouse lines are on BALB/c background. BALB/c mice were obtained from Harlan-Winkelmann (Germany). All experiments were performed in accordance with institutional, state, and federal guidelines.

Induction of intestinal inflammation

For the induction of inflammation via adoptive transfer of autoreactive T cells, transgenic VILLIN-HA mice and non transgenic littermates were pretreated with 0.1% SiO_2 in the chow or placebo-chow (both Ssniff, Germany) for one week before starting the adoptive transfer of $CD8^+$ T cells from CL4-TCR mice and during the development of intestinal inflammation. For colitis-induction, $CD8^+$ T cells were isolated from CL4-TCR splenocytes using the MACS $CD8^+$ T cell isolation kit according to the manufacturer´s recommendations (Miltenyi Biotec,

Germany). A total of 3.5 x 10^6 HA-specific $CD8^+$ T cells were adoptively transferred intravenously into SiO_2-pretreated or nontreated VILLIN-HA transgenic mice and non transgenic littermates. Mice developed intestinal inflammation 5 days post transfer. Animals were weighted daily and monitored for rectal bleeding, diarrhea, and general signs of morbidity.

Induction of chronic and acute colitis in C57/BL6 mice was performed according to a method previously described, with some modifications[14]. In short, mice were pretreated with SiO_2- or placebo-chow for 14 days. Then chronic colitis was induced by 3 cycles of DSS-treatment. Each cycle consisted of one week of 2% (wt/vol) DSS in acidified drinking water ad libidum, while mice received normal chow, followed by two weeks with normal drinking water and SiO_2- or placebo-chow. After the last cycle, mice were sacrificed for further analysis.

For induction of acute colitis, mice were pretreated with SiO_2- or placebo-chow for 18 days. Then, colitis was induced with 2% DSS in drinking water for six days. During DSS-treatment, mice were offered normal breeding chow ad libidum. After day six, mice were left for additional two days, in which they received SiO_2- or placebo-chow and normal drinking water and were then sacrificed for further analysis.

To evaluate the severity of disease in DSS-treated mice, colon length was assessed and a clinical score according to Cooper et al. (1993), which consists of bleeding intensity, weight-loss and stool-consistency, was determined. Scores of the 3 criteria were added and divided by 3. In short, rectal bleeding was scored as 3, Hemocare$^+$ (Care diagnostica, Germany) as 2 and no bleeding was scored as 1. For weight loss, more than 20% weight loss was scored as 4, 10 - 20% as 3, 0 – 10% as 2 and no weight loss was scored as 1. For liquid stools 3 points were given. Pasty, soft stools were scored as 2 and well-formed pellets were scored as 1. After sacrificing, colons of the mice were removed and flushed with ice cold PBS. The entire colon was devided into 3 equal pieces and one half of each piece was frozen in liquid nitrogen for RNA-preparation or fixed in 4% PFA for histological analysis. Additionally, spleen weight was assessed.

Antibodies and Flow cytometry

The following antibodies were used for flow cytometry: α-CD8 (53-6.7), α-CD11b (M1/70) α-CD25 (PC61), α-CD69 (H1.2F3), α-F4/80 (BM8), α-Gr1 (RB68C5), and α-Vβ8 (F23.1). All antibodies were from BD Bioscience. Flow cytometry was performed with a LSR II instrument using the DIVA software (BD Biosciences). Single cell suspensions were prepared from spleen and mLN. Cells were counted, washed and resuspended at 1 x 10^6 cells/ml in FACS

buffer (PBS, supplemented with 2% fetal calf serum and 2mmol/l EDTA). Cells were stained for 10 minutes at 4°C, washed once in FACS buffer. Afterwards, cells were washed in FACS buffer and flow cytometry was performed.

Cytokine profile of small intestine biopsies of adoptively transferred mice

Small intestine biopsies were isolated at day 5 after transfer and cultured in medium for 6 h. Supernatants were then analyzed for cytokine secretion by Luminex technology. Staining was performed with a Procarta Cytokine assay kit (Panomics, Fremont, CA) according to the manufacturer`s recommendations. The assay was measured with a Luminex 200 instrument using the Luminex IS software (Luminex Corporation, Austin, TX).

Cell culture for proliferation and cytokine analysis of *ex vivo* cultivated cells

To analyze the proliferative capacity of lymphocytes from MLN and spleen, single-cell suspensions were prepared from SiO_2 pre-treated and non-treated VILLIN-HA transgenic mice and non transgenic littermates 5 days after adoptive transfer of $CD8^+$ T cells from CL4-TCR mice. Cells were labelled with CFSE (Invitrogen, Germany). For stimulation, 3 x 10^5 cells per well were incubated with or without 10 µg/ml of the MHC class I HA-Peptide HA 512-520 for 1 week in 200 µl IMDM medium containing 10% FCS, 25 µmol 2-β-mercaptoethanol and 100 µg/mL penicillin/streptomycin in a 96-well plate at 37° C. After 7 days, cells were harvested and stained for the expression of CD8. Gating on $CD8^+$ T cells, the proliferation was measured by reduction of CFSE dye.

For assessment of cytokine production in MLN, single cell suspensions were prepared, by DNAse (Sigma, Germany), Collagenase-D (Sigma, Germany) digestion (20 min at 37°C). Then cells were plated at a concentration of 2 x 10^6 cells/ml in RPMI1640 containing 10% FCS, 25 µmol 2-β-mercaptoethanol and 100 µg/mL penicillin/streptomycin. Cells were stimulated with 0,1µg/ml LPS. After 48 hours supernatants were analyzed for TNFα by ELISA (R&D, Germany) according to the manufacturer's instructions.

CFSE labeling

For labelling with CSFE (Invitrogen, Germany), T cells were resuspended in RPMI 1640 at a concentration of 1 x 10^7 cells/ml and incubated with 1 µl CSFE for 8 min at 37° C. For additional incubation of 5 min, two volumes of FCS were added. After washing in complete medium, followed by washing with PBS, CSFE-labeled cells were used for the proliferation assay.

RNA preparation

RNA extraction from snap frozen colon specimen was carried out using the RNeasy mini kit (Qiagen, Germany) according to the manufacturer's instructions. First-strand cDNA was synthesized from 1µg RNA according to standard protocol.

Quantitative PCR

SYBR-green master mix (ThermoScientific. UK) was used to detect accumulation of PCR products during cycling on an Rotor-Gene 3000 Cycler (Quiagen, Germany). RNA expression levels of samples of experimental groups were normalized to β-actin and were displayed as fold-change relative to the mean of samples of untreated controls. Primers were designed using Universal ProbeLibrary (Roche).

Histology

Paraffin sections from the small intestine of adoptively transferred mice were stained with H&E for histological analysis. Mucosal inflammation was evaluated in cross sections of the small intestine. Sections were scored in a blinded fashion on a scale from 0 to 30, based on the degree of lamina propria mononuclear cell infiltration, crypt hyperplasia, goblet cell depletion and architectural distortion as previously described in detail (Westendorf et al., 2006).

Statistics

Data are expressed as mean ± standard deviation for each group. Student´s t-test was used to compare groups; P values less than 0.05 were considered significant.

Results

Amorphous SiO_2 NP exacerbate intestinal inflammation in VILLIN-HA-transgenic mice, adoptively transfered with MHC-I-restricted HA-specific T cells.

To analyze the effects of ingested amorphous SiO_2 NP on the pathology of IBD, we first exploited a T cell-dependent model of intestinal inflammation. HA-specific $CD8^+$ T cells were isolated from the spleen of CL4-TCR transgenic mice and 3-4 x 10^6 cells were injected intravenously into VILLIN-HA transgenic mice or nontransgenic littermates. After five days, mice were sacrificed and disease serverity was evaluated. To assess the effect of SiO_2 NP on disease severity, mice received SiO_2-chow (SiO_2) or particle-free chow (placebo) for one

week before the transfer and during induction of T cell mediated inflammation. Disease developed from day 3 on, and at day 5 VILLIN-HA mice displayed severe symptoms of intestinal inflammation. At this time point, body weight was reduced to about 95% of initial weight in VILLIN-HA recipient mice, whereas body weight was stable in non-transgenic littermate controls (Fig. 1 A). Histological sections of small intestinal biopsies from Villin-HA mice treated with a particle-free chow exhibited inflammatory cell infiltrates, which reached a mean score of about 15 points out of a maximum of 42 points (Fig. 1 B). However, body weight of VILLIN-HA mice, which had ingested SiO_2 NP with their chow before and during the onset of inflammation, was reduced to about 90% of initial weight, significantly different from the mice that had received particle-free chow (Fig. 1 A). Additionally, histological examination revealed that mucosal inflammation of the small bowel was more severe in SiO_2-treated VILLIN-HA mice, when compared to placebo-treated VILLIN-HA mice (Fig. 1 B). As described earlier, transfered HA-specific $CD8^+$ T-cells display an activated phenotype[16]. Therefore, we assessed the expression of the activation marker CD69 on $CD8^+$ T cells in the MLN of VILLIN-HA recipient mice by flow cytometry (Fig. 2 A). For further analysis of the activation status of the transferred $CD8^+$ transgenic T cells, isolated MLN cells were restimulated *in vitro* with the corresponding HA-peptide for 7 days and proliferation of $CD8^+$ T cells was assessed by CFSE-labeling assay. T cells, that had been isolated from MLN of transplanted VILLIN-HA mice displayed a much higher proliferative activity compared with transplanted littermate controls. The frequency of proliferating T cells, however, was even further enhanced in SiO_2-treated VILLIN-HA mice in comparison to placebo-treated VILLIN-HA mice (Fig. 2 B). Additionally, small intestinal biopsies were isolated, and cultured for 6h, after which supernatants were collected and analyzed for cytokine-expression by Luminex technology. IL-10 production from small intestines of transplanted placebo-treated VILLIN-HA mice did not differ from that of transplanted littermate controls. In contrast, biopsies of SiO_2-treated VILLIN-HA mice secreted significantly higher amounts of IL-10, compared to placebo-treated controls (Fig. 3 A). Similar results were obtained for TNFα- and IFNγ-production. Both cytokines were not or only slightly enhanced in placebo-treated VILLIN-HA mice in comparison to SiO_2- or placebo-fed littermate controls, whereas intestinal biopsies of SiO_2-treated VILLIN-HA mice produced elevated levels of TNFα and IFNγ (Fig. 3 B-C). In control mice, which did not develop symptoms of IBD upon T cell transfer, neither in turns of inflammation, nor of weight loss, administration of SiO_2 NP had no effect whatsoever. In summary, these data clearly show an exacerbated disease activity in VILLIN-HA mice, after treatment with SiO_2 NP-containing diet in comparison to mice

SiO_2 NP aggravate symptoms in DSS-induced acute colitis

DSS-induced colitis is generally believed to be dependent on bacteria, which penetrate through the epithelium and elicit strong immune responses in the colonic mucosa. Inflammation goes along with bloody diarrhea and infiltrates of granulocytes in the colonic tissue. This model also works well in Rag1-deficient mice, which lack all mature lymphocytes, therefore DSS-induced colitis seems to be mainly induced by innate immune mechanisms. To assess the influence of SiO_2 NP in DSS-induced acute colitis, mice were fed with SiO_2- or particle free-chow ad libidum for 18 days before induction of colitis. After 6 days with 2% DSS in the drinking water, in the absence of experimental chow, mice received SiO_2- or placebo-chow for additional 2 days. During the onset of disease, mice were analyzed every other day and clinical symptoms were scored. Both DSS-treated groups showed symptoms of colitis, including bloody diarrhea and weight-loss. Whereas mice which had received DSS and particle-free chow (DSS/placebo) recovered from day 25 to day 26, disease persisted in DSS-treated, SiO_2-treated (DSS/SiO_2) mice (Fig. 4 A). Additionally, the colon length was further reduced in DSS/SiO_2-treated mice in comparison to DSS/placebo-treated mice (Fig. 4 B). While total cell numbers of MLN were similar comparing the two DSS-treated groups, analysis of cytokine-production revealed a slightly enhanced secretion of TNFα from MLN cells of DSS/placebo-treated mice after 48h stimulation with LPS, which was further upregulated in DSS/SiO_2-treated mice (Fig. 5).

SiO_2 NP enhance the inflammatory response in DSS-induced chronic colitis

To evaluate the effect of SiO_2 NP in the diet during chronic DSS-induced inflammation, C57BL/6 mice were pretreated with SiO_2-containing or particle-free chow for 14 days and chronic colitis was induced in 3 intervals of DSS-treatment. Each interval consisted of one week feeding with 2% DSS in the drinking water, while mice received normal chow, followed by two week with normal drinking water and SiO_2- or placebo-chow. During the entire experiment, mice were monitored every other day, determining weight-loss and stool-consistency. During each cycle of DSS-treatment, symptoms worsened and the clinical score was highest about 10 days after the beginning of the treatment. Regarding these clinical parameters, we observed no differences between DSS/SiO_2-treated and DSS/placebo-treated groups (Fig. 6 A). Additionally, colon length, another parameter, which correlates with disease activity, was measured. In both DSS-treated groups there was a significant reduction in colon length, but there was no difference between DSS/SiO_2- and DSS/placebo-treated mice (Fig. 6 B). As a marker for systemic inflammation, spleen weight was analyzed. In both DSS-treated groups spleen weights were significantly enhanced compared to the untreated

groups, and were higher in DSS/SiO_2- compared to DSS/placebo-treated mice (Fig. 7 A). MLN are the main gut draining lymph nodes, in which induction of adaptive immune responses by gut-derived APC takes place. Therefore, we analyzed the total cellularity and cellular composition of MLN after DSS-induced chronic colitis. In both DSS-treated groups, total cell numbers of MLN were higher than those of MLN of DSS-untreated mice. When comparing MLN cell numbers of DSS/SiO_2-treated with DSS/placebo-treated mice, we observed significantly enhanced cell numbers in the MLN of SiO_2-treated mice (Fig. 7 B). To identify the cell population that was expanded in MLN of colitis mice, we performed FACS analysis. Absolut cell numbers of T cells and B cells were only slightly increased, whereas DC cell numbers remained unchanged in DSS-treated mice (Suppl. Fig. 1). The most prominently enhanced cell population expressed Gr1, a marker for granulocytes, monocytes and some macrophages (Fig. 7 C-D) and intermediate levels of CD11b and F4/80 (Fig. 7 E-F). To further analyze the effect of SiO_2 NP on cells of the colonic mucosa during DSS-induced chronic colitis, we assessed the production of inflammatory mediators in colonic tissue via quantitative PCR. In DSS/placebo-treated mice, there was no altered expression of either IFNγ or IL-17, two proinflammatory cytokines, which are closely linked to the pathology of DSS-induced colitis[30]. IFNγ-expression was upregulated only in DSS/SiO_2-treated mice (Fig. 8 A). This NP-mediated effect was not seen for IL-17 expression, which remained unchanged in both DSS-treated groups (Fig. 8 B). IL-1β is an inflammatory cytokine, which contributes largely to the tissue destruction in DSS-induced colitis[31]. In line with previous findings by others, we observed a significant upregulation of IL-1β mRNA-levels in DSS/placebo-treated mice, which was slightly further enhanced in DSS/SiO_2-treated mice (Fig. 8 C). During inflammation the inducible form of nitric oxide synthase (iNOS) is upregulated, resulting in the production of high amounts of NO, which exerts an essential anti-microbial function. However, high amounts of NO also lead to the formation of peroxynitrite, which induces cell toxicity and tissue distruction. In both DSS-treated groups iNOS was significantly upregulated compared to the untreated controls. Furthermore, iNOS mRNA levels were even higher in DSS/SiO_2-treated mice compared with DSS/placebo-treated mice (Fig 8 D). Taken together these data clearly indicate an adverse effect of food-contained SiO_2 NP in this DSS-dependent model of chronic colitis by exacerbation of the inflammatory response.

Taken together we could show, that amorphous SiO_2 NP lead to exacerbation of intestinal inflammation in 3 independent murine models of IBD. We conclude, that SiO_2 NP uptake with the diet might also lead to adverse effects in people, who have a predisposition for IBD or suffer from chronic or active disease.

Discussion:

NP, which are defined as particles with a diameter ≤ 100 nm, are increasingly utilized for food production. SiO_2 NP, for example, are used as anti-caking agents in spices, or to enhance flow properties of viscous fluids. While inhalation of NP may cause severe inflammatory reactions in lung tissue, very little is known about uptake, distribution and effects after oral ingestion. Amorphous SiO_2 NP were shown by others to cause transient pulmonary fibrogenic effects, similar to the known carcinogen quartz[11,12]. Here, we report, that oral uptake of SiO_2 NP exacerbates inflammation in the intestine in several murine models of IBD.

The initial processes leading to the induction of inflammation in the intestinal mucosa are not yet fully understood, although there is evidence that both innate immune cells and autoreactive T cells might play a role. We first analyzed the effect of SiO_2 NP on intestinal inflammation in an autoimmune model of IBD. CL4-TCR transgenic T cells, which recognize an epitope of viral hemagglutinin (HA) presented by MHC class I, were adoptively transfered into VILLIN-HA mice, expressing the influenza virus A/PR8/34 HA under the control of the villin promoter along the entire crypt-villus axis[16-18]. Upon transfer of transgenic T cells, Villin-HA mice lost weight, developed bloody diarrhea and showed signs of inflammation in the mucosa of the small intestine within 5 days. When VILLIN-HA mice were treated with SiO_2-chow 1 week before the adoptive transfer and during the onset of enterocolitis, symptoms worsened dramatically. This was reflected in more rapid weight loss, and more severe histological lesions, when compared to placebo-treated mice. Additionally, small intestinal biopsies of SiO_2-treated VILLIN-HA mice produced high amounts of the cytokines IL-10, TNFα and IFNγ, whereas tissue of placebo-treated VILLIN-HA mice secreted cytokine levels similar to non-transgenic controls. SiO_2 NP had no effect in non-transgenic control mice, and did not lead to inflammation on their own.

Recently, NP of different chemical compositions were tested for their ability to enhance therapeutic efficiency by delivering drugs specifically to inflamed sites of the intestine. It was shown, that polymeric particles adhere preferably to inflamed tissue, due to elevated levels of mucus production at these sites. Additionally, a higher uptake of particles into the mucosa was reported, as a result of a disrupted epithelial integrity together with a highly increased number of immune cells at sites of inflammation. Uptake was dependent on particle size and was more efficient, the smaller the particles were[19,20]. We hypothesize, that SiO_2 NP might be adsorbed via similar mechanisms to inflamed mucosa, where they could then be engulfed by macrophages or DC. Once SiO_2 NP are taken up into intestinal phagocytes, they may induce secretion of proinflammatory cytokines like IL-1β and TNFα, and expression of iNOS. The

latter induces secretion of NO as a second messenger, as was shown previously for peritoneal macrophages, which had been stimulated by i.p. injection of SiO_2 NP with an average diameter of 12 nm[21]. Additionally, SiO_2 NP exposure induced apoptosis and the production of reactive oxygen species (ROS) in a macrophage cell line *in vitro*[21]. In our hands, SiO_2 NP induced apoptosis and NLRP3 inflammasome-dependent IL-1β secretion in bone marrow derived DC, but no significant ROS-production[10]. These observations suggest, that SiO_2 NP might possibly lead to the secretion of inflammatory mediators in intestinal phagocytes, which could then induce activation of T cells as a secondary effect. In line with these thoughts, $CD8^+$ splenocytes from SiO_2-chow treated colitic VILLIN-HA mice displayed a more mature phenotype and higher proliferative activity upon restimulation with HA-peptide.

We next assessed the effect of SiO_2 NP ingestion in an acute model of DSS-induced colitis. Generally, it is thought that during DSS-colitis, mainly innate immune mechanisms contribute to inflammation. DSS leads to destruction of the epithelial layer and, as a consequence, microbiota from the gut lumen infiltrate the mucosa and elicit an immune response. In addition, it was shown that DSS may activate the NLRP3 inflammasome in mice[15]. In the present study, C57BL/6 mice were given SiO_2- or placebo-chow for 18 days, before inflammation was induced with 2% DSS in the drinking water. We refrained from feeding mice with NP-containing chow in parallel with DSS to avoid possible adsorption of DSS to the NP. After DSS was stopped at day 6, mice again received SiO_2-chow for additional 2 days. DSS-treated mice developed severe signs of rectal bleeding, diarrhea and weight loss, starting from day 2 on. When mice were sacrificed on day 8, DSS-placebo-treated mice already showed remission of symptoms, whereas DSS-SiO_2-treated mice were still in severe conditions. As another parameter, which correlates with severity of inflammation, colon length was measured. Only in SiO_2-treated mice colon length was clearly reduced, indicating a more serious inflammatory response in the colonic mucosa of these mice. In concordance with the effects of SiO_2 NP in the VILLIN-HA colitis model, we additionally observed significantly elevated levels of TNFα in cultures of MLN cells. TNFα is a proinflammatory cytokine, which is mainly produced by mononuclear cells like macrophages in IBD[22,23], indicating that intestinal phagocytes might indeed be a primary target of NP exposure. TNFα represents one of the most important inflammatory cytokines in IBD-associated immunopathology. It leads to the activation of neutrophils and macrophages, stimulates B cells and induces T cells to produce IFNγ[24]. During the last decade a new generation of therapeutica has been designed, targeting mediators of IBD like TNFα and IL-1β, instead of a general immunosuppression. This approach has been very successful with regard to

amelioration of symptoms during flares and incidence of remission[25]. The clear upregulation of TNFα in SiO_2-treated mice in both acute models of colitis analyzed in this study, further strengthens the significance of NP induced enhancement of intestinal inflammation. In contrast, SiO_2 NP had no effect whatsoever in untreated control mice.

Since IBD is typically a chronic, relapsing disease, we also analyzed the influence of SiO_2 NP in a DSS-dependent model of chronic colitis[26]. SiO_2 NP-induced effects were not as strong as during acute inflammation, but nevertheless, we observed significant differences in the cellular composition of MLN and spleen. Colitic mice, which had been fed with SiO_2-chow for 2 weeks before the first cycle of DSS-treatment, in between DSS-treatments and after the last round of DSS-administration, had enlarged spleens and significantly enhanced absolut cell numbers in MLN in DSS-SiO_2-treated mice, when compared to DSS-placebo-treated colitic mice. We were able to identify the cell population, which was mainly enhanced in MLN of SiO_2-treated colitic mice as Gr-1^+, $CD11b^+$ cells. In several models of tumorigenesis a similar cell type, termed myeloid suppressor cell (MSC) has been described to act immunosuppressive via the inhibition of T cell activation[27, 28]. The occurence of this newly identified cell population also increases during intestinal inflammation, probably to prevent fatal sepsis[29]. We speculate, that MSC are induced by SiO_2 NP in DSS-treated mice, which counteract inflammation. Yet the presence of such a high proportion of regulatory cells in MLN of SiO_2-treated diseased mice argues for the induction of a more severe inflammatory response in SiO_2-treated mice in comparison to placebo-treated mice. In this model, we also assessed the expression of inflammatory mediators in the colonic mucosa. IL-1β and iNOS were both significantly upregulated in the intestines of DSS-placebo -treated mice, whereas IL-17 was only slightly enhanced and IFNγ expression was unchanged when compared to the control. No differences were observed regarding IL-17 production, when comparing DSS-placebo - and DSS-SiO_2-treated mice. Although IL-17 was described to play a major role in chronic DSS-induced colitis, we were not able to confirm this finding in our experiment[30]. IL-1β, as well as iNOS, were upregulated in DSS-SiO_2- in comparison to DSS-placebo-treated mice, eventhough the differences were not very strong. In contrast, IFNγ was clearly upregulated in DSS-SiO_2-treated mice, when compared to DSS-placebo-treated mice, suggesting that SiO_2 NP directly of indirectly excacerbate the Th1 response during intestinal inflammation. In the light of recent findings, that activation of the NLRP3 inflammasome influences the strength of DSS-colitis[15,39-42], and our own observations that SiO_2 NP activate the inflammasome in DC[10], it is possible that SiO_2 NP exacerbate inflammation in this model of chronic DSS-induced colitis at least partly by activating the inflammasome in intestinal phagocytes. It will be interesting to investigate the mechanisms of SiO_2 NP-dependent

amplification of intestinal inflammation in more detail, e.g. in DSS-induced colitis in NLRP3, ASC and Caspase1-deficient mice.

In summary, our findings clearly show, that SiO_2 NP in the diet can enhance inflammation in IBD, in particular after the disease has already manifested. Nevertheless, it is also possible that SiO_2 NP can accelerate the onset of mucosal inflammation in people, who are genetically predisposed to develop IBD, as many genes associated with an increased predisposition for IBD are related to inflammasomes[4,5,33]. This point should be given further attention in the future. It has also been shown, that poly(lactic-co-glycolic acid) NP, which are to be used in different therapeutical approaches, including the delivery of drugs to the inflamed mucosa of IBD patients, also act as potent activators of the inflammasome [34]. Therefore, we suggest that these particles, as well as NP of other materials such as TiO_2, ZnO, MnO or CaO, which are already used by the food industry, should also be tested critically for counter indications *in vivo*.

The concentration of 0.1% SiO_2 NP in the chow used in this study is not very different from the estimated actual uptake of SiO_2 food additives by humans. Therefore, we consider our results alarming and suggest that IBD patients should be cautious in consuming NP-rich foods.

Figure legends

Figure 1 **Severity of colitis in particle-treated VILLIN-HA mice 5 days after colitis induction.** 3.5 x 10^6 HA-specific $CD8^+$ T cells were adoptively transferred intravenously into VILLIN-HA transgenic mice and non-transgenic littermates. Where indicated, mice were pretreated with SiO_2- chow for one week (SiO_2). Disease development was measured daily and is expressed in terms of body weight loss at day 5 (A). Small intestines were isolated at day 5 and histologically scored (B). Statistics were calculated by Student's t-test * $p \leq 0.05$ (comparison as indicated); $^{\#}p \leq 0.05$, $^{\#\#}p \leq 0{,}01$ (versus control).

Figure 2 **Percentage of activated CD8 T cells and proliferation of CD8 T cells of mLN in particle-treated VILLIN-HA mice 5 days after colitis induction.** 3.5 x 10^6 HA-specific $CD8^+$ T cells were adoptively transferred intravenously into VILLIN-HA transgenic mice and non-transgenic littermates. Where indicated, mice were pretreated with SiO_2-chow for one week (SiO_2). MLN were isolated at day 5 after transfer and cells were stained for the expression of CD8 and the activation marker CD69 (A). MLN cells were CFSE labeled and stimulated with the corresponding HA peptide. Proliferation of CD8 T cells were measured by dilution of CFSE-dye (B). Statistics were calculated by Student's t-test * $p \leq 0.05$ (comparison as indicated).

Figure 3 **Cytokine production in gut tissue of particle-treated VILLIN-HA mice 5 days after colitis induction.** 3.5 x 10^6 HA-specific $CD8^+$ T cells were adoptively transferred intravenously into VILLIN-HA transgenic mice and non-transgenic littermates. Where indicated, mice were pretreated with SiO_2-chow for one week (SiO_2). At day 5 after transfer, small intestine biopsies were isolated and cultured for 6h in medium. Supernatants were collected and analyzed for cytokines by Luminex technology. Statistics were calculated by Student's t-test * $p \leq 0.05$ (comparison as indicated).

Figure 4 **Clinical score and colon length of particle-treated mice with acute DSS-induced colitis.** C57/BL6 mice were pretreated with SiO_2-chow for 18 days, followed by induction of acute colitis by six days of DSS-treatment and two days on normal drinking water and SiO_2-chow. The clinical score was assessed about every second day (A), and colon length was measured. After sacrificing the mice after the experiment (B). Statistics were calculated by Student's t-test $^{\#\#\#}p \leq 0{,}005$ (versus control).

Figure 5 **Production of TNFα in the MLN of particle-treated mice with acute DSS-induced colitis.** C57/BL6 mice were pretreated with SiO_2-chow for 18 days, followed by induction of acute colitis by six days of DSS-treatment and two days on normal drinking water and SiO_2-chow. After the experiment, single cell suspensions of MLN were incubated in the presence of LPS for 48 hours and TNFα was analysed in the supernatant. Statistics were calculated by Student's t-test $^{\#}p \leq 0,05$ (versus control).

Figure 6 **Clinical score and colon length of particle-treated mice with chronic DSS-induced colitis.** C57/BL6 mice were pretreated with SiO_2-chow for 14 days, followed by induction of chronic colitis by 3 cycles of DSS-treatment. Each cycle consisted of one week with 2% (wt/vol) DSS in drinking water and two weeks with normal drinking water and SiO_2-chow. The clinical score was assessed about every second day (A), and colon length was measured after sacrificing the mice after the experiment (B). Statistics were calculated by Student's t-test $^{\#\#\#}p \leq 0,005$ (versus control).

Figure 7 **Cellular composition of MLN and spleen in particle-treated mice with chronic DSS-induced colitis.** C57/BL6 mice were pretreated with SiO_2-chow for 14 days, followed by induction of chronic colitis by 3 cycles of DSS-treatment. Each cycle consisted of one week on 2% (wt/vol) DSS in drinking water and two weeks on normal drinking water and SiO_2-chow. Mice were sacrificed and total cell numbers of spleens and MLN were calculated (A-B). Additionally total amounts of $Gr1^+$ cells in MLN were assessed by FACS analysis (C-D). Statistics were calculated by Student's t-test * $p \leq 0.05$, ** $p \leq 0.01$ (comparison as indicated); $^{\#\#}p \leq 0,01$, $^{\#\#\#}p \leq 0,005$ (versus control).

Figure 8 **Production of inflammatory mediators in colon tissue of particle-treated mice with chronic DSS-induced colitis.** C57/BL6 mice were pretreated with SiO_2-chow for 14 days, followed by induction of chronic colitis by 3 cycles of DSS-treatment. Each cycle consisted of one week on 2% (wt/vol) DSS in drinking water and two weeks on normal drinking water and SiO_2-chow. After the experiment, colon biopsies were dissected and mRNA levels of cytokines (A-C) and iNOS (D) were assessed by qPCR as described in Material and Methods. Statistics were calculated by Student's t-test $^{\#}p \leq 0,05$, $^{\#\#}p \leq 0,01$, $^{\#\#\#}p \leq 0,005$ (versus control).

References

1. Gent AE, Hellier MD, Grace RH, Swarbrick ET, Coggon D. Inflammatory bowel disease and domestic hygiene in infancy. Lancet 1994;343:766-767.

2. Hampe J, Heymann K, Krawczak M, Schreiber S. Association of inflammatory bowel disease with indicators for childhood antigen and infection exposure. Int J Colorectal Dis 2003;18:413-417.

3. Geerling BJ, Dagnelie PC, Badart-Smook A, Russel MG, Stockbrugger RW, Brummer RJ. Diet as a risk factor for the development of ulcerative colitis. Am J Gastroenterol 2000;95:1008-1013.

4. Heap GA, van Heel DS. The genetics of chronic inflammatory diseases. Hum Mol Genet 2009;18:101-106.

5. Shih DQ, Targan SR, McGovern D. Recent advances in IBD pathogenesis: Genetics and immunobiology. Curr Gastroenterol Rep 2008;10:568-575.

6. Vignal C, Singer E, Peyrin-Biroulet L, Desreumaux P, Chmaillard M. How NOD2 mutations predispose to Crohn's disease. Microbes Infect 2007;9:658-663.

7. Strober W, Murray PJ, Kitani A, Watanabe T. Signalling pathways and molecular interactions of NOD1 and NOD2. Nat Rev Immunol 2006;6:9-20.

8. Watanabe T, Kitani A, Murray PJ, Strober W. NOD2 is a negative regulator of Toll-like receptor 2-mediated T helper type 1 responses. Nat Immunol 2004;5:800-808.

9. Baumgart DC, Carding SR. Inflammatory bowel disease: Cause and immunobiology. Lancet 2007;369:1627-1640.

10. Winter et al. submitted

11. Cho WS, Choi M, Han BS, Cho M, Oh J, Park K, Kim SJ, Kim SH, Jeong J. Inflammatory mediators induced by intratracheal instillation of ultrafine amorphous silica particles. Toxicol Letters 2007;175:24-33.

12. Choi M, Cho WS, Han BS, Cho M, Kim SY, Yi JY, Ahn B, Kim SH, Jeong J. Transient pulmonary fibrogenic effect induced by intratracheal instillation of ultrafine amorphous silica in A/J mice. Toxicol Letters 2008;182:97-101.

13. Hillyer JF, Albrecht RM. Gastrointestinal persorption and tissue distribution of differently sized colloidal gold nanoparticles. Journal of Pharm Sci 2000;90:1927-1936.

14. Okayasu I, Hatakeyama S, Yamada M, Ohkusa T, Inagaki Y, Nakaya R. A novel method in the induction of reliable experimental acute and chronic ulcerative colitis in mice. Gastroenterol 1990;98:694-702.

15. Bauer C, Duewell P, Mayer C, Lehr HA, Fitzgerald KA, Dauer M, Tschopp J, Endres S, Latz E, Schnurr M. Colitis induced in mice with dextran sulfate sodium (DSS) is mediated by the NLRP3 inflammasome. Gut 2010;online first

16. Westendorf AM, Fleissner D, Deppenmeier S, Gruber AD, Bruder D, Hansen W, Liblau R, Buer J. Autoimmune-mediated intestinal inflammation-impact and regulation of antigen-specific $CD8^+$ T cells. Gastroenterol 2006;131:510-524.

17. Morgan DC, Liblau R, Scott B Fleck S, McDevitt HO, Sarvetnick N, Lo D, Sherman LA. CD8(+) T cell-mediated spontaneous diabetes in neonatal mice. J Immunol 1996;169:6677-6680.

18. Westendorf AM, Templin M, Gefferes R, Deppenmeier S, Gruber AD, Probst-Kepper M, Hansen W, Liblau RS, Gunzer F, Bruder D, Buer J. $CD4^+$ T cell mediated intestinal immunity: chronic inflammation versus immune regulation. Gut 2004;54:60-69.

19. Lamprecht A, Schäfer U, Lehr CM. Size-dependent bioadhesion of micro- and nanoparticluate carriers to the inflamed colonic mucosa. Pharm Res 2001;18:788-793

20. Lamprecht A, Yamamoto H, Takeuchi H, Kawashima Y. Nanoparticles enhance therapeutic efficiency by selectively increased local drug dose in experimental colitis in rats. JPET 2005;315:196-202.

21. Park EJ, Park K. Oxidative stress and pro-inflammatory responses induced by silica nanoparticles in vivo and in vitro. Toxicol Letters 2009;184:18-25.

22. MacDonald TT, Hutchings P, Choy MY, Murch S, Cooke A. Tumour necrosis factor-alpha and interferon gamma production measured at the single cell level in normal and inflamed human intestine. Clin exp Immunol 1990;81:301-305.

23. Olson AD, Ayass m, Chensue S. Tumor Necrosis Factor and IL-1β expression in pediatric patients with inflammatory bowel disease. J Pediatr Gastroenterol Nutr 1993;16:241-246.

24. Lukacz NW, Chensue SW, Stricter RM, Warmington K, Kunkel SL. Inflammatory granuloma formation is mediated by TNF-alpha-inducible intercellular adhesion molecule-1. J Immunol 1994;152:5883-5889.

25. Bosani M, Ardizzone S, Bianchi Porro G. Biologic targeting in the treatment of inflammatory bowel diseases. Biologics 2009;3:77-97.

26. Kaser A, Zeissig S, Blumberg RS. Inflammatory Bowel Disease. Annu Rev Immunol 2010;28:573–621.

27. Bunt SK, Sinha P, Clements VK, Leips J, Ostrand-Rosenberg S. Inflammation induces myeloid-derived suppressor cells that facilitate tumor progression. J Immunol 2006;176:284-290.

28. Song X, Krelin Y, Dvorkin T, Bjorkdahl O, Segal S, Dinarello CA, Voronov E, Apte RN. CD11b+/Gr-1+ immature myeloid cells mediate suppression of T cells in mice bearing tumors of IL-1{beta}-secreting cells. J Immunol 2005;175:8200-8208.

29. Haile LA, von Wasielewski R, Gamrekelashvili J, Krüger C, Bachmann O, Westendorf AM, Buer J, Liblau R, Manns MP, Korangy F, Greten TF. Myeloid-derived suppressor cells in inflammatory bowel disease: A new immunoregulatory pathway. Gastroenterol 2008;135:871-881.

30. Fitzpatrick LR, Deml L, Hofmann C, Small JS, Groeppel M, Hamm S, Lemstra S, Leban J, Ammendola A. 4SC-101, a novel immunosuppressive drug, inhibits IL-17 and attenuates colitis in two murine models of inflammatory bowel disease. Inflamm Bowel Dis 2010;0:1-15.

31. Siegmund B, Lehr HA, Fantuzzi G, Dinarello C. IL-1β-converting enzyme (caspase-1) in intestinal inflammation. PNAS 2001;98:13249-13254.

32. Allen IC, TeKippe EM, Woodford RM, Uronis JM, Holl EK, Rogers AB, Herfarth HH, Jobin C, Ting JP. The NLRP3 inflammasome functions as a negative regulator of tumorigenesis during colitis-associated cancer. J Exp Med 2010;207:1045-1056.

33. Glinsky GV. SNP-guided microRNA maps (MirMaps) of 16 common human disorders identify a clinically accessible therapy reversing transcriptional aberrations of nuclear import and inflammasome pathways. Cell Cycle 2008;7:3564-3576.

34. Demento SL, Eisenbarth SC, Foellmer HG, Platt C, Caplan MJ, Saltzman WM, Mellman I, Ledizet M, Fikrig E, Flavell RA, Fahmy TM. Inflammasome-activating nanoparticles as modular systems for optimizing vaccine efficacy. Vaccine 2009;27:3013-3021.

35. Hugot JP, Chamaillard M, Zouali H, Lesage S, Cezard JP, Belaiche J, Almer S, Tysk C, O'Morain CA, Gassull M, Binder V, Finkel Y, Cortot A, Modigliani R, Laurent-Puig P, Gower-Rousseau C, Macry J, Colombel JF, Sahbatou M, Thomas G. Association of NOD2 leucine-rich repeat variants with susceptibility to Crohn's disease. Nature 2001;31:599-603.

36. Ogura Y, Bonen DK, Inohara N, Nicolae DL, Chen FF, Ramos R, Britton H, Moran T, Karaliuskas R, Duerr RH, Achkar JP, Brant SR, Bayless TM, Kirschner BS, Hanauer SB, Nuñez G, Cho JH. A frameshift mutation in NOD2 associated with susceptibility to Crohn's disease. Nature 2001;31:603-606.

37. Powell JJ, Faria N, Thomas-McKay E, Pele LC. Origin and fate of dietary nanoparticles and microparticles in the gastrointestinal tract. J Autoimmun 2010;34:226-233.

38. Hamilton RF, Thakur SH, Holian A. Silica binding and toxicity in alveolar macrophages. Free Rad Biol Med 2008;44:1246-1258.

39. Zaki H, Boyd KL, Vogel P, Kastan MB, Lamkanfi M, Kanneganti T-D. The NLRP3 inflammasome protects against loss of epithelial integrity and mortality during experimental colitis. Immunity 2010; 32:379-391.

40. Allen IC, TeKippe E M, Woodford R-MT, Uronis JM, Holl EK, Rogers AB, Herfarth HH, Jobin C, Ting JP-Y. The NLRP3 inflammasome functions as a negative regulator of tumorigenesis during colitis-associated cancer. J Exp Med 2010;207:1045-1056.

41. Siegmund B. Interleukin-18 in intestinal inflammation: friend and foe? Immunity 2010;32:300-302.

42. Dupaul-Chicoine J, Yeretssian G, Doiron K, Bergstrom KSB, McIntire CR, LeBlanc PM, Meunier C, Turbide C, Gros , Beauchemin N, Vallace BA, Saleh M. Control of intestinal homeostasis, colitis, and colitis-associated colorectal cancer by the inflammatory caspases. Immunity 2010;32:367-378.

43. Westendorf AM, Templin M, Geffers R, Deppenmeier S, Gruber AD, Probst-Kepper M, Hansen W, Liblau RS, Gunzer F, Bruder D, Buer J. CD4+ T cell mediated intestinal immmunity: chronic inflammation versus immune regulation. Gut 2005;54:60-69.

Figure 1

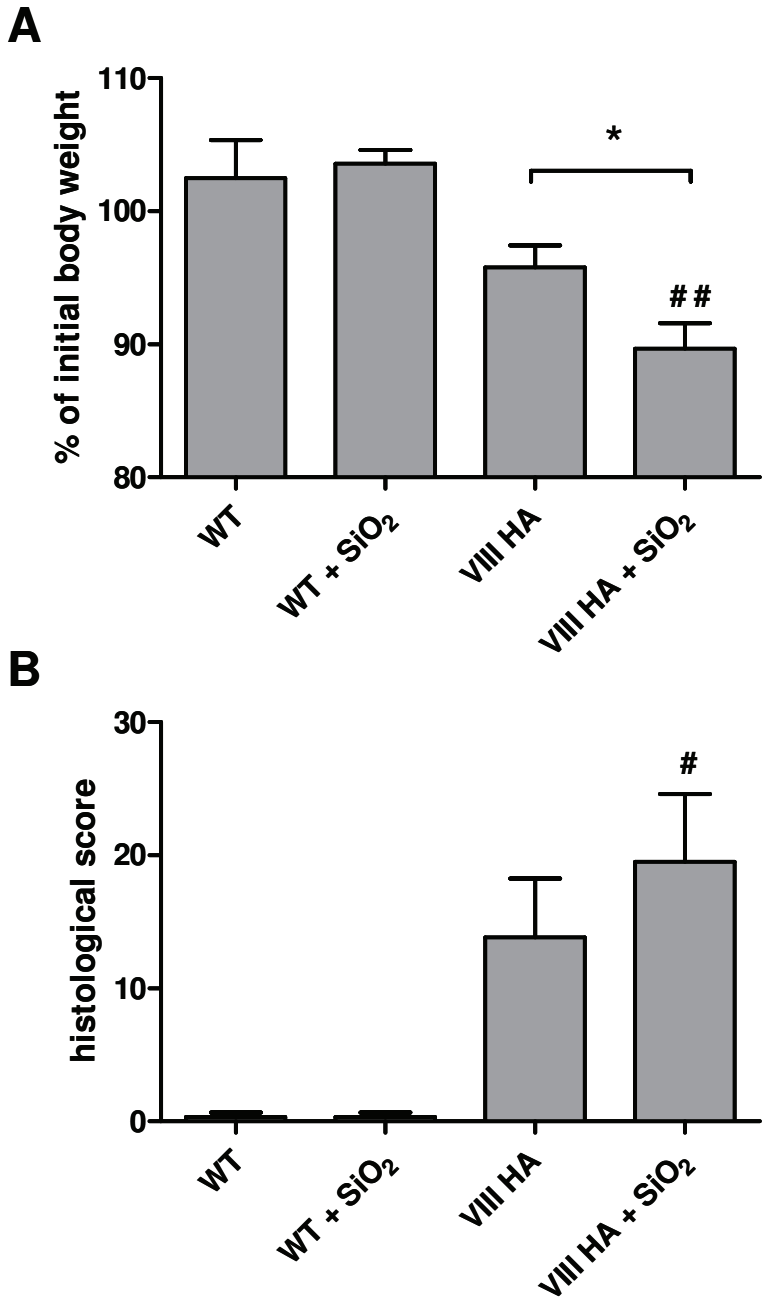
A
% of initial body weight
110
100
90
80
*
##
WT
WT + SiO2
VIII HA
VIII HA + SiO2
B
histological score
30
20
10
0
#
WT
WT + SiO2
VIII HA
VIII HA + SiO2

Figure 2

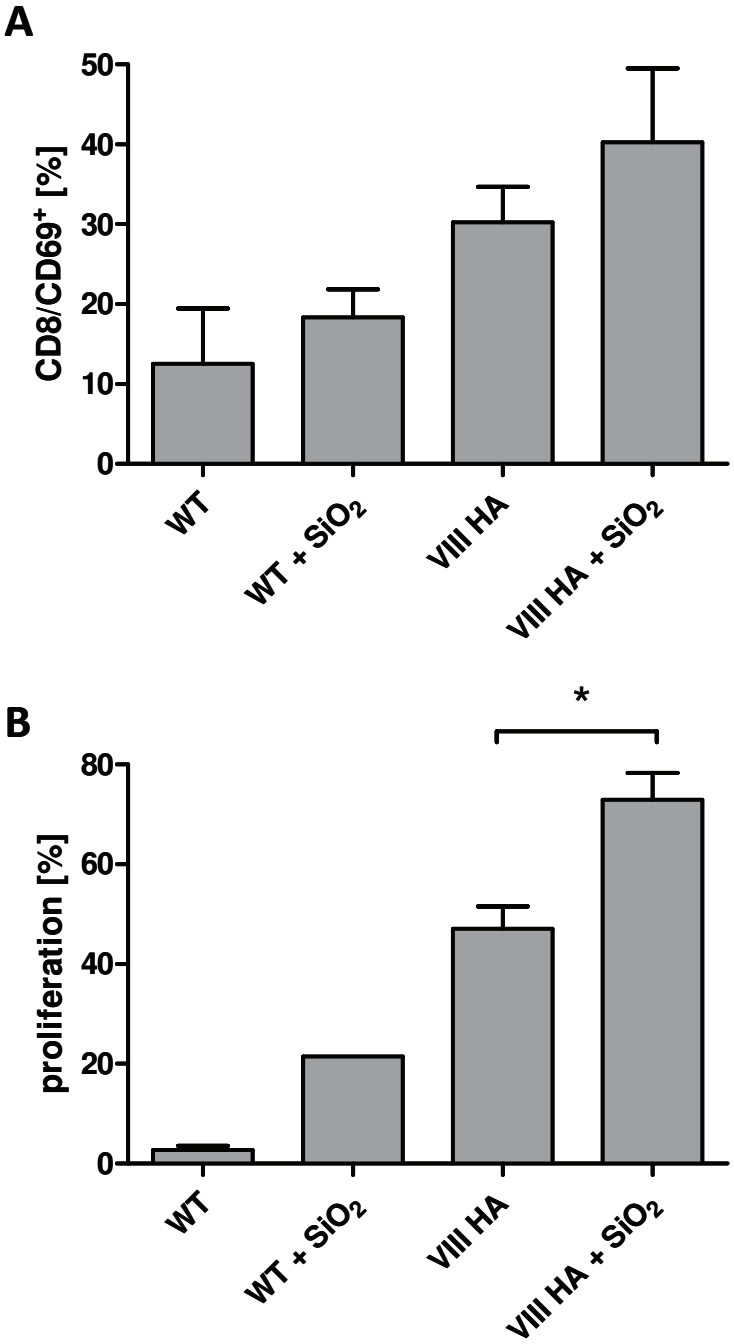
A
CD8/CD69+ [%]
50
40
30
20
10
0
WT
WT + SiO2
VIII HA
VIII HA + SiO2
B
*
proliferation [%]
80
60
40
20
0
WT
WT + SiO2
VIII HA
VIII HA + SiO2

Figure 3

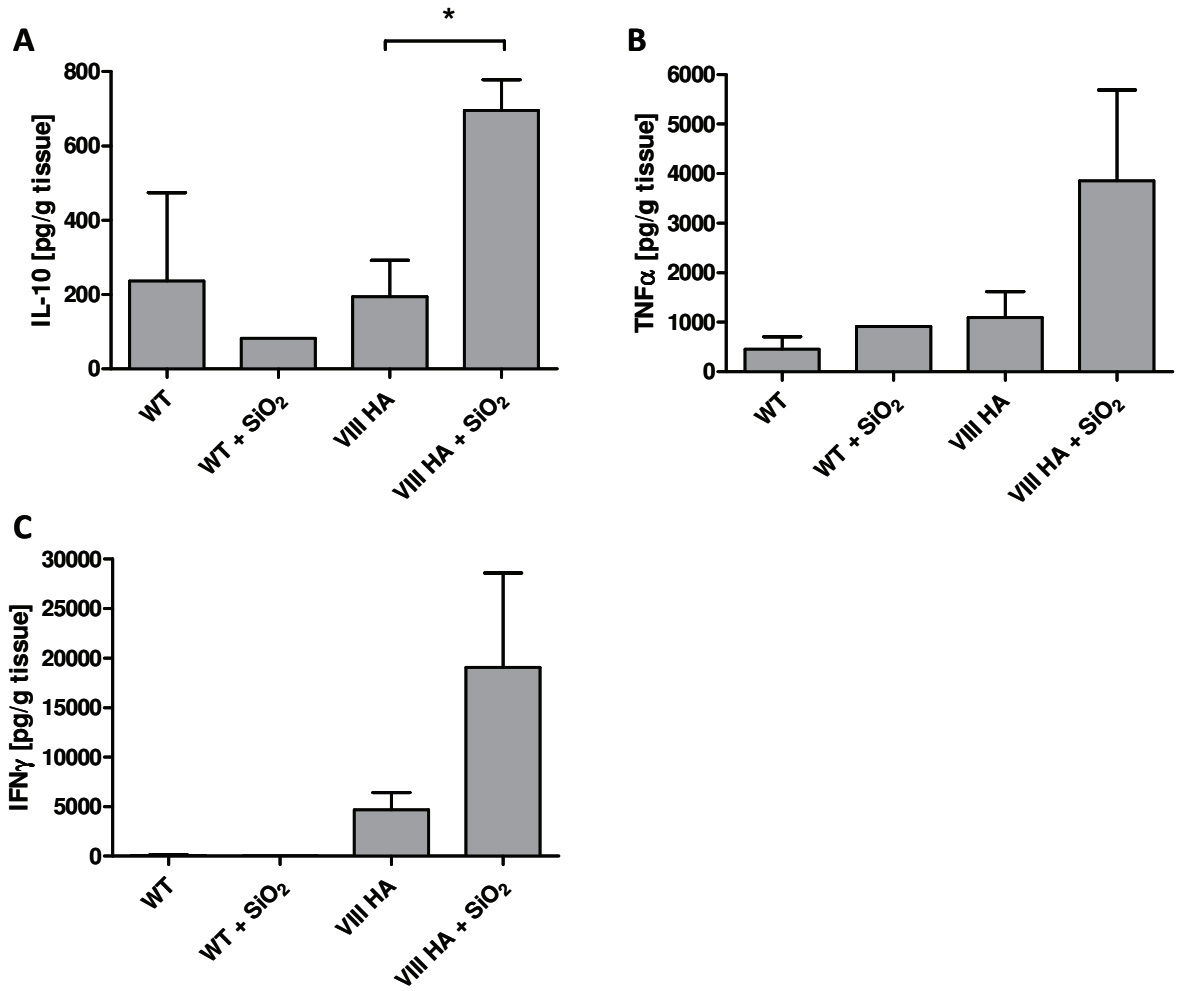
A
*
IL-10 [pg/g tissue]
800
600
400
200
0
WT
WT + SiO2
VIII HA
VIII HA + SiO2
B
TNFα [pg/g tissue]
6000
5000
4000
3000
2000
1000
0
WT
WT + SiO2
VIII HA
VIII HA + SiO2
C
IFNγ [pg/g tissue]
30000
25000
20000
15000
10000
5000
0
WT
WT + SiO2
VIII HA
VIII HA + SiO2

Figure 4

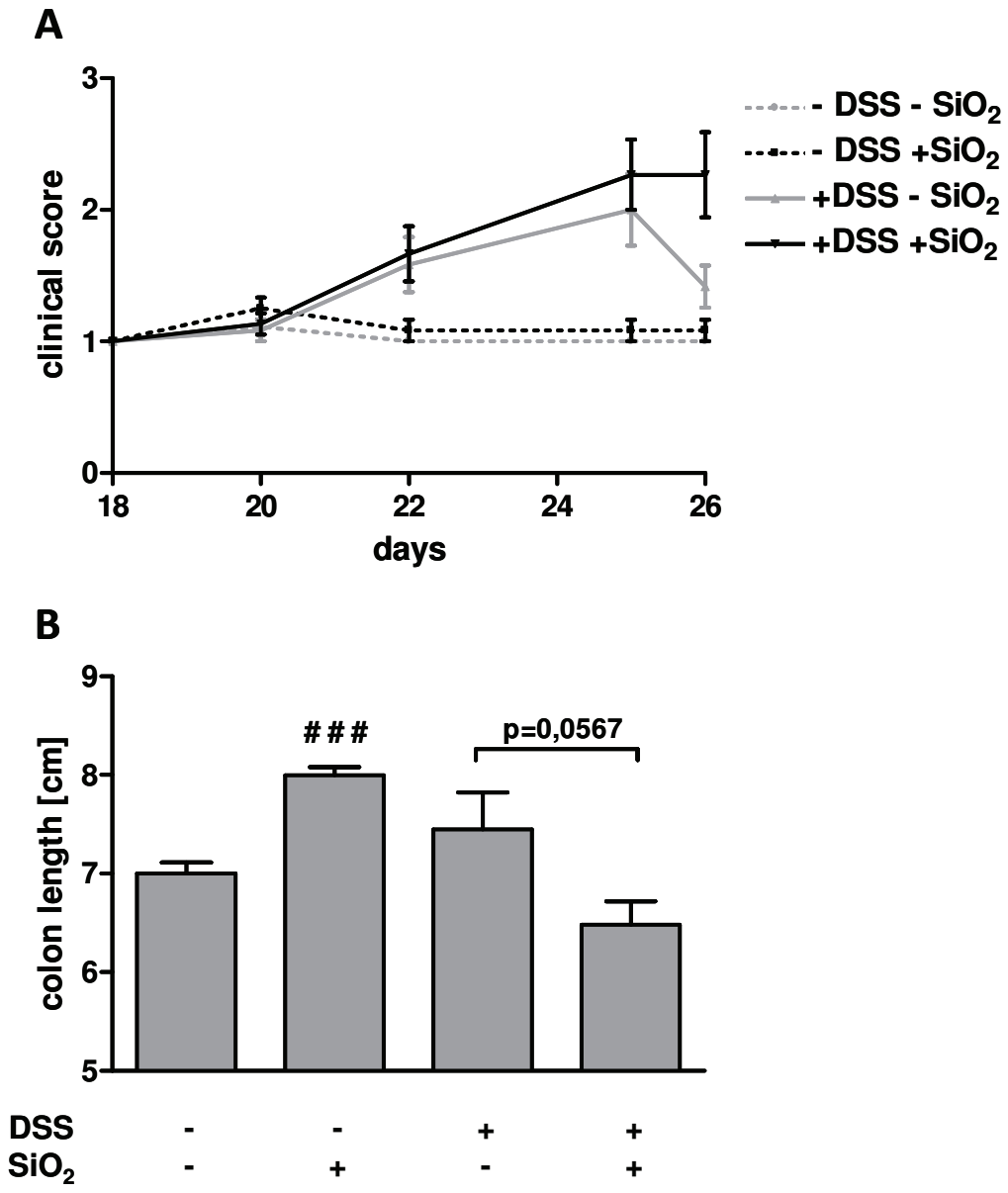
A
clinical score
days
- DSS - SiO2
- DSS +SiO2
+DSS - SiO2
+DSS +SiO2
B
colon length [cm]
###
p=0,0567
DSS
SiO2

Figure 5

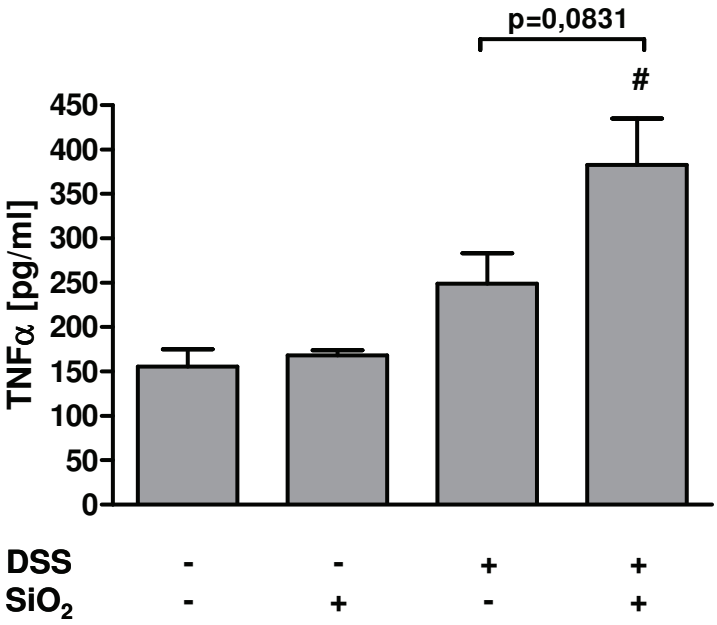

Figure 6

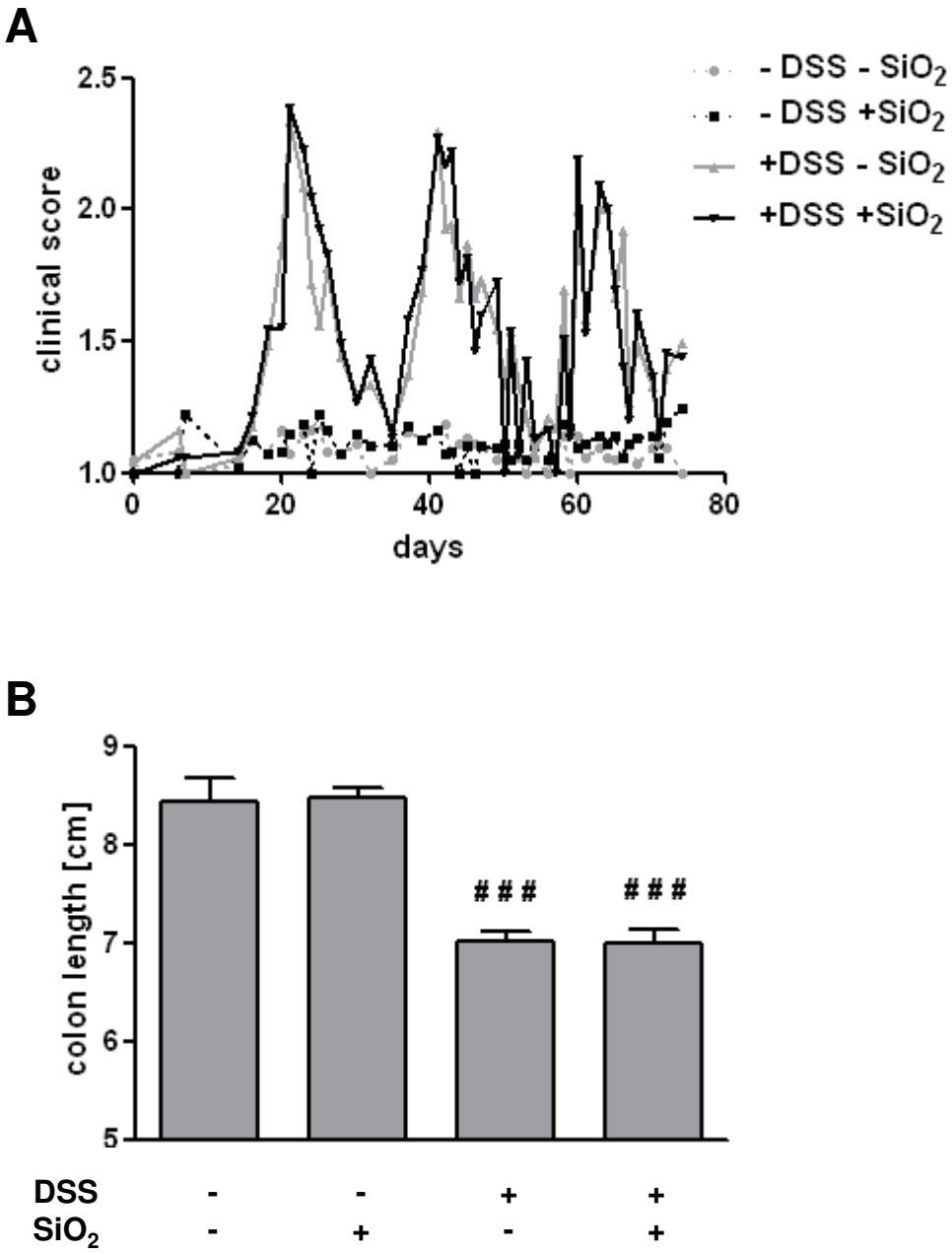
A
2.5
2.0
1.5
1.0
clinical score
0
20
40
60
80
days
- DSS - SiO2
- DSS +SiO2
+DSS - SiO2
+DSS +SiO2
B
9
8
7
6
5
colon length [cm]
###
###
DSS
SiO2
-
-
+
+
-
+
-
+

Figure 7

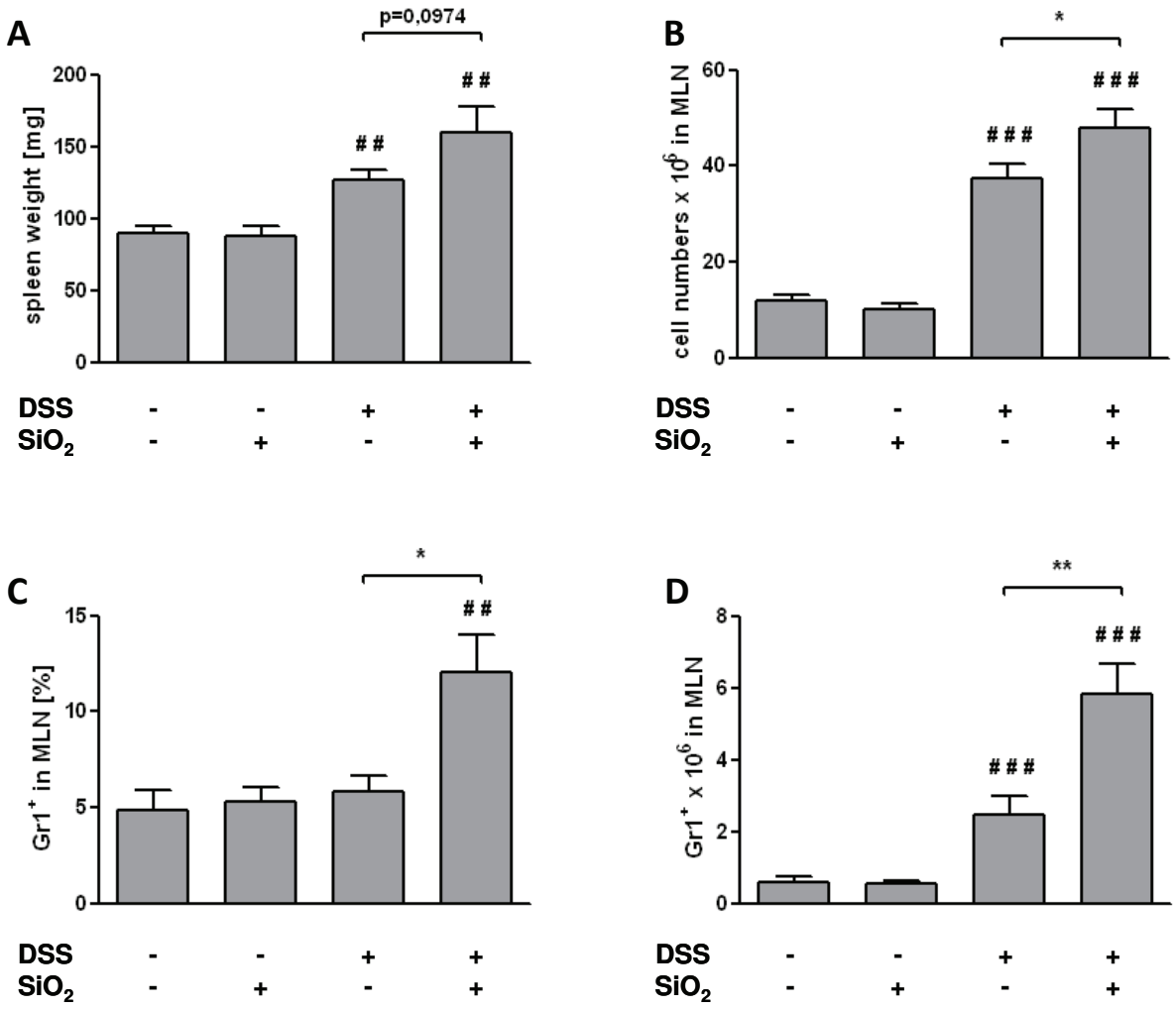
A
p=0,0974
spleen weight [mg]
200
150
100
50
0
##
##
DSS - - + +
SiO2 - + - +
B
*
cell numbers x 10^6 in MLN
60
40
20
0
###
###
DSS - - + +
SiO2 - + - +
C
*
Gr1+ in MLN [%]
15
10
5
0
##
DSS - - + +
SiO2 - + - +
D
**
Gr1+ x 10^6 in MLN
8
6
4
2
0
###
###
DSS - - + +
SiO2 - + - +

Figure 8

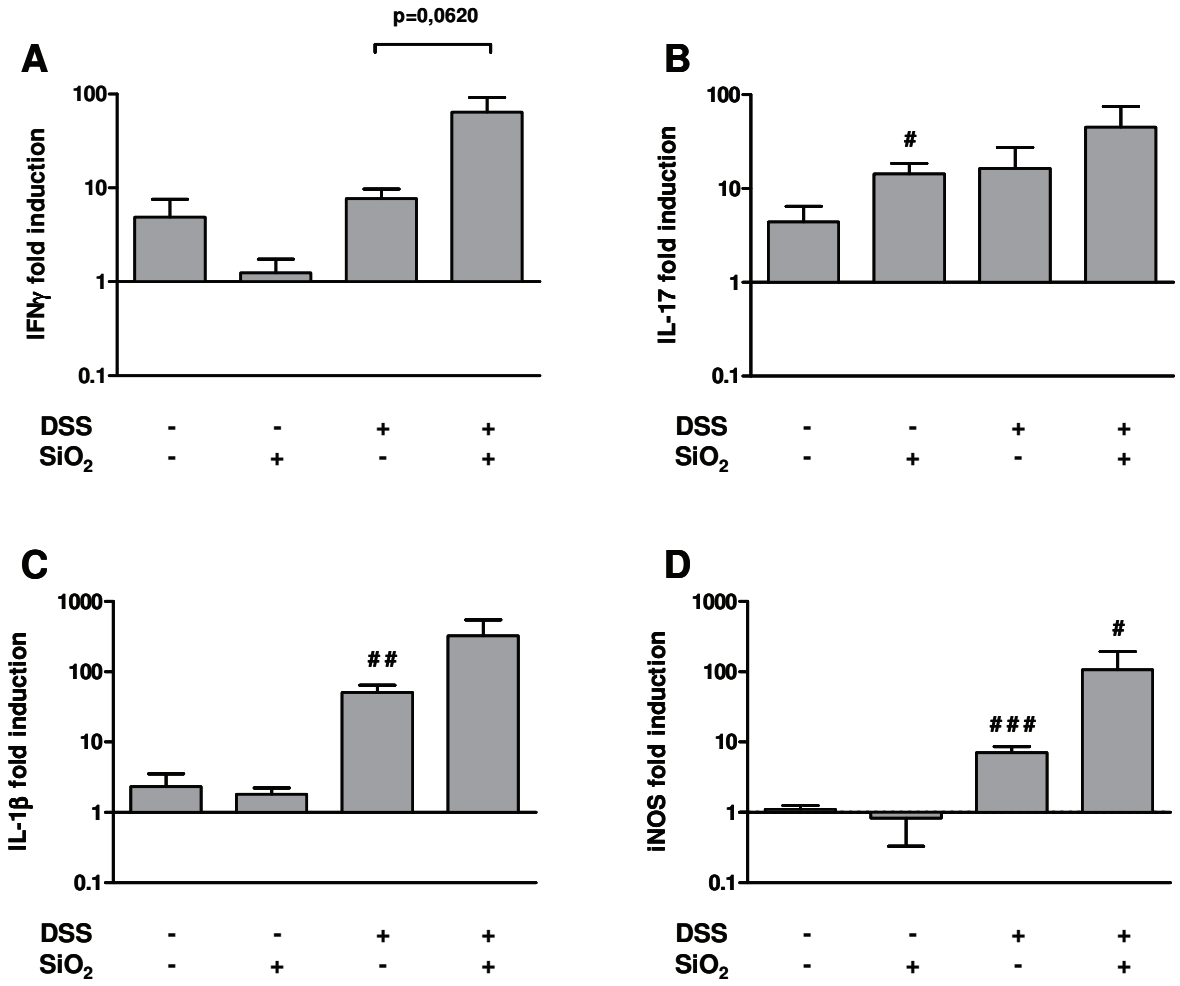
A
p=0,0620
IFNγ fold induction
100
10
1
0.1
DSS - - + +
SiO2 - + - +
B
IL-17 fold induction
#
C
IL-1β fold induction
1000
##
D
iNOS fold induction
###
#

Activation of the inflammasome by amorphous silica and TiO_2 nanoparticles in murine dendritic cells

MEIKE WINTER[1], HANS-DIETMAR BEER[2], VEIT HORNUNG[3], ROEL P.F. SCHINS[4], IRMGARD FÖRSTER[1]

[1]Molecular Immunology, Institut für Umweltmedizinische Forschung at the Heinrich-Heine University, Düsseldorf, Germany
[2]Institute of Cell Biology, Eidgenössische Technische Hochschule, Zürich, Switzerland.
[3]Institute for Clinical Chemistry and Pharmacology, Unit for Clinical Biochemistry, University Hospital, University of Bonn, Germany
[4]Particle Research, Institut für Umweltmedizinische Forschung at the Heinrich-Heine University, Düsseldorf, Germany

Inflammasome activation by NP

Keywords: nanoparticles, amorphous silica, TiO_2, NLRP3, dendritic cells

*Corresponding author:

Irmgard Förster, Prof. Dr.
Institut für umweltmedizinische Forschung (IUF)
Auf'm Hennekamp 50
D-40225 Düsseldorf, Germany
tel: +49-211-3389-210
fax: +49-211-3190910
email: irmgard.foerster@uni-duesseldorf.de

Abstract

Nanomaterials are increasingly used in various food applications, although there is little known about toxicological endpoints after oral uptake. Since intestinal dendritic cells (DC) could be critical targets for ingested particles, we compared the *in vitro* effects of amorphous silica nanoparticles with fine crystalline silica, and micron-sized with nano-sized TiO_2 particles on DC. TiO_2- and SiO_2-nanoparticles, as well as crystalline silica particles led to an upregulation of MHC-II, CD80, and CD86 on DC. Furthermore, these particles activated the inflammasome, leading to significant IL-1β-secretion in wild-type (WT) but not Caspase-1- or NLRP3-deficient mice. Silica nanoparticles and crystalline silica induced apoptosis, while TiO_2 nanoparticles led to enhanced production of reactive oxygen species (ROS). Since amorphous silica and TiO_2 nanoparticles had strong effects on the activation-status of DC, we suggest that nanoparticles, used as food additives, should be intensively studied *in vitro* and *in vivo*, to ensure their safety for the consumer.

Introduction

In the past decade, the use of nano-materials in various industrial applications has steadily increased. Nanoparticles offer many useful properties, due to their enlarged surface in comparison to larger particles. Currently, nano-materials are used for many different purposes, including surface coatings, as food additives, or in microelectronics. Because of their great potential to enhance the uptake and prolong the half-life of drugs, and their adjuvant properties, they find entrance into clinical use as drug delivery vectors or for vaccination approaches (Aline et al., 2009; Elamanchili et al., 2007; Lamprecht et al., 2001; Lamprecht et al., 2005; Li et al., 2007). While the major route for accidental uptake is via the respiratory route, nanoparticles are also effectively taken up via the intestinal mucosa (Behrens et al., 2002; Hillyer and Albrecht, 2001). Humans ingest an estimated number of 10^{12}-10^{14} inorganic particles per day, including a nano-sized fraction (Chaudhry et al., 2008). This number will probably rise in the next few years, since nanoparticles are now increasingly used in the food sector (Bouwmeester et al., 2009; Powell et al., 2009).

Nano-sized particles induce a stronger acute inflammatory reaction than larger sized particles, when tested at the same mass dose, as was shown by inhalation (Oberdörster et al., 2000) or intratracheal instillation (Sager et al., 2008). In fact, for several types of poorly soluble particles (e.g. TiO_2, carbonaceous particles) a strong correlation has been found between pulmonary toxic responses and the particle surface area (Oberdörster et al., 2005; Stoeger et al., 2006). When applied intraperitoneally, TiO_2 was distributed throughout the entire body, but was mainly retained in liver and spleen (Chen et al., 2009). After intratracheal instillation, both fine and ultrafine TiO_2 particles caused pulmonary fibrosis and tumours in rat lungs (reviewed by Borm et al., 2004). Application of TiO_2 nanoparticles with a primary particle size of 21 nm in drinking water of mice was recently shown to cause genotoxic effects in blood cells, bone marrow and liver, as well as DNA deletions in the offspring (Trouiller et al., 2009). In contrast, TiO_2 nanoparticles with a very small primary size (i.e. < 5 nm) were found to cause only rather mild symptoms and transient damage (Grassian et al., 2007).

Inhalation of crystalline silica particles induces a severe lung disease, known as Potter's rot or silicosis. Crystalline silica, in the form of quartz or crystoballite, has also been classified as a human carcinogen by the International Agency for Research on Cancer (IARC, 1997). The silicotic response to inhalation of crystalline silica is associated with the persistent activation of alveolar macrophages, which secrete inflammatory cytokines like Tumor Necrosis Factor-α (TNF-α) or Interleukin (IL)-1β. It also leads to fibrosis and in later stages to lung cancer (Saffiotti, 2005). The inflammatory effect in quartz-induced silicosis is mediated by activation of the NLRP3 inflammasome through phagosomal destabilisation as was currently revealed

in pioneering *in vitro* studies (Cassel et al., 2008; Hornung et al., 2008). The NLRP3 inflammasome is a multi-protein complex within the cytoplasm of antigen-presenting cells (APC), neutrophils and keratinocytes. It can be activated by conserved pathogen structures, by intrinsic danger signals like ATP, uric acid or low intracellular potassium concentrations, but also by inorganic materials like crystalline silica and aluminium salts (Hornung et al., 2008; Petrilli et al., 2007). Activation of NOD-like proteins leads to ASC recruitment and activation of Caspase-1, which in turn cleaves proIL-1β and proIL-18. In contrast to the rather well-understood mechanism by which crytalline silica induces persistent inflammation, relatively little is known about adverse health effects caused by amorphous silica nanoparticles after inhalation (Merget et al., 2002). Amorphous silica nanoparticles are known to induce a strong, but transient inflammatory reaction and fibrosis in the lungs of mice (Cho et al., 2007; Choi et al., 2008) and rats (Johnston et al., 2000). Yet, the molecular mechanism whereby amorphous silica triggers an acute inflammatory response is incompletely understood.

NOD receptor-activation and subsequent cytokine release is associated with a variety of diseases besides silicosis, including inflammatory diseases of the intestine (Kidd et al., 2009; Li et al., 2009b). Although the intestine generally appears to be less sensitive to inflammatory challenges compared with the lung, a higher susceptibility to inflammatory stimuli may occur in the context of inflammatory bowel diseases (IBD). In experimental colitis, it was shown that the IL-18 level was strongly elevated in mice upon treatment with dextrane sodium sulphate. Moreover, colitis could be blocked by inhibition of Caspase-1, indicating an important role for inflammasome-induced effects in IBD (Bauer et al., 2007). Intestinal immune homeostasis is regulated to a great extent by DC, which are the main inducers of adaptive immune responses upon stimulation with pathogenic components. In the intestinal mucosa, distinct subsets of DC are in charge of keeping the balance between tolerance towards harmless food compounds and gut commensals on the one hand and inflammatory reactions towards pathogens on the other hand (Rescigno, 2009). This delicate balance might be affected by nanoparticles present in our food. In this study, we analysed the effect of TiO_2 and silica nanoparticles as model particles with potential relevance for intestinal uptake on the activation status of DC and the elicitation of inflammasome activation.

Methods

Particles. The well-known inflammogenic and fibrotic quartz dust DQ12 (Dörentruper quartz, batch 6), with a mean diameter of 0.96 µm and a BET surface area of 10 m^2/g was used as a positive control. Detailed size distribution characteristics are described elsewhere (Albrecht et al., 2004). For all other particles, information on surface area and primary particle size was provided by the companies. In addition to DQ12, a fine TiO_2 (TiO_2f) sample, pure anatase with a BET of 10 m^2/g and a primary particle size range from 40 – 300 nm was used (Sigma Aldrich). The nanosized samples used in our study were p25 TiO_2 (TiO_2uf; Degussa/Evonik, composed of 77% anatase and 23% rutile, with a BET of 50 m^2/g and a primary particle size range from 20 – 80 nm), and amorphous fumed silica (SiO_2uf; Sigma Aldrich, with a BET of 200 m^2/g and a mean primary particle diameter of 14 nm). Both samples of TiO_2 as well as the amorphous silica nanoparticles have been used in previous studies (Borm et al., 2004; Singh et al., 2007; Gerloff et al., 2009). Before particles were used in experiments, they were baked at 220°C for 18 hours to destroy potential contaminating endotoxins. Thereafter, particles were suspended in complete medium and sonicated for 30 min in a Sonorex TK52 waterbath (60 W, 35 kHz). Cells were treated with the various particles at concentrations and time intervals as specified in the Results section.

Flow cytometry (FACS). Anti-MHC-II (M5/114.15.2, APC labelled), anti-CD11c (N418, FITC labelled), anti-CD80 (16-10A1, PE labelled) and anti-CD86 (PO3.1, PE labelled) were purchased from eBioscience. Anti-CD11c (HL3, PE labelled) was from BD Pharmingen. For FACS analysis, cells were stained in phosphate buffered saline (PBS), containing 0.5% FCS (PAN) and 2 mmol EDTA (FACS buffer) on ice for 15 min.

To stain apoptotic cells, cells were incubated with 0.5 µg/ml ethidium monoazide bromide (Invitrogen) on ice in the dark for 10 min and for another 20 min under direct light. Cells were washed twice in FACS buffer and further stained with PE-labelled anti-CD11c and APC-labelled anti-MHC-II antibodies in FACS buffer for 15 min on ice in the dark. Cells were washed once and stained with Alexa 488-labelled Annexin-V (Alexis) in Annexin-V (BD Pharmingen) binding buffer for 15 min at room temperature. Cells were then immediately analysed by FACS.

In order to assess the production of reactive oxygen species (ROS), particle-treated bone marrow-derived DC (BMDC) were harvested on d7 and incubated with 100 µM cell permeable 2'.7'-dichlorodihydrofluorescein diacetate (DCFDA; Sigma) for 30 min at 37 °C in RPMI 1640 (PAA), washed once and stained with anti-CD11c and anti-MHC-II for 15 min in FACS buffer on ice. Flow cytometry was performed using a FACSCalibur flow cytometer (BD

Bioscience). Data were acquired by CellQuest (BD Bioscience) and analysed by FlowJo software (Tree Star).

Mice. C57BL/6 mice were originally purchased from Harlan-Winkelmann and bred at the IUF animal facility under specific pathogen free conditions. Caspase-1-deficient mice (Li et al., 1995) and littermate control mice were bred at the Institute of Cell Biology, ETH, Zürich, Switzerland. NLRP3-deficient mice were kindly provided by Genentech (Mariathasan et al., 2006). All other mice used in the experiments were kept under specific pathogen-free conditions in the animal facility of the Institut für Umweltmedizinische Forschung, Düsseldorf, Germany

DC Preparation. Bone marrow cells were flushed from tibias and femurs of the mice with ice-cold PBS, resuspended and filtered once through a cell strainer (BD Falcon). Cells were washed once in PBS and plated at a concentration of 5 x 10^5 cells/ml in RPMI 1640, supplemented with 10% FCS, L-glutamine, penicillin-streptomycin and β-mercaptoethanol (Invitrogen). For differentiation, 2% supernatant of GM-CSF transfected X63Ag8-653-cells (Karasuyama and Melchers 1988) was added to the cultures. On d3 the same volume of complete medium was added to the cultures and on d6 non-adherent cells were harvested and used for experiments.

In vitro stimulation of BMDC. BMDC were harvested at d6 and plated at a concentration of 1 x 10^6 cells/ml in 2 ml onto six well plates (Grainer bio-one) in complete medium. For FACS analysis, cells were stimulated with 1 µg/ml LPS E.coli 0111:B4 (Sigma-Aldrich) or particles at concentrations from 5 – 50 µg/cm^2 in a total volume of 4 ml for 18 hours. Cells were then scraped from the bottom of the dishes and stained for FACS analysis.
To assess inflammasome activation, BMDC were plated at 1 x 10^6 cells/ml and stimulated with 0.1 µg/ml LPS on d6. After 6 hours 20 or 40 µg/cm^2 particles were added to the cultures and supernatants were harvested, centrifuged and immediately frozen at -80°C. In some experiments cells were incubated with 1.5 µg/ml Cytochalasin-D (Sigma) for 30 min at 37°C in serum-free RPMI 1640 to block actin-polymerisation (Haberzettl et al., 2007) after prestimulation with LPS and before particles were added to the cultures for additional 2 hours. Cells were then harvested and supernatants collected. Alternatively, ATP (Roche) was added to the cultures at a concentration of 5 mM, 90 min after Cytochalasin-D-treatment. Cells were harvested and supernatants collected after additional 30 min.

Particle uptake by DC. Uptake of particles by DC was evaluated by means of flow-cytometry according to an established method (Haberzettl et al., 2007; Haberzettl et al., 2008).

ELISA. IL-1β concentrations in cell culture supernatants were determined using an IL-1β ELISA DuoSet Development kit from R&D Systems, according to the manufacturer's instructions. Extinction (OD) was measured at 450 and 570 nm with an ELx 800 universal microplate reader (Bio-Tek).

Statistics. Means were calculated from at least three experiments and are expressed as mean + standard error of the mean (SEM) or as median + interquartile range. Statistical analysis was performed with the Student's paired or unpaired t-test as indicated in the Figure legends.

Results

To analyse the effect of particles on the differentiation of DC, BMDC were incubated in the presence or absence of LPS (TLR4 ligand) as controls, or 20 and 50 μg/cm^2 particles for 18 hours. Toxicity was measured by cell counting and the maturation status of the cells was assessed by FACS analysis. MHC-II, CD80 and CD86 molecules are strongly upregulated on the cell surface of DC upon maturation and were therefore used as maturation markers. The frequency of CD11c$^+$ DC in BMDC cultures was between 60 and 90% in all experiments as depicted in Figure 1 A and B. Stimulation with LPS led to an increase in cell number, whereas treatment with SiO_2uf particles significantly reduced cell numbers by about 50%. DQ12 also led to a decrease in cell numbers, even though the effect was not as strong as with silica nanoparticles. Neither TiO_2uf nor TiO_2f had a notable influence on cell viability (Fig.1 C). While MHC-II molecules were strongly upregulated on the DC surface after culture with TiO_2uf, MHC-II expression was only slightly elevated by TiO_2f at the highest concentration. Both types of silica particles caused a significantly enhanced MHC-II expression in BMDC, independent of their size and structure (Fig.1 D). After loading of BMDC with TiO_2uf and both types of silica, CD80 and CD86 expression was slightly increased. However, there was no increase in CD80 and CD86 expression on BMDC treated with TiO_2f (Fig.1 E-F). Taken together, all particles tested, with the exception of TiO_2f, induced maturation of the cells, while only SiO_2uf significantly affected cell viability, indicating that particles can directly stimulate DC.

[Insert Figure 1 about here]

To investigate whether the reduced cell numbers were due to enhanced apoptosis, BMDC were incubated with 5, 20 and 40 µg/cm^2 particles or LPS for 18 hours and analysed by Annexin V staining. The highest frequency of apoptotic BMDC was observed in the SiO_2uf-treated group with 47.08% +/- 5.913%, and 25.43% +/- 21.11% in the DQ12 cultures at a concentration of 40 µg/cm^2 (Fig.2 C-D). TiO_2uf and TiO_2f particles did not lead to notably enhanced frequencies of apoptotic cells at the concentrations applied (Fig.2 A-B). Immature BMDC were defined as CD11c$^+$ MHC-II^{low} cells and mature DC as CD11c$^+$MHC-II^{high} cells. Remarkably, SiO_2uf and DQ12 particle-induced apoptosis was mainly seen in immature BMDC, whereas mature cells were only moderately affected. Taken together, crystalline as well as amorphous silica, but not TiO_2 particles, induce apoptosis in BMDC. For BMDC treated with SiO_2 particles, the enhanced frequency of MHC-II^{high} DC, shown in Fig. 1D may partly be explained by selective loss of MHC-II^{low} immature DC through particle induced apoptosis.

[Insert Figure 2 about here]

Next, we determined the capacity of the tested particles to induce oxidative stress in DC. For this purpose, BMDC were treated with 20 and 40 µg/cm^2 particles and were then loaded with cell permeable DCFDA, which is converted to the fluorescent DCF by ROS within the cell. In TiO_2uf particle-treated BMDC but not in TiO_2f particle-treated cells, there was a strong, concentration-dependent enhancement of ROS-production (Fig.3 A). The quartz sample and the amorphous SiO_2 nanoparticles did not have a significant effect on the overall oxidative stress in BMDC regardless of their size and chemical structure (Fig.3 B). LPS also did not induce ROS production. These data indicate a size-dependency of the TiO_2-induced oxidative stress response in DC.

[Insert Figure 3 about here]

To test, whether particles activate DC directly, we also assessed the production of the inflammatory cytokine IL-1β from particle-treated cells. It is known that after inhalation of quartz, active IL-1β can be detected in the lungs of mice. Quartz induces IL-1β secretion from immune cells via activation of the NLRP3 inflammasome (Hornung et al., 2008). To investigate whether the particles - and in particular nanoparticles - used in this study activate DC via a similar mechanism, production of mature IL-1β was analysed in the supernatant of BMDC after cultivation with 20 and 40 µg/cm^2 particles. To induce transcription of the pro-form of IL-1β, cells were pre-stimulated with LPS six hours prior to particle loading. IL-1β was detected in the supernatant already after stimulation with LPS only, but was enhanced

markedly after stimulation with both silica particles. Cells treated with SiO_2uf particles secreted 2060 pg/ml +/- 445.3 pg/ml and DQ12-treated cells released 2174 pg/ml +/- 778.5 pg/ml at the highest concentration in comparison to 253.2 pg/ml +/- 75.0 pg/ml after LPS stimulation. TiO_2uf particles also induced a significant upregulation of IL-1β to 973.9 pg/ml +/- 209.8 pg/ml, whereas TiO_2f particles had no effect on IL-1β secretion (Fig.4). Thus, all particles tested, with the exception of TiO_2f, were able to induce the maturation of IL-1β.

[Insert Figure 4 about here]

Maturation of proIL-1β is mediated by activated Caspase-1, which is cleaved upon activation of the inflammasome and then in turn cleaves proIL-1β. To verify the involvement of Caspase-1 in nanoparticle-mediated IL-1β-production, BMDC from WT and Caspase-1-deficient mice were cultured with 20 and 40 µg/cm^2 particles after prestimulation with LPS. As described above, IL-1β release was strongest in WT cells cultured with silica nanoparticles, whereas TiO_2uf-treated cells produced only low amounts of mature IL-1β. In contrast, using BMDC from Caspase-1 deficient mice, IL-1β levels were reduced to near background level after treatment with TiO_2uf, and reduced significantly in both silica particle treated groups (Fig.5 A, B and C). We noticed that IL-1β levels were generally higher in the experiments performed with Caspase-1-deficient BMDC and respective WT littermate control cells compared with all other experiments shown in this study. This difference may depend on different genetic backgrounds of the mice, or differences in animal housing. Taken together, these data show that particle-induced IL-1β release is dependent on Caspase-1 activation, and therefore likely mediated by the inflammasome. In addition, we assessed whether particle-mediated Caspase-1 activation takes place in association with the NLRP3 inflammasome, as was described for quartz particles (Hornung et al., 2008). We therefore analysed IL-1β expression in NLRP3-deficient DC and WT DC, after cultivation with particles. IL-1β secretion was reduced to background levels after culture of NLRP3-deficient DC with all particles (Fig. 5 D-F), strongly indicating an activation of the NLRP3 inflammasome in DC by TiO_2uf as well as SiO_2uf, similar to DQ12.

[Insert Figure 5 about here]

Since inflammasome activation by quartz is known to depend on particle uptake and delivery in lysosomes (Hornung et al., 2008), we blocked actin-dependent uptake with Cytochalasin-D to determine if uptake was also necessary to activate the inflammasome for the TiO_2 and SiO_2 nanoparticles tested in this study. Since the granularity of the cells has been proven to be a valid estimate of particle uptake (Haberzettl et al., 2007; Haberzettl et al., 2008), we

determined the granularity of the cells by FACS. A strongly enhanced granularity was observed when cells were cultured in the presence of both titanium particles and DQ12 (Fig.6 A, B and D). In contrast, SiO_2uf particles only led to a slightly increased side scatter (Fig.6 C). By inhibiting endocytosis via Cytochalasin-D, granularity was reduced in BMDC, treated with both TiO_2 particles regardless of their size and both silica particles (Fig.6 A - D), indicating that particle uptake is at least partly mediated by an actin-dependent mechanism.

[Insert Figure 6 about here]

To assess whether the inhibition of actin-dependent uptake of the particles has an influence on the production of active IL-1β, cytokine release was measured in the presence or absence of Cytochalasin D. IL-1β secretion from particle-treated BMDC was reduced to background levels in all groups (Fig.7 A-D), when actin polymerisation was blocked by Cytochalasin D. To assure that Cytochalasin D treatment did not affect IL-1β secretion as such, inflammasome activation was also induced by ATP, which occurs independent of endocytosis. In contrast to particle-induced IL-1β-production, release of IL-1β was unchanged after ATP-stimulation (Fig.7 E), indicating that the IL-1β secretion machinery was still intact after Cytochalasin D treatment. We therefore conclude that particle uptake via actin-dependent mechanisms is essential for the induction of the inflammasome by TiO_2 and SiO_2 nanoparticles.

[Insert Figure 7 about here]

Discussion

DC act as gatekeepers in the intestine and are indispensable for the induction of immune responses against pathogens and the maintenance of tolerance towards food antigens and luminal commensals (Rescigno and Matteoli, 2008; Varol et al., 2009). In addition, DC and macrophages are important regulators of intestinal homeostasis and directly influence the pathogenesis and severity of IBD (Abe et al., 2007; Reindl et al., 2007; Takeda et al., 1999). In this study, the immunogenic potential of TiO_2 and SiO_2 particles was analysed in murine BMDC in comparison to crystalline silica particles, which are known to exert inflammatory reactions (Albrecht et al., 2004). Micronsized TiO_2 and amorphous silica particles have been used in the food sector for a long time already. Amorphous, fumed SiO_2 nanoparticles with identical properties and size as the ones that were analysed in this study, are already contained in food, and it seems conceivable that nanosized TiO_2, or newly engineered

nanoparticles of other chemical composition may also be used for food production in the future (Chaudhry et al., 2008; Powell et al., 2009). We therefore tested SiO_2, and TiO_2 nanoparticles as model particles for their potential ability to influence the activation status of DC. Whereas micronsized TiO_2 particles were relatively inert and had only minor influences on BMDC viability, maturation, and activation of the inflammasome, amorphous silica nanoparticles and the nanosized TiO_2 particles induced partial maturation of BMDC and activation of the inflammasome comparable to crystalline silica. Amorphous silica particles, in particular, induced apoptosis in a substantial fraction of immature BMDC, whereas TiO_2uf particles stood out as significant inducers of ROS generation in BMDC cultures. Although composed of primary particles in the nanosize range, both the TiO_2uf and SiO_2uf used in our study are known to appear mainly as larger aggregates and/or agglomerates in cell culture conditions. However, this typical aggregation/agglomeration is also likely to occur when these nanoparticles are present in food.

Inflammasomes are multiprotein complexes that consist of intracellular receptors of the Nod-like family, ASC adaptor proteins and Caspase-1, eventhough inflammasomes are known, that do not require NLR-triggering and ASC-recruitment (Bryant et al., 2009). The latter is activated upon stimulation and cleaves the pro-forms of the pro-inflammatory cytokines IL-1β and IL-18 to become functionally active. Recently, it was reported that crystalline silica potently activates the inflammasome in APC via a mechanism termed lysosomal rupture, mediated via release of Cathepsin B into the cytosol (Hornung et al., 2008). At the same time it was reported that crystalline silica triggers NLRP3 inflammasome activation via the induction of ROS (Dostert et al., 2008). Further studies will be required to reconcile these two different concepts. To analyse whether TiO_2 particles and amorphous silica nanoparticles can also activate the inflammasome, we measured the production of the active form of IL-1β in the supernatant of particle-treated cells. For this purpose, BMDC were pretreated with LPS to induce transcription of the pro-form of IL-1β, which is then cleaved to its mature form following activation of the inflammasome (Dinarello et al., 2010). As expected, a strong secretion of IL-1β was observed in BMDC treated with crystalline silica. Remarkably, amorphous silica nanoparticles induced IL-1β to similar amounts as crystalline particles. Furthermore, TiO_2 nanoparticles induced maturation of IL-1β in BMDC as well, whereas TiO_2 micron-sized particles did not. Using Caspase-1 or NLRP3-deficient BMDC, we demonstrated that the secretion of mature IL-1β was dependent on Caspase-1 and NLRP3, implicating activation of the NLRP3-inflammasome by the particles tested, with the exception of micron-sized TiO_2 particles. Since IL-1β secretion was not entirely absent in Caspase-1 or NLRP3-deficient BMDC cultures, it is apparent that some cleavage of IL-1β can also be achieved by alternative mechanisms, independent of Caspase-1. In line with this, neutrophil- and mast cell-derived serine proteases were shown to be able to produce bioactive IL-1β

after LPS stimulation (Guma et al., 2009). In a recent study, in which BMDC were treated with various nanoparticles, production of mature IL-1β was not observed, in contrast to our study (Palomäki et al., 2010). This discrepancy might be explained by the fact that Palomäki et al. did not induce the expression of pro-IL-1β by pretreatment of the cells with LPS. Recent studies however have shown that not only pro-IL-1β expression, but also NLRP3 expression itself has to be primed by microbial stimuli such as LPS (Bauernfeind et al. 2009, Franchi et al., 2009). Thus a bona fide NLRP3 stimulus might not be active in resting, unprimed cells. Nanoparticles that pass through the gut, however, might likely be coated with microbial components like LPS from the gut flora, which may enhance their reactivity (Powell et al., 2000).

To further identify the mechanisms that lead to particle-induced inflammasome activation, we assessed, whether particle uptake into the cells is essential, as was shown for crystalline silica particles (Hornung et al., 2008), or whether amorphous silica and TiO_2 nanoparticles induce the inflammasome by alternative pathways. For the DQ12 particles used in the present study, uptake into alveolar macrophages was previously shown to occur via actin-dependent phagocytosis (Haberzettl et al., 2007). For nanoparticles, various mechanisms of uptake have been described (reviewed in Unfried et al., 2007). The materials used in our present study typically appear in agglomerated form. DC sample their surrounding continuously via macropinocytosis. Therefore, it seems very likely that the nanoparticles used in our current study preferably enter DC via this actin-dependent mechanism, which like endocytosis can be blocked by Cytochalasin-D (Amyere et al., 2002). As depicted in Figure 7, the amounts of IL-1β secreted from Cytochalasin-D pretreated cells were reduced below background level in all groups. In contrast, ATP-treated BMDC released normal amounts of IL-1β after Cytochalasin-D-treatment, proving that the ability of the cells to secrete IL-1β was not affected by blocking actin polymerisation as has been described earlier (Hornung et al., 2008). Taken together, these data indicate, that particle uptake via actin-dependent mechanisms is required for the activation of the inflammasome.

It is well established, that inflammasome activation mediated by crystalline silica particles is induced via lysosomal rupture in DC, which goes along with induction of necrosis or apoptosis (Hornung et al., 2008; Li et al., 2009a). At least for alveolar macrophages it was shown that ROS formation is a trigger of inflammasome activation (Cassel et al., 2008; Dostert et al., 2008). We believe that amorphous silica nanoparticle-mediated inflammasome activation in murine BMDC might be triggered by processes involving the induction of cell death independently of ROS formation, whereas TiO_2 nanoparticles might induce the NLRP3 inflammasome via a ROS-dependent mechanism.

Inflammasome activation is associated with several human diseases. It is for instance a main event in the development of lung fibrosis following chronic inhalation of crystalline silica dusts (Cassel et al., 2008), and is associated with inflammatory diseases of the intestine. Interestingly, elevated IL-1β levels were found in colonic biopsies of colitis patients (Olson et al., 1993), and in mice with experimental colitis. Symptoms of DSS-induced colitis were ameliorated when Caspase-1 was inhibited or absent, arguing for an involvement of inflammasome activation in IBD (Bauer et al., 2007; Siegmund et al., 2001).

Besides inflammasome activation, we also assessed the expression of maturation markers on primary BMDC after culture with particles for 18 hours. Upon treatment with TiO_2 nanoparticles, MHC-II expression was upregulated almost to the same extent as after LPS stimulation. Our data show that the effect of TiO_2 strongly depends on particle size and surface area, as was shown for other endpoints before (Oberdörster et al., 1994; Oberdörster et al., 2005; Rahman et al., 2002). In contrast to these findings, Palomäki et al. found no upregulation of maturation markers on BMDC at comparable concentrations of TiO_2 nanoparticles (Palomäki et al., 2010). These differences might be explained by differences in the mouse-strains used, since for this study, we used C57BL/6 mice, whereas Palomäki et al. used BALB/c mice. These two mouse strains are known for their contrasting sensitivity to crystalline silica-induced fibrosis (Moore and Hogaboam, 2008). Besides TiO_2 nanoparticles, also amorphous silica nanoparticles and crystalline silica significantly increased expression of MHC-II as well as CD80/CD86 on BMDC, independently of their chemical structure. To assess whether the mature phenotype of the BMDC cultures after particle exposure might also result from selective death of immature BMDC as opposed to mature BMDC, we next assessed whether particles directly induce cytotoxicity. A significantly lower cell number was only observed in cultures with amorphous silica nanoparticles. In contrast to other more reactive particles, TiO_2 particles induce cytotoxicity only at relatively high concentrations (Monteiller et al., 2007; Wang et al., 2007; Singh et al., 2007). These observations are in line with the relatively mild decrease in cell number with both types of TiO_2 when compared with other particles (Fig.1). In contrast to TiO_2, crystalline silica is a highly reactive and cytotoxic material. It was shown that crystalline silica particles potently induce cytotoxicity in many cell types (Iyer et al., 1996; Sarih et al., 1993; Thakur et al., 2009). Although amorphous silica is less potent than crystalline silica in causing chronic lung disease after inhalation (Merget et al., 2002), several studies could demonstrate cytotoxicity by amorphous nanoparticles with size-dependent induction of cell death in different cell types (Napierska et al., 2009; Park and Park, 2009; Waters et al., 2009). In our experiments with BMDC, amorphous silica nanoparticles were the most toxic particles. This indicates that these particles are not inert and do have proinflammatory properties.

For further analysis of the toxic effects of the particles, we assessed which cells are primarily affected by apoptosis following particle exposure using Annexin-V- and EMA-staining. Apoptosis has been observed after inhalation of high concentrations of amorphous silica (Johnston et al., 2000), and has also been discussed as an important mechanism whereby crystalline silica causes fibrosis (Borges et al., 2001). Neither nanosized nor micronsized TiO_2 particles induced apoptosis in the cells. However, amorphous silica nanoparticles as well as crystalline silica dose dependently induced cell death mainly in immature BMDC, whereas the mature fraction of BMDC remained largely unaffected by crystalline silica and showed only a moderate increase in cell death when treated with amorphous silica nanoparticles. We hypothesize, that due to a more active metabolism, enhanced macropinocytosis and higher proliferative activity, immature BMDC are more prone to undergo apoptosis upon particle exposure than fully mature BMDC. Thus, our results identify immature DC as sensitive target cells for particle induced toxicity, which might be especially important in the gut, where immature DC play an important role in the maintenance of homeostasis (Turnbull et al., 2005).

In addition to particle-induced apoptosis, we analysed the generation of ROS, which is critically involved in cell death (Broaddus et al., 1996). ROS may also serve as cellular mediators in inflammatory processes by activation of inflammasomes and the secretion of proinflammatory cytokines (Martinon et al., 2009). Interestingly, only TiO_2 nanoparticles but not larger TiO_2 particles led to the formation of ROS at equal mass dose, indicating that this effect is dependent on the particle surface. Neither SiO_2 nanoparticles nor quartz induced ROS in our experiments. It is well known, that nanosized TiO_2 particles are much more reactive than micronsized TiO_2 particles (Oberdörster et al., 1994; Oberdörster et al., 2005; Rahman et al., 2002). Thus TiO_2 nanoparticles induce ROS formation in mouse macrophage, brain microglia, human epithelial and fibroblast cell lines, with TiO_2 anatase nanoparticles inducing greater amounts of ROS than TiO_2 rutile nanoparticles. The TiO_2 nanoparticles used in our experiments were composed of 77% anatase and 23% rutile. This structural distribution is reported to cause intermediate levels of ROS, starting at 3 mg/ml TiO_2 in human dermal fibroblast- and lung epithelial-cell lines (Long et al., 2006; Oberdörster et al., 2005; Sayes et al., 2006). In A549 human lung epithelial cells, TiO_2 nanoparticle-induced ROS generation was observed upon incubation of the cells at very high concentrations, i.e. 400 µg/cm² (Singh et al., 2007). In contrast, others did not observe ROS formation under TiO_2 nanoparticle-induced stress in mouse RAW 264.7 macrophages and also not in human monocyte-derived DC (Muller et al., 2010; Xia et al., 2006). These high variabilities in particle-induced ROS generation appear to be dependent on the cell-type analysed. Nevertheless, it is difficult to compare the susceptibilities of the different cell-types, because of non-uniformly depicted mass doses of the particles that were used in the experiments.

Taken together, our data demonstrate that materials other than crystalline silica activate the NLRP3 inflammasome, an important pro-inflammatory pathway. Indeed, this indicates a potential health hazard for these materials, although cumulative dosimetry aspects need to be taken into account: Crystalline silica is much more biopersistent in lung tissue after inhalation than amorphous silica because of its specific physicochemical properties. The resulting dose accumulation and associated persistent inflammatory response provides an explanation for the severe pathogenicity of crystalline silica (i.e. fibrosis, tumorigenesis). Johnston et al. (2000) compared the pulmonary toxicity of crystalline (fine) and amorphous (nano) SiO_2 and demonstrated that the latter also causes inflammation, but in contrast to the former, this effect was transient. With regard to the rather insoluble TiO_2uf, we refer to the recent study by Trouiller et al. (2009). They showed strong genotoxic effects after oral application of the same nanoparticles as used in our study and suggested that genotoxicity might be linked to the systemic inflammatory responses observed in the exposed animals. Taken together, our current findings on the activation of the inflammasome for both types of nanoparticles support their reported ability to cause inflammation (*in vivo*) and, depending on dosimetry issues, associated pathogenicity. In the gut, DC activated through nanoparticles could act as inducers of immune responses in the absence of pathogens or amplify immune reactions in the presence of pathogens. After oral uptake, particles thus might have adverse effects during ongoing chronic inflammatory diseases of the intestine. Therefore, we conclude that nanoparticles considered to be used as food constituents in the future, should be carefully studied for their immunostimulatory capacity.

Acknowledgements

This study was financially supported by grants from the German Research Council (Deutsche Forschungsgemeinschaft – Graduate College GK 1427 (to I.F. and R.P.F.S.), SFB 704 (to I.F. and V.H.), and FOR 729 (to I.F.). We are grateful to Heike Weighardt, Catrin Albrecht, Ursula Krämer and Jason Cline for discussion and help on the manuscript.

References

Abe K, Nguyen KP, Fine SD, Mo JH, Shen C, Shenouda S, Corr M, Jung S, Lee J, Eckmann L, Raz E. Conventional dendritic cells regulate the outcome of colonic inflammation independently of T cells. Proc Natl Acad Sci U S A 2007;104(43):17022-17027.

Albrecht C, Schins RPF, Höhr D, Becker A, Shi T, Knaapen AM, Borm PJA. Inflammatory time course following quartz instillation: role of TNF-alpha and particle surface. Am J Respir Cell Mol Biol 2004; 31: 292-301.

Aline F, Brand D, Pierre J, Roingeard P, Severine M, Verrier B, Dimier-Poisson I. Dendritic cells loaded with HIV-1 p24 proteins adsorbed on surfactant-free anionic PLA nanoparticles induce enhanced cellular immune responses against HIV-1 after vaccination. Vaccine 2009;27(38):5284-5291.

Amyere M, Mettlen M, Van Der Smissen P, Platek A, Payrastre B, Veithen A, Courtoy PJ. Origin, originality, functions, subversions and molecular signalling of macropinocytosis. Int J Med Microbiol 2002;291(6-7):487-494.

Bauer C, Loher F, Dauer M, Mayer C, Lehr HA, Schonharting M, Hallwachs R, Endres S, Eigler A. The ICE inhibitor pralnacasan prevents DSS-induced colitis in C57BL/6 mice and suppresses IP-10 mRNA but not TNF-alpha mRNA expression. Dig Dis Sci 2007; 52(7):1642-1652.

Bauernfeind FG, Horvath G, Stutz A, Alnemri ES, Mac Donald K, Speert D, Fernandes-Alnemri T, Wu J, Monks BF; Fitzgerald KA, Hornung V, Latz E. J Immunol. 2009; 15;183(2):787-791.

Behrens I, Pena AI, Alonso MJ, Kissel T. Comparative uptake studies of bioadhesive and non-bioadhesive nanoparticles in human intestinal cell lines and rats: the effect of mucus on particle adsorption and transport. Pharm Res 2002;19(8):1185-1193.

Borges VM, Falcao H, Leite-Junior JH, Alvim L, Teixeira GP, Russo M, Nobrega AF, Lopes MF, Rocco PM, Davidson WF et al. Fas ligand triggers pulmonary silicosis. J Exp Med 2001;194(2):155-164.

Borm PJ, Schins RP, Albrecht C. Inhaled particles and lung cancer, part B: paradigms and risk assessment. Int J Cancer 2004;110(1):3-14.

Bouwmeester H, Dekkers S, Noordam MY, Hagens WI, Bulder AS, de Heer C, ten Voorde SE, Wijnhoven SW, Marvin HJ, Sips AJ. Review of health safety aspects of nanotechnologies in food production. Regul Toxicol Pharmacol 2009;53(1):52-62.

Broaddus VC, Yang L, Scavo LM, Ernst JD, Boylan AM. Asbestos induces apoptosis of human and rabbit pleural mesothelial cells via reactive oxygen species. J Clin Invest 1996;98(9):2050-2059.

Bryan NB, Dorfleutner A, Rojanasakul Y, Stehlik C. Activation of inflammasomes requires intracellular redistribution of the apoptotic speck-like protein containing a caspase recruitment domain. J Immunol 2009;182(5):3173-3182.

Bryant C, Fitzgerald KA. Molecular mechanisms involved in inflammasome activation. Trends in Cell Biology 2009;19(9):455-464

Cassel SL, Eisenbarth SC, Iyer SS, Sadler JJ, Colegio OR, Tephly LA, Carter AB, Rothman PB, Flavell RA, Sutterwala FS. The Nalp3 inflammasome is essential for the development of silicosis. Proc Natl Acad Sci U S A 2008;105(26):9035-9040.

Chaudhry Q, Scotter M, Blackburn J, Ross B, Boxall A, Castle L, Aitken R, Watkins R. Applications and implications of nanotechnologies for the food sector. Food Addit Contam Part A Chem Anal Control Expo Risk Assess 2008;25(3):241-258.

Chen J, Dong X, Zhao J, Tang G. In vivo acute toxicity of titanium dioxide nanoparticles to mice after intraperitioneal injection. J Appl Toxicol 2009;29(4):330-337.

Cho WS, Choi M, Han BS, Cho M, Oh J, Park K, Kim SJ, Kim SH, Jeong J. Inflammatory mediators induced by intratracheal instillation of ultrafine amorphous silica particles. Toxicol Lett 2007;175(1-3):24-33.

Choi M, Cho WS, Han BS, Cho M, Kim SY, Yi JY, Ahn B, Kim SH, Jeong J. Transient pulmonary fibrogenic effect induced by intratracheal instillation of ultrafine amorphous silica in A/J mice. Toxicol Lett 2008;182(1-3):97-101.

Dinarello CA. IL-1: Discoveries, controversies and future directions. Eur. J. Immunol. 2010;40:595–653.

Dostert C, Petrilli V, Van Bruggen R, Steele C, Mossman BT, Tschopp J. Innate immune activation through Nalp3 inflammasome sensing of asbestos and silica. Science 2008;320(5876):674-677.

Elamanchili P, Lutsiak CM, Hamdy S, Diwan M, Samuel J. "Pathogen-mimicking" nanoparticles for vaccine delivery to dendritic cells. J Immunother 2007;30(4):378-395.

Franchi L, Egnebrod T, Nunez G. Cutting edge: TNF-alpha mediates sensitization to ATP and silica via the NLRP3 inflammasome in the absence of microbial stimulation. J Immunol 2009;15;183(2):792-796.

Grassian VH, O'Shaughnessy P T, Adamcakova-Dodd A, Pettibone JM, Thorne PS. Inhalation exposure study of titanium dioxide nanoparticles with a primary particle size of 2 to 5 nm. Environ Health Perspect 2007;115(3):397-402.

Gerloff K, Albrecht C, Boots AW, Förster I, Schins RPF. Cytotoxicity and oxidative DNA damage by nanoparticles in human intestinal Caco-2 cells. Nanotoxicology 2009;3(4):355-364.

Guma M, Ronacher L, Liu-Bryan R, Takai S, Karin M, Corr M. Caspase 1–Independent Activation of Interleukin-1 in Neutrophil-Predominant Inflammation. Arthritis & Rheumatism 2009;60(12):3642-3650.

Haberzettl P, Schins RPF, Borm PJA, Albrecht C. Actin plays a crucial role in the phagocytosis and biological reponse to respirable quartz particles in macrophages. Arch Toxicol 2007;81:459-470.

Haberzettl P, Schins RPF, Höhr D, Wilhelmi V, Borm PJA, Albrecht C. Impact of the FcII-receptor on quartz uptake and inflammatory response by alveolar macrophages. Am J Physiol Lung Cell Mol Physiol 2008;294:L1137-L1148.

Hillyer JF, Albrecht RM. Gastrointestinal persorption and tissue distribution of differently sized colloidal gold nanoparticles. J Pharm Sci 2001;90(12):1927-1936.

Hornung V, Bauernfeind F, Halle A, Samstad EO, Kono H, Rock KL, Fitzgerald KA, Latz E. Silica crystals and aluminum salts activate the NALP3 inflammasome through phagosomal destabilization. Nat Immunol 2008;9(8):847-856.

International Agency for Research on Cancer. IARC Working Group on the evaluation of carcinogenic risks to humans: Silica, some silicates, coal dust and para-aramid fibrils. Monographs on the Evaluation of the Carcinogenic Risks to Humans. 1997;Vol. 68, IARC, Lyon, France.

Iyer R, Hamilton RF, Li L, Holian A. Silica-induced apoptosis mediated via scavenger receptor in human alveolar macrophages. Toxicol Appl Pharmacol. 1996;141(1):84-92.

Johnston CJ, Driscoll KE, Finkelstein JN, Baggs R, O'Reilly MA, Carter J, Gelein R, Oberdorster G. Pulmonary chemokine and mutagenic responses in rats after subchronic inhalation of amorphous and crystalline silica. Toxicol Sci 2000;56:405–413.

Karasuyama,H. & Melchers,F. Establishment of mouse cell lines which constitutively secrete large quantities of interleukin 2, 3, 4 or 5, using modified cDNA expression vectors. Eur J Immunol 1988;18:97-104.

Kidd M, Gustafsson BI, Drozdov I, Modlin IM. IL1beta- and LPS-induced serotonin secretion is increased in EC cells derived from Crohn's disease. Neurogastroenterol Motil 2009;21(4):439-450.

Lamprecht A, Schafer U, Lehr CM. Size-dependent bioadhesion of micro- and nanoparticulate carriers to the inflamed colonic mucosa. Pharm Res 2001;18(6):788-793.

Lamprecht A, Yamamoto H, Takeuchi H, Kawashima Y. Nanoparticles enhance therapeutic efficiency by selectively increased local drug dose in experimental colitis in rats. J Pharmacol Exp Ther 2005.315(1):196-202.

Li H, Ambade A, Re F. Cutting edge: Necrosis activates the NLRP3 inflammasome. J Immunol 2009a;183(3):1528-1532.

Li KS, Wang BY, Liu SY, Yao SP, Guo L, Mao DW. The combination of polymorphisms within MCP-1 and IL-1beta associated with ulcerative colitis. Int J Immunogenet 2009b;36(3):135-139.

Li MG, Lu WL, Wang JC, Zhang X, Wang XQ, Zheng AP, Zhang Q. Distribution, transition, adhesion and release of insulin loaded nanoparticles in the gut of rats. Int J Pharm 2007;329(1-2):182-191.

Li P, Allen H, Banerjee S, Franklin S, Herzog L, Johnston C, Mc Dowell J, Paskind M, Rodman L, Salfeld J, et al. Mice deficient in IL-1 beta-converting enzyme are defective in production of mature IL-1 beta and resistant to endotoxic shock. Cell 1995;10;80(3):401-411.

Long TC, Saleh N, Tilton RD, Lowry GV, Veronesi B. Titanium dioxide (P25) produces reactive oxygen species in immortalized brain microglia (BV2): implications for nanoparticle neurotoxicity. Environ Sci Technol 2006;40(14):4346-4352.

Mariathasan S, Weiss DS, Newton K, McBride J, O'Rourke K, Roose-Girma M, Lee WP, Weinrauch Y, Monack DM, Dixit VM. Cryopyrin activates the inflammasome in response to toxins and ATP. Nature 2006;9;440(7081):228-232.

Martinon F, Mayor A, Tschopp J. The inflammasomes: guardians of the body. Annu Rev Immunol 2009;27:229-265.

Merget R, Bauer T, Küpper HU, Philippou S, Bauer HD, Breitstadt R, Bruening T. Health hazards due to the inhalation of amorphous silica. Arch Toxicol 2002;75:625-634.

Moore BB, Hogaboam CM. Murine models of pulmonary fibrosis. Am J Physiol Lung Cell Mol Physiol 2008;294:L152-160.

Monteiller C, Tran L, MacNee W, Faux S, Jones A, Miller B, Donaldson K. The pro-inflammatory effects of low-toxicity low-solubility particles, nanoparticles and fine particles, on epithelial cells in vitro: the role of surface area. Occup Environ Med 2007;64(9):609-615.

Muller L, Riediker M, Wick P, Mohr M, Gehr P, Rothen-Rutishauser B. Oxidative stress and inflammation response after nanoparticle exposure: differences between human lung cell monocultures and an advanced three-dimensional model of the human epithelial airways. J R Soc Interface. 2010;6;7 Suppl 1:S27-40.

Napierska D, Thomassen LC, Rabolli V, Lison D, Gonzalez L, Kirsch-Volders M, Martens JA, Hoet PH. Size-dependent cytotoxicity of monodisperse silica nanoparticles in human endothelial cells. Small 2009;5(7):846-853.

Oberdörster G, Ferin J, Lehnert BE. Correlation between particle size, in vivo particle persistence, and lung injury. Environ Health Perspect 1994;102 Suppl 5:173-179.

Oberdörster G, Finkelstein JN, Johnston C, Gelein R, Cox C, Baggs R, Elder AC. Acute pulmonary effects of ultrafine particles in rats and mice. Res Rep Health Eff Inst 2000; 96: 5-86.

Oberdörster G, Oberdörster E, Oberdörster J. Nanotoxicology: an emerging discipline evolving from studies of ultrafine particles. Environ Health Perspect 2005;113(7):823-839.

Olson AD, Ayass M, Chensue S. Tumor necrosis factor and IL-1 beta expression in pediatric patients with inflammatory bowel disease. J Pediatr Gastroenterol Nutr 1993;16(3):241-246.

Palomäki J, Karisola P, Pylkkänen L, Savolainen K, Alenius H. Immunological effects of engineered nanomaterials on mouse antigen presenting cells in vitro. Toxicology 2010;267(1-3):125-131.

Park EJ, Park K. Oxidative stress and pro-inflammatory responses induced by silica nanoparticles in vivo and in vitro. Toxicol Lett 2009;184(1):18-25.

Petrilli V, Papin S, Dostert C, Mayor A, Martinon F, Tschopp J. Activation of the NALP3 inflammasome is triggered by low intracellular potassium concentration. Cell Death Differ 2007;14(9):1583-1589.

Powell JJ, Harvey RS, Ashwood P, Wolstencroft R, Gershwin ME, Thompson RP. Immune potentiation of ultrafine dietary particles in normal subjects and patients with inflammatory bowel disease. J Autoimmun 2000;14(1):99-105.

Powell JJ, Faria N, Thomas-McKay E , Pele LC. Origin and fate of dietary nanoparticles and microparticles in the gastrointestinal tract. J Autoimm 2009;34(3):J226-J233.

Rahman Q, Lohani M, Dopp E, Pemsel H, Jonas L, Weiss DG, Schiffmann D. Evidence that ultrafine titanium dioxide induces micronuclei and apoptosis in Syrian hamster embryo fibroblasts. Environ Health Perspect 2002;110(8):797-800.

Reindl W, Weiss S, Lehr HA, Forster I. Essential crosstalk between myeloid and lymphoid cells for development of chronic colitis in myeloid-specific signal transducer and activator of transcription 3-deficient mice. Immunology 2007;120(1):19-27.

Rescigno M. Before they were gut dendritic cells. Immunity 2009;31(3):454-456.

Rescigno M, Matteoli G. Lamina propria dendritic cells: for whom the bell TOLLs? Eur J Immunol 2008;38(6):1483-1486.

Saffiotti U. Silicosis and lung cancer: a fifty-year perspective. Acta Biomed 76 Suppl 2005;2:30-37.

Sager TM, Kommineni C, Castranova V. Pulmonary response to intratracheal instillation of ultrafine versus fine titanium dioxide: role of particle surface area. Part Fibre Toxicol 2008;5:17.

Sarih M, Souvannavong V, Brown SC, Adam A. Silica induces apoptosis in macrophages and the release of interleukin-1 alpha and interleukin-1 beta. J Leukoc Biol 1993;54(5):407-413.

Sayes CM, Wahi R, Kurian PA, Liu Y, West JL, Ausman KD, Warheit DB, Colvin VL. Correlating nanoscale titania structure with toxicity: a cytotoxicity and inflammatory response study with human dermal fibroblasts and human lung epithelial cells. Toxicol Sci 2006;92(1):174-185.

Siegmund B, Lehr HA, Fantuzzi G, Dinarello CA. IL-1 beta -converting enzyme (caspase-1) in intestinal inflammation. Proc Natl Acad Sci U S A 2001;98(23):13249-13254.

Singh S, Shi T, Duffin R, Albrecht C, van Berlo D, Hohr D, Fubini B, Martra G, Fenoglio I, Borm PJ et al. Endocytosis, oxidative stress and IL-8 expression in human lung epithelial cells upon treatment with fine and ultrafine TiO2: role of the specific surface area and of surface methylation of the particles. Toxicol Appl Pharmacol 2007;222(2):141-151.

Stoeger T, Reinhard C, Takenaka S, Schroeppel A, Karg E, Ritter B, Heyder J, Schulz H. Instillation of six different ultrafine carbon particles indicates a surface-area threshold dose for acute lung inflammation in mice. Environ Health Perspect 2006;114: 328-333.

Takeda K, Clausen BE, Kaisho T, Tsujimura T, Terada N, Forster I, Akira S. Enhanced Th1 activity and development of chronic enterocolitis in mice devoid of Stat3 in macrophages and neutrophils. Immunity 1999;10(1):39-49.

Thakur SA, Hamilton R, Jr., Pikkarainen T, Holian A. Differential binding of inorganic particles to MARCO. Toxicol Sci 2009;107(1):238-246.

Trouiller B, Reliene R, Westbrook A, Solaimani P, Schiestl RH. Titanium dioxide nanoparticles induce DNA damage and genetic instability in vivo in mice. Cancer Res 2009;69:8784-8789.

Turnbull EL, Yrlid U, Jenkins CD, Macpherson GG. Intestinal dendritic cell subsets: differential effects of systemic TLR4 stimulation on migratory fate and activation in vivo. J Immunol 2005;174(3):1374-1384.

Unfried K, Albrecht C, Klotz LO, von Mikecz A, Grether-Beck S, Schins RPF. Cellular responses to nanoparticles: target structures and mechanisms. Nanotoxicol 2007;1:52-71.

Varol C, Vallon-Eberhard A, Elinav E, Aychek T, Shapira Y, Luche H, Fehling HJ, Hardt WD, Shakhar G, Jung S. Intestinal lamina propria dendritic cell subsets have different origin and functions. Immunity 2009;31(3):502-512.

Wang JJ, Sanderson BJ, Wang H. Cyto- and genotoxicity of ultrafine TiO2 particles in cultured human lymphoblastoid cells. Mutat Res 2007;628(2):99-106.

Waters KM, Masiello LM, Zangar RC, Tarasevich BJ, Karin NJ, Quesenberry RD, Bandyopadhyay S, Teeguarden JG, Pounds JG, Thrall BD. Macrophage responses to silica nanoparticles are highly conserved across particle sizes. Toxicol Sci 2009; 107(2):553-569.

Xia T, Kovochich M, Brant J, Hotze M, Sempf J, Oberley T, Sioutas C, Yeh JI, Wiesner MR, Nel AE. Comparison of the abilities of ambient and manufactured nanoparticles to induce cellular toxicity according to an oxidative stress paradigm. Nano Lett 2006; 6(8):1794-1807.

Figure legends

Figure 1 **Viability and maturation status of DC after particle treatment.** On day six, BMDC were harvested and incubated with medium, 20 and 50 µg/cm^2 particles, or 1 µg/ml LPS for 18 hours as indicated. (A and B) Representative FACS analysis for CD11c and MHCII expression in the absence (A) or presence of LPS (B). Numbers indicate the frequency of CD11c$^+$ cells in the cultures. (C) Total cell number at the end of the culture. (D-F) The expression of maturation markers was analysed via FACS analysis, and is depicted as the frequency of MHCII^{high} DC (D), or the mean fluorescence intensity (MFI) for CD80 (E) and CD86 (F). Values are expressed as median + interquartile range; n ≥ 12 (C) or mean + SEM; n ≥ 5 (D-F). We calculated whether particle-treated groups differed significantly from the untreated control group by paired t-test. * p≤0.05, ** p≤0.01 *** p≤0.001 (versus control)

Figure 2 **Induction of apoptosis in DC by particles.** BMDC were incubated with particles at concentrations of 5, 20 and 40 µg/cm^2 or 1 µg/ml LPS on day six. After 18 hours, the frequency of apoptotic cells was measured by FACS analysis within the immature (grey) or mature (black) DC subset, as determined by MHC-II expression; n = 4. Values are expressed as mean + SEM. $^{\#}$ indicates significance of particle-treated groups versus control; * indicates significance of immature versus mature DC. Significance was calculated by paired t-test.

$^{\#}$ p≤0.05, $^{\#\#}$ p≤0.01 $^{\#\#\#}$ p≤0.001 (versus control)

*p≤0.05, ** p≤0.01 *** p≤0.001 (immature versus mature DC)

Figure 3 **Induction of oxidative stress in DC by particles.** Generation of oxidative stress was visualized by DCFDA cleavage into fluorescent DCF after incubation of BMDC with 5, 20 and 40 µg/cm^2 particles or 1 µg/ml LPS for 18 hours. Values are expressed as mean + SEM; n = 4. $^{\#}$ indicates significance of particle-treated groups versus control; * indicates significance of TiO_2uf- versus TiO_2f-treated groups. Significance was calculated by paired t-test.

$^{\#}$ p≤0.05, $^{\#\#}$ p≤0.01 $^{\#\#\#}$ p≤0.001 (versus control)

*p≤0.05, ** p≤0.01 *** p≤0.001 (TiO_2uf versus TiO_2f)

Figure 4 **Particle-induced IL-1β secretion.** BMDC were prestimulated with 0.1 µg/ml LPS on d6. After 6 hours, particles were added to the cultures for another 18 hours. Active IL-1β was measured in the supernatant by ELISA. As a control, unstimulated and LPS-stimulated cells are depicted. Values are expressed as mean + SEM; n ≥ 6. * indicates significance of particle-treated groups versus control + LPS. Significance was calculated by paired t-test.
* p≤0.05, ** p≤0.01 *** p≤0.001 (versus control + LPS)

Figure 5 **Particle-induced IL-1β secretion is dependent on Caspase-1 and NLRP3.** BMDC of WT, Caspase-1-deficient mice (A-C) and NLRP3-deficient mice (D-F) were prestimulated with 0.1 µg/ml LPS on d6. After 6 hours, particles were added to the cultures for another 18 hours. Active IL-1β was measured in the supernatant by ELISA. As a control, unstimulated and LPS-stimulated cells are depicted. (A – C) Values are expressed as mean + SEM; n = 3. (D-F) For the NLRP3-deficient mice 1 representative experiment is shown out of 2. # indicates significance of particle-treated groups versus WT control + LPS * indicates significance of WT versus Caspase-1 deficient mice. Significance was calculated by t-test.
p≤0.05, ## p≤0.01 ### p≤0.001 (versus control)
p≤0.05, ** p≤0.01 *** p≤0.001 (WT versus Caspase-1 deficient mice)

Figure 6 **Uptake of particles into DC.** BMDC were prestimulated with 0.1 µg/ml LPS on d6 for 6 hours. Particle uptake was partially blocked with Cytochalasin-D before particles were added to the cultures for another 2 hours. Cell granularity was measured by FACS. As a control, unstimulated and LPS-stimulated cells are depicted. Values are expressed as mean + SEM; n = 4. # indicates significance of particle-treated groups versus WT control + LPS. * indicates significance of groups - Cytochalasin-D versus + Cytochalasin-D. Significance was calculated by paired t-test.
p≤0.05, ## p≤0.01 ### p≤0.001 (versus LPS-stimulated control)
*p≤0.05, ** p≤0.01 *** p≤0.001 (–Cytochalasin-D versus +Cytochalasin-D)

Figure 7 **Particle-induced IL-1β secretion in DC is dependent on particle uptake.** BMDC were prestimulated with 0.1 µg/ml LPS on d6 for 6 hours. Actin-

polymerisation was blocked with Cytochalasin-D before particles were added to the cultures for another 2 hours (A-D). Active IL-1β was measured in the supernatant by ELISA. As controls, IL-1β production by unstimulated, LPS-, or ATP-stimulated cells (E) are depicted. Values are expressed as mean + SEM; n = 4. # indicates significance of particle-treated groups versus WT control + LPS. * indicates significance of groups -Cytochalasin-D versus +Cytochalasin-D. Significance was calculated by paired t-test.

p≤0.05, ## p≤0.01 ### p≤0.001 (versus LPS-stimulated control)

*p≤0.05, ** p≤0.01 *** p≤0.001 (–Cytochalasin-D versus +Cytochalasin-D)

Figure 1

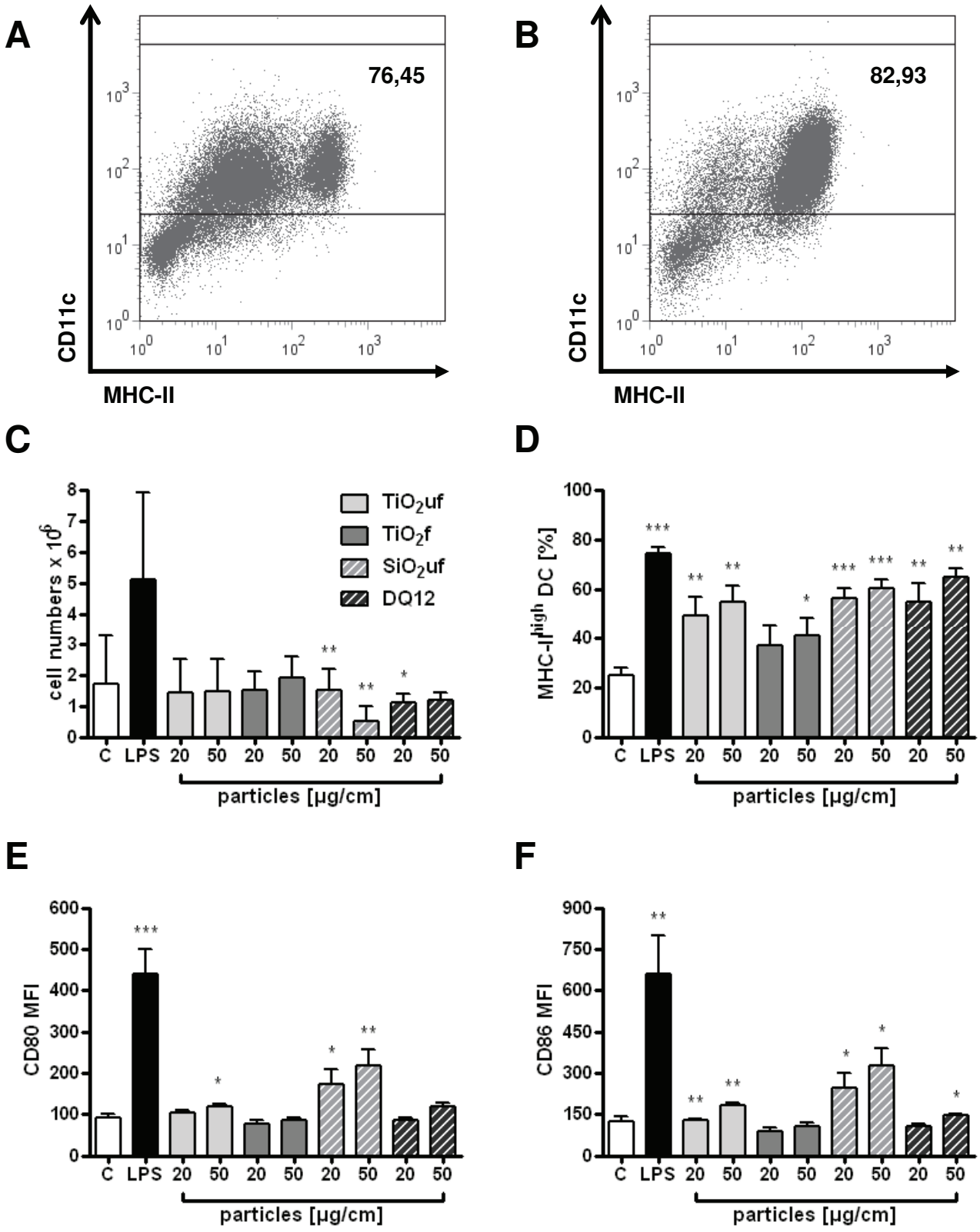
A
76,45
CD11c
MHC-II
B
82,93
CD11c
MHC-II
C
cell numbers x 10^6
TiO2uf
TiO2f
SiO2uf
DQ12
C LPS 20 50 20 50 20 50 20 50
particles [µg/cm]
D
MHC-II^high DC [%]
C LPS 20 50 20 50 20 50 20 50
particles [µg/cm]
E
CD80 MFI
C LPS 20 50 20 50 20 50 20 50
particles [µg/cm]
F
CD86 MFI
C LPS 20 50 20 50 20 50 20 50
particles [µg/cm]

Figure 2

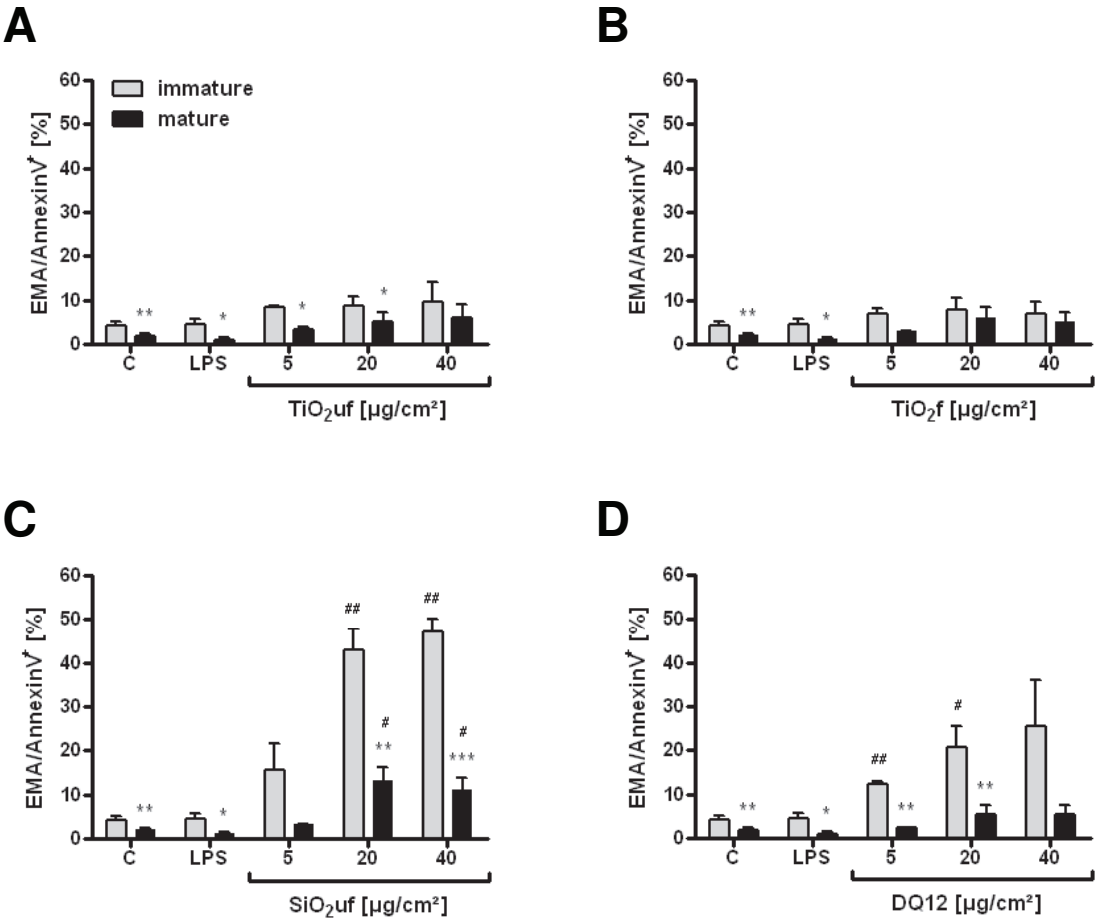
A
B
C
D
immature
mature
EMA/AnnexinV+ [%]
C
LPS
5
20
40
TiO2uf [µg/cm²]
TiO2f [µg/cm²]
SiO2uf [µg/cm²]
DQ12 [µg/cm²]

Figure 3

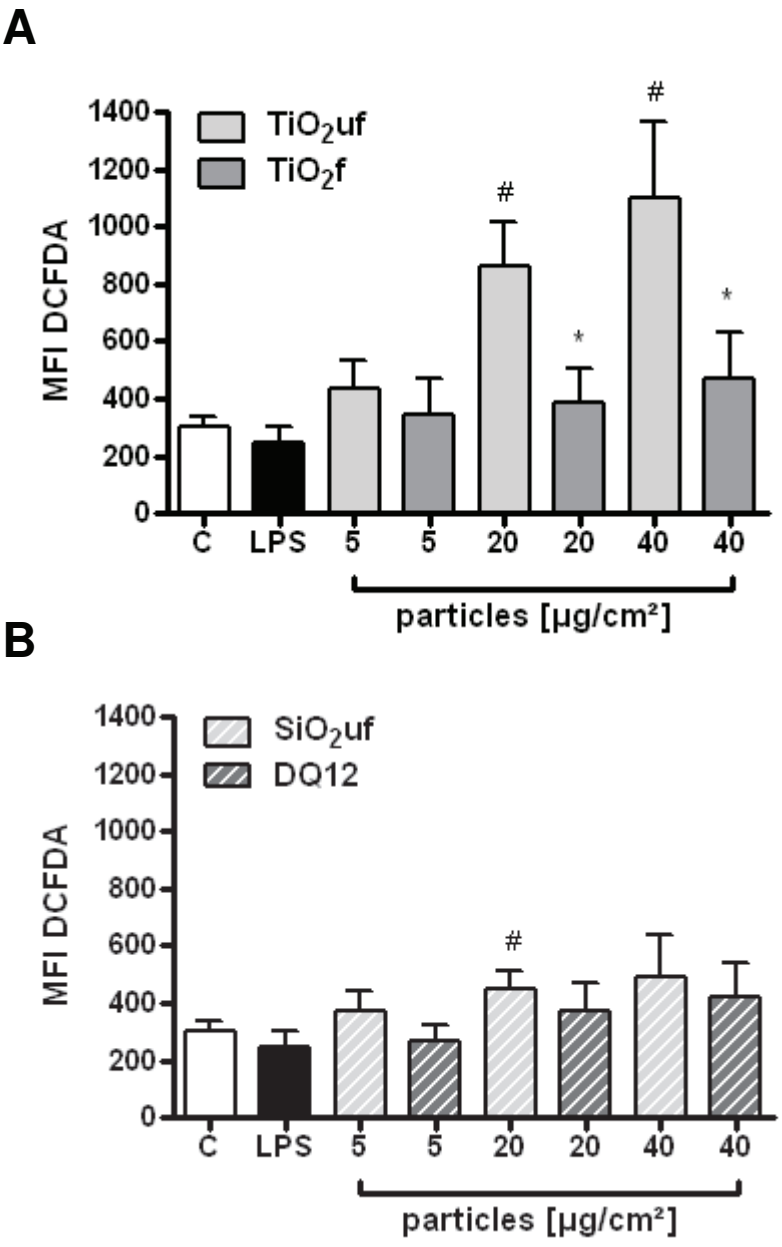
A
1400
1200
1000
800
600
400
200
0
MFI DCFDA
TiO2uf
TiO2f
#
#
*
*
C
LPS
5
5
20
20
40
40
particles [µg/cm²]
B
1400
1200
1000
800
600
400
200
0
MFI DCFDA
SiO2uf
DQ12
#
C
LPS
5
5
20
20
40
40
particles [µg/cm²]

Figure 4

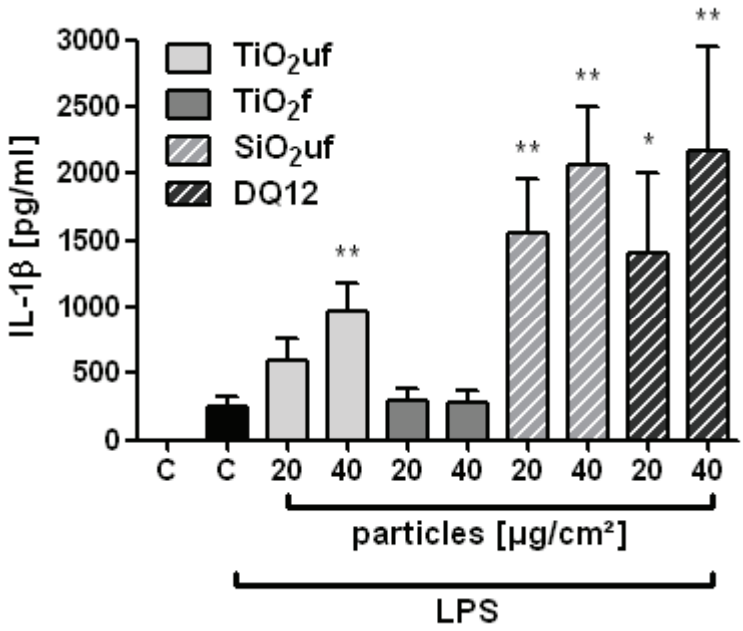
IL-1β [pg/ml]
3000
2500
2000
1500
1000
500
0
TiO2uf
TiO2f
SiO2uf
DQ12
**
**
**
*
**
C
C
20
40
20
40
20
40
20
40
particles [µg/cm²]
LPS

Figure 5

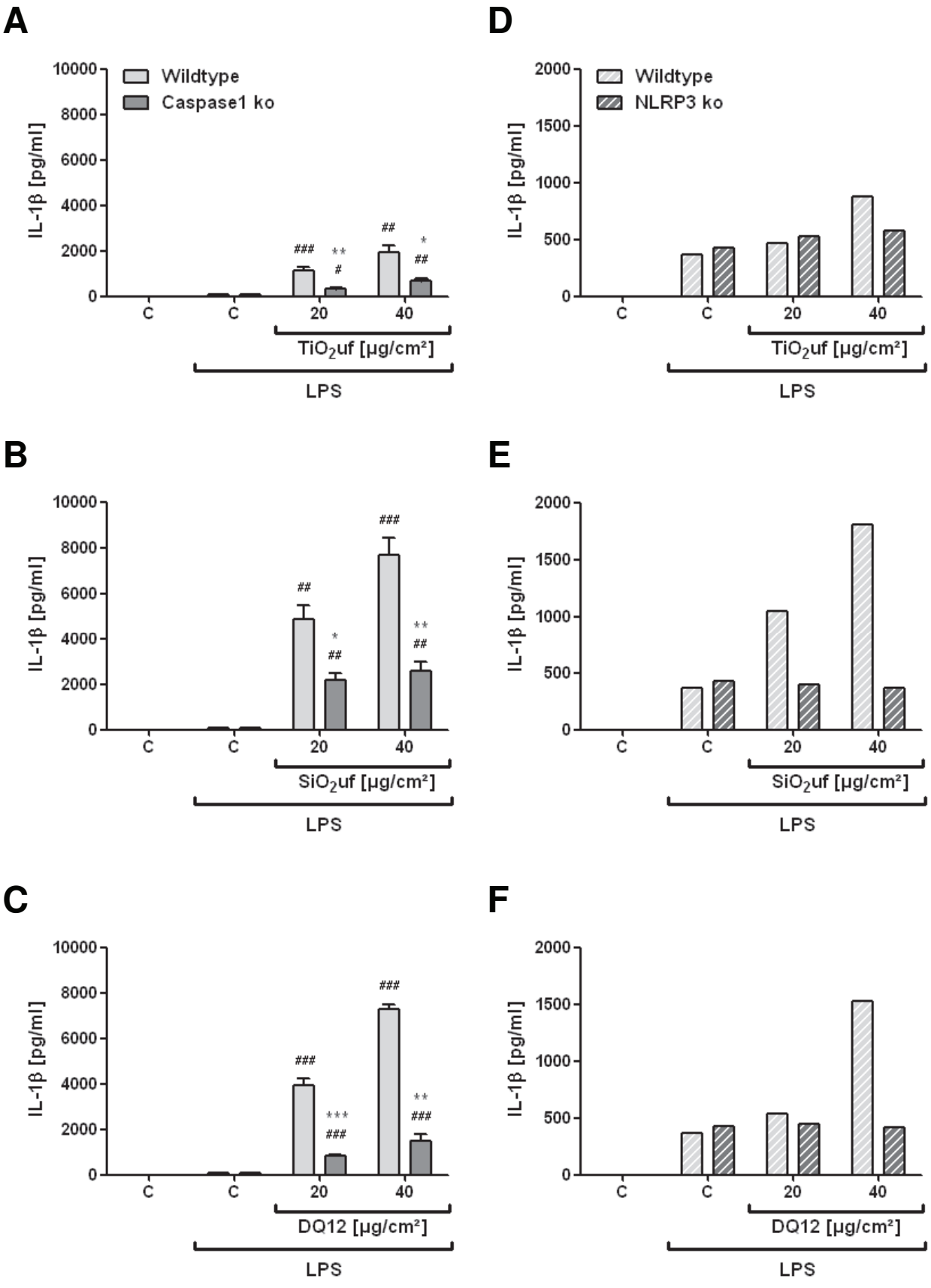
A
Wildtype
Caspase1 ko
IL-1β [pg/ml]
10000
8000
6000
4000
2000
0
C
C
20
40
TiO2uf [µg/cm²]
LPS
D
Wildtype
NLRP3 ko
IL-1β [pg/ml]
2000
1500
1000
500
0
C
C
20
40
TiO2uf [µg/cm²]
LPS
B
IL-1β [pg/ml]
SiO2uf [µg/cm²]
LPS
E
IL-1β [pg/ml]
SiO2uf [µg/cm²]
LPS
C
IL-1β [pg/ml]
DQ12 [µg/cm²]
LPS
F
IL-1β [pg/ml]
DQ12 [µg/cm²]
LPS

Figure 6

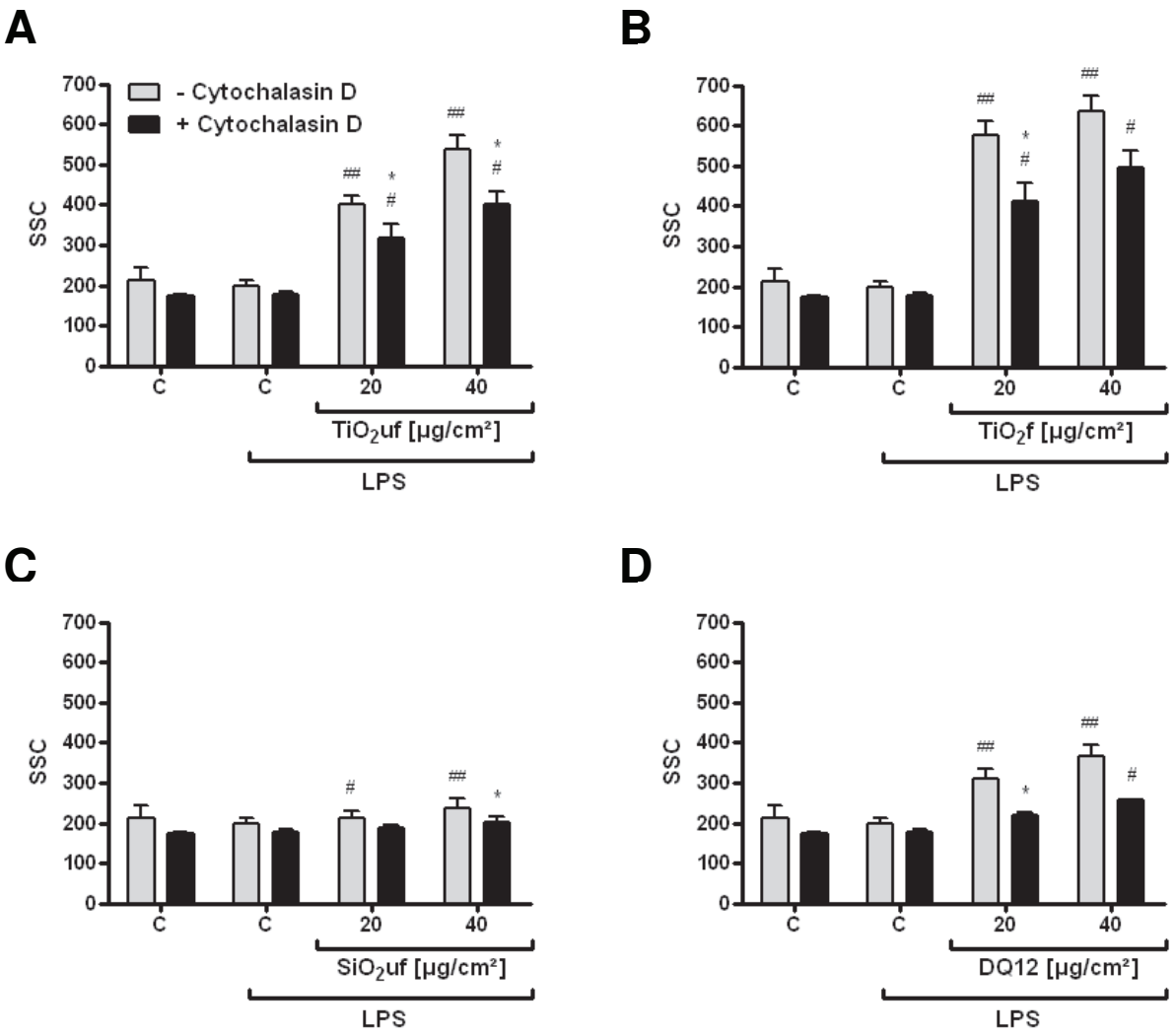
A
B
C
D
- Cytochalasin D
+ Cytochalasin D
SSC
700
600
500
400
300
200
100
0
C
C
20
40
TiO2uf [µg/cm²]
TiO2f [µg/cm²]
SiO2uf [µg/cm²]
DQ12 [µg/cm²]
LPS
#
##
*

Figure 7

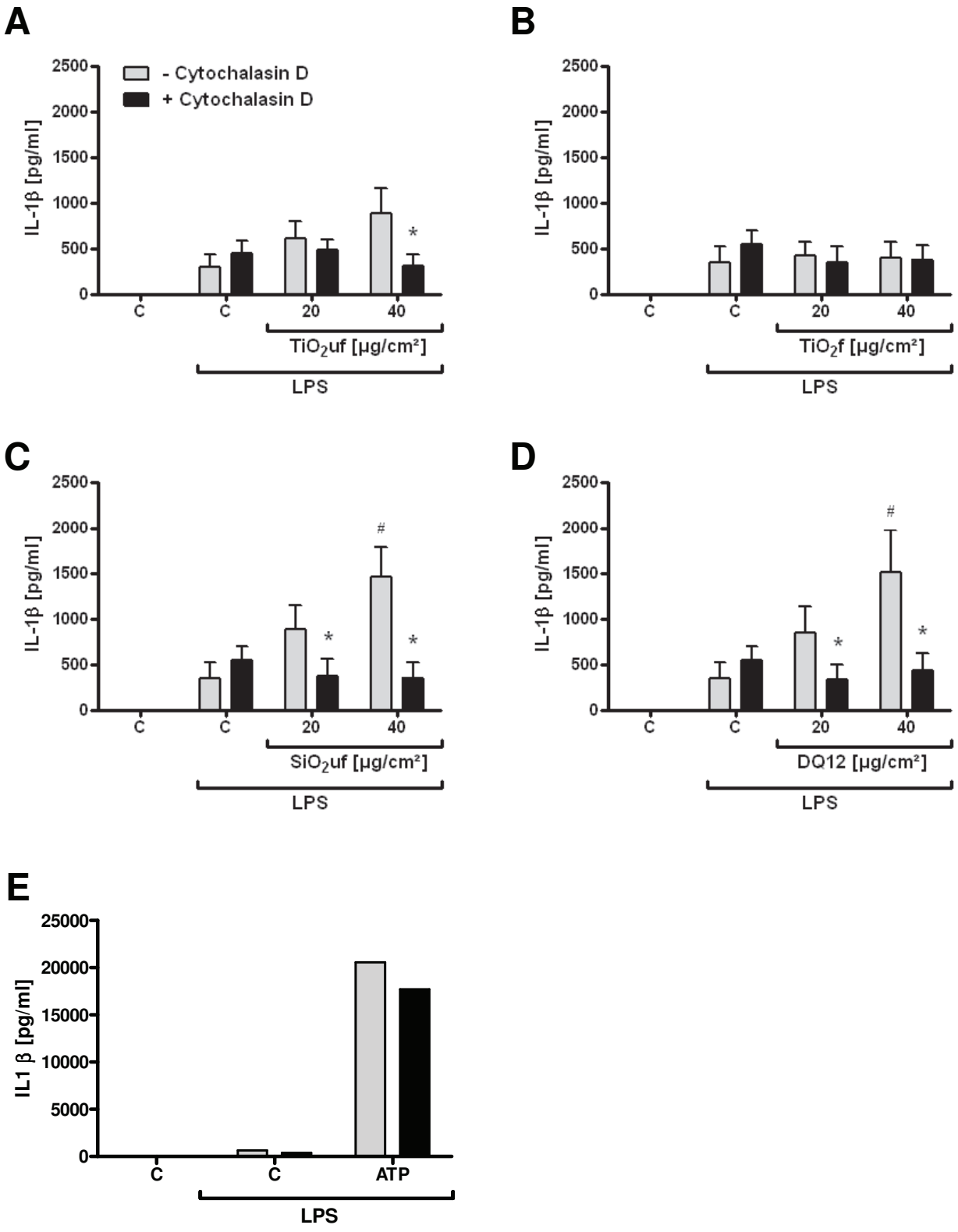
A
- Cytochalasin D
+ Cytochalasin D
IL-1β [pg/ml]
2500
2000
1500
1000
500
0
C
C
20
40
TiO2uf [µg/cm²]
LPS
B
IL-1β [pg/ml]
TiO2f [µg/cm²]
LPS
C
IL-1β [pg/ml]
SiO2uf [µg/cm²]
LPS
D
IL-1β [pg/ml]
DQ12 [µg/cm²]
LPS
E
IL1 β [pg/ml]
25000
20000
15000
10000
5000
0
C
C
ATP
LPS

In vitro and in vivo investigations on the effect of amorphous silica on DNA damage in the inflamed intestine

KIRSTEN GERLOFF[1], MEIKE WINTER[2], AGNES W. BOOTS[1], DAMIEN VAN BERLO[1], JULIA KOLLING[1], CATRIN ALBRECHT[1], IRMGARD FÖRSTER[2], ROEL P.F. SCHINS[1*]

[1] Particle Research and [2] Molecular Immunology, Institut für Umweltmedizinische Forschung (IUF) at the Heinrich Heine University Düsseldorf, Germany.

Abstract

The discussion about possible adverse effects of ingested nanoparticles towards the human body is currently gaining much attention. One of the major contributors to regular nanoparticle ingestion includes amorphous SiO_2 which is already widely used in cosmetics, pharmaceutical products and foods. Recently we demonstrated that these particles are can cause cytotoxicity and oxidative DNA damage to human intestinal Caco-2 cells, as well as upregulation of the expression of the potent neutrophil chemoattractant interleukin-8. To elaborate whether the toxic potency of ingested nanoparticles differs between healthy individuals and those with (chronic) inflammatory bowel diseases (IBD) we have investigated the oxidative DNA damaging properties of SiO_2 (i) *in vitro* in Caco-2 cells during co-exposure to primary human neutrophils (PMN) and (ii) *in vivo* by evaluation of the effects of SiO_2 enriched chow in acute and chronic dextrane sulphate sodium (DSS) induced colitis in mice. Genotoxicity was evaluated by the formamidopyrimidine glycosylase (Fpg)-modified comet assay and immunohistochemistry for 8-hydroxydeoxyguanosine (8-OHdG). It was found that activated human neutrophils potently induced DNA strand breakage and oxidative lesions *in vitro*. However, SiO_2 did not lead to PMN activation, and no PMN mediated DNA damage was determined in a co-culture model with Caco-2 cells. The outcome of the *in vivo* study were in support of these findings: analysis of DNA damage in whole colonic tissue by the *in vivo* Fpg-modified comet assay did not

reveal elevated strand breakage after receiving a SiO_2 enriched chow. However, a mild increase of 8-OHdG lesions was shown by immunohistochemical staining after chronic, but not after acute colitis induction.

Introduction

Throughout the last few years, the discussion about possible adverse effects of ingested nanoparticles towards the human body is gaining much attention. The use of nanoparticles, defined by a size smaller 100 nm, for food and food-related products becomes more popular (Oberdöster *et al.,* 2005; Chaudhry *et al*., 2008; Tiede *et al*., 2008; Schmid and Riediker, 2008; homepage nanotechproject.org). A daily ingestion of 10^{12}-10^{14} particles per day has been suggested already several years ago, with increasing tendency each year (Lomer *et al*., 2001, 2004). One of the major contributors to regular nanoparticle ingestion includes the amorphous SiO_2 which is already widely used in cosmetics, pharmaceutical products and foods (Johnston *et al*., 2000; Chaudhry *et al*., 2008). SiO_2 in general is accepted as a common food additive (E551) and mainly used as an anticaking agent (homepage food.gov.uk). The uptake of such nanoparticles into the intestinal epithelium is still not fully understood and appears to vary with different particle compositions and applications (Unfried *et al*., 2007; Powell *et al*., 2010). In general, particle uptake by intestinal tissue is low (< 10 %) (Jani *et al*., 1994, Hillery *et al*., 1994) but reported to be a 15-250 fold higher for small particles (~110-120 nm) compared to larger particles (Desai *et al*, 1996). Intestinal particle internalisation is mainly driven by the so-called Peyer´s Patches, i.e. lymphoid tissue rich of specified M-cells (reviewed in Powell *et al*., 2010), but epithelial cells are also reported to be capable of considerable particle uptake (Hillery *et al*., 1994). Trouiller and co-workers recently showed marked systemic DNA damage and mutagenesis in mice after oral uptake of TiO_2 nanoparticles and suggested that this may be due to uptake and subsequent induction of systemic inflammation (Trouiller *et al*., 2009).

Recently, we have addressed the potential hazards of a selection of nanoparticles that are likely to find their way into engineered food or food packaging in the future. In these studies we observed for instance that nanosize SiO_2 and ZnO induce marked cytotoxicity, and also can cause oxidative DNA damage and the release of the pro-inflammatory mediator interleukin-8 from human intestinal Caco-2 cells. In contrast, TiO_2 only showed rather negligible cytotoxic and DNA damaging effects in our investigations (Gerloff *et al*., 2009, Gerloff *et al*., submitted). Remarkably however and contrasting to findings in lung epithelial cells (e.g. Singh *et al*., 2007; Monteiller et al., 2007), the aforementioned effects could not be predicted

by the primary particle size or specific surface area of the different compounds (Gerloff *et al*., 2009, Gerloff *et al*., submitted). In the respiratory tract, particles of low solubility and toxicity, such as TiO_2 and carbon black, have been shown to cause inflammation in proportion to their specific surface area. This observation is of major importance for risk assessment of inhaled particles, since their adverse effects have been demonstrated to be associated with their intrinsic inflammatory potency (Oberdörster *et al*., 2005; Duffin *et al.,* 2007). In contrast, relatively little is known about possible inflammatory properties and possibly associated effects of nanoparticles in the gut. In the respiratory tract, the particle-driven inflammatory response is associated with tissue damage, remodelling and mutagenesis (Donaldson *et al*., 2005; Duffin *et al*. 2007; Schins and Knaapen, 2007). An important player in the relationship between inflammation and carcinogenesis is the formation of reactive oxygen species (ROS) during inflammatory phagocyte respiratory burst (Babbs, 1992; Knaapen *et al*., 2006). Indeed, activated polymorphonuclear neutrophils (PMN) have been shown to cause oxidative DNA damage in rat lung epithelial cells (Knaapen *et al*., 1999; Knaapen *et al*., 2002a), and the amounts of recruited neutrophils was shown to be correlated with genotoxic and mutagenic effects in the lung epithelium of particle-exposed rats (Driscoll *et al*., 1997; Knaapen *et al*. 2002b).

Inflammatory effects of particles might also play an important role in particle risk assessment for the intestine. For example, bacterial components such as LPS are shown to bind to TiO_2 particles which then, by serving as a carrier for these toxins, may lead to highly increased inflammatory responses in peripheral blood mononuclear cells, characterized by the release of various inflammatory cytokines. Interestingly, the inflammatory response induced by the LPS-particle complex is synergistic as it was shown to be more pronounced than that caused by incubation with either the particles or LPS alone (Ashwood *et al*., 2007). Since large amounts of bacterial compounds are present, such particle-endotoxin complexes might be easily formed within the colon. Transportation of these bacterial composites into the mucosa via binding to nanoparticles might lead to aggravation of inflammatory events induced by unintentional ingestion of nanoparticles via food uptake and exacerbate inflammatory bowel diseases (IBD) as ulcerative colitis. However, the influence of particles on the etiopathology of IBD is currently under discussion but not yet confirmed (Lomer *et al*., 2001, 2004; Schneider *et al*., 2007).

The main hallmark of colitis is the imbalance of the intestinal immune system. This is characterised by continous migration of activated lymphocytes, granulocytes and macrophages into the mucosa as well as an increased production of various pro-inflammatory cyto- and chemokines (Mitsuyama *et al*., 1994; Rogler and Andus, 1998; MacDermott, 1999). In colonic tissue of colitis patients, increased levels of the potent chemoattractant interleukin-8 (IL-8), secreted by epithelial cells, macrophages or fibroblasts, are found. These elevated IL-8 levels are directly linked to the attraction and thus the infiltration of neutrophils, and therefore also correlate with the grade of local inflammation (Kunkel *et al*., 1991; Mazzucchelli *et al*., 1994; Mitsuyama *et al*., 1994; Kucharzik and Williams, 2002-2003). The respiratory burst of activated neutrophils will lead to an increased production of reactive oxygen species (ROS) that can further enhance inflammation and may introduce DNA damage. Persistent activation of neutrophils and ROS has been considered to contribute to carcinogenesis in the respiratory tract as well as the intestine (Itzkowitz *et al*., 2004; Knaapen et al., 2006; Westbrook *et al.,* 2009).

Recently, we have shown that amorphous SiO_2 is capable of inducing cytotoxicity, oxidative DNA lesions and pro-inflammatory responses in Caco-2 cells, including the upregulation of mRNA expression and protein secretion of IL-8 (Gerloff *et al*., 2009, Gerloff *et al*., submitted), one of the most prominent cytokines expressed by these cells (Jung *et al*., 1995). In the present study, we aimed to investigate the potential consequences of the pro-inflammatory properties of SiO_2 for DNA damage induction in intestinal cells using both an *in vitro* and *in vivo* model of intestinal inflammation. For the *in vitro* experiments, we used a co-incubation model composed of Caco-2 cells and primary human neutrophils. Using this co-incubation, we analysed the potential genotoxic effects of SiO_2 nanoparticles in Caco-2 cells in the presence or absence of neutrophils. For the *in vivo* experiments, we used a colitic mouse model using dextrane sulphate sodium (DSS), known to induce experimental ulcerative colitis by disturbance of the epithelial integrity (Wirtz and Neurath, 2007). Upon inducing either acute or chronic inflammation, the colon was analyzed for DNA strand breakage and oxidative DNA damage

Methods

Materials. Trypsin, Dulbecco's Ca^{2+}/Mg^{2+}-free phosphate buffered saline (PBS), agarose, low melting point (LMP) agarose, Triton X-100, DMSO, ethidium bromide, fetal calf serum (FCS), phorbol-12-myristate-13-acetate (PMA) and deferoxamine (DFO) were all purchased from Sigma (Germany). Minimum essential Medium (MEM) with Earle´s salts, Hanks´ Balanced Salt Solution (HBSS), penicillin/streptomycin were purchased from Invitrogen (Germany). Lymphoprep was obtained from Axis-Shield (Norway). 1-hydroxy-3-carboxy-pyrrolidine (CPH) was purchased from Alexis Biochemicals (Germany), lucigenin (N,N´-Dimethyl-9,9´-biacridinium dinitrate) was obtained from Fluka and Rneasy Tibrous Tissue Mini Kit was from Quiagen (Germany). Dextran sulfate sodium (DSS; mol wt 36.000-50.000) was obtained from MP Biomedicals (USA). Hemocare was from Carediagnostica (Germany). The antibody against 8-OHdG was obtained from the Japan Institute of Aging, mouse IgG was purchased from Vector Laboratories (USA). Histomouse^{TM}-SP Kit was sourced from Zymed Laboratories (USA) and DePex was obtained from Serva (Germany). Formamidopyrimidine-glycosylase (Fpg)-enzyme was kindly provided by Dr. Andrew Collins (Institute for Nutrition Research, University of Oslo, Norway). All other chemicals were from Merck (Germany).

Nanoparticles. SiO_2 (amorphous Silica, fumed; Sigma, Germany) was used for all experiments in present study. The sample has been reported to have a surface area according to according to Brunauer, Emmett and Teller (BET) of 200 m^2/g and a mean primary particle diameter of 14 nm. For the *in vitro* studies, SiO_2-nanoparticles were suspended in HBSS, sonicated for 10 min (Sonorex TK52 water-bath; 60 Watt, 35 kHz) and then directly added to the cells at the indicated concentrations. Although the primary size of the SiO_2 particles is well in the nanosize range, the material is well-known to occur as aggregates/agglomerates. This was also confirmed by Mastersizer analysis in the suspensions used for cell treatment (Gerloff *et al*., submitted). For the *in vivo* study, chow was purchased from Ssniff (Germany), either supplemented with or without 0.1 % w/w SiO_2 (SiO_2-chow).

Animals. C57BL/6 mice were originally purchased from Harlan-Winkelmann and bred at the IUF animal facility under specific pathogen free (SPF) conditions. The animals

were housed and maintained in an accredited on-site testing facility under SPF conditions, according to the guidelines of the Society for Laboratory Animals Science (GV-SOLAS). Food and water were available ad libitum. Female mice were used at 9 weeks of age. Mice were painlessly sacrificed in a CO_2 chamber, according to German guidelines. The experiment was performed with the permission of the Regierung von Nordrhein-Westfalen, Germany.

Cell culture and co-incubation. The human colon adenocarcinoma cell line Caco-2 was obtained from the *Deutsche Sammlung von Mikroorganismen und Zellkulturen* (DSMZ) GmbH**,** Germany and grown in MEM with Earle´s salts and Non Essential Amino Acids, supplemented with 20 % FCS, 1 % L-glutamine and 30 IU/ml penicillin–streptomycin. For experiments, cells were trypsinized at near confluency and $4x10^4$ cells per cm^2 were seeded into 60 mm culture plates and grown overnight. Experiments were performed in HBSS between cell passages 5 to 30 after starvation of the cells for 20 h in serum free medium. Neutrophils (PMN) were isolated freshly from blood of healthy, non-smoking volunteers as described in Knaapen *et al*. (1999) using Lymphoprep. PMN were suspended in HBSS (+ Ca^{2+}/Mg^{2+}) and counted using a Neubauer chamber. Cell viability was tested via Trypan Blue staining (viability > 95%). PMA (100 ng/ml) was used for PMN-activation. For the co-incubation experiments, PMN were incubated with PMA or SiO_2 and added directly to the Caco-2 cells for 30 min at 37°C at the indicated ratios. SiO_2 particles were administered to the cell cultures at the indicated concentration immediately after sonication as described above. After treatment, cell monolayers were rinsed twice with PBS to remove excess of extracellular particles, neutrophils and detached (dead) cells or cell debris.

ROS measurements by luminescence and Electron Paramagnetic Resonance (EPR). ROS production was measured using either lucigenin-enhanced chemiluminescence or EPR spectroscopy. For luminescence, PMN (2.5 mil/ml) were stimulated with SiO_2 (31.25 and 312.5 µg/cm^2) or PMA (100 ng/ml) in a white maxisorp 96-well plate (Nunc, Germany). Subsequently, 0.25 mM lucigenin was added to preferentially detect superoxide formation and chemiluminescence was recorded directly for 50 min at 37°C using a Luminometer (Multi-Bioluminat, Berthold, Germany). Results were expressed as the area under the curve (RLU=relative light units).

For EPR spectroscopy the spin probe CPH was used. Caco-2 cells were previously seeded in a 96 well plate and grown to 70-80 % confluency before 30 min co-incubation with PMN (1.3 million/ml) at 37°C in the presence of 0.5 mM CPH in 10 µM DFO. Furthermore, PMN alone were preincubated with 20 or 80 µg/cm^2 SiO_2 for 30 min at 37°C in the presence of 0.5 mM CPH in 10 µM DFO. ROS generation was evaluated using a MiniScope MS200 Spectrometer (Magnettech, Berlin, Germany) at room temperature using the following instrumental settings: Magnetic field: 3360 G; sweep width: 97 G; scan time: 60 sec; number of scans: 1; modulation amplitude: 2000 mG. Data shown are calculated from the average peak amplitude of CPH characteristic triplet spectrum and expressed in arbitrary units (AU).

Colitis induction in C57/BL6 mice. Induction of chronic and acute colitis was performed by a method previously described, with some modifications (Okayasu *et al*., 1990). In short, mice were pretreated with conventional or SiO_2-enriched chow for 14 days. Chronic colitis was induced by 3 cycles of DSS-treatment. Each cycle consisted of one week of 2 % (wt/vol) DSS in acidified drinking water ad libidum, while the mice received normal chow, followed by two weeks on normal drinking water and SiO_2-chow. After the last cycle, mice were sacrificed on day 77 for further analysis. For induction of acute colitis, mice were pretreated with SiO_2-chow for 17 days. Then colitis was induced by 2 % DSS in drinking water for six days. During DSS-treatment, mice were offered normal breeding chow ad libidum. After day six, mice were left for additional two days, in which they were set on SiO_2 chow and normal drinking water, after which they were sacrificed for further analysis. Thus, both the acute and the chronic exposure model represented each 4 different treatment groups, i.e. the i.e. (i) animals without any treatment, (ii) animals treated with DSS, (iii) animals treated with SiO_2, and finally, (iv) animals exposed to both DSS and SiO_2. To evaluate the severity of disease, colon length was assessed as an established marked. A clinical score according to Cooper *et al*. (1993), which consists of bleeding intensity, weight loss and stool consistency was determined. Scores of these three categories were added and divided by three. In short, rectal bleeding was scored as 3, hemocare+ (i.e. the detection of minor amounts of haemoglobin in the faeces) as 2 and no bleeding was scored as 1. For weight loss, more than 20% weight loss was scored as 4, 10 - 20% as 3, 0 – 10% as 2 no weight loss was scored

as 1. For liquid stools 3 points were given, pasty, soft stools were scored as 2 and well-formed pellets were scored as 1.

Detection of oxidative DNA damage in Caco-2 cells and in cells obtained from mouse small intestine or colon tissues by Fpg-modified comet assay. The Fpg-modified comet assay was used to determine DNA strand breaks and alkali labile sites as well as specifically oxidative DNA damage in the Caco-2 cells, based on the method by Speit *et al*., (2004) and modifications as described earlier (Gerloff *et al*., 2009). Comet appearances were analyzed using an Olympus BX60 fluorescence microscope at 400× magnification. A comet image analysis software program (Comet Assay II, Perceptive Instruments, Haverhill, UK) was used for quantification of DNA damage by analysis of % DNA in tail. A total of 50 cells were analyzed per slide per experiment. A detailed description of the method in Caco-2 cells is provided in Gerloff *et al.* (2009). For the *in vivo* comet assay, after sacrificing the colons of the mice were removed and flushed with ice cold PBS. The entire colon was divided into 3 equal pieces, and one third of each piece was used to assess DNA strand breakage and oxidative DNA lesions. The tissue pieces of each colon were then pooled and processed for the *in vivo* Fpg-modified comet assay as described in Risom *et al*., 2003 with minor modifications. Shortly, the tissue samples were minced with the plunger of a syringe in 1ml ice cold *in vivo* comet assay buffer (IVCAB, 0.14 M NaCl, 1.47 mM KH_2PO_4, 2.7 mM KCl, 8.1 mM Na_2HPO_4 and 10 mM EDTA, pH 7.4). The cell-homogenate was filtered through a 40 µm sieve and subsequently centrifuged at 180 g for 10 min at 4°C. Supernatant was discarded and the pellet resuspended in 50µl IVCAB. Afterwards, 25 µl of the suspension were mixed with 235 µl 0.5 % low melting point agarose and applied to pre-coated slides (coated with 1.5 % agarose). From here, the Fpg-modified comet assay was performed as described for the *in vitro* measurements (Gerloff *et al*., 2009). Data are shown both as % comet tail values for each individual animal in the presence (+Fpg) or absence (-Fpg) of Fpg, and as the calculated group means and standard deviations (SD) of the differences in % tail DNA as measured in the presence (+Fpg) or absence (-Fpg) of the Fpg enzyme (i.e. delta (Δ)Fpg = [% tail DNA_{+Fpg}] – [% tail DNA_{-Fpg}])

Colon fixation and immunohistochemistry of 8-hydroxydeoxyguanosine. Three colonic sections of each animal were removed, fixed in 4% paraformaldehyde/PBS

and paraffin embedded. The tissue sections were mounted on slides and stained for 8-OHdG. Mouse IgG staining was used as a negative control. RNA digestion was performed using RNase (100 µg/ml) in Tris buffer (5 mM Tris, 1 mM EDTA, pH 7.5; 60 min at 37 °C) and DNA-denaturation was conducted by 70 mM NaOH with 0.14 M NaCl and 40 % Ethanol. Zymed Histomouse^{TM}-SP Kit was used according to the supplier's manual to block unspecific binding. The sections were then incubated over night with a primary antibody against 8-OHdG (1:250) or against IgG (1:250) as a negative control and counter stained with hematoxylin. After washing with water slides were dehydrated and covered in DePex. Slides were analysed using a light microscope (Olympus BX60).

Statistics. For all experiments, all means were calculated from three independent experiments, with the error bars representing standard deviation (SD). Analysis of statistical significance was done by Student's t-test with *$p < 0.05$, **$p < 0.01$ and ***$p < 0.001$ as levels of significance.

Results

The potential of human primary blood derived neutrophils (PMN) to induce DNA strand breakage and/or oxidative DNA damage in human intestinal Caco-2 cells was evaluated using a co-incubation model consisting of both cell types. As depicted in Figure 1, only activated neutrophils were able to induce both DNA strand breaks and, more pronounced, oxidative lesions. A non-significant induction of oxidative damage was already observed at a 1:1 ratio of both cell types, whereas a 3:1 ratio (PMN:Caco-2) resulted in significant DNA strand breakage and oxidative DNA damage.

Next, we investigated the ROS formation in this co-incubation model using EPR with the spin probe CPH, which has been introduced for the specific detection of superoxide anion radicals ($O_2^{\cdot -}$). Caco-2 cells alone, either with or without the addition of PMA, did not induce any detectable $O_2^{\cdot -}$ production (Figure 2) . Non-activated PMN were capable of mild ROS-formation, but this production could no longer be detected in the unstimulated co-incubation with Caco-2 cells. PMA-activated PMN did cause a pronounced and significant ROS generation, both in the absence and presence of Caco-2 cells. Interestingly, this PMN-induced ROS generation was slightly reduced in the presence of the intestinal epithelial cells although this reduction was not significant.

The effect of PMN on SiO_2 induced DNA damage in Caco-2 cells is shown in Figure 3. The SiO_2 particles caused a significant induction of DNA damage in Caco-2 cells in the absence of PMN. Notably, the level of induction observed with the SiO_2 in the Caco-2 cells was similar to the effect observed with PMA-treated PMN used as positive control in these series of experiments. Surprisingly, the presence of PMN did not augment the SiO_2-induced DNA strand breakage, but in fact resulted in markedly reduced effect in the intestinal epithelial cells. Application of the Fpg enzyme revealed an increased, albeit not significant induction of oxidative lesions after SiO_2 incubation alone. In the presence of PMN however, a significant increase in oxidative DNA damage was detected.

Possible effects of SiO_2 on PMN-induced $O_2^{\cdot -}$ generation were analysed using two independent methods, i.e. both lucignenin-enhanced chemiluminescence (Figure 4 A) and EPR spectroscopy with CPH as spin probe (Figure 4 B). ROS detection via chemiluminescence occurs via constant measurement over 50 minutes and results in

a typical curve as depicted in Figure 4 a. Compared to non-stimulated PMN, the presence of SiO_2 did not affect the overall formation of superoxide (area under the curve). In contrast, stimulation with PMA resulted in a significant ROS induction (Figure 4 A). EPR spectroscopy allows for a quantification of the amount of CPH that has reacted with superoxide anions over the 30 min incubation. Similar to our findings in chemiluminescence measurement, ESR confirmed that SiO_2 did not activate neutrophilic burst, since no increase in ROS formation was detected (Figure 4 B). In contrast, a clear effect was observed with the well-known neutrophil activator PMA. Figure 4 b shows representative EPR spectra of ROS formation.

To analyse the genotoxic properties of SiO_2 *in vivo* in healthy intestine as well as during inflammation, mice were fed normal or SiO_2 chow for 14 days, followed by 3 alternating cycles of DSS or SiO_2 treatment for the induction of colitis. The occurrence of symptoms of colitic inflammation was confirmed by measure of colon length (Figure 5 A) and the clinical score, with 3 indicating severest symptoms (Figure 5 B). The colon lengths were reduced markedly after colitis induction, whereas mice receiving SiO_2 exhibited normal colon lengths. The clinical score, reflecting bleeding intensity, weight loss and stool consistency, revealed an increase in symptoms after each DSS treatment followed by states of remission. Interestingly, DNA damage as measured by *in vivo* Fpg-comet assay (see Figure 6) was already high in the colons of the control animals, i.e. the mice that were neither treated with SiO_2 nor with DSS. Consequently, chronic colitis did not result in an increased DNA damage in the colon of DSS-treated animals compared to these high controls (Figure 6 A). Interestingly, the SiO_2-enriched diet even led to a reduced oxidative DNA damage, both in the colon tissues of healthy and colitic mice. However, calculation of the ΔFpg showed that the reduction in oxidative lesions was not statistically significant, as a result of high individual variations (Figure 6 B). Interestingly, detection of 8-OHdG by immunohistochemistry (IHC, Figure 7) revealed a clear increase of oxidative lesions, mainly located in the nuclei of epithelial cells, in both SiO_2 (Figure 7 B) and DSS (Figure 7 C) treated mice when compared to the control animals (Figure 7 A). Combined treatment with SiO_2 and DSS (Figure 7 D) also induced increased 8-OHdG sites compared to the control, however these seem less pronounced than the lesions induced by SiO_2 or DSS alone. All IgG stained (control) slides were found to be without marked core staining (not shown).

In the same animals we also evaluated the small intestines. In contrast to colon, no differences in DNA damage or induction of oxidative lesions were observed between any of the various treatments in the small intestine by Fpg-comet assay (Figure 8 A and B).

Since the above findings in colon tissue during chronic colitis might have been due to feedback and/or adapative response mechanisms we also evaluated the genotoxic effects of SiO_2 after shorter particle exposures and/or acute colitis. The treatment consisted of administration of DSS for 6 days (acute colitis animals) following 17 days of normal or SiO_2 chow. Results of these investigations are shown in figure 9. Slightly elevated levels of oxidative lesions were observed after a SiO_2 containing diet, although they did not reach a statistical significance. Remarkably, in the presence of Fpg, the % of tail DNA was found to be significantly lower in the DSS-SiO_2 group when compared to the SiO_2 groups (Figure 9 A). However, no significant reduction was found for the ΔFpg values indicating that there was no significant reduction of oxidative DNA damage (Figure 9 B). The absolute levels of DNA damage in the DSS and DSS-SiO_2 groups of the acute colitis study were comparable to the damage in the corresponding groups of the chronic study, but revealed higher interindividual variations. Moreover, IHC staining of the respective colonic tissue did not show marked differences in staining for 8-OHdG within the nuclei, as shown by representative images in Figure 10.

Discussion

In the present study we evaluated the DNA damaging potential of SiO_2 in the presence or absence of neutrophils on intestinal epithelial cells *in vitro*, as well as in a colitic mouse model *in vivo*.

Our *in vitro* model for intestinal inflammation consisted of a co-culture of Caco-2 cells and human primary neutrophils (PMN) at direct cell-cell contact. The model is similar to the one introduced by Vermeer and co-workers (Vermeer *et al.*, 2004) and a widely applied model in our laboratory to address effects of PMN on alveolar epithelial cell lines (Knaapen *et al.*, 1999, 2002a, 2006; Boots *et al.*, submitted). The presently applied co-incubation model allowed us to investigate the effect of activated neutrophils on the genome integrity of human intestinal cells and by varying the number of neutrophils present, different degrees of neutrophilic inflammation could be simulated. Importantly, we used non-confluent undifferentiated Caco-2 cells, which are still capable of cell division and differentiation. As such the influence of a neutrophilic inflammation on the potential genotoxic effects of SiO_2 could be addressed in an optimal manner, since intestinal inflammation is marked by the presence of hyperproliferative epithelial cells (Huang *et al.*, 1997; Arai *et al.*, 1999). Our results clearly show the potential of activated PMN to induce both DNA strand breakage and oxidative lesions in Caco-2 cells. Interestingly, this effect was shown to be dependent on both the number of PMN present and their activation.

A likely explanation for the observed PMN-driven DNA damage is the marked ROS production which is initiated during the respiratory burst of these inflammatory cells. Indeed, it is known that increased ROS formation also occurs in the inflamed tissue of patients suffering from ulcerative colitis (Babbs, 1992) accompanied by a reduced antioxidant potential, as lower levels of glutathione (Sido *et al.*, 1998). Since a huge amount of superoxide anion radicals could be found after activation of neutrophils alone or in the co-culture, we hypothesize that these ROS are the main cause of DNA damage in the Caco-2 cells.

Our previous studies demonstrated the potential of SiO_2 alone to induce oxidative lesions in Caco-2 cells after 4 hours incubation (Gerloff *et al.*, 2009). In the present work, we adapted the application of this nanoparticle to the co-incubation model and determined possible interference of PMN and SiO_2 on DNA damage in the co culture. Surprisingly, the SiO_2 particles alone now induced only significant DNA

strand breaks, but no oxidative lesions. The most likely explanation for this apparent discrepancy between the results of both studies is the difference in treatment time and cell culture conditions. In the present study, to adapt to the conditions of the co-incubation model a shorter incubation time was applied and all experiments were performed in HBSS instead of serum free cell culture media in order to minimise scavenging effects of culture medium constituents. Interestingly, the effects of SiO_2 were not enhanced in the co-incubation, i.e. when neutrophils were also present. Current results indicate that the SiO_2 particles do not activate the neutrophils to induce comparable DNA damage as detected in the presence of PMA, but that the presence of neutrophils in fact decreases the potential of SiO_2 to induce DNA damage in Caco-2 cells.

SiO_2-induced ROS formation by PMN was determined by two independent methods. No potential of SiO_2 to induce neutrophilic burst could be revealed. This absence correlates nicely with the observed absence of DNA damage within the co-incubation model. The observation that the DNA damaging effect of SiO_2 was abrogated in the presence of PMN may be explained by the presence of an increased number of total cells in culture (i.e. a 3-fold number of PMN), which thereby reduces the particle (number) dose per Caco-2 cell. The SiO_2 might preferentially interact with the phagocytosing PMN and thereby the amount of particles faced by Caco-2 cells is reduced, which in turn leads to reduced direct SiO_2 effects on Caco-2 cells. Moreover, the neutrophils are known to contain various antioxidants including superoxide dismutase (Zakhireh *et al.*, 1979), which may scavenge to moderate oxidative effects of the SiO_2 to the Caco-2 cells.

The actual influence of SiO_2 on DNA integrity *in vivo* was further investigated in a mouse model of colitis via the application of SiO_2 in the chow. The polysaccharide DSS was used for induction of experimental colitis as it reduces the integrity of the mucosal barrier by causing a direct toxicity to gut epithelial cells (Gaudio *et al.*, 1999; Wirtz and Neurath, 2007). Our *in vivo* comet assay analyses of fresh whole colonic tissue in this model surprisingly revealed reduced DNA lesions after SiO_2 ingestion in both healthy and colitic animals compared to control animals fed a SiO_2-free diet. The finding that DNA strand breaks were markedly reduced in the colitic mice leads to the assumption that DNA repair mechanisms might be upregulated in colitis. Such upregulation would be in accordance with the results of a previous study performed by Wessels and co-workers in our lab in an experimental

model of pulmonary exposure to nanoparticles (Wessels *et al.*, submitted). In this study, no induction of DNA strand breaks or oxidative lesions could be detected in the lungs of mice upon inhalation of spark generated carbon nanoparticles, while several genes regulating DNA repair enzymes tended to be upregulated within this tissue. However, immunohistochemical staining of 8-OHdG revealed a clear induction of oxidative lesions in the DNA of epithelial cells after treatment with SiO_2 or DSS. Moreover, the intensity of the induced staining tended to be slightly lower after combined DSS-SiO_2 treatment compared to treatment with either SiO_2 or DSS alone. The discrepancies between the immunohistochemical findings and the comet assay data might lie within the fact that not only epithelial cells are analysed by the latter method, but whole colon tissue. Thus, this also includes other cell types present in the colon, including infiltrated immune cells or small muscle cells, which might lead to a “dilution” of the overall determined effect. Moreover, one should take into account that the *in vivo* comet assay method requires processing time to isolate cells and nuclei from the tissue homogenates, during which potential artefacts may be induced. In contrast, IHC staining allows for the specific detection of 8-OHdG formation in individual cells.

Caco-2 cells, although isolated from a colon adenocarcinoma, form an apical brush border and microvilli upon differentiation (Chantret *et al.*, 1988) and thus show several properties of the small intestine. To investigate the influence of ingested SiO_2 on the gene integrity of the small intestine *in vivo*, the comet assay was also performed in whole small intestinal tissue. In line with our findings within the colonic tissue, no DNA damage was detectable in the small intestine after chronic ingestion of SiO_2. In contrast to a short-term study of Hong *et al.* (2005) who administered DSS in the drinking water for 48 hours, we also could not find any oxidative DNA damage in whole tissue samples of the small intestine after DSS treatment in our chronic study by Fpg-modified comet-assay analysis.

To address whether the observations were due to the chronic exposure conditions we also performed an acute colitis study. Comparably to our results of the chronic study, no induction of DNA strand breaks or oxidative lesions were found in colons of DSS treated mice. However, oxidative DNA damage tended to be increased after treatment with SiO_2 alone, although this did not reach statistical significance and may be due to the limited number of animals investigated. Remarkably, the oxidative DNA damage in the SiO_2 treatment group was significantly

higher than the damage found in the DSS+SiO_2 treatment group when the absolute amount of strand breaks plus oxidative lesions were considered (Figure 9 A), whereas IHC staining for 8-OHdG lesions did not show marked differences within the four treatment groups. However, the comet assay results are in concordance to our *in vitro* results, where the DNA damaging potential of SiO_2 seemed to be reduced in an inflammatory environment. The mechanisms of these *in vivo* effects require further investigation in view of their relevance for hazard and risk assessment of ingested SiO_2 and other nanoparticles, but also because of potential preventive or therapeutic strategies in patients suffering from inflammatory bowel diseases.

It should be emphasized that the *in vivo* comet assay used in our study reflects alterations in the whole tissue, and therefore not solely the DNA of epithelial cells which are considered relevant target cells for colon carcinogenesis (Itzkowitz *et al*., 2004). The DNA damage measured by the *in vivo* comet assay also may reflect integrity changes in endothelial cells, smooth muscle cells or, most importantly inflammatory cells, which might dilute a possible damage of the epithelial DNA. Earlier studies detected increased levels of 8-hydroxydeoxyguanosine (8-OHdG) in isolated colonic mucosal cells of DSS treated rats by HPLC (Tardieu *et al*., 1998) or in whole colonic rat tissue, measured by quantitative immunohistochemistry (Hong *et al*., 2005). The latter finding could be confirmed in our chronic colitis model for treatment with DSS, but not after co-treatment with DSS and SiO_2. This suggests that the *in vivo* comet assay of whole tissue might not be sensitive or specific enough to detect slight alterations in epithelial DNA damage. Additionally, Westbrook and co-workers could detect systemic DNA damage after chronic DSS treatment in mice, as found in peripheral leukocytes, detected with the alkaline comet assay during acute colitis, whereas a slight decrease of DNA strand breaks was reported during remission cycles (Westbrook *et al*., 2009), as in our study of chronic colitis.

Here we highlighted the effects of amorphous SiO_2, possibly present in food or pharmaceuticals, on the genome integrity of the healthy or inflammatory intestinal epithelium *in vitro* and *in vivo*. We analysed the effects of activated human primary neutrophils on the genome integrity of Caco-2 cells in an *in vitro* model of intestinal inflammation. The induction of oxidative lesions was dependent on the amount of activated inflammatory cells and associated with the neutrophilic burst. In the presence of SiO_2 no significant neutrophil-activation was detected, as measured by reactive oxygen species formation. In line with these observations, the concurrent

incubation of Caco-2 cells with neutrophils and SiO_2 did not lead to an augmented DNA damage when compared to the effect of SiO_2 alone. We further analysed the DNA damaging properties of ingested SiO_2 on the intestine in a DSS-induced colitic mouse model. DSS alone did not induce DNA strand breakage in the colons in both acute and chronic colitis studies. Treatment with SiO_2 in healthy or colitis mice also did not lead to a significant enhancement of DNA damage measured by the *in vivo* Fpg-comet assay, whereas slight induction of 8-OHdG lesions was shown in immunohistochemichal stainings in the chronically, but not in the acutely treated colons. We conclude that the risk of SiO_2 ingestion on the genome integrity of the intestine is low, also in the inflamed gut, taken into account that a rather high concentration was used. Importantly however, slightly increased oxidative lesions were found locally after chronic SiO_2 treatment. Moreover, systemic or long-term damage could not be excluded, and extrapolation of our current results to the human situation is limited and should be done with caution. Concern about the potential genotoxic hazard of nanoparticles in food was recently expressed on the basis of the investigations by Trouiller and co-workers, who showed marked systemic DNA damage and mutagenesis in mice after oral uptake of TiO_2 nanoparticles (Trouiller *et al*., 2009). However, in contrast to our investigations no data were provided in their study on local (geno)toxic effects in the intestine. In our present study, the mice chow contained 0.1 mass % of SiO_2, which is considerably lower than the cumulative exposure of TiO_2 applied via the drinking water as estimated by Trouiller *et al*. (2009). An appropriate interpretation of our current findings can only be made upon a thorough further evaluation of both quantitative (mass and number dose) and qualitative (size, aggregation/agglomeration, etc) particle properties such as size exposure assessments in consumers for SiO_2 and other types of nanoparticles.

References

Arai N, Mitomi H, Ohtani Y, Igarashi M, Kakita A, Okayasu I. Enhanced epithelial cell turnover associated with p53 accumulation and high p21WAF1/CIP1 expression in ulcerative colitis. Mod Pathol 1999;12(6):604-11

Ashwood P, Thompson RP, Powell JJ. Fine particles that adsorb lipopolysaccharide via bridging calcium cations may mimic bacterial pathogenicity towards cells. Exp Biol Med (Maywood) 2007;232(1):107-17.

Babbs CF. Oxygen radicals in ulcerative colitis. Free Radic Biol Med 1992;13(2):169-81

Boots AW, Gerloff K, van Berlo F, Ledermann K, Haenen GRMM, Bast A, Albrecht C, Schins RPF. Neutrophils augment LPS-mediated pro-inflammatory signaling in human lung epithelial cells, submitted

Chantret I, Barbat A, Dussaulx E, Brattain MG, Zweibaum A. Epithelial polarity, villin expression, and enterocytic differentiation of cultured human colon carcinoma cells: a survey of twenty cell lines. Cancer Res 1988;48(7):1936-42

Chaudhry Q, Scotter M, Blackburn J, Ross B, Boxall A, Castle L, Aitken R, Watkins R. Applications and implications of nanotechnologies for the food sector. Food Addit Contam Part A Chem Anal Control Expo Risk Assess 2008;25(3):241-58

Cooper HS, Murthy SN, Shah RS, Sendergran DJ. Clinicopathologic study of dextran sulphate sodium experimental murine colitis. Lab Invest 1993;69(2):238-249

Desai MP, Labhasetwar V, Amidon GL, Levy RJ. Gastrointestinal uptake of biodegradable microparticles: effect of particle size. Pharm Res 1996;13(12):1838-45

Donaldson K, Tran L, Jimenez LA, Duffin R, Newby DE, Mills N, MacNee W, Stone V. Combustion-derived nanoparticles: a review of their toxicology following inhalation exposure. Part Fibre Toxicol 2005;2:10

Driscoll KE, Deyo LC, Carter JM, Howard BW, Hassenbein DG, Bertram TA, 1997. Effects of particle exposure and particle-elicited inflammatory cells on mutation in rat alveolar epithelial cells. Carcinogenesis 18: 423-430.

Duffin R, Tran L, Brown D, Stone V, Donaldson K. Proinflammogenic effects of low-toxicity and metal nanoparticles in vivo and in vitro: highlighting the role of particle surface area and surface reactivity. Inhal Toxicol 2007;19(10):849-56

Fatahzadeh M. Inflammatory bowel disease. Oral Surg Oral Med Oral Pathol Oral Radiol Endod 2009;108(5):e1-10

food.gov.uk homepage: http://www.food.gov.uk/safereating/chemsafe/additivesbranch/enumberlist May 2010

Gaudio E, Taddei G, Vetuschi A, Sferra R, Frieri G, Ricciardi G, Caprilli R. Dextran sulfate sodium (DSS) colitis in rats: clinical, structural, and ultrastructural aspects. Dig Dis Sci 1999;44(7):1458-75

Gerloff K, Albrecht C, Boots AW, Förster I, Schins RPF. Cytotoxicity and oxidative DNA damage by nanoparticles in human intestinal Caco-2 cells. Nanotoxicol 2009; 3(4):355-364

Gerloff K, Pereira D, Faria N, Boots AW, Förster I, Albrecht C, Powell JJ, Schins RPF. Influence of simulated gastro-intestinal conditions on particle-induced cytotoxicity and interleukin-8 regulation in differentiated and undifferentiated Caco-2 cells, submitted

Hillery AM, Jani PU, Florence AT. Comparative, quantitative study of lymphoid and non-lymphoid uptake of 60 nm polystyrene particles. J Drug Target 1994;2(2):151-6

Hong MY, Turner ND, Carroll RJ, Chapkin RS, Lupton JR. Differential response to DNA damage may explain different cancer susceptibility between small and large intestine. Exp Biol Med (Maywood) 2005;230(7):464-71

Huang N, Katz JP, Martin DR, Wu GD. Inhibition of IL-8 gene expression in Caco-2 cells by compounds which induce histone hyperacetylation. Cytokine 1997;9(1):27-36

Itzkowitz SH, Yio X. Inflammation and cancer IV. Colorectal cancer in inflammatory bowel disease: the role of inflammation. Am J Physiol Gastrointest Liver Physiol 2004;287(1):G7-17.

Jani PU, McCarthy DE, Florence AT. Titanium dioxide (rutile) particle uptake from the rat GI tract and translocation to systemic organs after oral administration. J Pharm 1994;105(2):157-168

Johnston CJ, Driscoll KE, Finkelstein JN, Baggs R, O'Reilly MA, Carter J, Gelein R, Oberdörster G. Pulmonary chemokine and mutagenic responses in rats after subchronic inhalation of amorphous and crystalline silica. Toxicol Sci 2000;56(2):405-13

Jung HC, Eckmann L, Yang SK, Panja A, Fierer J, Morzycka-Wroblewska E, Kagnoff MF. A distinct array of proinflammatory cytokines is expressed in human colon epithelial cells in response to bacterial invasion. J Clin Invest 1995;95(1):55-65

Knaapen AM, Seiler F, Schilderman PA, Nehls P, Bruch J, Schins RP, Borm PJ. Neutrophils cause oxidative DNA damage in alveolar epithelial cells. Free Radic Biol Med 1999;27(1-2):234-40

Knaapen AM, Schins RP, Polat D, Becker A, Borm PJ. Mechanisms of neutrophil-induced DNA damage in respiratory tract epithelial cells. Mol Cell Biochem 2002a;234-235(1-2):143-51

Knaapen AM, Albrecht C, Becker A, Höhr D, Winzer A, Haenen GR, Borm PJA, Schins RPF. DNA damage in lung epithelial cells isolated from rats exposed to quartz: role of surface reactivity and neutrophilic inflammation. Carcinogenesis 2002b; 23: 1111-1120.

Knaapen AM, Güngör N, Schins RP, Borm PJ, Van Schooten FJ. Neutrophils and respiratory tract DNA damage and mutagenesis: a review. Mutagenesis 2006;21(4):225-36.

Kucharzik T, Williams IR. Neutrophil migration across the intestinal epithelial barrier--summary of in vitro data and description of a new transgenic mouse model with doxycycline-inducible interleukin-8 expression in intestinal epithelial cells. Pathobiology 2002-2003;70(3):143-9

Kunkel SL, Standiford T, Kasahara K, Strieter RM. Interleukin-8 (IL-8): the major neutrophil chemotactic factor in the lung. Exp Lung Res 1991;17(1):17-23

Lomer MC, Harvey RS, Evans SM, Thompson RP, Powell JJ. Efficacy and tolerability of a low microparticle diet in a double blind, randomized, pilot study in Crohn's disease. Eur J Gastroenterol Hepatol 2001;13(2):101-6

Lomer MC, Hutchinson C, Volkert S, Greenfield SM, Catterall A, Thompson RP, Powell JJ. Dietary sources of inorganic microparticles and their intake in healthy subjects and patients with Crohn's disease. Br J Nutr 2004;92(6):947-55

MacDermott. Chemokines in the inflammatory bowel disease. J Clin Immunol 1999;19(5):266-72

Mazzucchelli L, Hauser C, Zgraggen K, Wagner H, Hess M, Laissue JA, Mueller C. Expression of interleukin-8 gene in inflammatory bowel disease is related to the histological grade of active inflammation. Am J Pathol 1994;144(5):997-1007

Mitsuyama K, Toyonaga A, Sasaki E, Watanabe K, Tateishi H, Nishiyama T, Saiki T, Ikeda H, Tsuruta O, Tanikawa K. IL-8 as an important chemoattractant for neutrophils in ulcerative colitis and Crohn's disease. Clin Exp Immunol 1994;96(3):432-6

Monteiller C, Tran L, MacNee W, Faux S, Jones A, Miller B, Donaldson K. The pro-inflammatory effects of low-toxicity low-solubility particles, nanoparticles and fine particles, on epithelial cells in vitro: the role of surface area. Occup Environ Med 2007;64(9):609-15

Nanotechproject homepage http://www.nanotechproject.org/inventories/consumer/browse/products/5107/ April 2010

Oberdörster G, Oberdörster E, Oberdörster J. Nanotoxicology: an emerging discipline evolving from studies of ultrafine particles. Environ Health Perspect 2005;113(7):823-39

Okayasu I, Hatakeyama S, Yamada M, Ohkusa T, Inagaki Y, Nakaya R. A novel method in the induction of reliable experimental acute and chronic ulcerative colitis in mice. Gastroenterol 1990;98(3):694-702

Powell JJ, Faria N, Thomas-McKay E, Pele LC. Origin and fate of dietary nanoparticles and microparticles in the gastrointestinal tract. J Autoimmun 2010;34(3):J226-33

Risom L, Møller P, Vogel U, Kristjansen PE, Loft S. X-ray-induced oxidative stress: DNA damage and gene expression of HO-1, ERCC1 and OGG1 in mouse lung. Free Radic Res 2003;37(9):957-66

Rogler G, Andus T. Cytokines in inflammatory bowel disease. World J Surg 1998;22(4):382-9

Schins RP, Knaapen AM. Genotoxicity of poorly soluble particles. Inhal Toxicol 2007;19 (Suppl 1):189-98

Schmid K, Riediker M. Use of nanoparticles in Swiss Industry: a targeted survey. Environ Sci Technol 2008;42(7):2253-60

Schneider JC. Can microparticles contribute to inflammatory bowel disease: innocuous or inflammatory? Exp Biol Med (Maywood) 2007;232(1):1-2

Sido B, Hack V, Hochlehnert A, Lipps H, Herfarth C, Dröge W. Impairment of intestinal glutathione synthesis in patients with inflammatory bowel disease. Gut 1998;42(4):485-92

Singh S, Shi T, Duffin R, Albrecht C, van Berlo D, Höhr D, Fubini B, Fenoglio I, Martra G, Borm PJA, Schins RPF. Endocytosis, oxidative stress and IL-8 expression in human lung epithelial cells upon treatment with fine and ultrafine TiO2: role of particle surface area and of surface methylation of the particles. Toxicol Applied Pharmacol 2007:222:141-151

Speit G, Schütz P, Bonzheim I, Trenz K, Hoffmann H. Sensitivity of the FPG protein towards alkylation damage in the comet assay. Toxicol Lett 2004;146(2):151-8

Tardieu D, Jaeg JP, Cadet J, Embvani E, Corpet DE, Petit C. Dextran sulfate enhances the level of an oxidative DNA damage biomarker, 8-oxo-7,8-dihydro-2'-deoxyguanosine, in rat colonic mucosa. Cancer Lett 1998;134(1):1-5

Tiede K, Boxall AB, Tear SP, Lewis J, David H, Hassellov M. Detection and characterization of engineered nanoparticles in food and the environment. Food Addit Contam Part A Chem Anal Control Expo Risk Assess 2008;25:795-821

Trouiller B, Reliene R, Westbrook A, Solaimani P, Schiestl RH. Titanium dioxide nanoparticles induce DNA damage and genetic instability in vivo in mice. Cancer Res 2009;69(22):8784-9

Unfried K, Albrecht C, Klotz LO, von Mikecz A, Grether-Beck S, Schins RPF. Cellular responses to nanoparticles: target structures and mechanisms. Nanotoxicol 2007;1:52-71

Vermeer IT, Henderson LY, Moonen EJ, Engels LG, Dallinga JW, van Maanen JM, Kleinjans JC. Neutrophil-mediated formation of carcinogenic N-nitroso compounds in an in vitro model for intestinal inflammation. Toxicol Lett 2004;154(3):175-82

Wessels A, Van Berlo D, Boots AW, Gerloff K, Scherbart A, Cassee FR, Gerlofs-Nijland ME, Van Schooten FJ, Albrecht C, Schins RPF. Oxidative stress and DNA damage responses in rat and mouse lung to inhaled carbon nanoparticles. accepted in Nanotoxicology

Westbrook AM, Wei B, Braun J, Schiestl RH. Intestinal mucosal inflammation leads to systemic genotoxicity in mice. Cancer Res 2009;69(11):4827-34

Wirtz S, Neurath MF. Mouse models of inflammatory bowel disease. Adv Drug Deliv Rev 2007;59(11):1073-83

Zakhireh B, Block LH, Root RK. Neutrophil function and host resistance. Infection 1979;7(2):88-98

Legends

Figure 1 **DNA strand breakage and oxidative DNA damage in Caco-2 cells upon co-exposure to activated PMN.** DNA strand breakage and oxidative DNA damage were determined in Caco-2 cells using the Fpg-modified comet assay following 30 minutes co-incubation with PMA-activated or non-activated primary human neutrophils (PMN) at the indicated PMN:Caco-2 ratios in $HBSS^{+/+}$. PMA=phorbol-12-myristate-13-acetate. Values are expressed as mean and standard deviation, n=3.

* $p < 0.05$ versus control.

Figure 2 **ROS formation by PMN and Caco-2 cells.** The formation of superoxide anion radicals by Caco-2 cells alone, PMA activated or non-activated primary human neutrophils (PMN) alone or Caco-2 cells and PMN in co-incubation was determined via ESR after 30 minutes at 37°C using the spin probe CPH. PMA=phorbol-12-myristate-13-acetate. AU=arbitrary units. Values are expressed as mean and standard deviation, n=3. n.s.=not significant

*** $p < 0.001$ versus control.

Figure 3 **DNA strand breakage and oxidative DNA damage in Caco-2 cells by activated PMN and SiO_2.** DNA strand breakage and oxidative DNA damage were determined in Caco-2 cells using the Fpg-modified comet assay. Cells were (I) not incubated as controls, (II) 30 minutes co-incubated with PMA-activated primary human neutrophils (PMN), (III) 30 minutes incubated with SiO_2 alone or (IV) 30 minutes co-incubated with SiO_2 and PMN. SiO_2 concentration: 20 µg/cm^2. PMN:Caco-2 ratio: 3:1. PMA=phorbol-12-myristate-13-acetate. Values are expressed as mean and standard deviation, n=3.

* $p < 0.05$, ** $p < 0.01$ and *** $p < 0.001$ versus control.

Figure 4 **ROS generation from PMN upon treatment with SiO_2.** The formation of superoxide anion radicals by primary human neutrophils (PMN) was determined by chemiluminescence using lucigenin over an incubation

period of 50 minutes (A) and ESR after 30 minutes pre-incubation with the spin probe CPH (B). (a) Representative luminescence curve and (b) representative ESR spectra by non-activated PMN (ctr=control), PMA-activated PMN (PMA) and SiO_2-treated PMN (SiO_2; (a) 312.5 µg/cm^2, (b) 20 µg/cm^2). AU=arbitrary units. Values are expressed as mean and standard deviation, n=3.

** $p < 0.01$ and *** $p < 0.001$ versus control.

Figure 5 **Evaluation of the severity of the induced chronic colitis.** Colon lengths were determined as marker of colitic symptoms (A). The clinical score as a combined measure of changes in bleeding intensity, weight loss and stool consistency. 1 = no effect detectable to 3 = strongest colitic effects (B).

Figure 6 **Effect of oral SiO_2 on DNA strand breakage and oxidative DNA damage in murine colonic tissue in a chronic colitis model.** DNA strand breakage and oxidative DNA damage were determined in whole murine colonic tissue using the *in vivo* Fpg-modified comet assay (A). The total amount of oxidative DNA damage is depicted as ΔFpg, calculated by the difference between + Fpg and – Fpg values (B). Treated mice were fed with either DSS to induce chronic colitic symptoms, SiO_2 or both DSS and SiO_2. ctr=control, DSS=dextrane sulphate sodium. Values are expressed as mean and standard deviation, n=3 (ctr), n=4 (SiO_2) and n=6 (DSS, DSS+SiO_2).

* $p < 0.05$ and *** $p < 0.001$ versus control.

Figure 7 **Immunohistochemical analysis of 8-hydroxydeoxyguanosine in a murine colonic tissue in a chronic colitis model.** Representative images of colonic sections, obtained from controls (A), mice after receiving SiO_2 enriched-chow (B) DSS treated mice receiving normal chow (C) or DSS treated mice receiving SiO_2 enriched-chow (D), stained with an antibody against 8-OHdG (original magnification × 400). n=3 (ctr), n=4 (SiO_2) and n=6 (DSS, DSS+SiO_2).

Figure 8 **Effect of oral SiO_2 on DNA strand breakage and oxidative DNA damage in murine small intestinal tissue in a chronic colitis model.** DNA strand breakage and oxidative DNA damage were determined in whole murine small intestinal tissue using the *in vivo* Fpg-modified comet assay (A). The total amount of oxidative DNA damage damage is depicted as ΔFpg, calculated by the difference between + Fpg and - Fpg values (B). Treated mice were fed with either DSS to induce chronic colitic symptoms, SiO_2 or both DSS and SiO_2. ctr=control, DSS=dextrane sulphate sodium. Values are expressed as mean and standard deviation, n=4 (ctr, SiO_2) and n=6 (DSS, DSS+SiO_2).
* $p < 0.05$ and *** $p < 0.001$ versus control.

Figure 9 **DNA strand breakage and oxidative DNA damage in murine colonic tissue using *in vivo* Fpg-comet assay in an acute colitis model.** DNA strand breakage and oxidative DNA damage were determined in whole murine colonic tissue using the *in vivo* Fpg-modified comet assay (A). The total amount of oxidative DNA damage is depicted as ΔFpg, calculated by the difference between + Fpg and – Fpg (B). Treated mice were fed with either DSS to induce acute colitic symptoms, SiO_2 or both DSS and SiO_2. ctr=control, DSS=dextrane sulphate sodium. Values are expressed as, n=3 (ctr), n=4 (SiO_2, DSS) and n=5 (DSS+SiO_2).
** $p < 0.01$

Figure 10 **Immunohistochemical analysis of 8-hydroxydeoxyguanosine in a murine colonic tissue in an acute colitis model.** Representative images of colonic sections, obtained from controls (A), mice after receiving SiO_2 enriched-chow (B) DSS treated mice receiving normal chow (C) or DSS treated mice receiving SiO_2 enriched-chow (D), stained with an antibody against 8-OHdG (original magnification × 400). n=3 (ctr), n=4 (SiO_2, DSS) and n=5 (DSS+SiO_2).

Figure 1

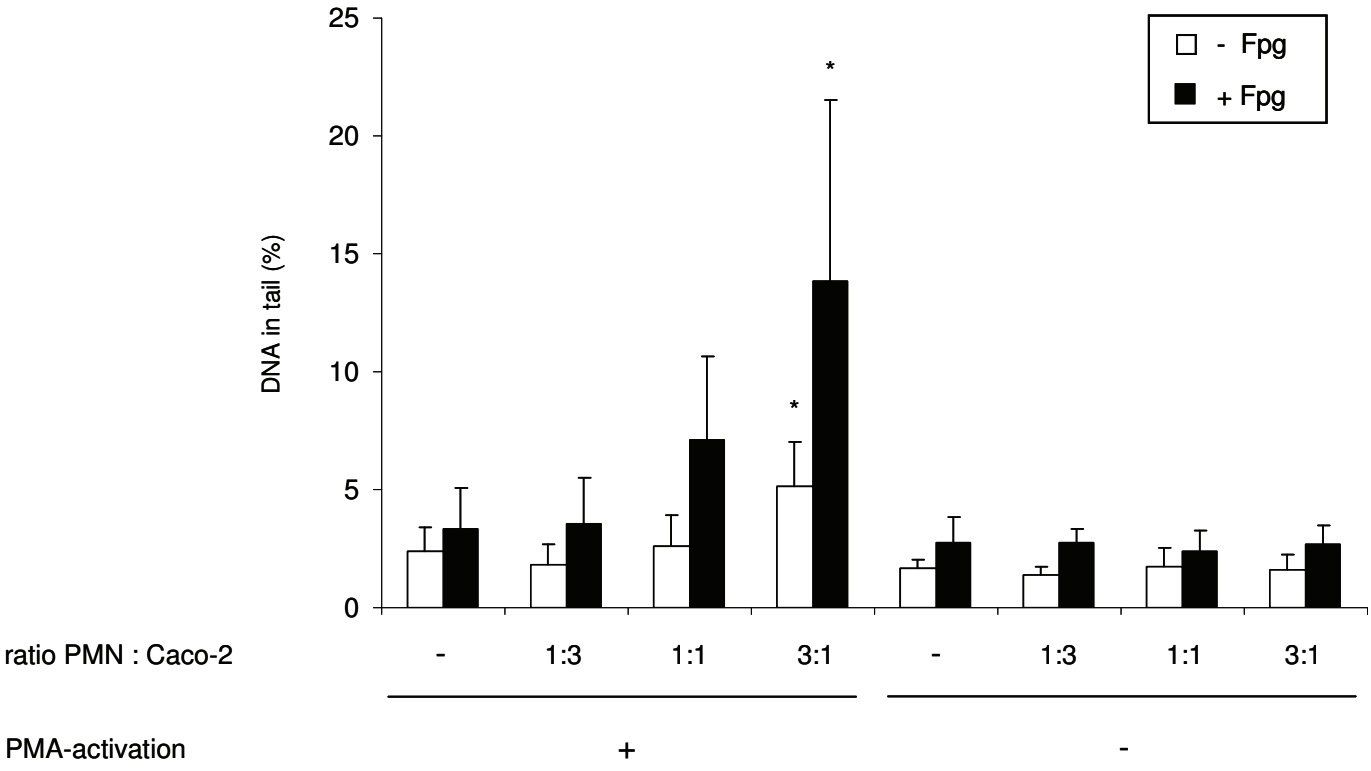
25
20
15
10
5
0
DNA in tail (%)
- Fpg
+ Fpg
*
*
ratio PMN : Caco-2
-
1:3
1:1
3:1
-
1:3
1:1
3:1
PMA-activation
+
-

Figure 2

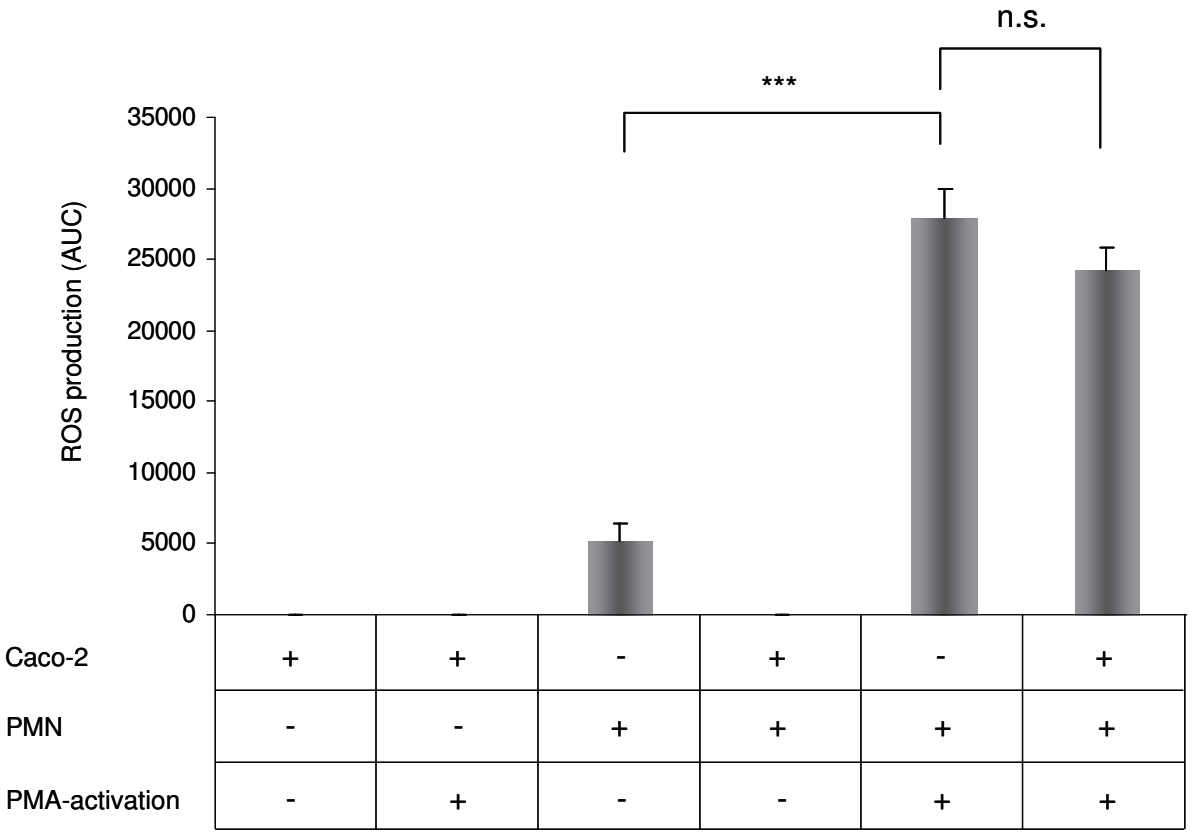
n.s.
***
35000
30000
25000
20000
15000
10000
5000
0
ROS production (AUC)
Caco-2
PMN
PMA-activation
+ + - + - +
- - + + + +
- + - - + +

Figure 3

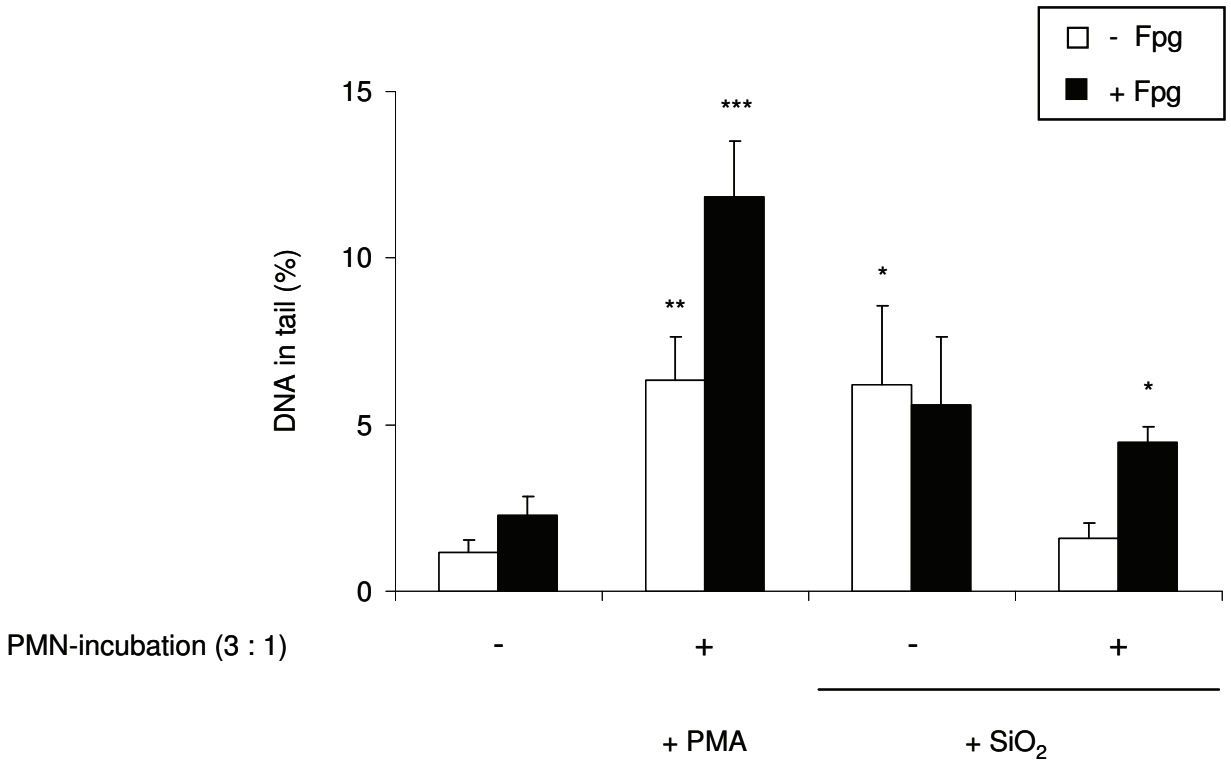

Figure 4

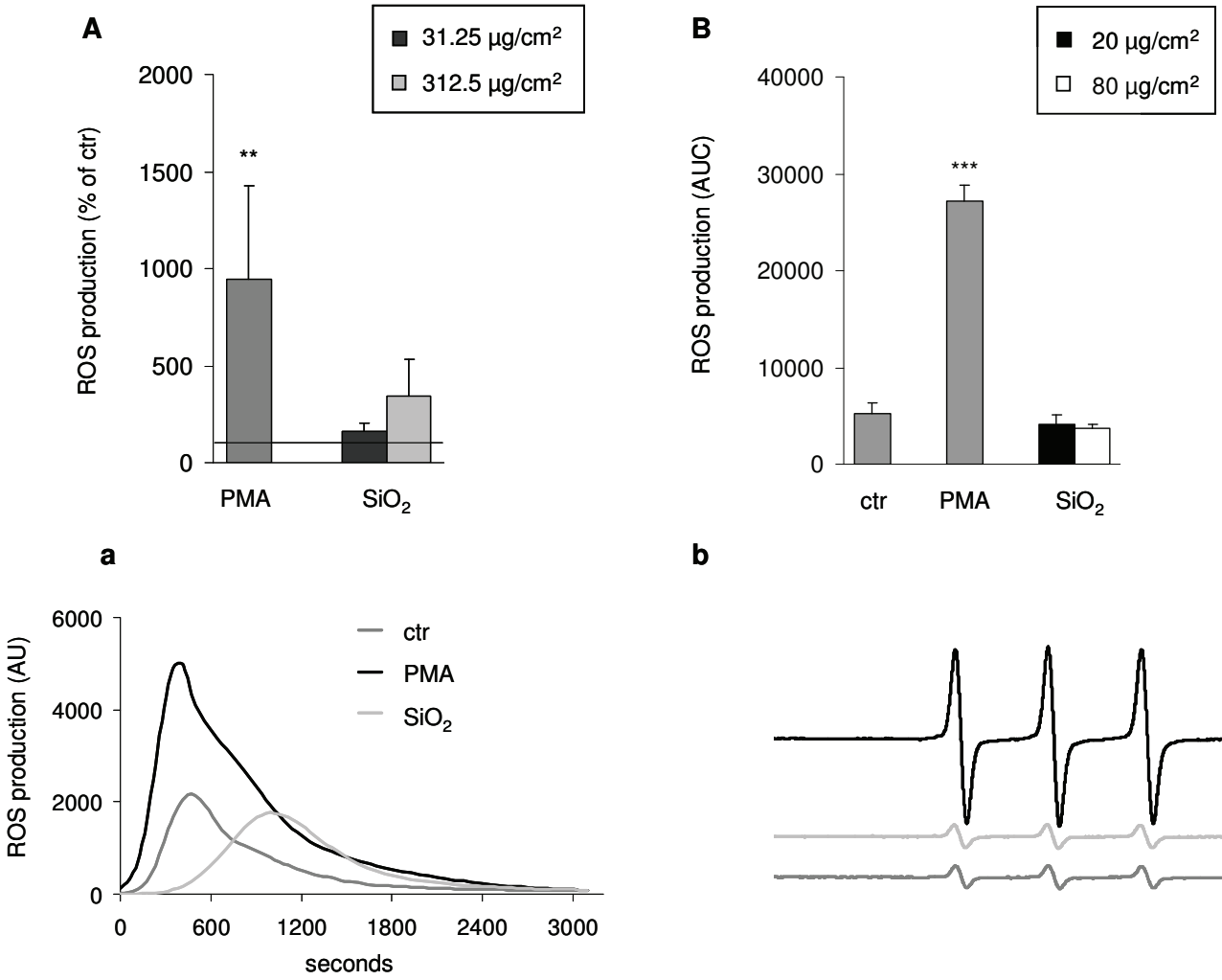
A
31.25 µg/cm²
312.5 µg/cm²
ROS production (% of ctr)
2000
1500
1000
500
0
**
PMA
SiO2
B
20 µg/cm²
80 µg/cm²
ROS production (AUC)
40000
30000
20000
10000
0
***
ctr
PMA
SiO2
a
ROS production (AU)
6000
4000
2000
0
ctr
PMA
SiO2
0
600
1200
1800
2400
3000
seconds
b

Figure 5

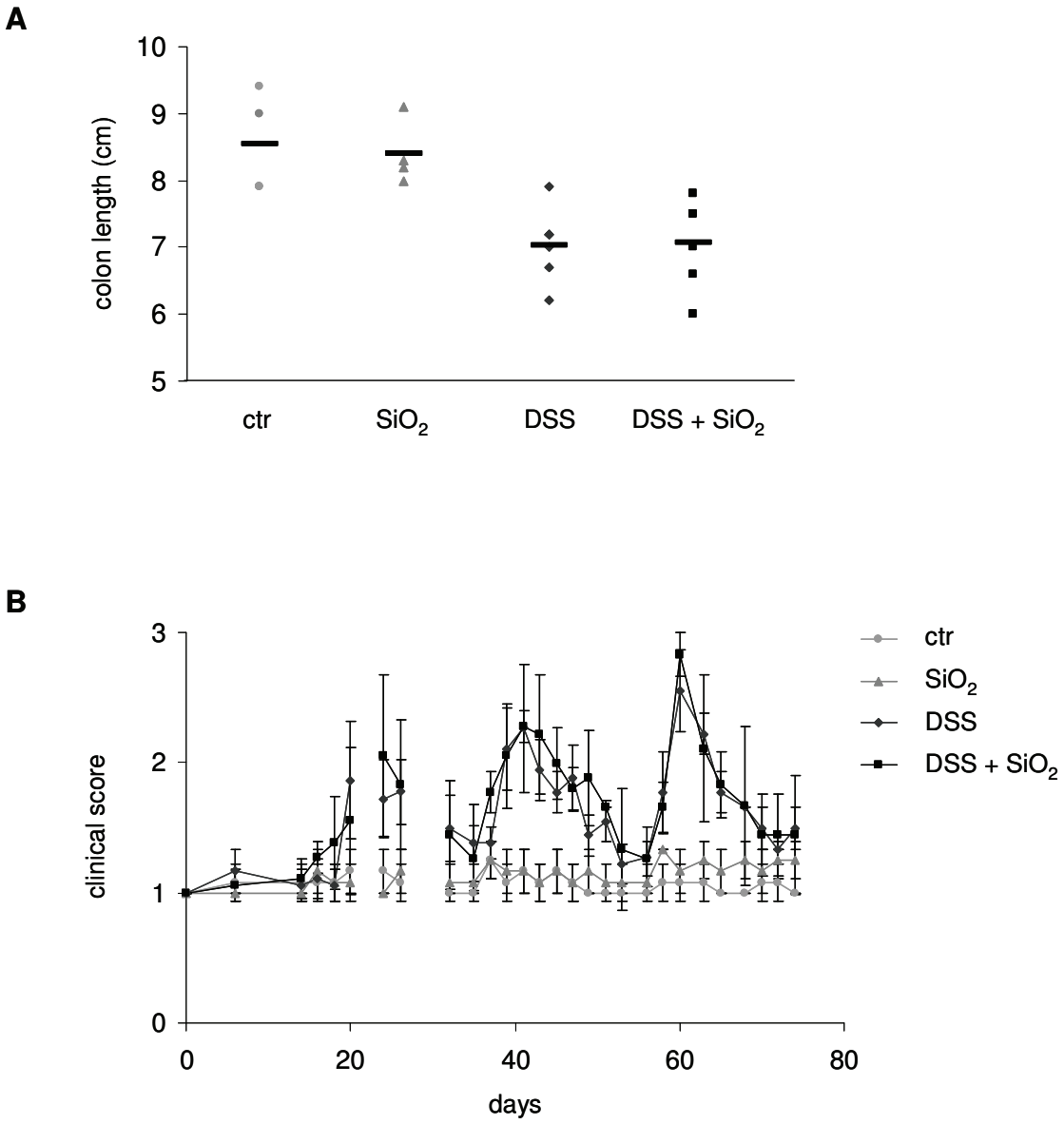
A
colon length (cm)
10
9
8
7
6
5
ctr
SiO2
DSS
DSS + SiO2
B
clinical score
3
2
1
0
0
20
40
60
80
days
ctr
SiO2
DSS
DSS + SiO2

Figure 6

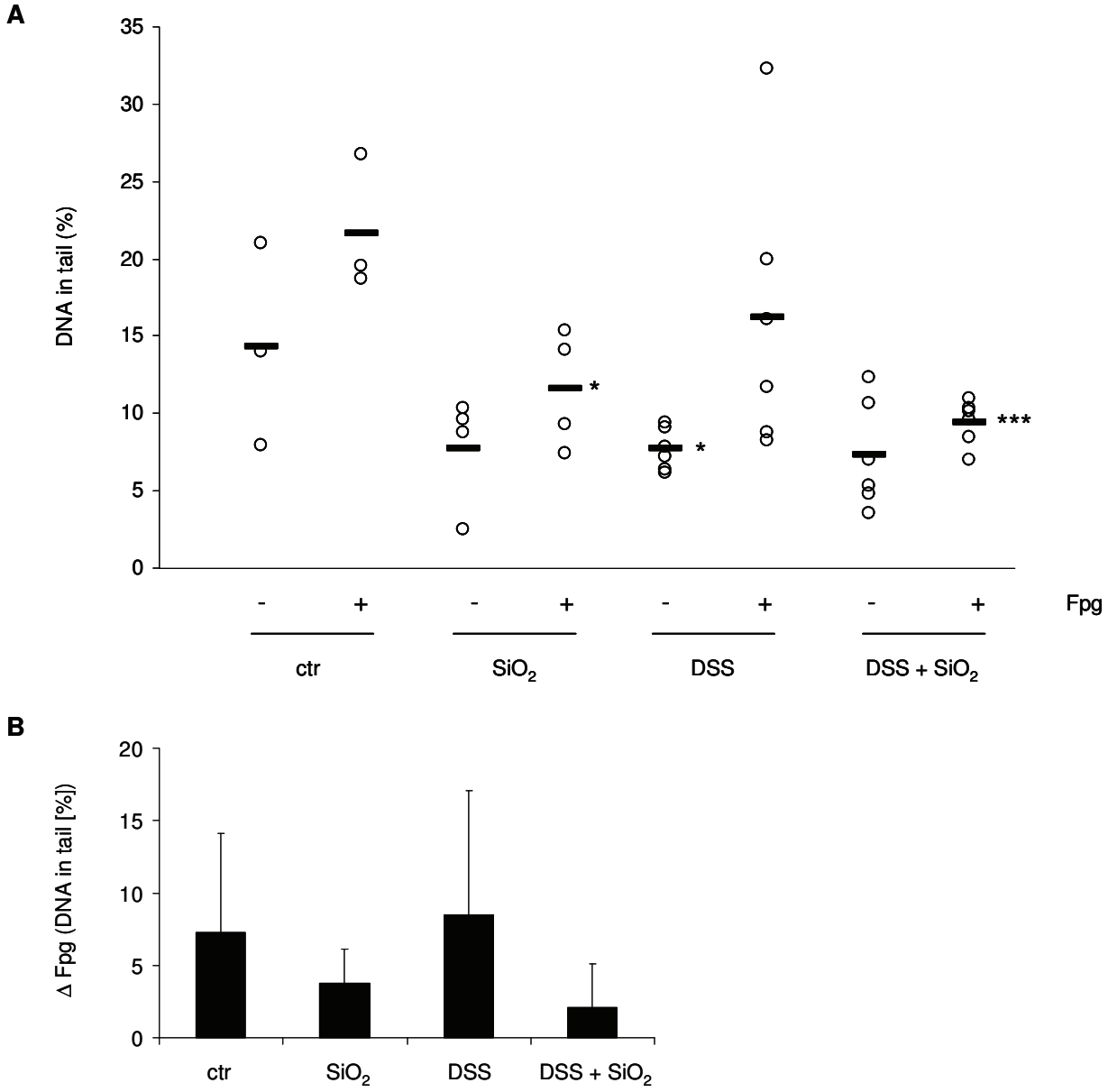
A
DNA in tail (%)
35
30
25
20
15
10
5
0
*
*
***
-
+
-
+
-
+
-
+
Fpg
ctr
SiO2
DSS
DSS + SiO2
B
Δ Fpg (DNA in tail [%])
20
15
10
5
0
ctr
SiO2
DSS
DSS + SiO2

Figure 7

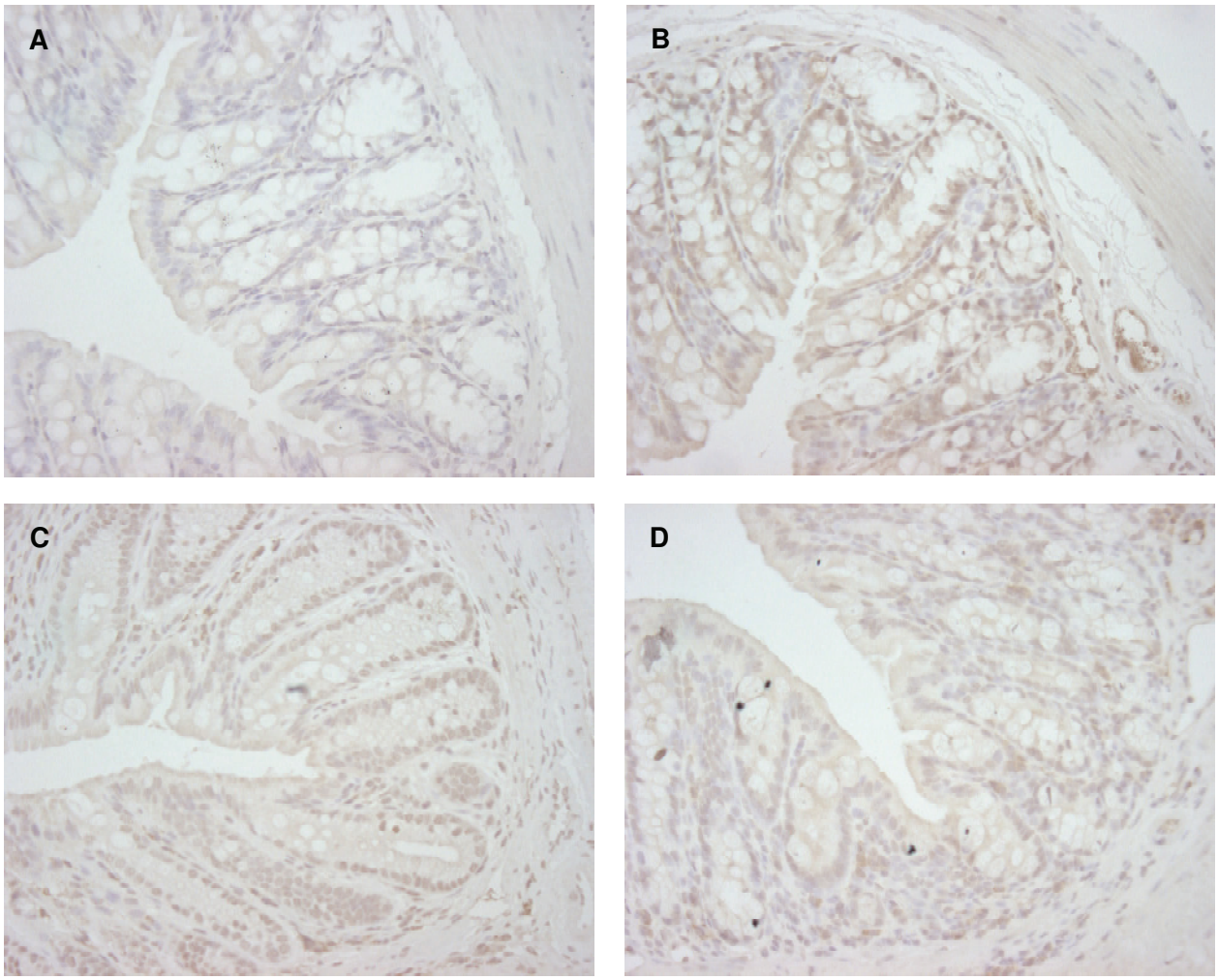

Figure 8

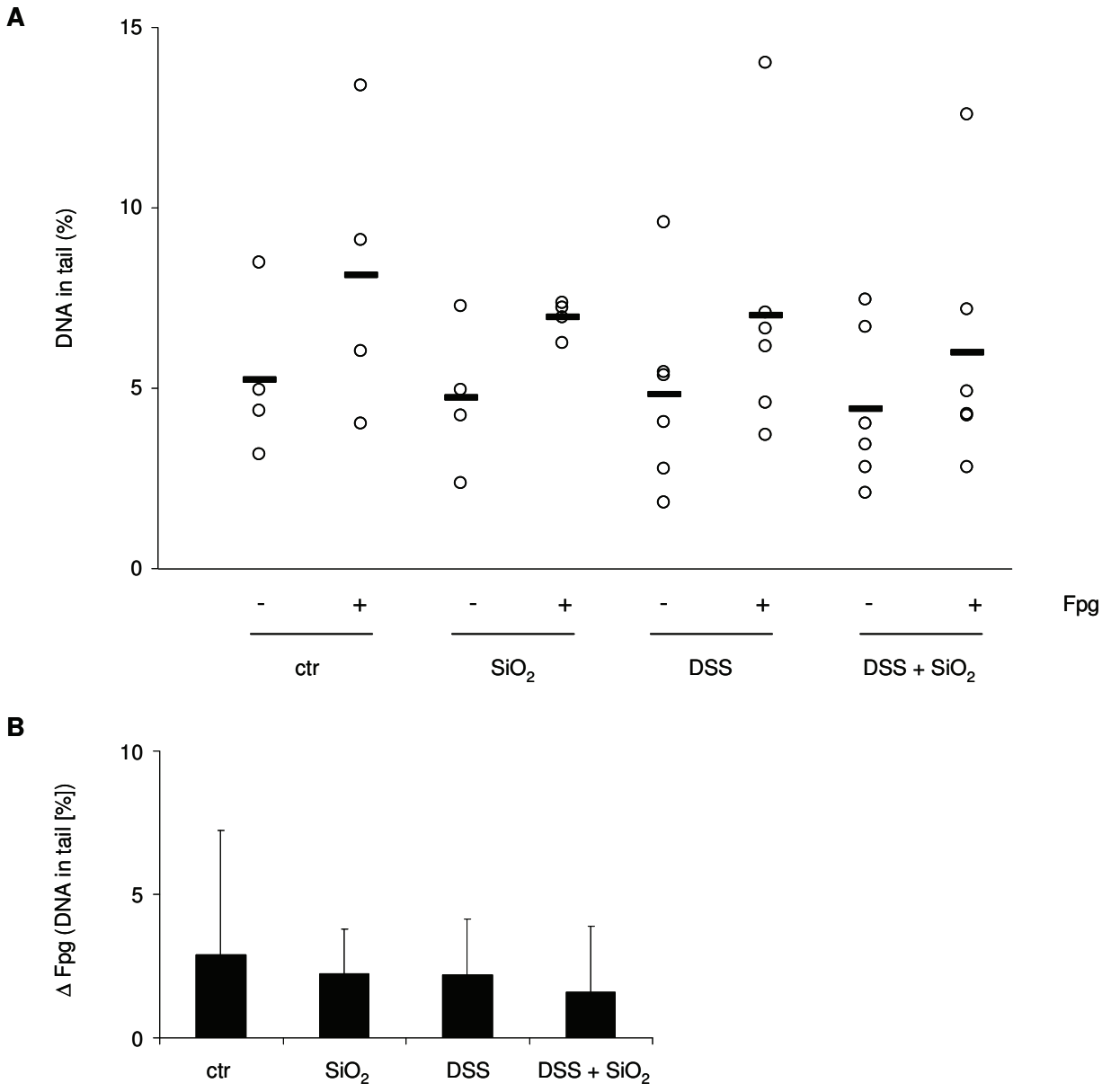
A
15
10
5
0
DNA in tail (%)
- + - + - + - +
Fpg
ctr
SiO2
DSS
DSS + SiO2
B
10
5
0
Δ Fpg (DNA in tail [%])
ctr
SiO2
DSS
DSS + SiO2

Figure 9

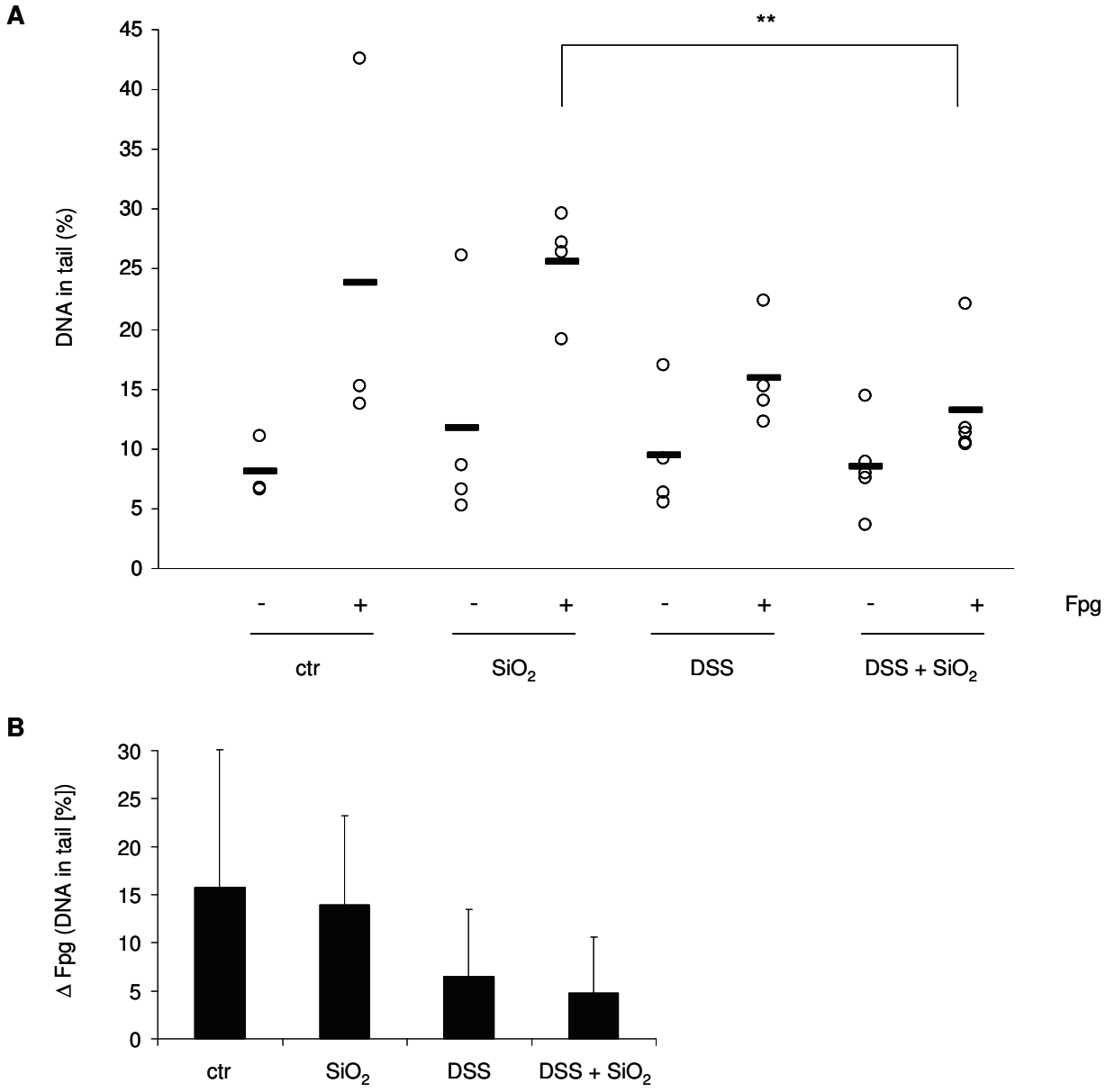
A
**
DNA in tail (%)
45
40
35
30
25
20
15
10
5
0
-
+
-
+
-
+
-
+
Fpg
ctr
SiO2
DSS
DSS + SiO2
B
Δ Fpg (DNA in tail [%])
30
25
20
15
10
5
0
ctr
SiO2
DSS
DSS + SiO2

Figure 10

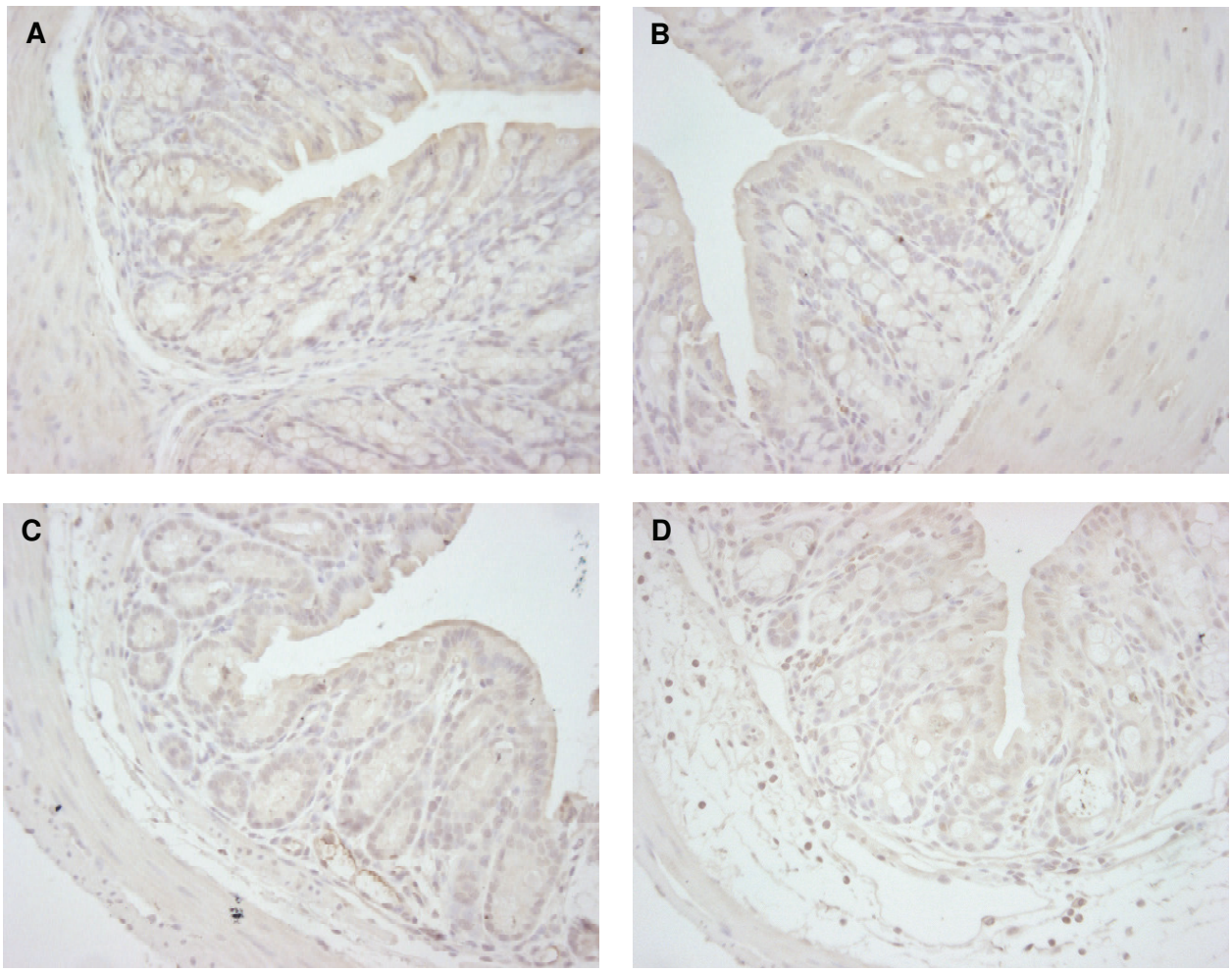

OXFORD UNIVERSITY PRESS Toxicological Sciences

2,3,7,8-Tetrachlorodibenzo-p-dioxin impairs stable establishment of oral tolerance in mice

Journal:	*Toxicological Sciences*
Manuscript ID:	TOXSCI-10-0266
Manuscript Type:	Research Article
Date Submitted by the Author:	25-Mar-2010
Complete List of Authors:	Esser, Charlotte; Institut für Umweltmedizinische Forschung, Immunology Chmill, Stefanie; Institut für Umweltmedizinische Forschung, Immunology Kadow, Stephanie; Institut für Umweltmedizinische Forschung, Immunology Winter, Meike; Institut für Umweltmedizinische Forschung, Immunology Weighardt, Heike; Institut für Umweltmedizinische Forschung, Immunology
Key Words:	gastrointestinal < Systems Toxicology, dioxin < Agents, cytokine, signalling < Immunotoxicology, food allergy < Immunotoxicology

2,3,7,8-TETRACHLORODIBENZO-*P*-DIOXIN IMPAIRS STABLE ESTABLISHMENT OF ORAL TOLERANCE IN MICE

Stefanie Chmill, Stephanie Kadow, Meike Winter, Heike Weighardt, and Charlotte Esser[§]

Molecular Immunology, Institute for Environmental Medical Research, Auf´m Hennekamp 50, 40225 Düsseldorf, Germany

[§] corresponding author

Charlotte Esser, Ph.D.

Auf´m Hennekamp 50

40225 Düsseldorf

Tel. +49-211-3389253

chesser@uni-duesseldorf.de

ABSTRACT

The toxic environmental pollutant 2,3,7,8-tetrachlorodibenzo-p-dioxin (TCDD) is a potent immunomodulatory chemical. TCDD activates the arylhydrocarbon receptor (AhR), and suppresses peripheral humoral and cellular adaptive immune responses. Though the major route of uptake is via food, little is known until now on the immunotoxic effects of TCDD on the gut associated lymphoid tissue. We show here that AhR is strongly expressed along the small intestine, especially in intestinal epithelial cells (IEC). The AhR marker gene *cyp1a1* is induced in IEC by oral TCDD exposure. Treatment of C57BL/6 mice with a non-toxic dose of 10μg/kg body weight TCDD prior to induction of oral tolerance against the model protein ovalbumin prevented the stable establishment of tolerance. We found an increase in IL-6 producing CD103+ dendritic cells present in the gut draining mesenteric lymph nodes and higher frequencies of Th17 cells. The results indicate a DC driven shift in the balance of regulatory T cells and pro-inflammatory Th17 upon oral TCDD treatment. Our data have implications for food allergies in settings of environmental exposure, but also raise concerns regarding the harmlessness of over-dosing potential AhR agonist in food.

KEY WORDS: mucosal immunity, Th17, aryl hydrocarbon receptor, tolerance, dendritic cells

INTRODUCTION

2,3,7,8-tetrachlorodibenzo-*p*-dioxin (TCDD) and other polyhalogenated hydrocarbons, including biphenyls and furans, are environmental pollutants with far-reaching toxic potential in humans and animals. They mediate toxicity via binding to and activating the aryl hydrocarbon receptor (AhR), a transcription factor and chemical sensor present in many (but not all) cell types. Classically, it mediates gene transcription in complex with ARNT, another PAS-bHLH protein, and targets promoter elements called DRE ("dioxin-responsive element") (Beischlag *et al.* 2008). Recently, alternative signalling of AhR via association with RelA or RelB was described, resulting in transcription of NFκB responsive genes (Tian 2009).

Immunotoxicological studies in mice exposed to TCDD showed drastic changes in thymocyte lineage decisions and impaired functions of many immune cells, including changes in cytokine profiles (Kerkvliet 2009; Lai *et al.* 1997; Laiosa *et al.* 2003). The correlated systemic effects are strong immunosuppression of the humoral, cellular, and innate immune responses (Kerkvliet 2002; Kerkvliet 2009; Majora *et al.* 2005; Schecter *et al.* 2006). A definite role for AhR in immunity emerged from studies on Th17 cells and dendritic cells (reviewed in Esser *et al.* 2009), two cell types with high expression of AhR (Jux *et al.* 2009; Platzer *et al.* 2009; Veldhoen *et al.* 2008).

In humans, approximately 90% of environmental exposure to TCDD is via food (Schecter *et al.* 2006; van Leeuwen *et al.* 2000). Moreover, abundant constituents of food, such as plant flavonoids and indoles, or bacterial tryptophan products are agonists of the AhR and may activate this pathway in the gut (Nguyen and Bradfield 2008). The gut is a highly active immune site in its own right, with about one third of all T cells of the body found intraepithelially and in the gut associated lymphoid tissue (GALT), i.e. lamina propria, Peyer's Patches and mesenteric lymph nodes. GALT differs from the peripheral immune

system, because is has to balance responsiveness between pathogenic and harmless antigens, including food constituents and the symbiotic gut flora. The gut is lined with a single layer of epithelia cells, connected by tight junctions, interspersed with goblet and paneth cells, which provide mucus and antimicrobial peptides, respectively (Artis 2008). Interspersed in the epithelium are intraepithelial lymphocytes (IEL), mostly $CD8^+$ cells, and in particular $CD8\alpha\alpha^+$ $TCR\gamma\delta^+$ T cells. The latter appear to strengthen the epithelial barrier function, e.g. by providing the lymphokine KGF (Chen *et al.* 2002). Immune cells in the lamina propria include $CD4^+$ T cells, plasma cells, DCs, macrophages, natural killer cells, and mast cells.

It has been known for decades that feeding protein antigens prevents a subsequent immune response against this antigen, a phenomenon called "oral tolerance". Oral tolerance is maintained by specialized $CD103^+$ dendritic cell, which sample the gut lumen, migrate to the mesenteric lymph nodes and present antigen (Jaensson *et al.* 2008; Worbs *et al.* 2006). While the role and effects of AhR and TCDD on the function of peripheral dendritic cells and differentiation of T cells have received considerable interest (Esser *et al.* 2009), surprisingly little is known on the effects of TCDD on cells of GALT. We asked whether TCDD exposure affects induction and maintenance of oral tolerance against the harmless food antigen ovalbumin (OVA). We show here, that this is indeed the case, and present possible mechanisms.

MATERIAL AND METHODS

Mice

C57BL/6 mice were from Janvier (Le Genest-St-Isle, France) and bred under specific pathogen-free conditions.

Chemicals and reagents

TCDD (Cambridge Isotope Laboratories, USA) was diluted in olive oil and applied at 10µg/kg body weight (b.w.).

Feeding and immunization regimen

To induce oral tolerance, mice were fed with 20mg OVA (Sigma-Aldrich, Munich, Germany) in 100µl PBS. TCDD treatment was 3 days prior to tolerance induction. Mice were immunized with 10µg OVA in 100µl PBS/CFA emulsion (first immunization) or PBS/IFA emulsion (booster immunizations) on days 12, 23 and 55. To trigger OVA-specific antibody secretion into the gut, mice were fed 3 times 1mg OVA in 100µl PBS by gavages on days 38, 41, 43.

Sample preparation

Serum was prepared from coagulated blood and frozen at -20^{o}C until further use. For faecal samples, 2-5 faecal pellets per mouse were collected and dried at 4°C. 100mg of faecal matter was dissolved in 1ml PBS/0.01% NaN_3 by shaking at RT for 3h. Particulate matter was removed by centrifugation and samples stored at -20°C.

ELISA

Total and OVA-specific antibody concentrations were measured by ELISA. For detection of OVA specific antibodies, ELISA plates were coated with 100µg OVA/ml and blocked. Serum or faecal samples were diluted (1:10.000 - 1:80.000 or 1:8, respectively) in 1% FCS in PBS and added. The plate was developed with biotinylated anti-IgG1 or IgA-antibodies (SBA, Birmingham, AL, USA. The amount of OVA specific antibodies is given relative to our own standard sera and faecal sample acquired from immunized mice.

Total antibody concentration was determined using isotype specific antibodies for coating. All antibodies were from Sigma (anti-IgA coating) or SBA. IgA and IgG1 standards

(hybridomas 233.1.3 and N1 G9), were a kind gift of C. Uthoff-Hachenberg (University of Cologne).

RT-PCR

RNA and cDNA preparation was according to standard procedures. For RNA from complete intestine, about 1cm² pieces were put on a shaker for 3h at 37°C in TRIzol™ (Invitrogen) before chloroform extraction. RT-PCR was performed as previously published (Frericks *et al.* 2007).

Single cell preparations of IEL and LPL

The small intestine was carefully removed and stripped of mesenterial tissue. The inside was flushed with PBS, Peyer's patches were removed with a scalpel, and the intestine was opened lengthwise. 1cm long segments were placed in 5mM EDTA in PBS (pH7.2) and shaken vigorously in a water bath at 37°C for 40min to release the epithelial cells and intraepithelial lymphocytes into the solution. Lymphocytes were purified further on on a 75%/40%/25% Percoll™ (Biochrom) gradient. Lamina propria cells were obtained by digesting the remaining solid gut pieces with 100 U/ml collagenase VII from *Clostridium histolyticum* (Sigma) for 1.5h at 37°C under constant stirring at 200rpm (Westendorf *et al.* 2009).

Flow cytometry

Single cell suspensions were incubated with Fc-block (anti-CD16/32) before staining with the indicated antibodies (10 minutes, 4°C). Antibodies used: anti-CD16/32 (Fc-Block, clone 2.4G2), anti-CD4 (clone RM4-5), anti-CD8a (clone 53-6.7), anti-CD8b (clone H35-17.2), anti-CD19 (clone 1D3), anti-TCRγδ (clone GL3) and anti-CD69 (clone H1.2F3), all from BD Pharmingen (Heidelberg, Germany). Anti-CD11c (clone N418), anti-MHCII (clone M5/114.15.2) and anti-CD103 (clone 2E7) antibodies for surface staining were from eBioscience (Frankfurt, Germany). The FoxP3 staining kit (antibody clone FJK-16s) from

eBioscience was used for staining regulatory T cells. $5*10^6$ cells/ml from mesenteric lymph nodes (MLN) or Peyer's Patches (PP) were stimulated in vitro with PMA (5ng/ml) and ionomycin (250ng/ml). 1µl/ml BrefeldinA (Golgi Plug, BD Pharmingen, Heidelberg, Germany) was added 5h prior to staining to inhibit cytokine secretion. After surface staining, cells were fixed in 2% paraformaldehyde (PFA) in PBS for 20min at RT, and permeabilizied with 0.5% saponin. Cells were then incubated for 20min at RT with the indicated intracellular antibodies in PBS/0.5% saponin and analyzed as above (Janke *et al.* 2010). Anti-IL-6, IL-17, IFNg, and IL-10 antibodies were from BD Pharmingen (Heidelberg, Germany).

Cell sorting

Mesenteric DC were enriched using CD11c MACS beads (Miltenyi, Bergisch Gladbach) and $CD11c^+$ $MHCII^+$ $CD103^+$ triple positive cells were FACS sorted to a purity greater 95%. $CD4^+$ and $CD8^+$ T cells were MACS sorted to purity greater 80%. IEC were identified based on their scatter prior to Percoll centrifugation and obtained more than 95% pure.

Statistics

Data was analyzed with GraphPad Prism™ software. Results are expressed as mean value ± SD (unless indicated otherwise). P-values <0.05 as determined with Student's *t*-test or ANOVA were considered significant.

RESULTS

GALT and gut epithelial cells express functional AhR

AhR is expressed abundantly in some organs, such as liver and lung, but absent in e.g. testis and muscle (Frericks *et al.* 2007). With respect to the immune system, analysis of sorted subsets has revealed differential and specific AhR expression in only some immune cell subsets, in particular differentiated Th17 cells, and $CCR6^+$ γδ T cells, Langerhans cells, and

other DC subsets (Jux *et al.* 2009; Martin *et al.* 2009; Veldhoen *et al.* 2008). We tested AhR expression in gut cells by semi-quantitative PCR. AhR transcripts were detectable in the duodenal, jejunal and ileal gut segments (Fig. 1a). Mesenteric lymph nodes (MLN) expressed AhR at levels similar to those of the thymus (an organ with known AhR-abundance). In Peyer's Patches (PP) AhR transcripts were barely detectable (Fig. 1b). Intestinal epithelial cells (IEC) and CD8$\alpha\alpha^+$ TCR$\gamma\delta^+$ IEL, a specialized T cell type probably responsible for epithelial integrity and immune surveillance (Hayday and Spencer 2009), also expressed AhR strongly (Fig. 1c). In contrast, CD103$^+$DC in MLN expressed far less AhR.

To test for functionality of the AhR in gut tissue, we treated C57BL/6 mice with 10µg/kg b.w. TCDD, a non-toxic moderate dose (Kerkvliet and Brauner 1990), and analyzed induction of *cyp1a1*, considered to be a biomarker of AhR activation. As shown in Fig. 2a, basal as well as inducible *cyp1a1* expression decreased in the jejunum and ileum compared to the more proximal intestine sections. Expression of another target gene and thus marker for AhR-activity, AhR-Repressor (*ahrr*), increased from low levels several-fold by TCDD. A spatial expression gradient could not be observed (data not shown). Taken together, AhR is functionally expressed in the gut, with *cyp1a1* gene induction by TCDD found decreasing in a gradient from proximal to distal in the small intestine.

AhRR represses AhR activity. We found that c*yp1a1* induction in the different GALT tissues and cell types was inversely related to *ahrr* expression. Thus, in MLN and PP (low in *ahrr* expression) *cyp1a1* transcripts increased strongly by TCDD. Similarly, *cyp1a1* RNA increased 100fold in IEC, in which *ahrr* transcripts were almost absent (Fig. 2a,b). In contrast, CD103$^+$DC co-expressed AhR and AhRR at considerably levels. Congruent with this finding, these cells did not induce *cyp1a1* transcripts upon TCDD exposure. Note that TCDD exposure of mice led to an even higher expression of *ahrr* in CD103$^+$DC (Fig. 2b).

TCDD and oral tolerance

Oral tolerance is defined as unresponsiveness of the immune system against foreign antigens, which are taken up through the gut after feeding or eating them. We fed C57/BL6 mice with 10µg/kg bodyweight TCDD in olive oil three days before starting a standard tolerization protocol of feeding OVA, followed by parenteral immunization against OVA. Serum samples were taken at the indicated time points and analyzed for total and OVA-specific IgG1. To detect OVA-specific IgA in faecal samples, mice were fed again with OVA after the end of the immunization scheme.

Fig. 3 shows the scheme of immunizations and serum/faecal sampling, which allows looking at the influence of TCDD on the humoral immune response against OVA in immunized versus tolerized animals.

First, TCDD treatment suppressed the humoral immune response after i.p. immunization with OVA. However, TCDD-suppression was abrogated by a second immunization and IgG1 titers reached levels of control animals (PBS treatment) (Fig. 4, white bars). In summary, TCDD alone induced immunosuppression in the non-tolerized mice, and the effect was abrogated after the second immunization.

Second, regarding tolerance, TCDD treatment prior to tolerization was permissive for IgG1 production at levels similar to those of non-tolerized mice, albeit only after two booster immunization (Fig. 4, dotted grey bars). The kinetics of OVA-specific IgG1 titer paralleled the total IgG1 titer (compare Fig. 4 and Fig. 5a).

The results of sera taken after the 3rd immunization are shown in Fig. 5b. The control groups behaved as expected: anti-OVA IgG1 titres in the non-tolerized group increased with each booster immunization, whereas OVA specific IgG1 was always absent in the tolerized mice. In contrast, TCDD-treated/OVA-tolerized mice produced significant amounts of OVA-specific IgG1 antibodies, albeit levels remained below those of the TCDD or PBS treated

control mice. Break of tolerance increased with booster injections. Only 4 or 5 out of 14 animals had high OVA-specific IgG1 in the serum after the 1st and 2nd immunization (Fig. 3), respectively, while after the 3rd immunization all TCDD treated mice had broken tolerance. Thus, TCDD-exposure prevented the stable establishment of oral tolerance.

IgA secretion into the gut lumen by TCDD treatment

Oral tolerance also prevents production of antigen-specific IgA into the gut lumen (Kato *et al.* 2001). We therefore measured OVA-specific IgA in faecal samples of tolerized and TCDD-exposed mice (see Fig. 3). In OVA-tolerized mice no OVA-specific IgA was present in the faecal samples. In contrast, after TCDD treatment and tolerization OVA-specific IgA antibodies were detected at the levels of non-tolerized mice (Fig. 6, white bars), affirming that TCDD breaks tolerance not only regarding peripheral antibody production, but also gut antibodies.

Immune cell distribution is only altered in MLN by TCDD

To exclude selective toxicity of 10µg TCDD/kg b.w. on IEL and LPL cells, we tested composition of immune cell subsets three days after exposure. IEL yield was approximately $1.5x10^6$ cells/small intestine in both TCDD-treated and control animals. Moreover, the immune cell subset frequencies did not differ between TCDD exposed and control mice (approximately 44% CD8ααTCRγδ, 20% CD8ααTCRαβ, 29% CD8αβTCRαβ, 2% CD8αβTCRγδ, 4% CD4). Similarly, neither the absolute number of cells, nor frequencies of $CD4^+$, $CD8^+$, $CD19^+$, $CD103^+$MHC-II^+CD11c^+ subsets in PP or LP cells were affected by 10µg/kg b.w. TCDD exposure. The data are summarized in Table 1. Thus, break of tolerance by TCDD, as described above, is not due to a toxic elimination of any or all effector subsets of immune cells in GALT.

Antigen-sampling $CD103^+$DC, which migrate to MLN, are critical for induction of regulatory T cells against gut antigens (Jaensson *et al.* 2008). TCDD might affect DC frequencies in the

MLN or their tolerogenic capacities. We determined the frequencies of DC in MLN three, 10, and 14 days after feeding TCDD. Confirming literature results (Coombes *et al.* 2007), we found about 2-3% MHC-II$^+$CD11c$^+$DC in MLN, of which 40% were CD103$^+$. At all time points after feeding TCDD the percentage of total DC in MLN was unchanged. However, on days 10 and 14 after TCDD exposure, CD103$^+$DC frequency was significantly increased by almost 15% to 61.2% ± 6,2% percent (see table 1a). Unfortunately, whether this correlates to significant changes in absolute number could not be determined, due the small numbers, and to biological variation between mice.

TCDD affects the regulatory T cell/ Th17 balance in MLN

DC produce cytokines which instruct T cell differentiation. The balance between regulatory T cells (Treg) and pro-inflammatory T cell subsets, in particular Th17 cells, is driven by IL-6 and TGFβ (Coombes *et al.* 2007; Stockinger *et al.* 2007). Treg generation is blocked in the presence of IL-6. Therefore, we analyzed IL-6 in MLN DC. As shown in Fig. 7a, TCDD exposed tolerized mice had a significantly higher frequency of IL-6 producing CD11c$^+$MHC-II$^+$ DC in their MLN. The frequency of IL10-producing DC remained unchanged between TCDD-exposed and control animals. Congruent with the IL-6 data, CD4$^+$ T cells in these MLN contained a significantly higher frequency of IL-17-producing T cells (Fig. 7b), suggesting that TCDD leads to misregulation of T cell differentiation towards an inflammatory phenotype. Our data fits with recent reports that AhR is important for Th17 differentiation (Veldhoen *et al.* 2008). Interestingly, no changes were detected in FoxP3$^+$ Treg, IL-10 or IFNγ positive cells. For representative FACS plots of the intracellular staining for DC and CD4$^+$T cells see Fig. 7 d,e, and f-h, respectively. In PP cells of TCDD-exposed mice and controls, none of these parameters differed (Fig. 7c).

DISCUSSION

It has been known for decades that the environmental pollutant TCDD suppresses the peripheral immune system. We show here that TCDD also affects mucosal immunity and prevented the stable establishment of oral tolerance. Associated with this, we found an increase in the frequency of IL-6 producing DC and $IL17^+$ T-cells in the gut-draining mesenteric lymph nodes, the site of tolerance induction against intestinal antigens (Worbs *et al.* 2006).

Rather than abrogating oral tolerance completely, our data indicate that the persistence of oral tolerance is impaired by TCDD. OVA-tolerized control mice resisted antigen challenge and two booster immunizations, i.e. they never mounted a gut (IgA) or systemic (IgG1) immune response. In contrast, oral tolerance did not persist after a repeated challenge with OVA in mice fed with 10µg/kg TCDD prior to tolerization. Interestingly, Kinoshita et al. reported that a dose of only 1µg TCDD/kg b.w. was permissive for generation of antibodies in OVA-tolerized mice upon two challenges (both given in CFA) (Kinoshita *et al.* 2006). At the late time-point these authors analyzed, TCDD would have been eliminated from the system. Thus, we think that TCDD affects cells responsible for tolerance induction and memory early after treatment, and TCDD presence, once the disruption is set, is no longer needed. Whether or not TCDD can break an already established tolerance remains to be shown.

We confirmed literature data that TCDD-treatment (*sine* tolerization) suppresses the humoral response (Kerkvliet *et al.* 1990), here against OVA. Moreover, we show for the first time that suppression does not persist after booster immunizations. Most likely, this is not due to an insufficient TCDD concentration in the mice at the time point measured, despite the fact that TCDD is eliminated much faster in mice than in humans (half life of 12 days versus a half life of 7 years (Van den *et al.* 1994). The estimated body burden at the time of the second immunization is 2.6µg/kg b.w. and immunosuppression was already described at doses as

low as 1µg/kg b.w. (Vorderstrasse *et al.* 2003). Adoptive transfer experiments with OVA-specific TCR-transgenic cells suggested that the TCDD-impaired humoral response was related to impaired CD4 help (Shepherd *et al.* 2000). Our results challenge this view, as suppression can be overcome with booster immunizations. Our results can explain why findings regarding the humoral immune response in humans after dioxin, furan or biphenyl exposure yielded ambiguous results regarding suppression of antibody responses, i.e. often normal antibody titres were observed in exposed persons (Esser 2005).

Recently, Ishikawa and colleagues analyzed IgA secretion into the gut lumen in mice after low-dose TCDD treatment via nursing, and reported an AhR-dependent decrease in faecal IgA (Ishikawa 2009). We were not able to confirm this result in our adult mice, but that might be due to experimental differences. However, similar to our results, Ishikawa et al. did not observe any TCDD-dependent gross changes in MLN cellularity or immune cell subset distribution of CD4, CD8, B cells, or $CD11c^{+}CD11b^{+}$ cells in MLN and PP. As they found an impaired migration of B1 B cells (a major source for intestinal IgA) towards B cell chemokines, and reduced chemokine receptor expression, they suggest, that TCDD-reduced faecal IgA is due to suppression of an appropriate B1 B cell response.

How could TCDD affect induction of oral tolerance? Two steps are needed for tolerance induction: first, antigen transfer by dendritic cells to the MLN and second, induction of antigen specific Treg in MLN (Worbs *et al.* 2006). Regarding the first step, we did not find fewer DC in the gut or MLN, ruling out DC-specific cell death or a failure of DC to migrate to MLN.

However, our data indicate TCDD effects on the capacity of DC to induce regulatory T cells. Recent studies reported that activation of AhR by TCDD affects the balance of regulatory and effector T cells. TCDD exposure ameliorated disease in a model of experimental autoimmune encephalitis (Quintana *et al.* 2008). Another study, however, found that AhR

activation by another ligand, 6-formylindolo[3,2-b]-carbazole, exacerbated the disease, due to an enhanced Th17 response (Veldhoen *et al.* 2008). DC as – presumably indirect - targets of TCDD were reported by ourselves for epidermal DC, (Jux *et al.* 2009), and for splenic DC by (Platzer *et al.* 2009). In the gut it was recently shown that the balance between DC derived retinoic acid (RA), IL-6 and TGFβ decides T-cell differentiation into Treg (RA, TGFβ) or Th17 (IL-6, TGFβ, IL21) (Lee *et al.* 2009; Nolting *et al.* 2009; von Boehmer H. 2007; Ziegler and Buckner 2009). Thus, DC are a pivot-point of balancing tolerance versus immune response. Gut derived $CD103^+$DC became known as "tolerogenic DC" (Coombes *et al.* 2005). These authors could show that under steady state conditions $CD103^+$DC secrete large amounts of TGFβ and RA, and preferentially drive T cell differentiation towards Treg. Albeit induction of Treg is the default, under inflammatory conditions $DC103^+$ DC may also induce an adaptive immune response (Johansson-Lindbom *et al.* 2005). Our data suggests that in the presence of TCDD mesenteric lymph node DC become less tolerogenic, produce IL-6 and thus switch from Treg to Th17 generation. Consequently, we observed a greater frequency of IL-17 producing T cells after TCDD. IL-6 can be produced by lymphoid cells and many non-lymphoid cells, including Macrophages and DC. IL-6 is a target gene of the NFκB signaling pathway, which can be hitchhiked by AhR (Kimura *et al.* 2009); the biological functions of IL-6 include T-cell activation/differentiation and support of antibody production by B cells.

We found that that $CD103^+$DC expressed very low amounts of AhR, and that the biomarker target gene *cyp1a1* was not induced by TCDD exposure. We therefore think it is unlikely that gut DC are a direct target of TCDD triggered AhR-mediated gene activation. Moreover, $CD103^+$DC expressed high amounts of *ahrr*, which indicates that at least the classical AhR-ARNT signalling pathway is blocked in gut DC. There is a possibility that AhR binds to RelA or RelB, and thus TCDD could trigger IL-6 via this pathway (Tian 2009). It is tempting to speculate that abundant AhRR in $CD103^+$DC is a control mechanism to push DC into

using the NFκB pathway preferentially, if AhR ligands are present. Note, that also another set of barrier organ DC, Langerhans cells in the skin, express high amounts of AhRR and do not use the classical AhR-ARNT pathway (Jux *et al.* 2009).

Whether gut DC will become tolerogenic is controlled to a large extent by IEC that transfer signals from nutrition and the bacterial flora of the gut lumen (Rimoldi *et al.* 2005). AhR was conspicuously abundant in IEC, conceivably it is related to the xenobiotic metabolism in IEC. IEC form a physical and biological barrier against the gut lumen. Recent evidence has revealed a role for IEC as an immunological barrier, instructing $CD103^+$DC to become tolerogenic or inflammatory (Shale and Ghosh 2009), e.g. by GM-CSF, TGFβ, IDO (indoleamin-2,3-dioxygenase), or TSLP (thymic stromal lymphopoetin) secretion. Moreover, induction of toll-like receptors signalling led to increased turnover and faster migration of $CD103^+$DC into the MLN (Schulz *et al.* 2009). It is currently not known whether AhR participates in the immunological functions of IEC.

The manipulation of Treg and T cell subsets in general, is of high therapeutic interest for the management of inflammatory and autoimmune disorders. Our data show that stability of mucosal Treg generation can be dependent on environmental chemicals encountered via the oral route. Further experiments will be needed to study the kinetics of DC changes, and the conceivable generation of memory Th17 cells in the setting of TCDD/oral tolerance.

TCDD is not the only AhR agonist in food. Flavonoids, bacterial tryptophane breakdown products, or bilirubins are abundant as well (Ciolino *et al.* 1999; Heath-Pagliuso *et al.* 1998). Indeed, some dietary supplements with flavonoids can peak AhR-agonist concentration in the gut in an unprecedented way. Further studies must explore, whether natural food constituents affect oral tolerance as well.

In summary, we have shown that a single moderate dose of TCDD prevents the stable induction of oral tolerance, possibly via Treg / Th17 unbalancing. Our data have implications

for food allergies in settings of environmental exposure, but also raise concerns regarding the harmlessness of over-dosing potential AhR agonists in food.

ACKNOWLEDGEMENTS

We thank Diana Fleissner, University of Essen, and Vladimir Temchura, Ruhr-University of Bochum, for help with isolation of gut lymphocytes. We thank Claudia Uthoff-Hachenberg (University of Cologne) and Frederic Heinrich (DRFZ, Berlin) for gifts of antibodies. This study was supported by the Deutsche Forschungsgemeinschaft, GRK1427 “Food constituents as triggers of nuclear receptors in the gut”.

The authors declare they have no competing financial interest.

REFERENCES

1. Artis, D. (2008). Epithelial-cell recognition of commensal bacteria and maintenance of immune homeostasis in the gut. *Nat. Rev. Immunol.* **8**(6), 411-420.

2. Beischlag, T. V., Luis, M. J., Hollingshead, B. D., and Perdew, G. H. (2008). The aryl hydrocarbon receptor complex and the control of gene expression. *Crit Rev. Eukaryot. Gene Expr.* **18**(3), 207-250.

3. Chen, Y., Chou, K., Fuchs, E., Havran, W. L., and Boismenu, R. (2002). Protection of the intestinal mucosa by intraepithelial gamma delta T cells. *Proc. Natl. Acad. Sci. U. S. A* **99**(22), 14338-14343.

4. Ciolino, H. P., Daschner, P. J., and Yeh, G. C. (1999). Dietary flavonols quercetin and kaempferol are ligands of the aryl hydrocarbon receptor that affect CYP1A1 transcription differentially. *Biochem. J.* **340 (Pt 3)**, 715-722.

5. Coombes, J. L., Robinson, N. J., Maloy, K. J., Uhlig, H. H., and Powrie, F. (2005). Regulatory T cells and intestinal homeostasis. *Immunol. Rev.* **204**, 184-194.

6. Coombes, J. L., Siddiqui, K. R., rancibia-Carcamo, C. V., Hall, J., Sun, C. M., Belkaid, Y., and Powrie, F. (2007). A functionally specialized population of mucosal CD103+ DCs induces Foxp3+ regulatory T cells via a TGF-beta and retinoic acid-dependent mechanism. *J. Exp. Med.* **204**(8), 1757-1764.

7. Esser, C. (2005). Dioxins and the immune system. In *Encyclopedic Reference of Immunotoxicology* (H.-W.Vohr, Ed.), Springer, Heidelberg.

8. Esser, C., Rannug, A., and Stockinger, B. (2009). The aryl hydrocarbon receptor and immunity. *Trends Immunol.* **9**, 447-454.

9. Frericks, M., Meissner, M., and Esser, C. (2007). Microarray analysis of the AHR system: tissue-specific flexibility in signal and target genes. *Toxicol. Appl. Pharmacol.* **220**(3), 320-332.

10. Hayday, A. C., and Spencer, J. (2009). Barrier immunity. *Semin. Immunol.* **21**(3), 99-100.

11. Heath-Pagliuso, S., Rogers, W. J., Tullis, K., Seidel, S. D., Cenijn, P. H., Brouwer, A., and Denison, M. S. (1998). Activation of the Ah receptor by tryptophan and tryptophan metabolites. *Biochemistry* **37**(33), 11508-11515.

12. Ishikawa, S. (2009). Children´s Immunology, what can we learn from animal studies (3):Impaired mucosal immunity in the gut by 2,3,7,8-tetrachlorodibenzo-p-dioxin (TCDD):a possible role for allergic sensitization. *J. Tox. Sci.* **34**(SP II), SP349-SP261.

13. Jaensson, E., Uronen-Hansson, H., Pabst, O., Eksteen, B., Tian, J., Coombes, J. L., Berg, P. L., Davidsson, T., Powrie, F., Johansson-Lindbom, B., and Agace, W. W. (2008). Small intestinal CD103+ dendritic cells display unique functional properties that are conserved between mice and humans. *J. Exp. Med.* **205**(9), 2139-2149.

14. Janke, M., Peine, M., Nass, A., Morawietz, L., Hamann, A., and Scheffold, A. (2010). In vitro-induced Th17 cells fail to induce inflammation in vivo and show an impaired migration into inflamed sites. *Eur. J. Immunol.*

15. Johansson-Lindbom, B., Svensson, M., Pabst, O., Palmqvist, C., Marquez, G., Forster, R., and Agace, W. W. (2005). Functional specialization of gut CD103+ dendritic cells in the regulation of tissue-selective T cell homing. *J. Exp. Med.* **202**(8), 1063-1073.

16. Jux, B., Kadow, S., and Esser, C. (2009). Langerhans cell maturation and contact hypersensitivity are impaired in aryl hydrocarbon receptor-null mice. *J. Immunol.* **182**(11), 6709-6717.

17. Kato, H., Fujihashi, K., Kato, R., Yuki, Y., and McGhee, J. R. (2001). Oral tolerance revisited: prior oral tolerization abrogates cholera toxin-induced mucosal IgA responses. *J. Immunol.* **166**(5), 3114-3121.

18. Kerkvliet, N. I. (2002). Recent advances in understanding the mechanisms of TCDD immunotoxicity. *Int. Immunopharmacol.* **2**(2-3), 277-291.

19. Kerkvliet, N. I. (2009). AHR-mediated immunomodulation: the role of altered gene transcription. *Biochem. Pharmacol* **77**(4), 746-760.

20. Kerkvliet, N. I., and Brauner, J. A. (1990). Flow cytometric analysis of lymphocyte subpopulations in the spleen and thymus of mice exposed to an acute immunosuppressive dose of 2,3,7,8-tetrachlorodibenzo-p-dioxin (TCDD). *Environ. Res.* **52**(2), 146-154.

21. Kerkvliet, N. I., Steppan, L. B., Brauner, J. A., Deyo, J. A., Henderson, M. C., Tomar, R. S., and Buhler, D. R. (1990). Influence of the Ah locus on the humoral immunotoxicity of 2,3,7,8-tetrachlorodibenzo-p-dioxin: evidence for Ah-receptor-dependent and Ah-receptor-independent mechanisms of immunosuppression. *Toxicol. Appl. Pharmacol.* **105**(1), 26-36.

22. Kimura, A., Naka, T., Nakahama, T., Chinen, I., Masuda, K., Nohara, K., Fujii-Kuriyama, Y., and Kishimoto, T. (2009). Aryl hydrocarbon receptor in combination with Stat1 regulates LPS-induced inflammatory responses. *J. Exp. Med.* **206**(9), 2027-2035.

23. Kinoshita, K., Abe, J., Akadegawa, K., Yurino, H., Uchida, T., Ikeda, S., Matsushima, K., and Ishikawa, S. (2006). Breakdown of mucosal immunity in gut by 2,3,7,8-tetrachlorodibenzo-p-dioxin. *Env. Health and Preventive Med.* **11**, 256-263.

24. Lai, Z. W., Hundeiker, C., Gleichmann, E., and Esser, C. (1997). Cytokine gene expression during ontogeny in murine thymus on activation of the aryl hydrocarbon receptor by 2,3,7,8-tetrachlorodibenzo-p-dioxin. *Mol. Pharmacol.* **52**(1), 30-37.

25. Laiosa, M. D., Wyman, A., Murante, F. G., Fiore, N. C., Staples, J. E., Gasiewicz, T. A., and Silverstone, A. E. (2003). Cell proliferation arrest within intrathymic lymphocyte progenitor cells causes thymic atrophy mediated by the aryl hydrocarbon receptor. *J. Immunol.* **171**(9), 4582-4591.

26. Lee, Y. K., Mukasa, R., Hatton, R. D., and Weaver, C. T. (2009). Developmental plasticity of Th17 and Treg cells. *Curr. Opin. Immunol.* **21**(3), 274-280.

27. Majora, M., Frericks, M., Temchura, V., Reichmann, G., and Esser, C. (2005). Detection of a novel population of fetal thymocytes characterized by preferential emigration and a TCRgammadelta+ T cell fate after dioxin exposure. *Int. Immunopharmacol.* **5**(12), 1659-1674.

28. Martin, B., Hirota, K., Cua, D. J., Stockinger, B., and Veldhoen, M. (2009). Interleukin-17-producing gammadelta T cells selectively expand in response to pathogen products and environmental signals. *Immunity.* **31**(2), 321-330.

29. Nguyen, L. P., and Bradfield, C. A. (2008). The search for endogenous activators of the aryl hydrocarbon receptor. *Chem. Res. Toxicol.* **21**(1), 102-116.

30. Nolting, J., Daniel, C., Reuter, S., Stuelten, C., Li, P., Sucov, H., Kim, B. G., Letterio, J. J., Kretschmer, K., Kim, H. J., and von, B. H. (2009). Retinoic acid can enhance conversion of naive into regulatory T cells independently of secreted cytokines. *J. Exp. Med.* **206**(10), 2131-2139.

31. Platzer, B., Richter, S., Kneidinger, D., Waltenberger, D., Woisetschlager, M., and Strobl, H. (2009). Aryl hydrocarbon receptor activation inhibits in vitro differentiation of human monocytes and Langerhans dendritic cells. *J. Immunol.* **183**(1), 66-74.

32. Quintana, F. J., Basso, A. S., Iglesias, A. H., Korn, T., Farez, M. F., Bettelli, E., Caccamo, M., Oukka, M., and Weiner, H. L. (2008). Control of T(reg) and T(H)17 cell differentiation by the aryl hydrocarbon receptor. *Nature* **453**(7191), 65-71.

33. Rimoldi, M., Chieppa, M., Salucci, V., Avogadri, F., Sonzogni, A., Sampietro, G. M., Nespoli, A., Viale, G., Allavena, P., and Rescigno, M. (2005). Intestinal immune homeostasis is regulated by the crosstalk between epithelial cells and dendritic cells. *Nat. Immunol.* **6**(5), 507-514.

34. Schecter, A., Birnbaum, L., Ryan, J. J., and Constable, J. D. (2006). Dioxins: an overview. *Environ. Res.* **101**(3), 419-428.

35. Schulz, O., Jaensson, E., Persson, E. K., Liu, X., Worbs, T., Agace, W. W., and Pabst, O. (2009). Intestinal CD103+, but not CX3CR1+, antigen sampling cells migrate in lymph and serve classical dendritic cell functions. *J. Exp. Med.* **206**(13), 3101-3114.

36. Shale, M., and Ghosh, S. (2009). How intestinal epithelial cells tolerise dendritic cells and its relevance to inflammatory bowel disease. *Gut* **58**(9), 1291-1299.

37. Shepherd, D. M., Dearstyne, E. A., and Kerkvliet, N. I. (2000). The effects of TCDD on the activation of ovalbumin (OVA)-specific DO11.10 transgenic CD4(+) T cells in adoptively transferred mice. *Toxicol. Sci.* **56**(2), 340-350.

38. Stockinger, B., Veldhoen, M., and Martin, B. (2007). Th17 T cells: linking innate and adaptive immunity. *Semin. Immunol.* **19**(6), 353-361.

39. Tian, Y. (2009). Ah receptor and NF-kappaB interplay on the stage of epigenome. *Biochem. Pharmacol* **77**(4), 670-680.

40. Van den, B. M., De, J. J., Poiger, H., and Olson, J. R. (1994). The toxicokinetics and metabolism of polychlorinated dibenzo-p-dioxins (PCDDs) and dibenzofurans (PCDFs) and their relevance for toxicity. *Crit Rev. Toxicol.* **24**(1), 1-74.

41. van Leeuwen, F. X., Feeley, M., Schrenk, D., Larsen, J. C., Farland, W., and Younes, M. (2000). Dioxins: WHO's tolerable daily intake (TDI) revisited. *Chemosphere* **40**(9-11), 1095-1101.

42. Veldhoen, M., Hirota, K., Westendorf, A. M., Buer, J., Dumoutier, L., Renauld, J. C., and Stockinger, B. (2008). The aryl hydrocarbon receptor links TH17-cell-mediated autoimmunity to environmental toxins. *Nature* **453**(7191), 106-109.

43. von Boehmer H. (2007). Oral tolerance: is it all retinoic acid? *J. Exp. Med.* **204**(8), 1737-1739.

44. Vorderstrasse, B. A., Bohn, A. A., and Lawrence, B. P. (2003). Examining the relationship between impaired host resistance and altered immune function in mice treated with TCDD. *Toxicology* **188**(1), 15-28.

45. Westendorf, A. M., Fleissner, D., Groebe, L., Jung, S., Gruber, A. D., Hansen, W., and Buer, J. (2009). CD4+Foxp3+ regulatory T cell expansion induced by antigen-driven interaction with intestinal epithelial cells independent of local dendritic cells. *Gut* **58**(2), 211-219.

46. Worbs, T., Bode, U., Yan, S., Hoffmann, M. W., Hintzen, G., Bernhardt, G., Forster, R., and Pabst, O. (2006). Oral tolerance originates in the intestinal immune system and relies on antigen carriage by dendritic cells. *J. Exp. Med.* **203**(3), 519-527.

47. Ziegler, S. F., and Buckner, J. H. (2009). FOXP3 and the regulation of Treg/Th17 differentiation. *Microbes. Infect.* **11**(5), 594-598.

FIGURE LEGENDS

Figure 1

mRNA levels of AhR in gut and gut associated immune cells.

Expression levels of AhR was determined by real time PCR in relation to house-keeping gene Rps6. (a) Total duodenal, jejunal and ileal sections. (b) Peyer´s Patches and mesenteric lymph nodes compared to liver and thymus (organs of high AhR expression). (c) IEC, $CD8\alpha\alpha^+$ $TCR\gamma\delta^+$ (TCRγδ) and $CD103^+$DC (CD103DC) were FACS-sorted to purity of more than 95 % from IEL or MLN. CD4 and CD8 T cells were sorted via MACS from MLN to purity greater 80%. Graphs show data are from n=3-6 mice, assayed in 2 independent experiments. ** $p<0.01$ *** $P<0.001$

Figure 2

Induction of the AhR target genes *cyp1a1* and *ahrr* in intestinal epithelial cells, GALT and immune cell subsets of TCDD treated mice.

C57BL/6 mice were fed with 10µg/kg body weight TCDD in olive oil. Three days later, gut was removed and *cyp1a1* (a) and *ahrr* (b) mRNA measured by real time PCR. White bars: tissue or cells form mice fed with solvent only. Grey bars: tissue or cells from TCDD fed mice. Shown is the expression ratio compared to the housekeeping gene RPS6. (n=3-6) ** $p<0.1$, *** $p<0.01$

Figure 3

Time scheme of TCDD feeding (flash arrow), tolerization (dashed arrows) and immunizations (black arrows). Numbers refer to the respective days after first feeding of OVA (=day 1). Diamonds denote time points of serum (♦) and faecal sampling (♦).

Figure 4

Serum concentrations of IgG1 in µg/ml serum. Samples were taken 10 days after the first immunization and 3 days after each booster injection and measured via ELISA. (n > 12, 2 independent experiments). Results are shown as mean ± SD. Significant differences were calculated using ANOVA.

Figure 5

Amount of OVA-specific IgG1 is given as relative units compared to a standard serum measured in ELISA. (a) Samples were taken 10 days after the first immunization and 3 days after each booster injection. TCDD induced immunosuppression was abrogated after the 2^{nd} immunization (TCDD). Tolerant mice (Tol-PBS) do not mount an immune response while pre-treatment with TCDD (Tol-TCDD) led to significant OVA-specific IgG1 production. Results are shown as mean ± SEM. (b) OVA-specific IgG1 three days after the third immunization. Results derived of two independent experiments and presented as mean ± SD; n > 12/group of mice. Significant differences were calculated using ANOVA.

Figure 6

OVA-specific IgA concentration was measured in faecal samples via ELISA (n > 12, 2 independent experiments) and is given as relative units compared to a standard sample. Samples were collected 1 day after oral challenge with OVA on days 38, 41, 43 (see Figure 3), dried and dissolved in PBS/NaN_3 at a concentration of 100mg/ml. Significant differences were calculated using ANOVA.

Figure 7

Mice were treated with TCDD, tolerized as shown in Fig. 3, and MLN or PP analyzed one day later. Frequencies of cytokine or FoxP3 expressing DC detected in MLN (a), or $CD4^+$ Tcells in MLN (b), or DC versus $CD4^+$ cells in PP (c) of TCDD-treated animals (grey dotted

bars), or controls (white dotted bars). (d,e): IL-6 expression in DC (previously gated as $CD11c^+$ (not shown) and $MHCII^+$). Numbers refer to percentage of cells in frame. Intracellular cytokine staining in CD4+ T cells from MLN in control mice (f,g) and TCDD treated mice (h,i). Results are shown as mean ± SD from 3 independent experiments, n =6-9. ** $p<0.1$, *** $p<0.01$

Table 1a. Lymphocyte frequencies in lamina propria, mesenteric lymph nodes and Peyer´s patches [a)]

	Lamina propria		Mesenteric lymph nodes		Peyer's patches	
	DMSO	TCDD	DMSO	TCDD	DMSO	TCDD
$CD4^+$	20.2 ± 7.9%	17.8 ± 3.8%	40.0 ± 7.4%	39.6 ± 8.0%	17.6 ± 6.8%	16.0 ± 6.2%
$CD69^+$ [b)]			16.2 ± 2.3%	17.2 ± 2.8%	50.3 ± 7.6%	53.2 ± 6.4%
$CD8^+$	4.3 ± 1.5%	4.1 ± 1.9%	29.5 ± 4.4%	30.1 ± 5.2%	7.0 ± 3.1%	5.9 ± 1.9%
$CD69^+$ [b)]			6.4 ± 3.6%	6.9 ± 2.8%	13.3 ± 4.5%	15.2 ± 6.0%
$CD19^+$	29.5 ± 9.9%	32.2 ± 15%	21.5 ± 6.4%	20.3 ± 6.5%	69.0 ± 6.8%	65.8 ± 7.6%
DC [c)]	3.4 ± 1.6%	3.0 ± 1.7%	2.3 ± 0.8%	2.0 ± 0.7%	2.8 ± 1.4%	3.0 ± 1.4 %
$CD103^+$ [b)]	51.5 ± 3.9%	55.0 ± 4.1%	***47.9±4.2% [d)] 46.7 ± 9.4%	***61.2±6.2% [d)] 45.3 ± 5.6%	38.8 ± 8.9%	36.1 ± 7.4%

[a)] The indicated organs were isolated, single cell suspensions prepared and analysed. The data shown are the percentages of life-gated cells expressing each marker as assessed by flow cytometry. Shown are the means ± SD of at least three independent experiments with 3 mice per group. Mice were treated with 10µg/kg b.w. TCDD ten days prior to cell isolation and staining. [b)] Frequencies of cells expressing subset markers (CD69, CD103) are given as percentages of the correspondent population. [c)] DC were defined as $CD11c^+$ $MHCII^+$.
[d)] Frequencies for $CD103^+$DC on day 3 after TCDD. *** $p<0.001$

Table 1b. Intraepithelial lymphocyte frequencies [a)]

	IEL	
	DMSO	TCDD
$CD4^+$	4.0 ± 2.5%	4.0 ± 2.1%
$CD8\alpha\alpha^+TCR\gamma\delta^+$	43.4 ± 10.0%	44.9 ± 9.2%
$CD8\alpha\alpha^+TCR\alpha\beta^+$	20.6 ± 8.6%	20.5 ± 5.8%
$CD8\alpha\beta^+TCR\gamma\delta^+$	2.6 ± 2.5%	2.3 ± 1.3%
$CD8\alpha\beta^+TCR\alpha\beta^+$	29.0 ± 12.5%	28.2 ± 12.3%

[a)] Intraepithelial lymphocytes were prepared from the small intestine as described in material and methods. The data shown are the percentages of life-gated cells expressing each cell surface marker as assessed by flow cytometry. Shown are the means ± SD of at least three independent experiments with 3 mice per group. Mice were treated with 10µg/kg b.w. TCDD ten days prior to cell isolation and staining.

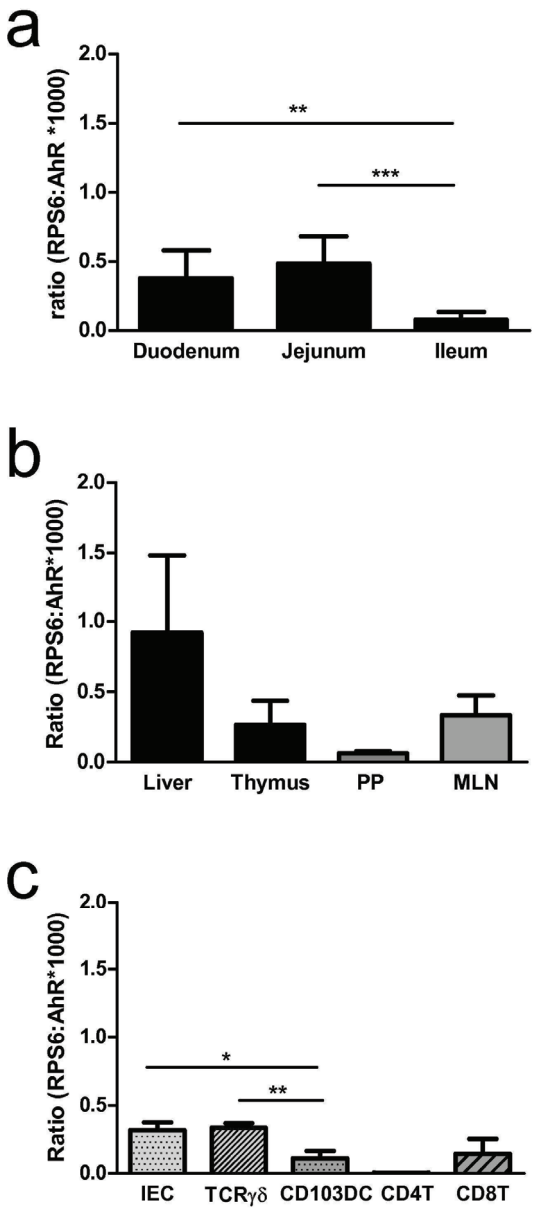

Figure 1
mRNA levels of AhR in gut and gut associated immune cells.
Expression levels of AhR was determined by real time PCR in relation to house-keeping gene Rps6. (a) Total duodenal, jejunal and ileal sections. (b) Peyer´s Patches and mesenteric lymph nodes compared to liver and thymus (organs of high AhR expression). (c) IEC, CD8αα+ TCRγδ+ (TCRγδ) and CD103+DC (CD103DC) were FACS-sorted to purity of more than 95 % from IEL or MLN. CD4 and CD8 T cells were sorted via MACS from MLN to purity greater 80%. Graphs show data are from n=3-6 mice, assayed in 2 independent experiments. ** p<0.01 *** P<0.001
53x123mm (600 x 600 DPI)

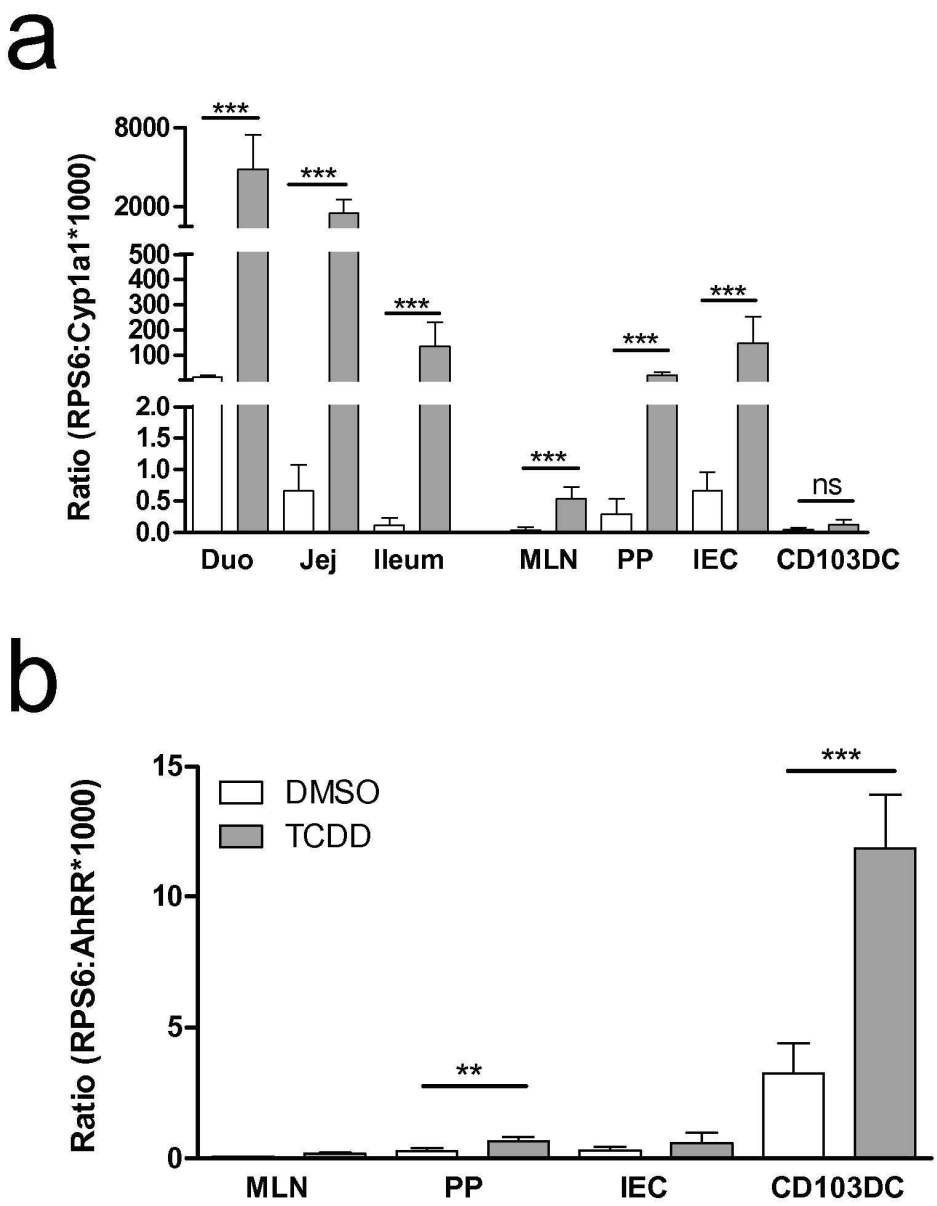

Figure 2
Induction of the AhR target genes cyp1a1 and ahrr in intestinal epithelial cells, GALT and immune cell subsets of TCDD treated mice.
C57BL/6 mice were fed with 10µg/kg body weight TCDD in olive oil. Three days later, gut was removed and cyp1a1 (a) and ahrr (b) mRNA measured by real time PCR. White bars: tissue or cells form mice fed with solvent only. Grey bars: tissue or cells from TCDD fed mice. Shown is the expression ratio compared to the housekeeping gene RPS6. (n=3-6) ** $p<0.1$, *** $p<0.01$

64x82mm (600 x 600 DPI)

Figure 3
Time scheme of TCDD feeding (flash arrow), tolerization (dashed arrows) and immunizations (black arrows). Numbers refer to the respective days after first feeding of OVA (=day 1).

168x98mm (600 x 600 DPI)

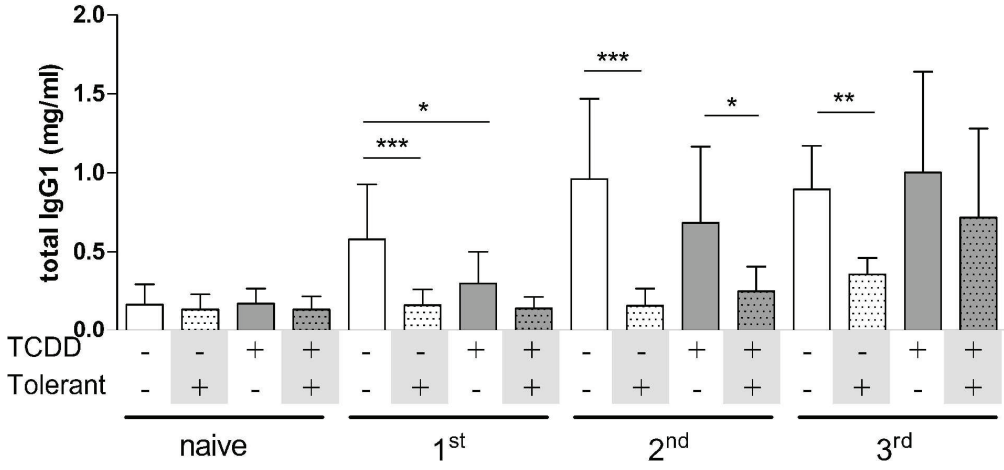

Figure 4
Serum concentrations of IgG1 in µg/ml serum. Samples were taken 10 days after the first immunization and 3 days after each booster injection and measured via ELISA. (n > 12, 2 independent experiments). Results are shown as mean ± SD. Significant differences were calculated using ANOVA.

161x73mm (600 x 600 DPI)

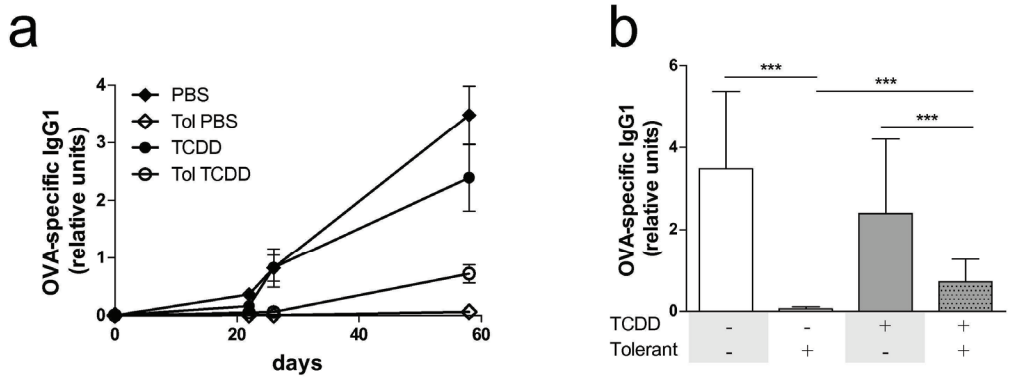

Figure 5
Amount of OVA-specific IgG1 is given as relative units compared to a standard serum measured in ELISA. (a) Samples were taken 10 days after the first immunization and 3 days after each booster injection. TCDD induced immunosuppression was abrogated after the 2nd immunization (TCDD). Tolerant mice (Tol-PBS) do not mount an immune response while pre-treatment with TCDD (Tol-TCDD) led to significant OVA-specific IgG1 production. Results are shown as mean ± SEM. (b) OVA-specific IgG1 three days after the third immunization. Results derived of two independent experiments and presented as mean ± SD; n > 12/group of mice. Significant differences were calculated using ANOVA.

120x45mm (600 x 600 DPI)

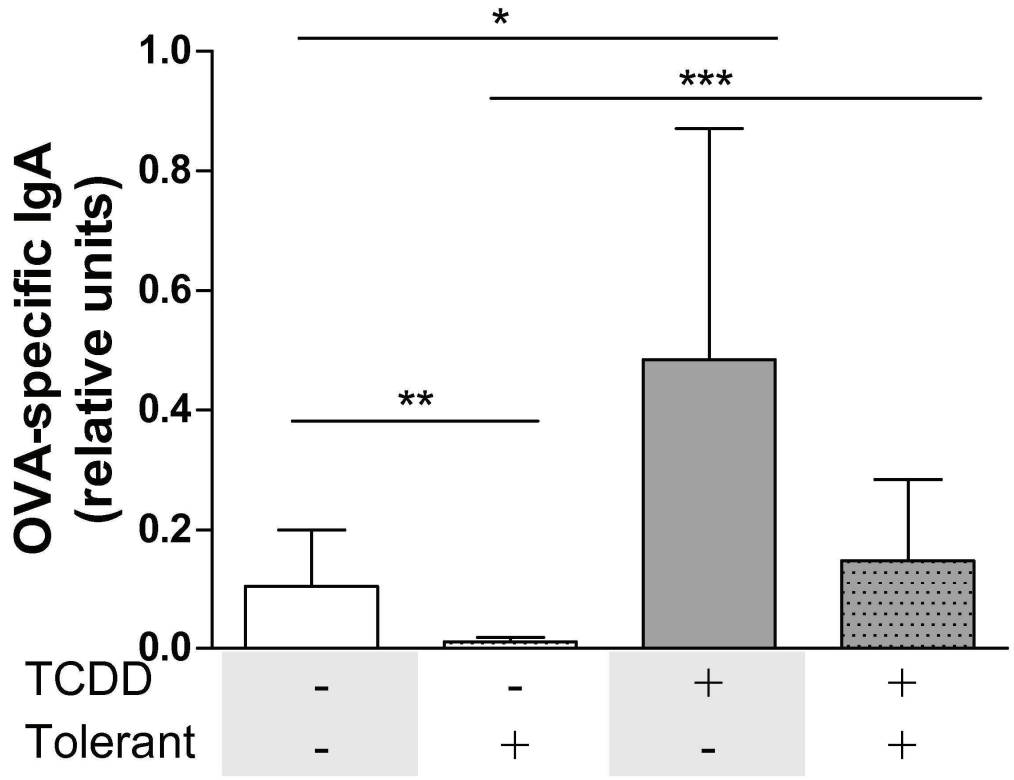

Figure 6
OVA-specific IgA concentration was measured in fecal samples via ELISA (n > 12, 2 independent experiments) and is given as relative units compared to a standard sample. Samples were collected 1 day after oral challenge with OVA on days 38, 41, 43 (see Figure 3), dried and dissolved in PBS/NaN3 at a concentration of 100mg/ml. Significant differences were calculated using ANOVA.

95x73mm (600 x 600 DPI)

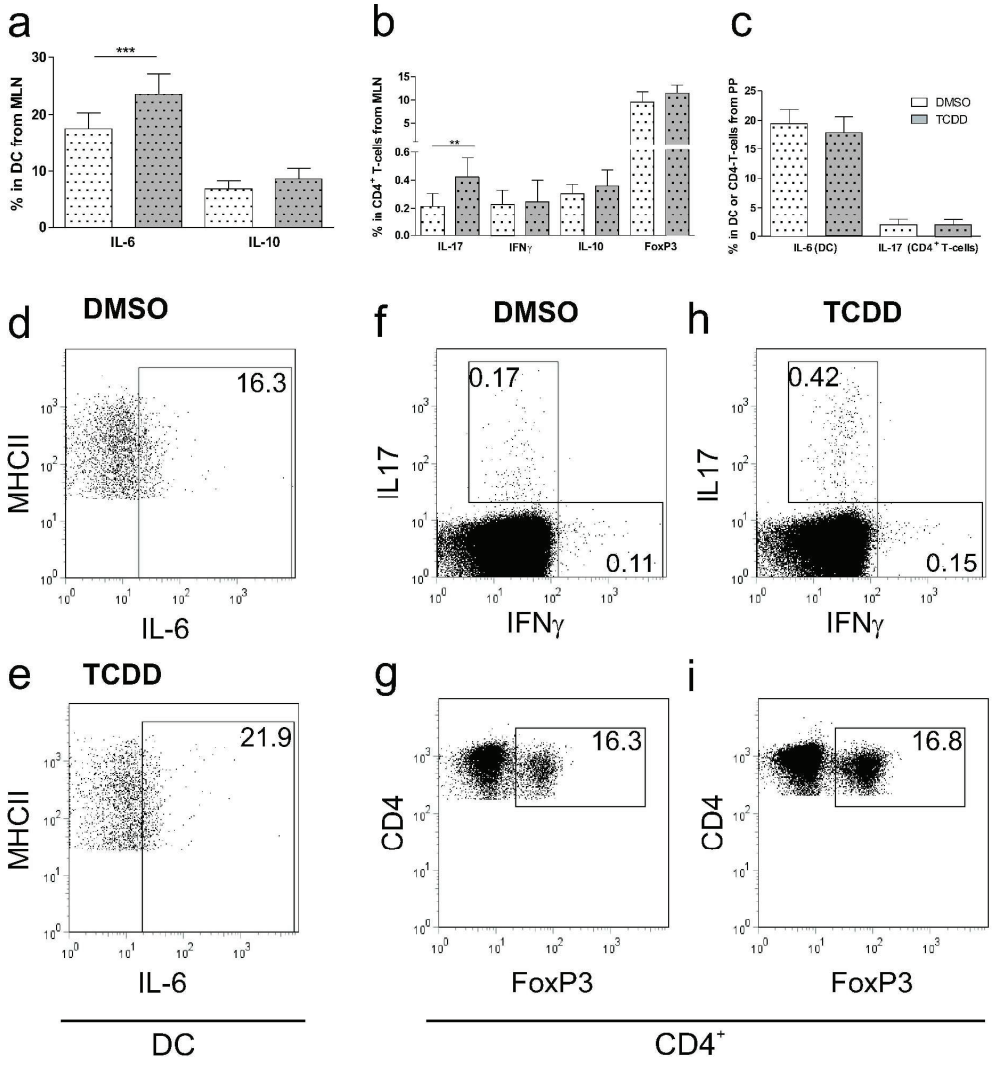

Figure 7
Mice were treated with TCDD, tolerized as shown in Fig. 3, and MLN or PP analyzed one day later. Frequencies of cytokine or FoxP3 expressing DC detected in MLN (a), or CD4+ Tcells in MLN (b), or DC versus CD4+ cells in PP (c) of TCDD-treated animals (grey dotted bars), or controls (white dotted bars). (d,e): IL-6 expression in DC (previously gated as CD11c+ (not shown) and MHCII+). Numbers refer to percentage of cells in frame. Intracellular cytokine staining in CD4+ T cells from MLN in control mice (f,g) and TCDD treated mice (h,i). Results are shown as mean ± SD from 3 independent experiments, n =6-9. ** $p<0.1$, *** $p<0.01$

159x167mm (600 x 600 DPI)

Cell-type specific expression of the aryl hydrocarbon receptor repressor in immune cells of barrier organs and regulation by Toll-like Receptor ligands

Heike Weighardt*, Olga Brandstätter*, Stefanie Zwicker*, Meike Winter*, Thomas Haarmann-Stemmann[#], Markus Korkowski*, Charlotte Esser*, Josef Abel[#] and Irmgard Förster*

*Department of Molecular Immunology, [#]Department of Molecular Toxicology, Leibniz-Institut für Umweltmedizinische Forschung (IUF) gGmbH, an der Heinrich-Heine Universität Düsseldorf

Auf´m Hennekamp 50 40225 Düsseldorf

Running title: AhRR expression *in vivo*

Key words: aryl hydrocarbon receptor repressor, dendritic cells, T cells, LPS, innate immune system

Corresponding author

Heike Weighardt, Institut für umweltmedizinische Forschung gGmbH (IUF), University of Duesseldorf, Auf´m Hennekamp 50, 40225 Duesseldorf, Germany

Phone: +49-211-3389-256 Fax: +49-211-3190-910

E-mail: Heike.Weighardt@uni-duesseldorf.de

ABSTRACT

The aryl hydrocarbon receptor (AhR) plays an essential role in the recognition and detoxification of environmental noxae. Within the immune system activation of the AhR was shown to have a major impact on dendritic cell (DC)- and T cell differentiation. The AhR itself is regulated by the AhR repressor (AhRR) through feedback inhibition. Using newly generated AhRR-reporter mice, we demonstrate that the AhRR is predominantly expressed in immune cells located in barrier organs. In the skin, AhRR expression was mainly detected in epidermal and dermal DC, besides some fibroblasts and keratinocytes. In the gut, AhRR expression was found to be strongest in DC and T cells of the lamina propria, was refined to $CD8^+$ T cells and DC in Peyers Patches, and to DC in mesenteric lymph nodes. Beyond this constitutive expression, AhRR expression could be further induced through AhR activation *in vivo*. Furthermore, we show for the first time that AhRR expression was equally induced by toll-like receptor (TLR) ligands independently of the AhR. Therefore, we postulate an important crosstalk of innate immunity with the AhR/AhRR system at environmental interfaces.

INTRODUCTION

The aryl hydrocarbon receptor (AhR), also known as the dioxin receptor, is a multifunctional ligand-activated transcription factor, which regulates the expression of drug metabolizing enzymes. Upon ligand binding, the AhR induces a battery of genes, including Cytochrome p450 (Cyp)1A1, Cyp1A2 and Cyp1B1, which are essential for the chemical modification and subsequent detoxification of xenobiotics (1-3). The AhR dimerizes with the cofactor AhR-nuclear translocator (Arnt) and binds to xenobiotic response elements (XRE) in the promoter regions of target genes and thereby regulates their expression. Besides the response to xenobiotics the AhR is activated by endogenous ligands and has many physiologic functions regarding cell growth and differentiation (4), including the regulation of immune responses. AhR-signaling is involved in the generation of Treg and Th17 cells in a ligand-dependent manner *in vivo* (5-9). Activation of AhR-signaling in DC leads to enhanced expression of costimulatory molecules, improves T cell proliferation in a mixed lymphocyte reaction *in vitro* (10), and provokes allograft survival in a mouse model by generation of Treg (11).

The activity of the AhR is regulated by the AhR-Repressor (AhRR), which, like the AhR, is a member of the basic helix loop helix Per-Arnt-Sim (PAS) family (12). AhRR transcription is induced by the AhR and in turn represses AhR activity by a negative feedback loop (12,13). The AhRR can also dimerize with Arnt, after which both proteins get SUMOylated. This facilitates the recruitment of ANKRA2, HDAC4 and -5 to the repressor complex and leads to efficient transcriptional repression of the AhR-pathway via XRE-binding (14). Besides this effect, the inhibitiory function of the AhRR also involves additional mechanisms which act independently from binding to XRE (15). The promoter of the AhRR itself contains several XRE, GC boxes and one NF-κB site, indicating that signals from other transcriptional pathways, potentially involving Sp1, c-Jun or NF-κB, may lead to expression of the AhRR (13). Inhibition of the GC box by mithramycinA inhibits AhRR expression in HepG2 cells *in*

vitro (16) and exposure of Hela cells to TPA induces an upregulation of *ahrr* transcription by activation of NFκB, which can be further enhanced by activation of the AhR pathway (13).

Expression analysis revealed that the AhRR mRNA is expressed and upregulated by AhR-ligands in a tissue specific manner in humans and rodents (17-22). Recently generated AhRR-deficient mice show an upregulation of the AhR-response gene Cyp1A1 in skin, stomach and spleen, while there is no altered Cyp1A1 expression in liver and heart, indicating a tissue specific induction of AhR-induced genes in AhRR-deficient mice. Further, these mice possess a reduced incidence to skin carcinogenesis induced by benzo[a]pyrene (18).

To analyze the expression and function of the AhRR within the immune system *in vivo,* we generated AhRR-reporter mice, which express the enhanced green fluorescent protein (EGFP) under control of the endogenous *ahrr* locus. These mice allow for efficient identification of AhRR expression at the single cell level by flow cytometry. Expression analyses in these mice revealed presence of the AhRR particularly in barrier organs like gut and skin. In skin, epidermal Langerhans cells (LC) as well as dermal DC expressed the AhRR. Further, expression of the AhRR was found in DC and T cells of the small intestinal lamina propria (LP) and in lymph node (LN) DC, but not in splenic DC. The expression of the AhRR could be significantly enhanced by AhR-signaling *in vivo* in LN DC as well as in LP DC. In addition, TLR stimulation was shown to upregulate the expression of the AhRR *in vitro* and *in vivo*, indicating a crosstalk between the innate immune system and the cellular response to xenobiotics.

MATERIAL AND METHODS

Targeting the murine *ahrr* locus by homologous recombination

The targeting vector was constructed in a way that an EGFP cDNA together with a polyA signal and a loxP-flanked neomycin resistance cassette was inserted into the second exon of the *ahrr*. To avoid transcription of a truncated protein by alternative splicing, the third exon was deleted additionally. Homologously recombined embryonic stem cell clones (E14K) were detected by Southern blot hybridization after digestion of embryonic stem cell DNA with DraI and hybridised to a 3`flanking probe (**see supplementary Figure 1A**) yielding a 6,6kb fragment for the wild-type (WT) allele and a 3,6kb fragment for the mutated allele. Germline transmission of the targeted allele was confirmed also by Southern blot analysis. The neomycin resistance cassette was removed from the targeted allele by crossing mutant mice with a Cre-Deleter-strain (CD11cCre3 mice; I. Förster, unpublished). In this study, heterozygous $AhRR^{E/+}$ reporter mice and homozygous $AhRR^{E/E}$ mice expressing EGFP but not AhRR were used. WT littermates were used as controls. Mice were originally generated on a mixed C57BL/6/129Ola genetic background and backcrossed to C57BL/6 for 2-5 generations. Primers for typing of mice were as follows: AhRR-rev:3`-tccttctcttcctaccggcg-5`; AhRR-fwd: 3`-catagtggaagtccagcacataga-5`; AhRR/GFP: 3-tccttgaagtcgatgcccttt-5` (see **supplementary Figure 1C**). Because the AhR of 129Ola mice has a low affinity to certain AhR-ligands, mice were screened for expression of the high affinity C57BL/6 allele by PCR as described (18). In all experiments mice with this allele of the AhR were used. For some experiments mice were injected i.p. with 200µl of either LPS (1mg/ml E.coli 0111:B4) in PBS or 3-Methylcholanthrene (3MC; 25 mg/ml, both Sigma, Deisenhofen, Germany) in PBS 1% DMSO for 16h or treated per gavage with 250 µg 3MC in DMSO/olive oil (1:4 v/v). Control animals received PBS, PBS 1%DMSO, or DMSO/olive oil, respectively. Mice were bred in the SPF animal facility of the Institut für Umweltmedizinische Forschung (IUF) according to German guidelines for animal care.

Immunohistology

Tissue samples (LN, skin and small intestine) were fixed for 3 h in 4% paraformaldehyde (PFA) at 4°C, saturated in a sucrose gradient from 5% over 10% to 20% sucrose before being embedded in tissue-freezing medium (Leica, Nussloch, Germany) and snap-frozen in 2-methylbutane (Merck, Darmstadt, Germany) prechilled with liquid nitrogen. Cryostat sections (7 µm) were fixed in acetone. For immunofluorescence analyses the sections were counterstained with 0,5 µg/ml DAPI (4,6-diamidino-2-phenylindole) in PBS and mounted in Moviol/DABCO (1,4-Diazabicyclo(2,2,2)octane, Carl-Roth GmbH, Karlsruhe, Germany). Images were acquired on an Axio Observer.D1 microscope (Zeiss, Jena, Germany) and analyzed with Axiovision Rel. 4.6 (Zeiss, Jena, Germany).

Preparation of cell suspensions for flow cytometry

Skin cell suspensions from dorsal skin were prepared as follows. Hairs were removed from back skin and skin specimens were explanted. After removal of subdermal fat, the skin explants were incubated for 2 h in PBS/0.25% trypsin, 5 mM EDTA (Invitrogen, Karlsruhe, Germany) at 37°C to separate the epidermis from the dermis. Epidermal sheets were mechanically disrupted and filtered through a 70 µm nylon filter to obtain a single cell suspension. Dermal sheets were cut into small pieces and incubated for 2.5 h in collagenase D (1.6 mg/ml, working activity: 226 U/mg; Roche, Mannheim, Germany) and were thereafter mechanically disrupted to obtain a homogenous cell suspension. Cell suspensions were stained with antibodies against MHCII (clone M5/114.15.2) and CD24a (M1/69, both eBioscience, San Diego,CA USA) .

For preparation of LP cells, the small intestine was flushed with PBS and Peyers Patches (PP) were removed. The intestinal tissue was opened longitudinally, cut into pieces and incubated in 3mM EDTA/PBS for 10 min at 37^{o}C, followed by 1%FCS, 1mM EGTA, 1,5mM $MgCl_2$ in RPMI 1640 for 15 min at 37^{o}C and digested in 20%FCS, 100U/ml CollagenaseA (Roche,

Mannheim, Germany) in RPMI 1640 for 1.5 h at 37°C with gentle agitation. The single cell suspensions were filtered through a 70µM cell strainer.

For preparation of PP, LN and splenic cell suspensions, tissues were digested for 15 min at 37°C with 1 mg/ml collagenase D and 300 U/ml DNaseI (both: Roche, Mannheim, Germany). Cell suspensions were stained with antibodies against CD3 (145-2C11), CD4 (RM4-5), CD8 (53-6.7), CD19 (MB19-1), CD25 (PC61, BD Biosciences, Heidelberg, Germany , MHCII (M5/114.15.2), CD11c (HL-3), F4/80 (CI:A3-1, Abd Serotec, Oxford, UK), CD11b (M1/70), NK1.1 (PK136), CD103 (2E7) (if not indicated otherwise, antibodies were purchased from eBioscience, San Diego,CA USA). All cell populations were analyzed with a FACScalibur flow cytometer (BD Biosciences Heidelberg, Germany,); data were analyzed with FlowJo software (Tree star, Ashland, USA).

Generation of bone-marrow derived DC (BMDC)

For differentiation of BMDC femurs of mice were flushed with PBS and the unfractionated cell populations were plated at a density of 5×10^5 cells/ml in suspension culture Petri dishes (Greiner, Frickenhausen, Germany) in RPMI 1640 supplemented with 2% supernatant of GM-CSF-transfected X63Ag8-653 cells (23). Cultures were fed with fresh medium containing 2% GM-CSF supernatant on d3. Cell cultures were used at day 6, purity of the DC population was assessed by FACS analysis using CD11c (HL30) and MHCII (M5/114.15.2) antibodies. For expression analysis DC were either stimulated with LPS (1µg/ml), CpG (ODN1668, 5µM, TIB Molbiol, Berlin, Germany), Pam3Cys (10µg/ml; emcMicrocollections, Tübingen, Germany), 3MC (10µM) or 3-Methoxy-4-nitroflavone (MNF, 5µM) or combinations thereof for 16 h.

Statistical analysis

Statistical analysis of the data was performed using the Student's *t* test. All data are presented as mean ± SEM. The level of significance for $p < 0.05$ was denoted as (*) or (§), for $p< 0,01$ as (**) or (§§), for $p<0,001$ as (***) or (§§§) as indicated in the figure legends.

RESULTS

Generation of AhRR/EGFP-mice

To analyze the expression and function of the AhRR *in vivo* we generated AhRR-reporter and -knockout mice, which allow to monitor expression of the AhRR by a fluorescence approach. Therefore, we inserted an EGFP-cassette into the second exon of the *ahrr* gene. To avoid expression of a truncated AhRR protein by alternative splicing, the third exon was deleted additionally. The targeting strategy is depicted in **Supplementary Figure 1A**. Recombinant AhRR/EGFP ES cell clones were analyzed by Southern blot for the presence of the mutant allele (**Supplementary Figure 1B**) and AhRR/EGFP mice were generated. Mice were intercrossed with a Cre-Deleter-strain to remove the neomycin resistance cassette. Both, heterozygous and homozygous mice can be used as reporter mice to track the expression of the *ahrr* gene. While heterozygous mice carry one mutant and one WT *ahrr* allele, homozygous mice are AhRR-deficient and can be used to study the function of the AhRR *in vivo*. The mice are fertile, and do not exhibit any obvious anatomic or behavioral abnormalities.

Expression of the AhRR in DC of the skin

The skin is the largest barrier organ of the body and protects the organism from environmental or pathogen-induced damage. The immune system of the skin includes a large network of DC, which senses antigen and induces immune activation or tolerance in the draining LN. LC are the DC of the epidermis, which are characterized by the expression of langerin and the occurrence of Birbeck granules. In the dermis, at least three different dDC populations are found and differentiated by their expression of langerin and CD103 (reviewed in (24)). Since mRNA of the AhRR was detected in epidermal LC of mice (25), we analyzed the skin of $AhRR^{E/+}$ and $AhRR^{E/E}$ mice using immunofluorescence and flow cytometry. Expression of the AhRR could be detected in the dermis and in the epidermis of $AhRR^{E/+}$ mice (**Figure 1A**).

To characterize the expression of the AhRR in more detail, freshly isolated epidermal and dermal cell suspensions were analyzed by flow cytometry. Expression of the AhRR could be detected in epidermal LC (appr. 67% and 77%) as well as in dDC (28% and 40%) of both $AhRR^{E/+}$and $AhRR^{E/E}$ mice (**Figure 1B**). The proportion of AhRR-expressing epidermal $MHCII^-$ cells, which mainly represent keratinocytes (11% in heterozygous mice and 16% in homozygous mice), as well as in dermal $MHCII^-$ cells, probably fibroblasts (11% and 17%) was lower compared to $MHCII^+$ fractions in both heterozygous and homozygous animals. For further analysis of dermal cells we included a CD24a staining in order to distinguish between $CD24a^{high}$ and $CD24a^{low}$ dDC. Previously, we could show that the $langerin^+$ dDC express CD24a whereas the $langerin^-$ fraction of dDC does not (26). The number of AhRR expressing cells was higher in the fraction of $CD24a^{high}$ expressing dDC compared to the $CD24a^{low}$ expressing dDC subset (**Figure 1C**), indicating that the highest proportion of AhRR-expressing cells can be found in the transmigrating LC or the $CD24a^+$, $langerin^+$ dDC subset. Analyzing the $MHCII^-$ fraction of dermal cells, we could show a higher expression of the AhRR in the $CD24a^{low}MHCII^-$ population, which includes dermal fibroblasts (**Figure 1C**). Thus, constitutive expression of the AhRR could be clearly demonstrated in immune cells of the skin, namely LC and dDC and, interestingly, to a lesser extent in non hematopoetic cells. High constitutive expression of the *ahrr* was previously demonstrated in primary human fibroblasts (16,27) and to a lesser degree in primary human keratinocytes (27). In the present study, however, a high constitutive transcription of the *ahrr* could not be demonstrated for fibroblasts and keratinocytes in mice *in vivo,* indicating a species difference or a difference of *in vivo* and *in vitro* experiments. Nevertheless, the expression of the AhRR could be upregulated in embryonic fibroblasts and primary murine keratinocytes *in vitro* by the AhR ligand 3MC (**supplementary Figure 2**). Interestingly, the intensity of EGFP expression was generally higher in $AhRR^{E/E}$ cells compared to $AhRR^{E/+}$ cells (**supplementary Figure 2 and 3**), indicating that the AhRR protein expressed from the residual *ahrr* WT allele in the

AhRR$^{E/+}$ animals may inhibit AhR-signaling, thereby repressing its own expression. Alternatively, the difference in EGFP expression levels of AhRR$^{E/E}$ - and AhRR$^{E/+}$ cells may result from a gene dosis effect.

Expression of the AhRR in the gut

Next, we focused on the analysis of AhRR expression in the gut, as another important barrier organ. AhRR/EGFP-expressing cells could be detected in the LP of the small intestine in AhRR$^{E/+}$ and AhRR$^{E/E}$ mice (**Figure 2A**). To further characterize the EGFP-expressing cells, the cells of the LP of the gut as well as of PP were analyzed by flow cytometry. In the LP, expression of the AhRR could be detected in T cells and CD11c$^+$ DC but not in CD19$^+$ B cells. AhRR-expression was found in 19% of CD4$^+$ and 27% of CD8$^+$ LP cells in AhRR$^{E/+}$ mice, and 29% of CD4$^+$ and 21% of CD8$^+$ cells in AhRR$^{E/E}$ mice. Analysis of CD4/CD25 double positive cells, including Treg and activated T cells, showed that 40% of these cells are EGFP$^+$ in both heterozygous and homozygous mice. Furthermore, 25% of the CD4$^+$/CD25$^-$ population expressed the AhRR in heterozygous and homozygous mice.

When analyzing AhRR expression in DC, we found that 66% or 80% of LP DC in AhRR$^{E/+}$ or AhRR$^{E/E}$ mice, respectively, expressed the AhRR (**Figure 2B**). The LP contains two DC populations of different origin, a CD103$^+$, CX3CR1$^-$ and a CD103$^-$, CX3CR1$^+$ population (28). The latter population extends dendrites between epithelial cells and is involved in antigen sampling from the mucosal lumen, which involves CX3CR1 (29) and MyD88 (30). The CD103$^+$, CX3CR1$^-$ DC population, however, plays a tolerogenic function and is able to induce the generation of Treg after migration into the mesenteric LN (MLN) in a TGF-β and retinoic acid-dependent manner (31). Expression of the AhRR could be detected in about 50% of CD11c$^+$, CD103$^-$ DC, whereas nearly all CD11c$^+$, CD103$^+$ DC were AhRR/EGFP positive (**Figure 3**).

The $CD103^+$ DC population localizes to the villous LP and also to the subepithelial dome region of SILT (32). In PP of both $AhRR^{E/+}$ and $AhRR^{E/E}$ mice expression of AhRR/EGFP can be localized to the dome region of the PP (**Figure 2A**). By flow cytometry we could show that in PP expression of the AhRR occurs in about 17% of CD8-T cells of $AhRR^{E/+}$- and 26% of CD8-T cells of $AhRR^{E/E}$ mice, but, in contrast to LP, not in CD4-T cells. In PP, only 20% of $CD11c^+/MHCII^+$ DC in both naive $AhRR^{E/+}$- and $AhRR^{E/E}$ mice were AhRR/$EGFP^+$ (**Figure 2B**). In contrast to skin and intestine, expression of the AhRR could not be detected in liver and lung (data not shown).

Thus, whereas AhRR expression in the LP can be found in $CD4^+$ and $CD8^+$ T cells and DC, it is restricted to $CD8^+$ T cells and DC in PP, indicating not only cell-type specific but also organ-specific expression of the AhRR.

Expression of the AhRR in dendritic cells of lymph nodes but not in spleen

The expression of the AhRR in the draining LN of the gut and skin, namely MLN and peripheral LN (PLN, a pool of brachial, axial, popliteal and inguinal LN) was analyzed by immunofluorescence and flow cytometry. The analysis of frozen sections of MLN and PLN revealed AhRR/EGFP expressing cells mainly in the paracortical and medullary regions of the LN. In contrast to LP and PP, no AhRR/EGFP expression was detectable in either MLN or PLN T cells. B cells were also shown to be $AhRR^-$ in LN, as in all other organs tested. $CD11c^+/MHCII^+$ DC, however, exhibited significant AhRR/EGFP expression. Interestingly, expression levels of the AhRR were higher in MLN DC compared to PLN DC (**Figure 4A and B**), with 30-40% of MLN DC expressing the AhRR, whereas in PLN only 7% of the DC population expresses the AhRR. In the spleen, however, no expression of the AhRR beyond background fluorescence level could be detected in naive mice.

In summary, we describe here for the first time a distinct expression pattern of the AhRR *in vivo*. In naive mice, the AhRR is predominantly observed in immune cells of the barrier

organs gut and skin. While highest expression of the AhRR could be seen in the LP of the intestine, the numbers of AhRR expressing cells decline with increasing distance to the gut.

Inducible expression of the AhRR by AhR- and TLR ligands

Expression of the AhRR is known to be induced by activation of the AhR (12,13). To analyze the influence of AhR induced signaling on the expression of the AhRR *in vivo,* $AhRR^{E/+}$ mice were injected i.p. with the AhR ligand 3MC. 16h later LN and spleen were collected and analyzed by flow cytometry. After 3MC application the expression of the AhRR was enhanced in LN DC, and AhRR-expression could be induced significantly in splenic DC, but not in T cells or B cells (**Figure 5A**). Further, feeding of mice with 3MC significantly enhanced the proportion of AhRR-expressing cells in LP DC and PP DC in both heterozygous $AhRR^{E/+}$ and homozygous $AhRR^{E/E}$ mice (**Figure 5B**), indicating that application of an AhR ligand enhances the expression of the AhRR as expected.

Since there is one NF-κB-site present in the AhRR promoter (13), we wondered whether activation of NF-κB could influence the expression of the AhRR. Therefore, we applied LPS i.p. to $AhRR^{E/+}$ mice and analyzed AhRR expression in a similar way as after the application of 3MC. Interestingly, administration of LPS induced the upregulation of AhRR expression in LN DC, but, in contrast to 3MC-treatment, not in splenic DC (**Figure 5C**). As already noted for 3MC-treatment, LPS-injection also did not lead to expression of the AhRR in either T- or B cells.

To further analyze the impact of TLR-ligation on the expression of the AhRR we generated BMDC and stimulated them with TLR ligands. In untreated BMDC, approximately 40% of DC expressed the AhRR. After stimulation with the TLR-ligands LPS, CpG and P3Cys, the expression could be enhanced up to 80%, indicating that stimulation of the innate immune system via TLR activates the expression of the AhRR (**Figure 5D**). Notably, 3MC did not enhance the expression of the AhRR in BMDC *in vitro*. Recent data revealed that the AhR is

upregulated in macrophages by LPS (33). Here, we found that this is also the case in BMDC (data not shown), but application of 3MC together with LPS does not further enhance expression of the AhRR. Since application of the AhR-inhibitor MNF did not alter the LPS or LPS/3MC-induced AhRR expression, we conclude that in BMDC AhR-signaling does not contribute to AhRR expression.

DISCUSSION

The AhR/AhRR system is important not only for the induction of the xenobiotic metabolism but also influences the immune system by the regulation of T cell responses. In this study we analyzed the expression of the AhRR using a novel AhRR reporter mouse strain. While no expression of the AhRR could be found in peripheral organs like liver and lung, expression of the AhRR in naive mice could be demonstrated mainly in immune cells of the skin and the mucosa, particularly in DC and T cells. AhRR expression could be modulated not only by AhR-activation but equally well by TLR-stimulation *in vitro* and *in vivo,* pointing to a unique function of the AhRR independently of the AhR. In addition, these data demonstrate that signals resulting in xenobiotic metabolism and innate immunity are tightly interconnected.

Expression of the AhRR is localized to LC and dDC in the skin, as well as to a smaller fraction of dermal fibroblasts and keratinocytes. In addition, only a small fraction of cultured, primary fibroblasts and keratinocytes was shown to express the AhRR constitutively. However, expression of the AhRR could be significantly enhanced in these cells by AhR activation. The percentage of $AhRR^{+}$ cells as well as the intensity of EGFP fluorescence increased clearly in $AhRR^{E/E}$ fibroblasts and keratinocytes compared to $AhRR^{E/+}$ cells (**Figure S2**). This indicates that the AhRR normally downregulates its own expression in these cells. In LC and dDC, however, the transcription of the AhRR locus seems not to be influenced by the presence or absence of the AhRR protein. This indicates that the AhRR regulates its own expression to a lesser degree in DC and may also point to a cell-type specific regulation of AhRR expression. It is already known that the AhR plays a role in several immune reactions of the skin. Thus, mice overexpressing a constitutively active AhR in keratinocytes develop hyperkeratosis and skin inflammation postnatally, resembling symptoms of atopic dermatitis (34). Furthermore, AhR-deficient mice show enhanced wound healing in the skin due to increased keratinocyte migration, elevated expression of TGF-β, and enhanced fibroblast function (35). In addition, LC of AhR-deficient mice are less mature and migratory and

therefore induce reduced contact hypersensitivity reactions upon challenge with the contact allergen FITC (25). This indicates that several cell populations of the skin are involved in skin pathologies in an AhR-dependent manner. Since all of these cell populations also express the AhRR, it is likely that the AhR/AhRR system plays an important function in allergic and inflammatory reactions of the skin. Further analysis of immune reactions in the skin of AhRR-deficient mice will help to delineate the interplay of environmental induced signals and immune reactions at the skin barrier.

In the small intestine, expression of the AhRR could be demonstrated in T cells and DC in the LP, as well as in $CD8^+$ T cells and DC of PP. The high expression of the AhRR in the dome region of PP is reminiscent of the expression of the inflammatory chemokine CCL17 (36). In addition $CCL17^+$ LN DC express a high level of AhRR-mRNA (data not shown). Interestingly, the highest expression levels of the AhRR are found in the LP of the gut and in the skin, whereas the frequency of AhRR expressing cells drops with increasing distance from interfaces to the environment. An overview of the data obtained in this study is depicted in **Figure 6** for AhRR expression in the intestine and in lymphoid organs. AhRR expression levels in DC gradually decline with distance from the mucosal barrier. Similarly, the expression of AhRR in T cells was only detectable in LP and PP, whereas it was absent in MLN, PLN and spleen. These findings indicate that expression of the AhRR may be induced by environmental stimuli, like food constituents, such as natural flavonoids or tryptophan metabolites, small chemicals, but also physical stress or microbial flora. Therefore, our data support the idea that the AhRR may play a unique function in the immunosurveillance of barrier organs like skin and intestine.

We describe a striking predominance of AhRR expression within cells of the immune system in naive mice. Expression of the AhRR was most prominent in a proportion of DC in all secondary lymphoid organs analyzed. In contrast, no AhRR expression could be found in liver and lung. Thus, the expression profile of the AhRR does not simply mirror the expression

profile of the AhR, which is highly expressed in liver and lung of rats and mice (37,38). Therefore, it is tempting to speculate that the AhRR may not only play a role in competing AhR-induced gene induction, but also exerts functions independently of the AhR. Within the immune system, AhR expression has previously been observed in LC of the epidermis (25,39). Here, we show that the AhRR is also expressed in LC and dermal DC of the skin. Further, it was shown that naive T cells do not express the AhR (5). In our study, we also did not observe expression of the AhRR in T cells of spleen and LN. In contrast, expression of the AhRR could be demonstrated in $CD4^+$ and $CD8^+$ T cells of the LP and $CD8^+$ T cells in PP, which are mostly activated T cells. Thus, it is possible that the activation state of T cells influences AhRR- and AhR-expression. However, more detailed analysis is necessary to precisely compare the expression of AhRR and AhR in immune cells.

A major finding of the present study is that expression of the AhRR could not only be upregulated through AhR-activation, but could be induced to the same extent after stimulation with TLR-ligands in DC *in vivo*. This suggests that the AhRR might play a role in early immune activation of antigen presenting cells. Upregulation of *ahrr* in spleen as well as in the gut was previously shown after AhR-activation by 3MC (18) and in spleen after benzo[a] pyrene treatment of mice (17) or TCDD treatment of rats (19). However, this is the first time that the regulation of *ahrr* gene expression is monitored at the single cell level within the immune system in the presence or absence of a functional AhRR protein. The AhR-pathway not only modifies T cell responses (5-9) but is also involved in the Th1/Th2 balance (40). In addition, TCDD confers enhanced susceptibility to endotoxin induced shock (41). Recently, it was shown that AhR-signaling plays an important role in the innate immune system. AhR-activation enhances the expansion of $CCR6^+$/IL-17-producing γδ T cells by microbial stimuli (42). Furthermore, the AhR negatively regulates the proinflammatory response to LPS in macrophages in a STAT-1- and NF-κB-dependent manner (33). AhR-deficient mice are highly susceptible to LPS induced shock, probably as a result of enhanced IL-1β production

by AhR-deficient macrophages (43). These data indicate multiple interactions of the AhR-pathway with the innate immune system, which may in turn be regulated by differential expression of the AhRR, as shown here for the first time.

In addition, the induction of the AhRR after AhR- and TLR-stimulation in DC might point to AhR-dependent and -independent roles of the AhRR in the immune system. It is known that members of the bHLH/PAS family can interact with each other. Besides binding to AhR, Arnt is able to interact with several other molecules of the PAS family like single minded (SIM) or hypoxia inducible factor (HIF) 1-α, and with estrogene receptor (ER), and thereby influences circadian rhythm, hypoxia and hormone signaling (reviewed in (44)). The AhR in turn is also able to interact with ER (45), the retinoblastoma protein (46) and also with the NF-κB family members RelA and RelB (47). The interaction with RelB after TCDD treatment involves binding to a novel RelBAhR responsive element in promoters of several genes, which are not part of the xenobiotic response machinery (48), leading to the induction of immune mediators as keratinocyte-derived chemokine (KC) and monocyte-chemoattractant protein (MCP) -1 (49). An interaction of the AhR with NF-κB and STAT-1 was also observed after LPS stimulation, thereby inhibiting IL-6 promoter activity (33). Recently, it was shown that the AhRR represses HIF-1α activation in a human cell line independently of Arnt (50). Since the AhRR is inducible by TLR-signaling, it might be possible that the AhRR, like the structurally closely related AhR, might also interact with members of the NF-κB family and may therefore fulfil other functions in the immune system besides the suppression of AhR-induced transcription.

Taken together, our data provide first evidence that the AhRR is not only regulated by xenobiotics but is also induced by TLR-dependent activation of antigen presenting cells especially in barrier organs. Therefore, the AhRR is likely to be involved in the controlled activation of the immune system in these organs. Further analysis of the role of the AhRR in the innate immune system will give insight in the interplay of the innate immune system and

environmental factors, which will be important to understand the pathophysiology of inflammatory or autoimmune disorders especially in barrier organs like skin or intestine.

.

ACKNOWLEDGMENTS

We are grateful to Nicole Küpper, Sandra Beer and Klaus Pfeffer for discussion and technical help in the generation of AhRR/EGFP mice, and thank Gabriele Vielhaber (Symrise AG, Holzminden) for providing MNF.

REFERENCES

1. Barouki, R., X. Coumoul, and P. M. Fernandez-Salguero. 2007. The aryl hydrocarbon receptor, more than a xenobiotic-interacting protein. *FEBS Lett.* 581:3608-3615.

2. Bock, K. W., and C. Kohle. 2006. Ah receptor: dioxin-mediated toxic responses as hints to deregulated physiologic functions. *Biochem. Pharmacol.* 72:393-404.

3. Nebert, D. W., T. P. Dalton, A. B. Okey, and F. J. Gonzalez. 2004. Role of aryl hydrocarbon receptor-mediated induction of the CYP1 enzymes in environmental toxicity and cancer. *J. Biol. Chem.* 279:23847-23850.

4. Nguyen, L. P., and C. A. Bradfield. 2008. The search for endogenous activators of the aryl hydrocarbon receptor. *Chem. Res. Toxicol.* 21:102-116.

5. Veldhoen, M., K. Hirota, A. M. Westendorf, J. Buer, L. Dumoutier, J. C. Renauld, and B. Stockinger. 2008. The aryl hydrocarbon receptor links TH17-cell-mediated autoimmunity to environmental toxins. *Nature* 453:106-109.

6. Marshall, N. B., W. R. Vorachek, L. B. Steppan, D. V. Mourich, and N. I. Kerkvliet. 2008. Functional characterization and gene expression analysis of CD4+ CD25+ regulatory T cells generated in mice treated with 2,3,7,8-tetrachlorodibenzo-p-dioxin. *J. Immunol.* 181:2382-2391.

7. Funatake, C. J., N. B. Marshall, L. B. Steppan, D. V. Mourich, and N. I. Kerkvliet. 2005. Cutting edge: activation of the aryl hydrocarbon receptor by 2,3,7,8-tetrachlorodibenzo-p-dioxin generates a population of CD4+ CD25+ cells with characteristics of regulatory T cells. *J. Immunol.* 175:4184-4188.

8. Quintana, F. J., A. S. Basso, A. H. Iglesias, T. Korn, M. F. Farez, E. Bettelli, M. Caccamo, M. Oukka, and H. L. Weiner. 2008. Control of T(reg) and T(H)17 cell differentiation by the aryl hydrocarbon receptor. *Nature* 453:65-71.

9. Kimura, A., T. Naka, K. Nohara, Y. Fujii-Kuriyama, and T. Kishimoto. 2008. Aryl hydrocarbon receptor regulates Stat1 activation and participates in the development of Th17 cells. *Proc. Natl. Acad. Sci. U. S. A* 105:9721-9726.

10. Vorderstrasse, B. A., E. A. Dearstyne, and N. I. Kerkvliet. 2003. Influence of 2,3,7,8-tetrachlorodibenzo-p-dioxin on the antigen-presenting activity of dendritic cells. *Toxicol. Sci.* 72:103-112.

11. Hauben, E., S. Gregori, E. Draghici, B. Migliavacca, S. Olivieri, M. Woisetschlager, and M. G. Roncarolo. 2008. Activation of the aryl hydrocarbon receptor promotes allograft-specific tolerance through direct and dendritic cell-mediated effects on regulatory T cells. *Blood* 112:1214-1222.

12. Mimura, J., M. Ema, K. Sogawa, and Y. Fujii-Kuriyama. 1999. Identification of a novel mechanism of regulation of Ah (dioxin) receptor function. *Genes Dev.* 13:20-25.

13. Baba, T., J. Mimura, K. Gradin, A. Kuroiwa, T. Watanabe, Y. Matsuda, J. Inazawa, K. Sogawa, and Y. Fujii-Kuriyama. 2001. Structure and expression of the Ah receptor repressor gene. *J. Biol. Chem.* 276:33101-33110.

14. Oshima, M., J. Mimura, H. Sekine, H. Okawa, and Y. Fujii-Kuriyama. 2009. SUMO modification regulates the transcriptional repressor function of aryl hydrocarbon receptor repressor. *J. Biol. Chem.* 284:11017-11026.

15. Evans, B. R., S. I. Karchner, L. L. Allan, R. S. Pollenz, R. L. Tanguay, M. J. Jenny, D. H. Sherr, and M. E. Hahn. 2008. Repression of aryl hydrocarbon receptor (AHR) signaling by AHR repressor: role of DNA binding and competition for AHR nuclear translocator. *Mol. Pharmacol.* 73:387-398.

16. Haarmann-Stemmann, T., H. Bothe, A. Kohli, U. Sydlik, J. Abel, and E. Fritsche. 2007. Analysis of the transcriptional regulation and molecular function of the aryl hydrocarbon receptor repressor in human cell lines. *Drug Metab Dispos.* 35:2262-2269.

17. Bernshausen, T., B. Jux, C. Esser, J. Abel, and E. Fritsche. 2006. Tissue distribution and function of the aryl hydrocarbon receptor repressor (AhRR) in C57Bl/6 and aryl hydrocarbon receptor deficient mice. *Arch. Toxikol.* 80:206-211.

18. Hosoya, T., N. Harada, J. Mimura, H. Motohashi, S. Takahashi, O. Nakajima, M. Morita, S. Kawauchi, M. Yamamoto, and Y. Fujii-Kuriyama. 2008. Inducibility of cytochrome P450 1A1 and chemical carcinogenesis by benzo[a]pyrene in AhR repressor-deficient mice. *Biochem. Biophys. Res. Commun.* 365:562-567.

19. Korkalainen, M., J. Tuomisto, and R. Pohjanvirta. 2004. Primary structure and inducibility by 2,3,7,8-tetrachlorodibenzo-p-dioxin (TCDD) of aryl hydrocarbon receptor repressor in a TCDD-sensitive and a TCDD-resistant rat strain. *Biochem. Biophys. Res. Commun.* 315:123-131.

20. Nishihashi, H., Y. Kanno, K. Tomuro, T. Nakahama, and Y. Inouye. 2006. Primary structure and organ-specific expression of the rat aryl hydrocarbon receptor repressor gene. *Biol. Pharm. Bull.* 29:640-647.

21. Tsuchiya, Y., M. Nakajima, S. Itoh, M. Iwanari, and T. Yokoi. 2003. Expression of aryl hydrocarbon receptor repressor in normal human tissues and inducibility by polycyclic aromatic hydrocarbons in human tumor-derived cell lines. *Toxicol. Sci.* 72:253-259.

22. Yamamoto, J., K. Ihara, H. Nakayama, S. Hikino, K. Satoh, N. Kubo, T. Iida, Y. Fujii, and T. Hara. 2004. Characteristic expression of aryl hydrocarbon receptor repressor gene in human tissues: organ-specific distribution and variable induction patterns in mononuclear cells. *Life Sci.* 74:1039-1049.

23. Karasuyama, H., and F. Melchers. 1988. Establishment of mouse cell lines which constitutively secrete large quantities of interleukin 2, 3, 4 or 5, using modified cDNA expression vectors. *Eur. J. Immunol.* 18:97-104.

24. Merad, M., F. Ginhoux, and M. Collin. 2008. Origin, homeostasis and function of Langerhans cells and other langerin-expressing dendritic cells. *Nat. Rev. Immunol.* 8:935-947.

25. Jux, B., S. Kadow, and C. Esser. 2009. Langerhans cell maturation and contact hypersensitivity are impaired in aryl hydrocarbon receptor-null mice. *J. Immunol.* 182:6709-6717.

26. Stutte, S., B. Jux, C. Esser, and I. Forster. 2008. CD24a expression levels discriminate Langerhans cells from dermal dendritic cells in murine skin and lymph nodes. *J. Invest Dermatol.* 128:1470-1475.

27. Akintobi, A. M., C. M. Villano, and L. A. White. 2007. 2,3,7,8-Tetrachlorodibenzo-p-dioxin (TCDD) exposure of normal human dermal fibroblasts results in AhR-dependent and -independent changes in gene expression. *Toxicol. Appl. Pharmacol.* 220:9-17.

28. Bogunovic, M., F. Ginhoux, J. Helft, L. Shang, D. Hashimoto, M. Greter, K. Liu, C. Jakubzick, M. A. Ingersoll, M. Leboeuf, E. R. Stanley, M. Nussenzweig, S. A. Lira, G. J. Randolph, and M. Merad. 2009. Origin of the lamina propria dendritic cell network. *Immunity.* 31:513-525.

29. Niess, J. H., S. Brand, X. Gu, L. Landsman, S. Jung, B. A. McCormick, J. M. Vyas, M. Boes, H. L. Ploegh, J. G. Fox, D. R. Littman, and H. C. Reinecker. 2005. CX3CR1-mediated dendritic cell access to the intestinal lumen and bacterial clearance. *Science* 307:254-258.

30. Chieppa, M., M. Rescigno, A. Y. Huang, and R. N. Germain. 2006. Dynamic imaging of dendritic cell extension into the small bowel lumen in response to epithelial cell TLR engagement. *J. Exp. Med.* 203:2841-2852.

31. Sun, C. M., J. A. Hall, R. B. Blank, N. Bouladoux, M. Oukka, J. R. Mora, and Y. Belkaid. 2007. Small intestine lamina propria dendritic cells promote de novo generation of Foxp3 T reg cells via retinoic acid. *J. Exp. Med.* 204:1775-1785.

32. Jaensson, E., H. Uronen-Hansson, O. Pabst, B. Eksteen, J. Tian, J. L. Coombes, P. L. Berg, T. Davidsson, F. Powrie, B. Johansson-Lindbom, and W. W. Agace. 2008. Small intestinal CD103+ dendritic cells display unique functional properties that are conserved between mice and humans. *J. Exp. Med.* 205:2139-2149.

33. Kimura, A., T. Naka, T. Nakahama, I. Chinen, K. Masuda, K. Nohara, Y. Fujii-Kuriyama, and T. Kishimoto. 2009. Aryl hydrocarbon receptor in combination with Stat1 regulates LPS-induced inflammatory responses. *J. Exp. Med.* 206:2027-2035.

34. Tauchi, M., A. Hida, T. Negishi, F. Katsuoka, S. Noda, J. Mimura, T. Hosoya, A. Yanaka, H. Aburatani, Y. Fujii-Kuriyama, H. Motohashi, and M. Yamamoto. 2005. Constitutive expression of aryl hydrocarbon receptor in keratinocytes causes inflammatory skin lesions. *Mol. Cell Biol.* 25:9360-9368.

35. Carvajal-Gonzalez, J. M., A. C. Roman, M. I. Cerezo-Guisado, E. M. Rico-Leo, G. Martin-Partido, and P. M. Fernandez-Salguero. 2009. Loss of dioxin-receptor expression accelerates wound healing in vivo by a mechanism involving TGF{beta}. *J. Cell Sci.* 122:1823-1833.

36. Alferink, J., I. Lieberam, W. Reindl, A. Behrens, S. Weiss, N. Huser, K. Gerauer, R. Ross, A. B. Reske-Kunz, P. Ahmad-Nejad, H. Wagner, and I. Förster. 2003. Compartmentalized Production of CCL17 In Vivo: Strong Inducibility in Peripheral Dendritic Cells Contrasts Selective Absence from the Spleen. *J. Exp. Med.* 197:585-599.

37. Carver, L. A., J. B. Hogenesch, and C. A. Bradfield. 1994. Tissue specific expression of the rat Ah-receptor and ARNT mRNAs. *Nucleic Acids Res.* 22:3038-3044.

38. Li, W., S. Donat, O. Dohr, K. Unfried, and J. Abel. 1994. Ah receptor in different tissues of C57BL/6J and DBA/2J mice: use of competitive polymerase chain reaction to measure Ah-receptor mRNA expression. *Arch. Biochem. Biophys.* 315:279-284.

39. Platzer, B., S. Richter, D. Kneidinger, D. Waltenberger, M. Woisetschlager, and H. Strobl. 2009. Aryl Hydrocarbon Receptor Activation Inhibits In Vitro Differentiation of Human Monocytes and Langerhans Dendritic Cells. *J. Immunol.*

40. Negishi, T., Y. Kato, O. Ooneda, J. Mimura, T. Takada, H. Mochizuki, M. Yamamoto, Y. Fujii-Kuriyama, and S. Furusako. 2005. Effects of aryl hydrocarbon receptor signaling on the modulation of TH1/TH2 balance. *J. Immunol.* 175:7348-7356.

41. Clark, G. C., and M. J. Taylor. 1994. Tumor necrosis factor involvement in the toxicity of TCDD: the role of endotoxin in the response. *Exp. Clin. Immunogenet.* 11:136-141.

42. Martin, B., K. Hirota, D. J. Cua, B. Stockinger, and M. Veldhoen. 2009. Interleukin-17-producing gammadelta T cells selectively expand in response to pathogen products and environmental signals. *Immunity.* 31:321-330.

43. Sekine, H., J. Mimura, M. Oshima, H. Okawa, J. Kanno, K. Igarashi, F. J. Gonzalez, T. Ikuta, K. Kawajiri, and Y. Fujii-Kuriyama. 2009. Hypersensitivity of AhR-deficient mice to LPS-induced septic shock. *Mol. Cell Biol.*

44. Kewley, R. J., M. L. Whitelaw, and A. Chapman-Smith. 2004. The mammalian basic helix-loop-helix/PAS family of transcriptional regulators. *Int. J. Biochem. Cell Biol.* 36:189-204.

45. Matthews, J., and J. A. Gustafsson. 2006. Estrogen receptor and aryl hydrocarbon receptor signaling pathways. *Nucl. Recept. Signal.* 4:e016.

46. Puga, A., Y. Xia, and C. Elferink. 2002. Role of the aryl hydrocarbon receptor in cell cycle regulation. *Chem. Biol. Interact.* 141:117-130.

47. Vogel, C. F., and F. Matsumura. 2008. A new cross-talk between the aryl hydrocarbon receptor and RelB, a member of the NF-kappaB family. *Biochem. Pharmacol.*

48. Vogel, C. F., E. Sciullo, W. Li, P. Wong, G. Lazennec, and F. Matsumura. 2007. RelB, a new partner of aryl hydrocarbon receptor-mediated transcription. *Mol. Endocrinol.* 21:2941-2955.

49. Vogel, C. F., N. Nishimura, E. Sciullo, P. Wong, W. Li, and F. Matsumura. 2007. Modulation of the chemokines KC and MCP-1 by 2,3,7,8-tetrachlorodibenzo-p-dioxin (TCDD) in mice. *Arch. Biochem. Biophys.* 461:169-175.

50. Karchner, S. I., M. J. Jenny, A. M. Tarrant, B. R. Evans, H. J. Kang, I. Bae, D. H. Sherr, and M. E. Hahn. 2009. The active form of human aryl hydrocarbon receptor (AHR) repressor lacks exon 8, and its Pro 185 and Ala 185 variants repress both AHR and hypoxia-inducible factor. *Mol. Cell Biol.* 29:3465-3477.

FOOT NOTES:

Grant support

This work was supported by the BMU project B5 (to I.F. and J.A.), the Jürgen-Manchot-Stiftung (to I.F.) and the "Stiftung zur Erforschung infektiös-immunologischer Erkrankungen" (to I.F.)

Abbreviations

AhR aryl hydrocarbon receptor

AhRR AhR-repressor

Arnt AhR-nuclear translocator

LN lymph nodes

MLN mesenteric LN

LP lamina propria

PLN peripheral LN

PP Peyers Patches

3MC 3-Methylcholanthrene

MNF 3-Methoxy-4-nitroflavone

XRE xenobiotic response elements

FIGURE LEGENDS

Figure 1: AhRR/EGFP expression in the skin

A) Immunofluorescence analysis of frozen sections of dorsal skin of WT and $AhRR^{E/+}$ mice counterstained with DAPI (200x)**. B, C**) Flow cytometric analysis of epidermal and dermal cell suspensions of WT, $AhRR^{E/+}$ and $AhRR^{E/E}$ mice. Skin biopsies were digested with 0,25% trypsin, after which the dermis was separated from the epidermis. After mechanical disruption, the epidermal cell suspensions were stained with antibodies against MHCII and CD24a. The dermis was further digested with collagenase P to produce a single cell suspension and stained for MHCII and CD24a expression. (**B**) Percentage of AhRR/EGFP positive cells in epidermis and dermis of either $MHCII^+$ (left) or $MHCII^-$ cells (right) (n=4) is shown. * $p < 0.05$, ** $p < 0.01$, *** $p < 0.001$ ($AhRR^{E/+}$ or $AhRR^{E/E}$ versus WT). (**C**) A representative staining pattern of dermal cells for MHCII and CD24a is shown (left). Percentages of $MHCII^+/CD24a^{low}$ (a), $MHCII^+/CD24a^{high}$ (b), $MHCII^-/CD24a^{low}$ (c) and $MHCII^-/CD24a^{high}$ (d) cells in the dermis are shown (n=4, right). * $p < 0.05$, ** $p < 0.01$, *** $p < 0.001$ ($AhRR^{E/+}$ or $AhRR^{E/E}$ versus WT).

Figure 2: AhRR/EGFP expression in the small intestine

A) Immunofluorescence analysis of frozen sections of the small intestine (top, 100x) and of PP (bottom, 200x) of WT, $AhRR^{E/+}$, $AhRR^{E/E}$ mice. **B**) Flow cytometric analyses of single cell suspensions of the LP and PP of the small intestine. The cells were stained with antibodies against CD3, CD3/CD4, CD3/CD8, CD3/CD4/CD25 to identify T cell subsets, CD19 to identify B cells, and CD11c and MHCII to identify DC. Percentages of EGFP-expressing cells in the indicated subsets are depicted (n= 3-5). * $p < 0.05$, ** $p < 0.01$, *** $p < 0.001$ ($AhRR^{E/+}$ or $AhRR^{E/E}$ versus WT).

Figure 3: AhRR/EGFP expression in the small intestine

Expression of AhRR/EGFP by $CD103^+$ and $CD103^-$ $CD11c^+$ /$MHCII^+$ DC in the LP analyzed by flow cytometry. Numbers indicate % $EGFP^+$ cells within the respective DC subset of WT, $AhRR^{E/+}$ and $AhRR^{E/E}$ mice.

Figure 4: AhRR/EGFP expression in MLN and PLN of naive mice

A) Immunofluorescence analysis of frozen sections of MLN and PLN of WT (left), $AhRR^{E/+}$ (middle) and $AhRR^{E/E}$ mice (right), counterstained with DAPI (100x). **B**) Single cell suspensions of MLN and PLN were stained with antibodies against CD3, CD4, CD8, CD19, CD11c and MHCII as described above (**Fig. 2B**) to identify T cells, B cells and DC. Percentages of EGFP-expressing cells are depicted (n=4-6) * $p < 0.05$, ** $p < 0.01$ ($AhRR^{E/+}$ or $AhRR^{E/E}$ versus WT).

Figure 5: AhRR/EGFP expression after 3MC and TLR ligand treatment

A) WT and $AhRR^{E/+}$ mice were injected with 200µl 3MC in PBS/1%DMSO (25mg/ml) i.p.. Control mice were injected with 200µl PBS/1%DMSO. After 16h single cell suspensions of LN (brachial, axial, inguinal and mesenteric) and spleen were stained with antibodies against CD3, CD4, CD8, CD19, CD11c and MHCII to identify T cells, B cells and DC as described above (**Fig. 2B**). Percentages of EGFP-expressing cells within each subset are depicted (n=3-4).* $p < 0.05$ ($AhRR^{E/+}$ versus WT),** $p < 0.01$ ($AhRR^{E/+}$/3MC versus WT), *** $p < 0.001$ ($AhRR^{E/+}$ versus WT) **B**) 3MC (250µl/ml) was applied per gavage in DMSO/olive oil (1:4 v/v). Control mice received solvent only. After 16h the small intestine was removed and single cell suspensions were stained with antibodies against MHCII and CD11c. Percentages of EGFP-expressing cells among all $MHCII^+$/$CD11c^+$ DC are depicted (n=3-6).* $p < 0.01$ (3MC-stimulated versus controls) **C**) Mice were injected with 200µl LPS in PBS (0,5 mg/ml) i.p. Control mice were injected with 200µl PBS. After 16h single cell suspensions of LN

(brachial, axial, inguinal and mesenteric) and spleen cells were stained with antibodies against CD3, CD4, CD8, CD19, CD11c and MHCII as described above (**Fig. 2B**) to identify T cells, B cells and DC. Percentages of EGFP-expressing cells are depicted within each subset (n=3-4).). * $p < 0.05$ ($AhRR^{E/+}$/LPS versus WT),.** $p < 0.01$ ($AhRR^{E/+}$ versus WT). **D**) BMDC of WT and $AhRR^{E/+}$ mice were stimulated with LPS (1µg/ml), CpG (100µM), P3Cys (10µg/ml), 3MC (10µM) or MNF (5µM), or with the indicated combinations (left picture). 16 h later cells were stained with antibodies against MHCII and CD11c. Percentages of EGFP-expressing cells among all $MHCII^+/CD11c^+$ DC are depicted (n=8). ** $p < 0.001$ (TLR-stimulated versus controls). **E**) BMDC of WT, $AhRR^{E/+}$ and $AhRR^{E/E}$ mice were stimulated with LPS (1µg/ml), 3MC (10µM) or MNF (5µM), or with the indicated combinations. 16 h later cells were stained with antibodies against MHCII and CD11c. Percentages of EGFP-expressing cells among all $MHCII^+/CD11c^+$ DC are depicted (n=3-7). ** $p < 0.01$ (TLR-stimulated BMDC from $AhRR^{E/+}$ or $AhRR^{E/E}$ mice versus controls).

Figure 6: Schematic illustration of expression levels of AhRR/EGFP in the intestine and lymphoid organs.

Highest expression levels of AhRR were found in LP and PP. Expression levels in DC drop gradually in MLN, PLN and spleen. Expression of AhRR in T cells was observed only in LP and in $CD8^+$ T cells in PP.

Figure 1

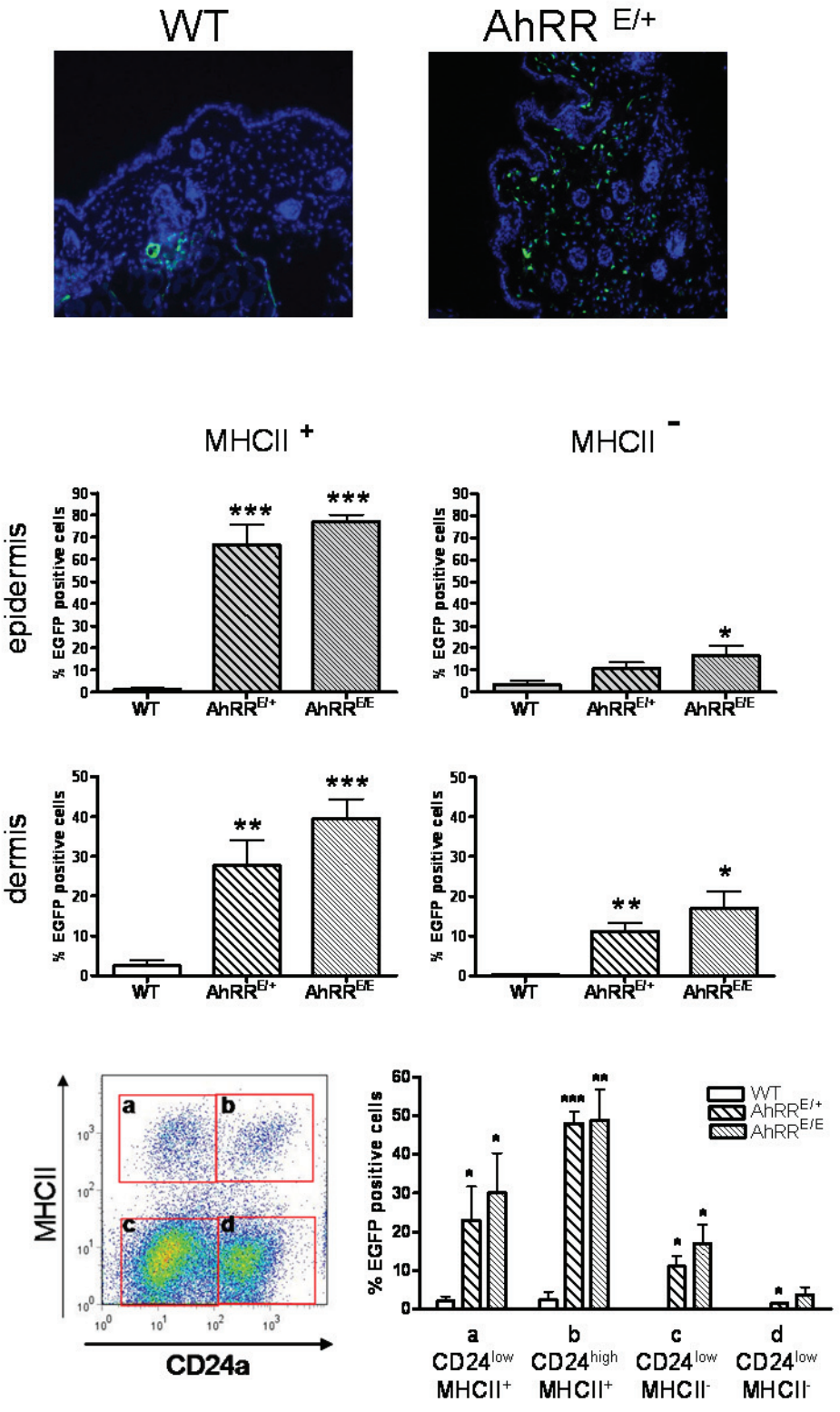
WT
AhRR E/+
MHCII +
MHCII -
epidermis
dermis
% EGFP positive cells
WT
AhRR E/+
AhRR E/E
MHCII
CD24a
a
b
c
d
WT
AhRR E/+
AhRR E/E
a CD24 low MHCII+
b CD24 high MHCII+
c CD24 low MHCII-
d CD24 low MHCII-

Figure 2

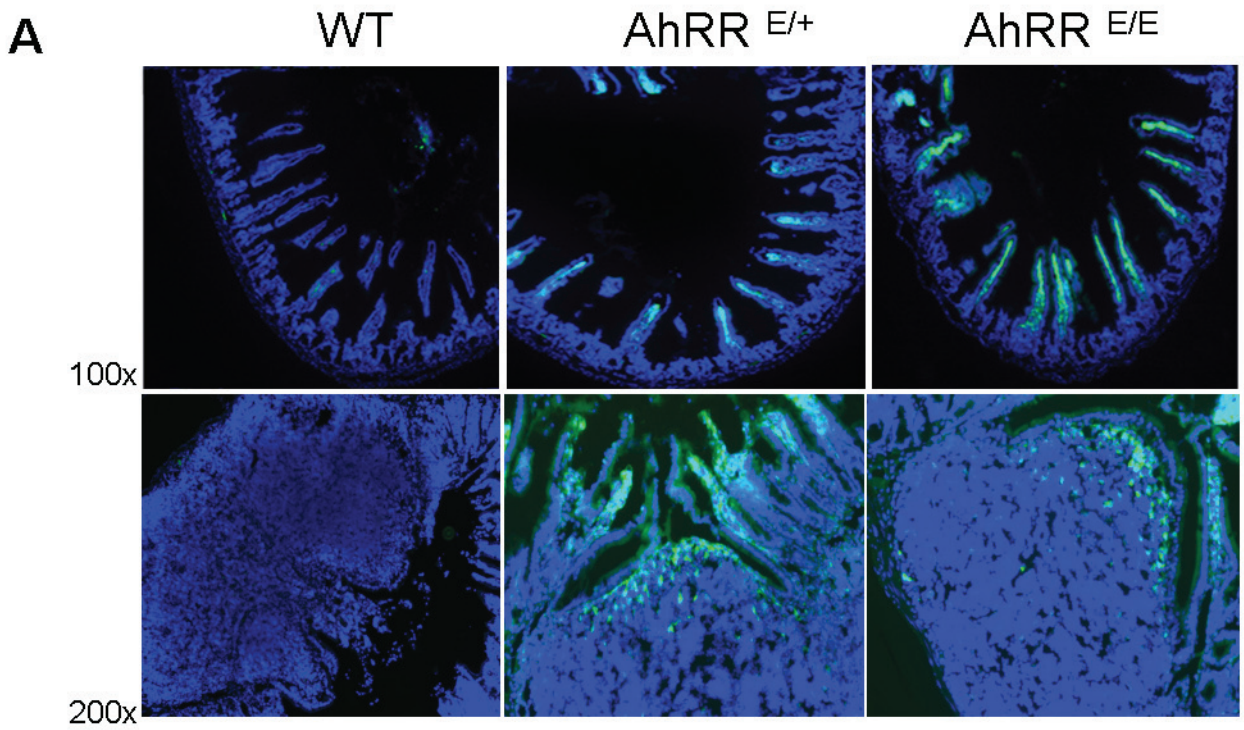
A
WT
AhRR E/+
AhRR E/E
100x
200x

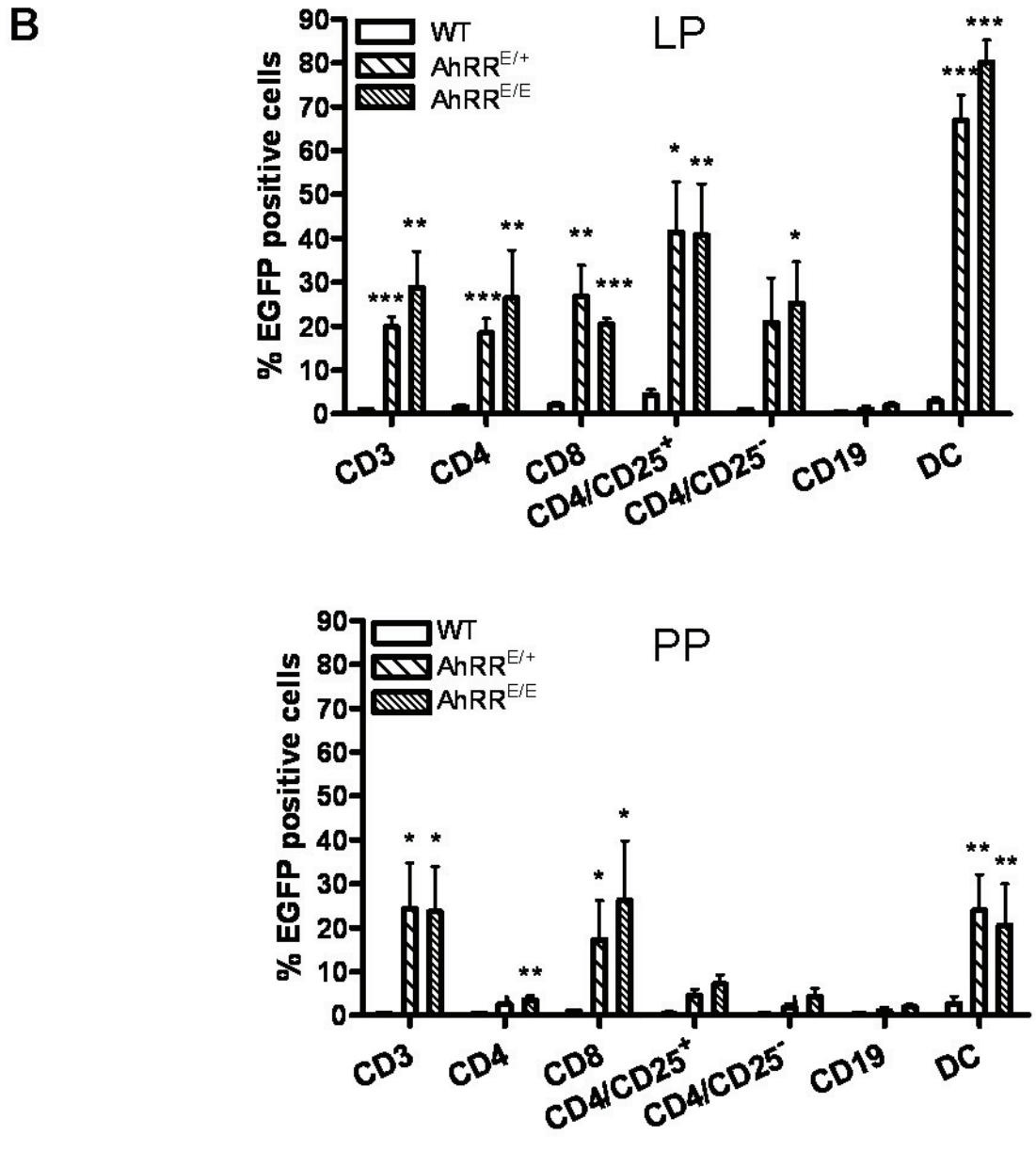
B
LP
WT
AhRR E/+
AhRR E/E
% EGFP positive cells
CD3
CD4
CD8
CD4/CD25+
CD4/CD25-
CD19
DC
PP
WT
AhRR E/+
AhRR E/E
% EGFP positive cells
CD3
CD4
CD8
CD4/CD25+
CD4/CD25-
CD19
DC

Figure 3

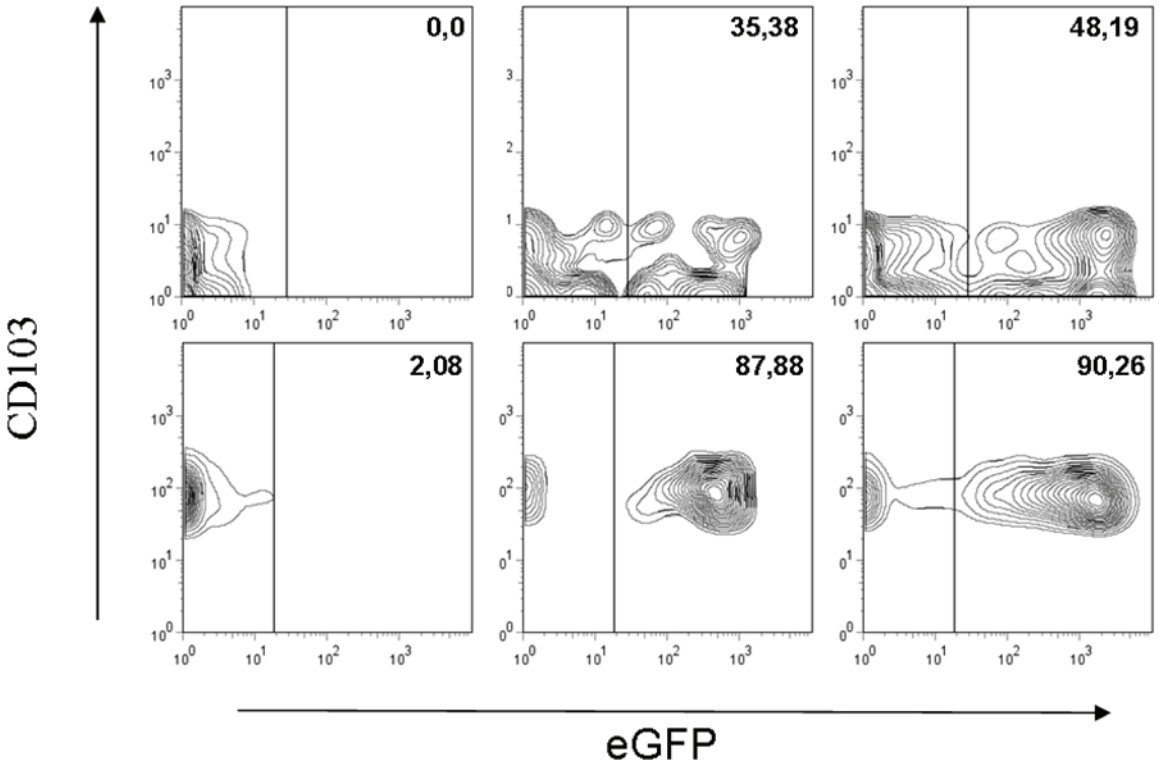

Figure 4

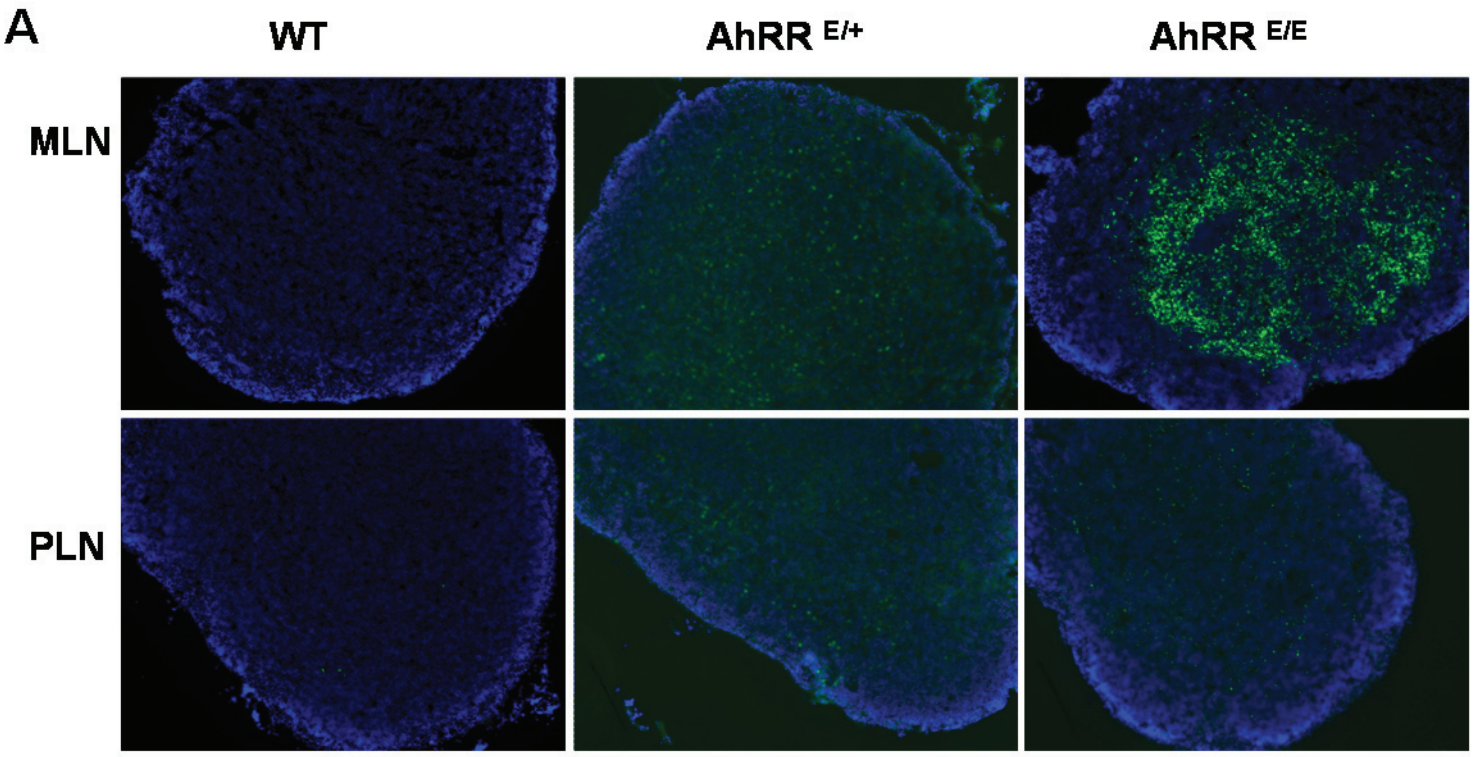
A
WT
AhRR E/+
AhRR E/E
MLN
PLN

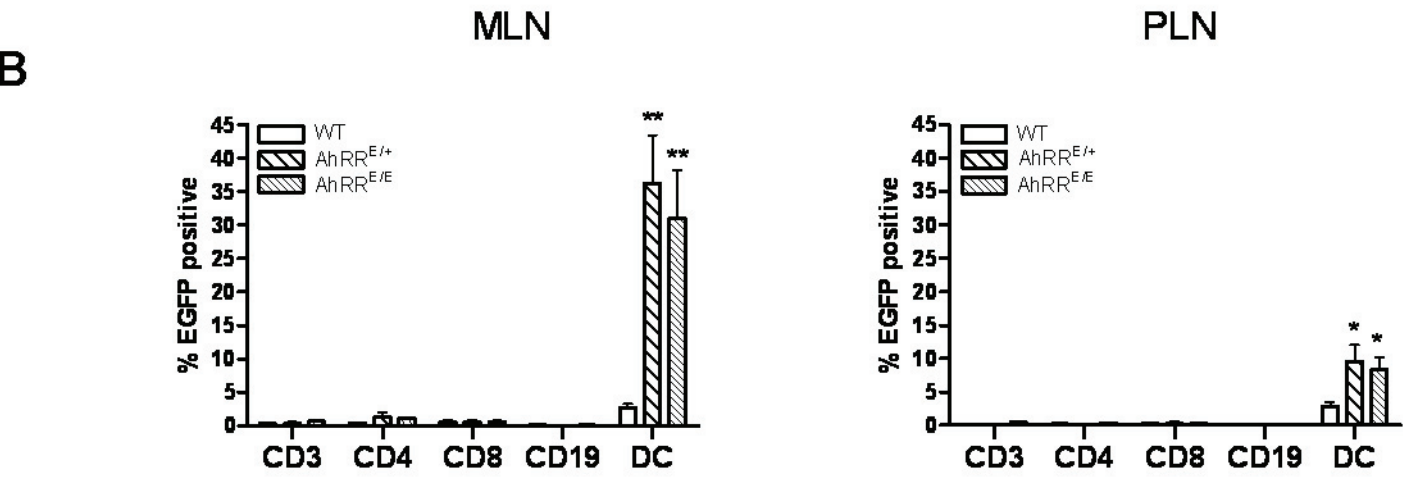
B
MLN
PLN
WT
AhRR E/+
AhRR E/E
% EGFP positive
0
5
10
15
20
25
30
35
40
45
CD3
CD4
CD8
CD19
DC
**
**
*
*

Figure 5

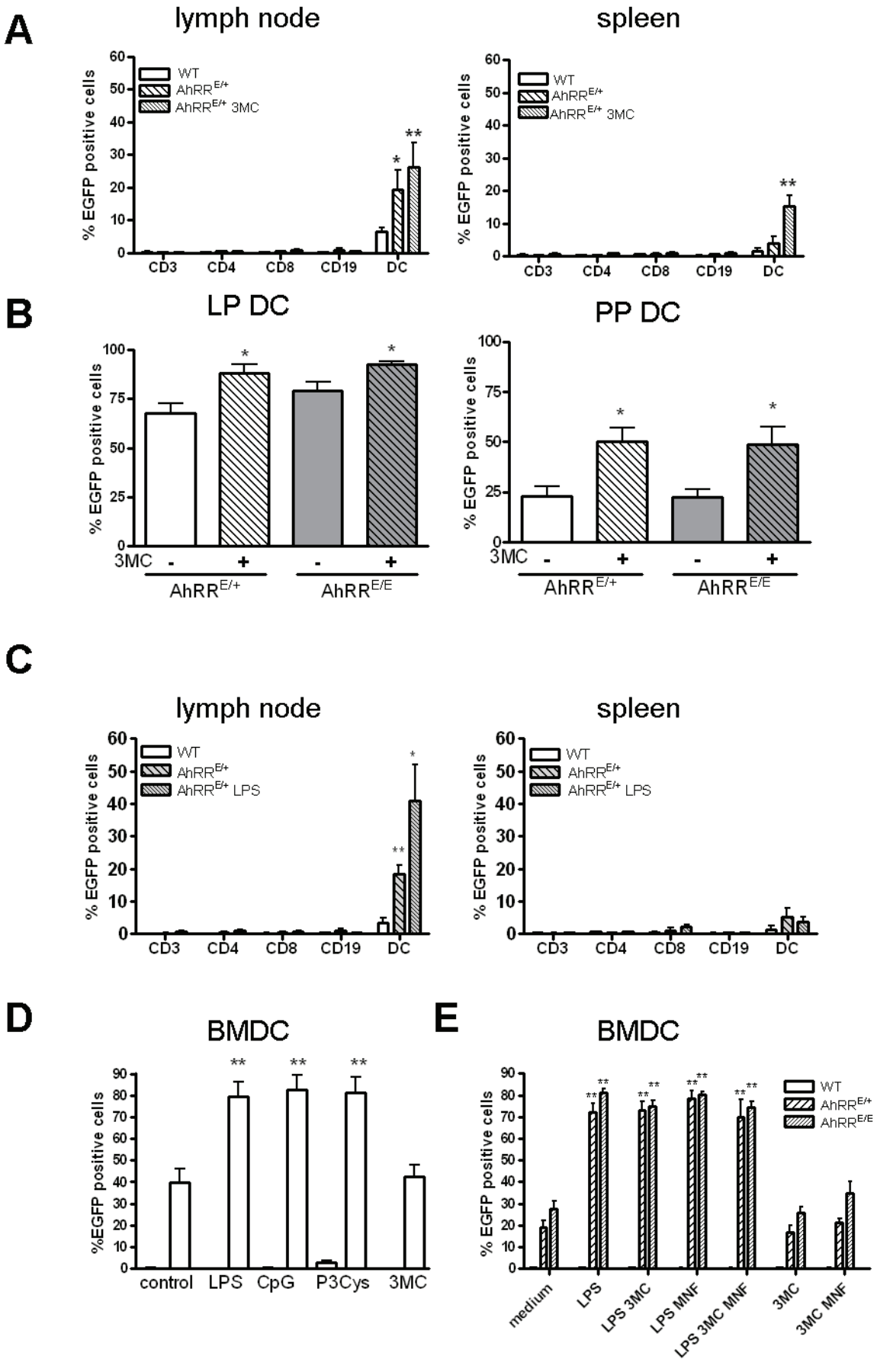
A
lymph node
spleen
% EGFP positive cells
WT
AhRR E/+
AhRR E/+ 3MC
CD3
CD4
CD8
CD19
DC
B
LP DC
PP DC
3MC
AhRR E/+
AhRR E/E
C
lymph node
spleen
AhRR E/+ LPS
D
BMDC
%EGFP positive cells
control
LPS
CpG
P3Cys
3MC
E
BMDC
medium
LPS
LPS 3MC
LPS MNF
LPS 3MC MNF
3MC
3MC MNF

Figure 6

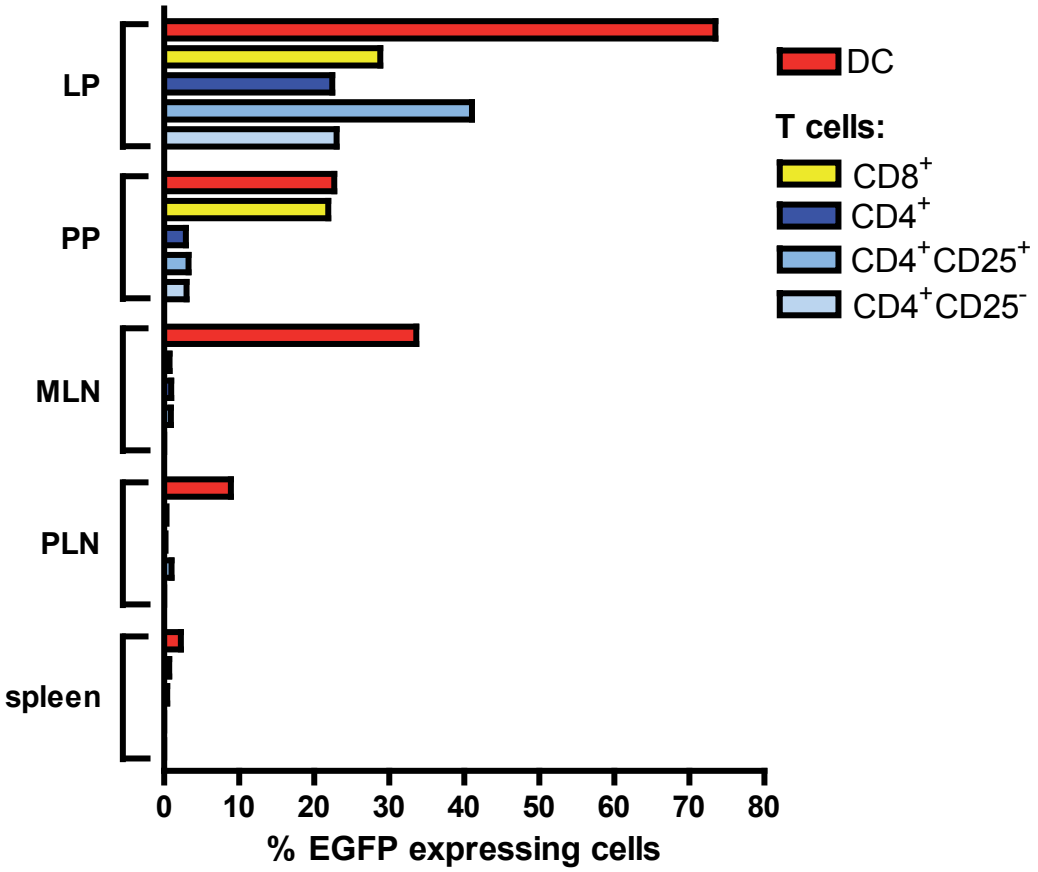
LP
PP
MLN
PLN
spleen
0
10
20
30
40
50
60
70
80
% EGFP expressing cells
DC
T cells:
CD8+
CD4+
CD4+CD25+
CD4+CD25-

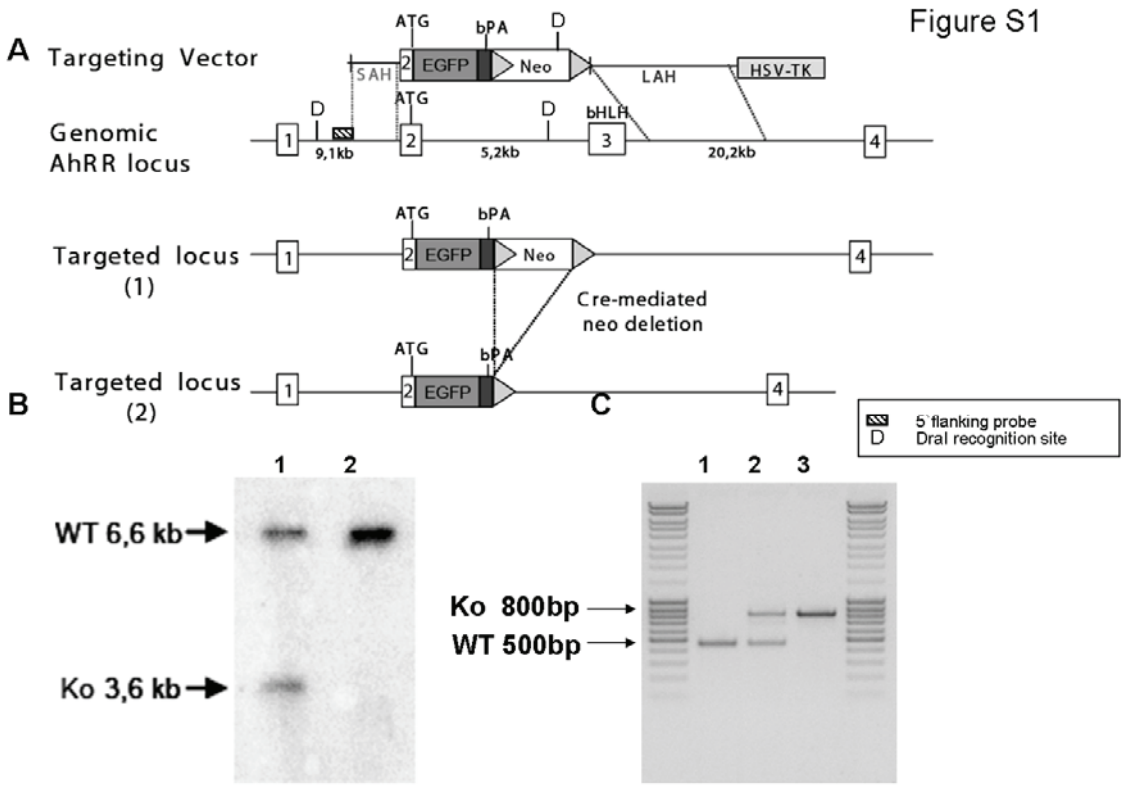

Supplementary Fig. 1: **Generation of AhRR-deficient mice**

A) Targeting-strategy to generate AhRR-deficient mice. The EGFP-cDNA was inserted into the second exon of AhRR and the third exon was deleted. In addition a loxP-flanked neomycin gene was inserted. For Southern blot analysis a 5`flanking probe was used (depicted as "probe"). **B)** For Southern blot analysis tail DNA of mutated and WT animals was digested with Dra1. Hybridisation with a 3`-flanking probe revealed a 6,6kb (WT) and a 3, 6 kb (KO) fragment in the targeted ES cell clone (1) compared to WT ES cells (2). **C)** PCR of tail DNA of WT (1), $AhRR^{E/+}$ (2) und $AhRR^{E/E}$ (3) mice shows a 500bp fragment for the WT allele and an 800bp fragment for the mutant allele.

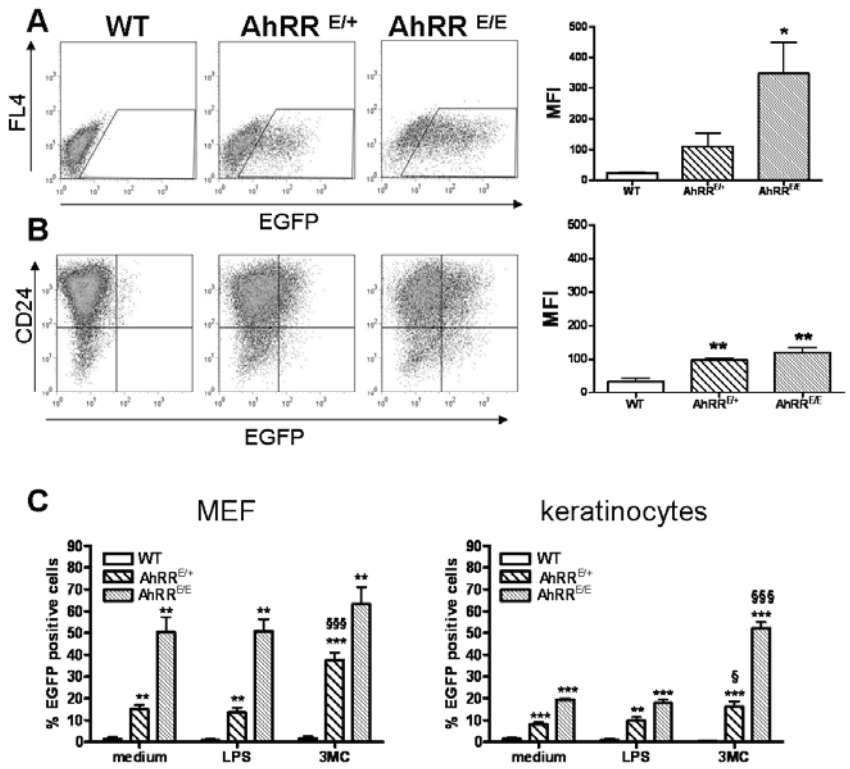

Figure S2

Supplementary Fig. 2: AhRR/EGFP-expression of MEF and keratinocytes

A) FACS analysis of WT-, AhRR$^{E/+}$- and AHRR$^{E/E}$-MEF (one of 3 representative experiments is shown). EGFP expression is plotted against an unstained channel (left). Mean fluorescence intensity (MFI) of EGFP^{+} cells is depicted (right picture). * $p < 0.05$ (AhRR$^{E/E}$ versus WT). **B)** FACS analysis of primary murine WT-, AhRR$^{E/+}$- and AHRR$^{E/E}$-keratinocytes (one representative of 3 individual experiments is shown). AhRR/EGFP-expression of CD24a^{+} keratinocytes is shown (left). MFI of EGFP^{+} cells is depicted (right picture). ** $p < 0.01$ (AhRR$^{E/+}$ or AhRR$^{E/E}$ versus WT). **C)** AhRR/EGFP-expression of WT-, AhRR$^{E/+}$- and AHRR$^{E/E}$-MEF (n=3, +/- SEM) and primary murine CD24a^{+} keratinocytes (n=3-4, +/- SEM) after LPS and 3MC treatment. ** $p < 0.01$, *** $p < 0.001$ (AhRR$^{E/+}$ or

AhRR$^{E/E}$ versus WT). § $p < 0.05$, §§§ $p < 0.001$ (3MC treated AhRR$^{E/+}$ or AhRR$^{E/E}$ vs control AhRR$^{E/+}$ or AhRR$^{E/E}$ cells).

Figure S3

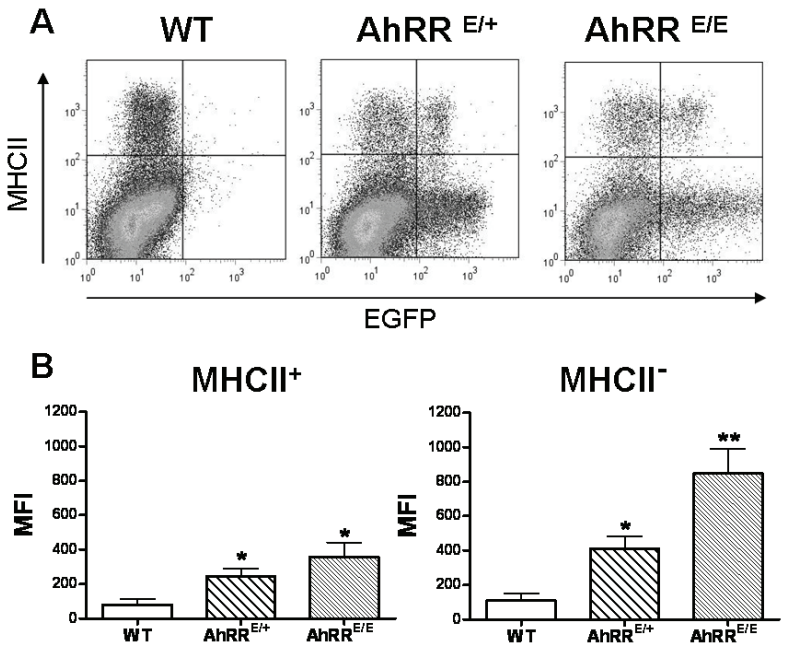

Supplementary Fig. 3: AhRR/EGFP-expression of dermal cells

A) FACS analysis of WT-, AhRR$^{E/+}$- and AHRR$^{E/E}$- MHCII+ and MHCII^{-} dermal cell populations (one representative of 4 individual experiments is shown). **B)** MFI of EGFP^{+} of MHCII^{+} and MHCII^{-} cell populations is calculated (n=4, +/- SEM). * $p < 0.05$ (AhRR$^{E/+}$ or AhRR$^{E/E}$ versus WT). ** $p < 0.01$ (AhRR$^{E/+}$ or AhRR$^{E/E}$ versus WT).

Proinflammatory cytokines down-regulate intestinal selenoprotein P biosynthesis via NOS-2 induction

Bodo Speckmann[a], Antonio Pinto[a], Meike Winter[b], Irmgard Förster[b], Helmut Sies[a,b,c] and Holger Steinbrenner[a]

[a] Institute for Biochemistry and Molecular Biology I, Heinrich-Heine University, Düsseldorf, Germany; [b] Institut für Umweltmedizinische Forschung (IUF) an der Heinrich-Heine-Universität, Düsseldorf, Germany; [c] College of Science, King Saud University, Riyadh, Saudi Arabia

Corresponding author:

Dr. Holger Steinbrenner,

Heinrich-Heine-University Düsseldorf, Institute for Biochemistry and Molecular Biology I,

Universitätsstrasse 1, Geb. 22.03, D-40225 Düsseldorf, Germany

Tel. +49-211-8112712;

Fax. +49-211-8113029;

Email: Holger.Steinbrenner@uni-duesseldorf.de

Abstract

Selenoprotein P (SeP), serving as selenium transporter and extracellular antioxidant, is assumed to have a protective role in the gastrointestinal tract, which is particularly susceptible to oxidative damage. Decreased SeP mRNA levels have been found in colon cancer; however, information on the control of intestinal SeP biosynthesis is scarce. We analysed SeP biosynthesis in human intestinal epithelial Caco-2 cells subject to differentiation from crypt- to villous-like enterocytes. In the course of Caco-2 cell differentiation, SeP mRNA expression and secretion increased concomitantly with three regulators of SeP transcription: hepatocyte nuclear factor 4α (HNF-4α), forkhead box class O1a (FoxO1a) and peroxisomal proliferator-activated receptor gamma coactivator 1α (PGC-1α). Treatment of differentiated Caco-2 cells with the proinflammatory cytokines IL-1β, TNF-α and IFN-γ caused a down-regulation of SeP biosynthesis, resulting from induction of nitric oxide synthase 2 (NOS-2). These observations were corroborated by declined SeP mRNA levels in the colon of dextran sodium sulphate (DSS)-treated mice, an animal model of experimental colitis. ***Conclusion:*** Inflammation of the intestinal mucosa causes a decline of locally produced selenoprotein P in the colon that eventually may contribute to the emergence of inflammatory bowel disease-related colorectal cancer.

Keywords: NOS-2; selenoprotein; HNF-4alpha; Caco-2; colitis

Introduction

Oxidative stress plays a major role in the pathogenesis of inflammatory bowel disease (IBD), which is characterised by intestinal mucosal damage and loss of the intestinal barrier function [1]. Intestinal oxidative damage in IBD results from excessive production of reactive oxygen and nitrogen species (ROS/RNS) and an impaired antioxidative capacity [2]. Many of these reactive species are generated by the reaction of cellular substrates and oxygen derivatives with nitric oxide (NO). Elevated expression and activity of the inducible form of nitric oxide synthase (NOS-2), resulting in high rates of NO release, are found in the inflamed mucosa of IBD patients [3]. Colonic and intestinal epithelial cells have been identified as the main source of NO formation in human IBD and in animal models of gut inflammation [4,5]. The biosynthesis of NOS-2 is induced in the human intestinal epithelial cell line Caco-2 by proinflammatory cytokines, whose mucosal concentrations are elevated in experimental and human IBD [6,7]. In the course of disease progression, accumulation of oxidative DNA damage in the inflamed mucosa is associated with colon carcinogenesis in patients suffering from ulcerative colitis [8].

Cellular antioxidant defence systems are supported by dietary micronutrients including vitamin C, flavonoids and selenium. The essential trace element selenium has beneficial effects in inflammatory disorders and certain types of cancer [9,10]. Supplementation with selenium protects rats against tissue damage induced by experimental colitis [11], and selenium intake is inversely correlated with colon cancer incidence in humans [12]. This protective role of selenium against oxidative stress-related diseases appears to rely primarily on antioxidative actions of selenoproteins. Most selenoproteins are oxidoreductases with selenocysteine being part of the catalytic center. The unique redox characteristics of selenocysteine make selenoenzymes effective reductants of ROS, thus preventing damage of cellular lipids, proteins and nucleic acids [9]. Selenoproteins that are abundantly expressed in the normal intestinal mucosa include glutathione peroxidases (GPx), thioredoxin reductase,

selenoprotein W and selenoprotein P (SeP) [13,14]. The expression pattern of selenoproteins is altered in intestinal sections of colorectal cancer patients: A significant decline of selenoprotein P mRNA levels has been described in colorectal cancer tissues in comparison to the corresponding normal mucosa [15]. In the progression of colorectal cancer, the GPx-2 expression increased, whereas the expression of GPx-1, GPx-3 and SeP decreased [13].

Selenoprotein P contains up to ten selenocysteine residues per molecule and is the major selenoprotein in human plasma. According to its high selenium content and its plasma localisation, the main function of SeP is to supply various tissues with selenium [16]. Additionally, two enzymatic activities of SeP have been demonstrated *in vitro*: a phospholipid hydroperoxide glutathione peroxidase and a peroxynitrite reductase activity [17,18]. The antioxidative function of SeP is attributed to its N-terminal selenocysteine residue, which has been found to be responsible for SeP-mediated protection of mice against oxidative tissue damage upon infection with *Trypanosoma congolense* [19]. SeP mRNA is ubiquitously expressed with highest levels found in liver, intestine and kidney [14]. As the liver represents the major source of plasma SeP, regulation of hepatic SeP biosynthesis has been studied extensively. Hepatic transcription of SeP is controlled by hepatocyte nuclear factor 4α (HNF-4α) and forkhead box O1a (FoxO1a), that are coactivated by peroxisomal proliferator activated receptor-γ coactivator 1α (PGC-1α) [20]. Liver-derived SeP has been suggested to be a negative acute phase reactant due to decreased plasma SeP levels in sepsis [21].

Information on regulation and function of selenoprotein P in extrahepatic tissues is scarce. Evidence for an intracellular SeP pool has been provided in human astrocytes: Specific SeP down-regulation by use of small interfering RNA (siRNA) impaired the viability of the cells and made them more susceptible to hydroperoxide-induced oxidative stress, pointing to a contribution of SeP to ROS clearance [22]. Regarding the intestine, SeP is of particular interest as it likely has a protective role against colon carcinogenesis and due to its abundant mRNA expression in comparison to other selenoproteins [13-15,23]. The factors regulating

SeP biosynthesis in the intestine remain to be clarified. In this study, we analysed the intestinal biosynthesis of selenoprotein P using differentiating Caco-2 cells as *in vitro* model for the human intestinal epithelium. In order to determine whether the observed down-regulation of SeP biosynthesis upon exposure of differentiated Caco-2 cells to proinflammatory cytokines may reflect the situation *in vivo* in the inflamed mucosa, SeP mRNA levels were examined in intestinal biopsies from dextran sodium sulphate (DSS)-treated mice.

Materials and Methods

Antibodies and reagents

The polyclonal antibody against human SeP was produced in rabbits as described.[25] The FoxO1 antibody was from Cell Signaling (Beverly, MA). Antibodies against E-Cadherin, PGC-1α and HNF-4α were from Santa Cruz Biotechnology (Santa Cruz, CA). The monoclonal antibodies against α-tubulin and α_1-antitrypsin were from Sigma (St. Louis, MO) and Abcam (Cambridge, UK), respectively. The secondary HRP-coupled anti-rabbit IgG antibody was obtained from Dianova (Hamburg, Germany). Recombinant human cytokines interleukin-1β (IL-1β), interferon-γ (IFN-γ) and tumor necrosis factor-α (TNF-α) were from Invitrogen (Karlsruhe, Germany). The NOS inhibitors L-N^5-(1-Iminoethyl)-ornithine dihydrochloride (L-NIO) and N^G-Monomethyl-L-arginine monoacetate (L-NMMA) were purchased from Tocris Bioscience (Ellisville, MO) and Alexis Biochemicals (San Diego, CA), respectively. Reagents for SDS-PAGE were from Roth (Karlsruhe, Germany). PCR primers were synthesized by Invitrogen.

Cell culture

Caco-2 human intestinal epithelial cells (ECACC number: 86010202) were kindly provided by Dr. R. Schins (IUF, Düsseldorf). Caco-2 cells were regularly tested for *mycoplasma*

contamination, and used for experiments between passages 13 and 30. Cells were cultivated at 37°C in a humidified 5% CO_2 atmosphere in EMEM supplemented with 20% foetal calf serum (PAA; Pashing, Austria), non-essential amino acids, 100 U/ml penicillin, 100 µg/ml streptomycin (PAA) and 2mM glutamax (Invitrogen). For differentiation studies, cells were seeded at a density of 32,000/cm² and grown until day 7 with respect to the day initially reaching confluency (day 0). Culture medium was changed every 2-3 days. Prior to time-course analysis of protein and mRNA levels as well as for experimental treatments, cells were cultivated for additional 24h in serum-free medium supplemented with 200nM sodium selenite to avoid interference with serum components and to provide sufficient selenium for selenoprotein biosynthesis. HepG2 and Huh-7 human hepatoma cells were cultured as described [20].

Isolation of RNA and Real-Time RT-PCR analysis

Total RNA was extracted from Caco-2 cells as well as from snap frozen mouse colon specimen using the RNeasy mini kit (Qiagen, Hilden, Germany) and subjected to RT-PCR analysis in a Lightcycler 2.0 qPCR system (Roche) as described [20]. Real-time RT-PCR was performed with 40ng cDNA in glass capillaries containing LightCycler FastStart DNA Master SYBR Green I Reaction Mix (Roche), 2mM $MgCl_2$ and 1µM of primers. Human hypoxanthine phosphoribosyltransferase 1 (HPRT1) or mouse β-actin were used as internal normalisation controls. Primers were designed using the Universal ProbeLibrary Assay Design Center (Roche) and are listed in Table 1. Specificity of all primer pairs was confirmed by melting curve analysis and agarose gel electrophoresis of PCR products.

Dual luciferase reporter gene assay

SeP-luc, containing a 1,800-bp fragment of the human SeP promoter in the firefly luciferase reporter gene plasmid pGL3basic (Promega; Madison, WI) [24], was a kind gift from Dr. J.

Abel (IUF, Düsseldorf). SeP-mutant-luc, containing an inactivated HNF-4α binding element within the SeP promoter, was generated from the wild-type construct SeP-luc and is equivalent to the SeP-Mut3-luc construct described elsewhere [20]. For reporter gene assays, Caco-2 cells grown in 6-well plates were co-transfected at days -1 or 6 with 2.5µg reporter gene construct (SeP-luc or SeP-mutant-luc) and 0.5µg renilla luciferase expression plasmid pRL-SV40 with 9µl FuGene HD transfection reagent (Roche) in serum-free medium. 24h after transfection, luciferase activities were measured in cell lysates in a Victor 1420 multi-label counter (Wallac; Freiburg, Germany) using the Dual Luciferase Reporter Assay (Promega). To assess cytokine-dependent regulation of SeP promoter activity, Caco-2 cells were transfected on day 5 analogously. 20h later, the medium was replaced by serum-free medium with or without cytomix composed of IL-1β (1,000 U/ml), IFN-γ (100 U/ml) and TNF-α (1,000 U/ml), and luciferase activities were measured after 24h of incubation.

Western Blot analysis

Detection of SeP and α_1-antitrypsin in culture supernatants was done as described [25]. Detection of proteins in cell lysates was done by immunoblotting with specific antibodies using standard techniques.

Enrichment and deglycosylation of secreted SeP

HepG2 and Huh-7 hepatoma cells at 80-90% confluency and differentiated Caco-2 cells (day 5) were serum-starved for 6h and then cultured in serum-free medium supplemented with 200nM sodium selenite for 24h. Cell supernatants containing secreted SeP were collected and concentrated 40-fold by ultrafiltration using Vivaspin 15R concentrator columns (Sartorius; Göttingen, Germany) as described [22,25]. Concentrated supernatants were treated with recombinant N-glycosidase F (Roche) for 16h at 37°C, according to the manufacturer's instructions.

Electrophoretic mobility shift assay (EMSA)

Nuclear fractions were extracted from proliferating (day -1) and differentiated (day 6) Caco-2 cells using NE-PER nuclear and cytoplasmic extraction reagent (Pierce Biotechnology; Rockford, IL). 5µg of nuclear proteins were used in gel shift assays with a biotinylated DNA duplex probe comprising the HNF-4α binding site in the human SeP promoter as described previously [20].

Induction of chronic experimental colitis in mice

C57BL/6 mice were purchased from Harlan-Winkelmann (Borchen, Germany) and bred at the animal facility of the IUF Düsseldorf under specific pathogen-free conditions. The mice were kept according to German guidelines for animal care, and were fed standard mouse chow (Ssniff; Soest, Germany) containing 0.3 mg selenium/kg. Female mice, deriving from the same litter, were recruited for experiments at the age of 9 weeks. For induction of chronic colitis, mice received three cycles of dextran sodium sulphate (DSS with a molecular weight of 36-50kDa; MP Biomedicals, LLC; Solon, OH) treatment. Each cycle consisted of 2% DSS in drinking water for 7 days, which was offered *ad libitum*, followed by a 14-day interval with normal drinking water. The control mice received acidified tap water *ad libitum* over the entire period. After the third cycle of DSS treatment (day 63), mice were sacrificed by asphyxiation in carbon dioxide according to German guidelines. The animal experiments were approved by the state government of Northrhine-Westphalia. For assessment of inflammation, colon length as well as cell numbers in the mesenteric lymph nodes were calculated. The clinical score, which combines weight loss, stool consistency and occurrence of blood in stool, was assessed as described previously [26]. The systemic selenium status of the animals was determined by measuring their serum selenium levels with a fluorimetric assay as described [16,22]. Selenium concentrations were calculated according to a standard curve of

serial dilutions of sodium selenite in water (2 ng/ml to 800 ng/ml), which were treated in parallel with the serum samples.

Statistics

Values are given as means ± standard deviation (SD) of three or more independent experiments. Differences between groups were tested for significance by Student's t-test.

Results

Induction of selenoprotein P biosynthesis in differentiating Caco-2 cells

Caco-2 cells undergo differentiation upon contact inhibition, thereby acquiring characteristics of normal enterocytes and colonocytes shortly after reaching confluency [27]. Differentiation is accompanied by phenotypic changes and an extensive genetic reprogramming, resembling the processes in intestinal epithelial cells migrating along the crypt axis *in vivo* [28]. We cultured Caco-2 cells over a period of 9 days, covering stages from subconfluent (proliferating) to postconfluent and differentiated cells. SeP mRNA levels increased continuously in the course of differentiation, being 8-fold (P = .0018) higher in differentiated (day 7) than in proliferating Caco-2 cells (day -1). The mRNA levels of the housekeeping gene HPRT1 remained unaffected, and HPRT1 was therefore used to normalise relative SeP mRNA expression in RT-PCR analysis (Figure 1A). Likewise, we determined the capability of Caco-2 cells to secrete SeP by immunoblotting of Caco-2 supernatants taken at different stages of differentiation. Whereas no SeP protein was detectable in supernatants of subconfluent and confluent cells (days -1 and 0), SeP was released from differentiated Caco-2 cells at days 5 and 7 post confluency (Figure 1B).

The differentiation of Caco-2 cells was monitored by analysing α_1-antitrypsin secretion and E-cadherin maturation, representing markers of differentiated enterocytes [27,29]. Secretion of α_1-antitrypsin was detectable beginning at day 0 and maximised at day 5 post confluency.

Expression and maturation of the cell adhesion protein E-cadherin increased from day -1 to day 7 (Figure 1C).

Next, we analysed the pattern of SeP isoforms secreted by differentiated Caco-2 cells. Liver-derived HepG2 and Huh-7 hepatoma cell lines were used for comparison as both secrete SeP as two isoforms that are found in human plasma as well [25,30]. SeP in supernatants of differentiated Caco-2 cells migrated in SDS polyacrylamide gels as two bands with molecular masses between 50 and 70 kDa, resembling SeP released from hepatoma cells. As liver-derived SeP is heavily N-glycosylated during intracellular processing [25], we examined whether SeP glycosylation also occurs in Caco-2 cells. Treatment of Caco-2 supernatants with N-glycosidase F resulted in a shift of both SeP isoforms towards lower molecular masses, displaying the same sizes as deglycosylated SeP from hepatoma cells (Figure 1D). The two isoforms correspond to full-length and truncated SeP, respectively [30]. In Caco-2 supernatants, the truncated SeP isoform was much more abundant than the full length isoform, in contrast to an evenly distribution of the SeP isoforms secreted by liver-derived cells.

Factors controlling the induction of selenoprotein P biosynthesis during Caco-2 cell differentiation

We hypothesised a stimulation of the SeP promoter in the course of Caco-2 differentiation regarding the sustained elevation of SeP mRNA levels. Therefore, we tested whether the stage of differentiation affects SeP promoter activity by applying a luciferase reporter gene construct harbouring a 1,800-bp fragment of the human SeP promoter, termed SeP-luc [24]. The SeP-luc construct was active in Caco-2 cells: SeP promoter activity was three-fold higher ($P < .001$) in differentiated (day 6) than in proliferating cells (day -1) (Figure 2A), pointing to transcriptional induction of SeP in Caco-2 cells during differentiation.

Recently, we identified *cis*- and *trans*-regulatory factors contributing to transcriptional regulation of SeP. In particular, a functional binding site for the transcription factor HNF-4α

is located within the SeP promoter and plays a role in cell type-specific expression of SeP [20]. Besides the liver, HNF-4α is abundantly expressed in the intestine, where it regulates intestinal epithelial cell functions [31,32]. In proliferating and differentiated Caco-2 cells transfected with a reporter gene construct containing a mutated (inactivated) HNF-4α binding site (SeP-mutant-luc) [20], the activity of the SeP promoter was strongly impaired to 5.3 % ($P < .001$) and 3.8 % ($P < .001$) of the activity of the wild-type promoter construct SeP-luc (Figure 2A). Given the vital importance of HNF-4α for SeP transcription, we analysed the expression of HNF-4α in Caco-2 cells: HNF-4α mRNA levels increased constantly from proliferating to differentiated Caco-2 cells, being ten-fold higher at day 7 compared to day -1 ($P < .05$) (Figure 2B). Moreover, an immunoreactive band corresponding to HNF-4α (54 kDa) was detected in cell lysates of confluent Caco-2 cells, and increased during differentiation (Figure 2C). To study the role of HNF-4α in the induction of SeP during Caco-2 differentiation more directly, nucleic extracts from proliferating and differentiated cells were subjected to gel shift analysis with a DNA duplex probe comprising the HNF-4α binding site of the human SeP promoter. Complex formation of HNF-4α with the DNA probe was much more pronounced in binding reactions with extracts from Caco-2 cells taken at day 7 than at day -1. Specific binding towards the HNF-4α binding site was confirmed by competition with excess non-labelled DNA probe and by supershift formation with an antibody directed against HNF-4α (Figure 2D).

In addition to HNF-4α, control of hepatic SeP transcription occurs through the transcription factor FoxO1a and the transcriptional coactivator PGC-1α [20]. Consequently, mRNA and protein expression of these two factors were analysed and found to be elevated in differentiated Caco-2 cells, even though to a lesser extent than HNF-4α. FoxO1a mRNA expression increased during differentiation, being four-fold ($P < .05$) and three-fold ($P < .05$) higher at days 5 and 7 in comparison to proliferating cells (day -1). FoxO1a protein was only detectable in lysates from differentiated Caco-2 cells. PGC-1α mRNA levels were slightly

(two-fold) elevated in differentiated cells in comparison to subconfluent cells. Likewise, a faint immunoreactive band of PGC-1α was detected in cell lysates of confluent and differentiated Caco-2 cells (Figures 2B, 2C).

The serum-free culture medium of the Caco-2 cells was usually supplemented with 200nM sodium selenite. Thus, we also performed a control experiment in order to ensure that the concomitant increases in gene expression of selenoprotein P and its transcriptional regulators indeed resulted from the differentiation process and did not reflect merely a response to enhanced selenium availability. Proliferating and differentiated Caco-2 cells were cultured for 24h with or without selenium supplementation. In proliferating (day -1) and differentiated (day 6) Caco-2 cells, selenite did not affect mRNA levels of HNF-4α and FoxO1a, whereas SeP and PGC-1α were slightly increased in selenium-supplemented cells. However, selenite produced only marginal effects compared to the pronounced up-regulation of selenoprotein P and its transcriptional regulators in the course of Caco-2 differentiation (day -1 vs. day 6), which occurred independently of the selenium status in selenium-deficient as well as in selenium-supplemented cells (Figures 3A, 3B). Moreover, protein expression of HNF-4α, FoxO1a and PGC-1α was not affected by selenite, but strongly elevated in differentiated cells (Figure 3C).

Down-regulation of SeP biosynthesis in Caco-2 cells by proinflammatory cytokines

Lowered selenium concentrations have been measured in the colon of rats subjected to experimental colitis [33]. As proinflammatory cytokines are major effectors in the pathogenesis of experimental colitis and inflammatory bowel disease [7], we analysed expression and secretion of SeP in differentiated Caco-2 cells exposed to interleukin-1β (IL-1β), interferon-γ (IFN-γ) and tumor necrosis factor-α (TNF-α). The individual cytokines had only minor effects on SeP mRNA levels, whereas a combination of all three cytokines (cytomix) caused a 50% inhibition of SeP mRNA expression compared to controls ($P < .001$)

(Figure 4A). Promoter activity and most notably secretion of SeP were suppressed even to a greater extent by the proinflammatory cytokines: Upon cytomix treatment for 24h, secretion of the full-length isoform of SeP was completely abrogated, and secretion of the truncated isoform of SeP was diminished to 21% of control values (Figures 4B, 4C). The cytomix-treated cells retained more than 95% viability compared to controls, as determined by MTT assay (data not shown). Thus, diminished SeP biosynthesis did not result from induction of cytotoxicity by the applied proinflammatory cytokines.

As SeP secretion appeared to be much stronger suppressed than its transcription by the proinflammatory cytokines, we investigated their influence on additional factors required for biosynthesis of selenoproteins: Selenophosphate synthetase-2 (SPS-2), selenocysteine synthetase (SecS) and phosphoseryl-tRNA[Ser]Sec kinase (Pstk) have been described to be down-regulated in the liver during an acute phase response [21], and the selenocysteine insertion sequence (SECIS)-binding protein-2 (SBP-2) has been found to be a major determinant for efficient translation of selenoprotein mRNAs [34]. The mRNA expression of all four factors was down-regulated in the cytomix-treated Caco-2 cells. The most pronounced effect was observed on SecS, which was inhibited by the cytokine combination to 45% of control values ($P < .01$) (Figure 4D).

The inducible nitric oxide synthase (NOS-2) is a well-characterised target gene and effector of proinflammatory cytokines [6]. Accordingly, we observed up-regulated NOS-2 mRNA expression in Caco-2 cells incubated for 24h with IL-1β, IFN-γ and TNF-α. When employed individually, TNF-α and IFN-γ moderately stimulated NOS-2 expression. Combined treatment with cytomix resulted in eight-fold ($P = .14$) induction of NOS-2 mRNA levels in comparison to controls, and the protein expression of NOS-2 was similarly increased by the cytokines (Figure 5A). Induction of NOS-2 thus correlated with inhibition of SeP biosynthesis. We used inhibitors of the enzymatic function of nitric oxide synthases to directly address the involvement of NOS-2 in cytokine-induced SeP down-regulation:

Incubation of Caco-2 cells with the L-arginine analogues L-NMMA or L-NIO alone did not affect basal SeP mRNA expression, but pre-incubation with the inhibitors partly reversed the cytomix-induced inhibition of SeP mRNA expression ($P < .05$). The effect of NOS-2 inhibition extended to SeP secretion: pre-incubation of differentiated Caco-2 cells with L-NIO almost completely reversed the cytokine-induced inhibition of SeP secretion (Figure 5B).

Selenoprotein P mRNA levels are lowered in the inflamed intestinal mucosa in vivo

Finally, we employed an animal model of experimental chronic colitis to test whether inflammation-induced inhibition of intestinal SeP expression also occurs *in vivo*. Three cycles of intermitting administration of dextran sodium sulphate (DSS) to mice resulted in intervals of worsening colitis, followed by recovery to near control values. The DSS-treated mice lost weight to about 85% of the control animals during the first cycle, but weight loss was less severe (to about 90% of controls) during the second and third cycle of DSS administration. At day 63, colitis was evident in DSS-treated mice by clinical scoring ($P < .001$), shortening in colon length ($P < .01$) and a higher cell count in mesenteric lymph nodes in comparison to control-treated mice ($P < .01$) (Figure 6A). DSS administration did not impair the systemic selenium status of the animals, as revealed by serum selenium levels of 238±25 ng/ml in the DSS-treated group compared to 236±16 ng/ml in the control group. However, chronic colitis was associated with a concomitant decrease in intestinal selenoprotein P and increase in NOS-2 mRNA levels: SeP mRNA was down-regulated in the colon of DSS-treated mice to 9.4% of the values measured in the colon of untreated animals ($P = .01$), which was accompanied by a 63% increase in NOS-2 mRNA ($P = .67$) (Figure 6B). The difference between the control and the DSS-treated group was statistically significant in regard to SeP mRNA levels, but failed to reach statistical significance in the case of NOS-2 due to low basal mRNA levels of NOS-2 and its high variation in both groups.

Discussion

Selenoprotein P biosynthesis is induced during in vitro enterocytic differentiation

Caco-2 intestinal epithelial cells differentiate in culture upon contact inhibition, undergoing phenotypic and genotypic changes of enterocytes migrating along the crypt axis [27,28]. The gene expression of Caco-2 cells changes in the course of differentiation from a tumorous-like pattern towards the profile of normal colon tissue [35]. We here show that Caco-2 cells acquire the capability to secrete selenoprotein P as a result of marked up-regulation in SeP transcription during their differentiation. The up-regulation of intestinal SeP biosynthesis is explained by applying our recently established model for the transcriptional control of SeP involving the tissue-specific transcription factor HNF-4α together with FoxO1a and the coactivator PGC-1α [20].

Selenoprotein P mRNA is expressed ubiquitously, but by far the highest levels were found in liver, kidney and intestine [14], in close correlation with the tissue distribution of HNF-4α [31]. The critical role of HNF-4α for high-level expression of SeP has been demonstrated for liver cells before [20], and is now extended to intestinal epithelial cells. High-level SeP expression in differentiated Caco-2 cells is consistent with a concomitant rise in HNF-4α levels during differentiation, shown before by northern blotting [36] and verified here in a detailed time course analysis using qPCR and immunoblotting. Dysregulation of HNF-4α has been demonstrated in colitis [32], and might contribute to lowered SeP mRNA levels in the inflamed intestinal mucosa of DSS-treated mice, as observed in this study. On the other hand, low-level expression of SeP in proliferating Caco-2 cells is consistent with down-regulation of SeP expression during progression of colorectal cancers [13].

In addition to HNF-4α, the expression of SeP transactivators FoxO1a and PGC-1α increased in the course of Caco-2 differentiation. In the brain and in vascular endothelial cells, PGC-1α regulates the expression of ROS-detoxifying enzymes such as catalase and superoxide

dismutases (SOD1/2) by co-activation of FoxO3, a FoxO1a-homologous transcription factor [37,38]. Enzymatic activities of SOD2 and catalase were found to be decreased in undifferentiated Caco-2 cells compared to primary human colonic epithelial cells [39], and catalase expression increases in the course of Caco-2 differentiation. We thus conclude that PGC-1α cooperates with FoxO transcription factors to enhance the transcription of oxidative stress-related genes (SOD2, catalase and selenoprotein P) in the course of enterocyte cell differentiation, thereby contributing to protection of the intestinal barrier. In this context, FoxO3- and FoxO4-*knock out* mice are more susceptible to tissue injury and inflammation in experimental colitis, and the expression of FoxO4 is decreased in IBD patients [40,41].

Selenoprotein P is predominantly known as extracellular plasma protein [9,42], although an intracellular SeP pool has been identified in astrocytes [22]. SeP secretion has been studied comprehensively *in vitro* using hepatocytes and liver-derived cell lines. This is the first study to demonstrate SeP secretion by intestinal cells. The relevance of this finding derives from the suggested secondary function of SeP as extracellular antioxidant in addition to its main role as selenium transporter [9,16-19,42]. Indirect evidence for a protective role of SeP in the gut is provided by epidemiological association of advanced adenoma risk with genetic polymorphisms in the SeP gene [23]. Interestingly, glutathione peroxidase 3 (GPx-3) has been found to be produced and secreted by mature epithelial cells of the large intestine as well [43]. The extracellular ROS-detoxifying selenoenzymes GPx-3 and selenoprotein P may constitute a first line of defense, protecting the villus epithelial cells of the intestine from damage induced by ingested oxidative compounds. Recently, it has been speculated that extrahepatic tissues may secrete mostly shorter isoforms of selenoprotein P for local use as redox enzyme or signalling molecule, whereas the liver-derived full-length SeP is destined for selenium supply of peripheral organs [42]. Given that we found a predominant secretion of truncated SeP by differentiated Caco-2 cells, it might be worthwhile to verify this hypothesis using the example of intestinal selenoprotein P.

Selenoprotein P is a negative acute phase reactant in the intestine

We observed a down-regulation of intestinal SeP biosynthesis by IL-1β, IFN-γ and TNF-α in differentiated Caco-2 cells *in vitro* and in experimental colitis *in vivo*. The proinflammatory cytokines used in the present study have been reported to decrease SeP promoter activity in liver-derived HepG2 cells as well [44], suggesting diminished SeP secretion by the liver during systemic inflammation. Indeed, levels of plasma selenium and SeP declined after injection of lipopolysaccharide (LPS) in mice, and mRNA levels of several enzymes with essential functions in selenoprotein biosynthesis were decreased in the liver of LPS-treated mice. In this animal model, hepatic mRNA levels of SeP were only slightly affected, and the authors concluded that the lowered plasma levels of SeP resulted from insufficient translation of SeP mRNA [21]. Apart from inhibition of hepatic SeP biosynthesis, enhanced binding of SeP to endothelial membranes has been discussed to contribute as well to the lowered SeP plasma concentrations during an acute phase response [42]. We here focus on the intestine and reinforce the notion of SeP being a negative acute phase reactant. In consensus with previous studies in hepatocytes [21,44], SeP biosynthesis was down-regulated during intestinal inflammation both at the transcriptional and the post-transcriptional level. However, the inhibition of SeP transcription appeared to be stronger and longer-lasting in intestinal cells than in hepatocytes.

As NOS-2 is considered to be a key player in the progression of IBD and target for pharmacological intervention (e.g. glucocorticoid treatment), we hypothesised its involvement in inhibition of intestinal SeP transcription during inflammation. Expression and activity of NOS-2 are increased in the inflamed mucosa of IBD patients [3], and this was also observed in the intestine of DSS-treated mice. Proinflammatory cytokines induced in differentiated Caco-2 cells an up-regulation of NOS-2 as well, concomitantly with inhibition of SeP biosynthesis. The regulation of NOS-2 expression was in consent with previous reports, using

the same combination of cytokines at similar doses [6]. A partial contribution of NOS-2 to cytokine-induced inhibition of SeP biosynthesis in Caco-2 cells was proven by the use of NOS inhibitors. *In vivo*, the induction of NOS-2 during endotoxemia has been shown to be much more pronounced in the intestine than in the liver of lipopolysaccharide (LPS)-injected mice [45], which might explain the modest impact of LPS-treatment on hepatic SeP mRNA levels reported by Renko *et al*. [21]. Moreover, basal and cytokine-stimulated NOS-2 levels were lower in liver-derived HepG2 cells than in intestinal Caco-2 cells (unpublished observations). Apart from the intestine, our finding of a NOS-2-mediated inhibition of SeP biosynthesis might also be applicable to other tissues. In particular, an inverse correlation between NOS-2 and SeP expression has been ascertained for the prostate, which is susceptible to malignant transformation as well: NOS-2 is selectively expressed in epithelia of prostate carcinoma tissue [46], whereas SeP mRNA levels are diminished in human prostate tumor samples and in a mouse model of prostate cancer progression [47]. A better understanding of functions and regulation of selenoprotein P in extrahepatic tissues may contribute to highlight the role of SeP in inflammatory diseases and in tumour development. Regarding the intestine, decreased biosynthesis of locally produced selenoprotein P at sites of inflammation may diminish the antioxidative capacity of the intestinal mucosa and thus add to inflammation-driven carcinogenesis in the colon.

Acknowledgments

This study was supported by Deutsche Forschungsgemeinschaft (DFG), Bonn, Germany (STE 1782/2-1, SFB 575/B4 and GRK1427/P9). B. Speckmann received a scholarship of the Ernst Jung-Stiftung für Wissenschaft und Forschung, Hamburg, Germany. H. Sies is a fellow of the National Foundation for Cancer Research (NFCR), Bethesda, MD.

The authors thank K. Gerloff for helpful discussions and A. Borchardt for technical assistance.

List of Abbreviations:

DSS, dextran sodium sulphate; FoxO1a, forkhead box O1 a; HNF-4α, hepatocyte nuclear factor-4 alpha; HPRT1, hypoxanthine phosphoribosyltransferase 1; IBD, inflammatory bowel disease; IFN-γ, interferon gamma; IL-1β, interleukin 1 beta; NOS-2, nitric oxide synthase 2; PGC-1α, peroxisomal proliferator-activated receptor gamma coactivator 1 alpha; Pstk, phosphoseryl-tRNA[Ser]Sec kinase; ROS, reactive oxygen species; SBP-2, selenocysteine insertion sequence-binding protein 2; SecS, selenocysteine synthetase; SeP, selenoprotein P; SOD, superoxide dismutase; SPS-2, Selenophosphate synthetase 2; TNF-α, tumor necrosis factor alpha; UC, ulcerative colitis

References

1. Grisham, M. B. Oxidants and free radicals in inflammatory bowel disease. *Lancet* **24**:859-861; 1994.
2. Kruidenier, L.; Kuiper, I.; Lamers, C. B.; Verspaget, H. W. Intestinal oxidative damage in inflammatory bowel disease: Semi-quantification, localization and association with mucosal antioxidants. *J. Pathol*. **201**:28-36; 2003.
3. Rachmilewitz, D.; Stamler, J. S.; Bachwich, D.; Karmeli, F.; Ackerman, Z.; Podolsky, D. K. Enhanced colonic nitric oxide generation and nitric oxide synthase activity in ulcerative colitis and Crohn's disease. *Gut* **36**:718-723; 1995.
4. Singer, I. I.; Kawka, D. W.; Scott, S.; Weidner, J. R.; Mumford, R. A.; Riehl, T. E.; Stenson, W. F. Expression of inducible nitric oxide synthase and nitrotyrosine in colonic epithelium in inflammatory bowel disease. *Gastroenterology* **111**:871-885; 1996.
5. Tepperman, B. L.; Brown, J. F.; Whittle, B. J .R. Nitric oxide synthase induction and intestinal epithelial cell viability in rats. *Am. J. Physiol.* **265**:214-218; 1993.

6. Cavicchi, M.; Whittle, B. J. R. Regulation of induction of nitric oxide synthase and the inhibitory actions of dexamethasone in the human intestinal epithelial cell line, Caco-2: influence of cell differentiation. *Br. J. Pharmacol.* **128**:705-715; 1999.
7. Papadakis, K. A.; Targan, S. R. Role of cytokines in the pathogenesis of inflammatory bowel disease. *Annu. Rev. Med.* **51**:289-298; 2000.
8. D'Incà, R.; Cardin, R.; Benazzato, L.; Angriman, I.; Martines, D.; Sturniolo, G. C. Oxidative DNA damage in the mucosa of ulcerative colitis increases with disease duration and dysplasia. *Inflamm. Bowel Dis.* **10**:23-27; 2004.
9. Steinbrenner, H.; Sies, H. Protection against reactive oxygen species by selenoproteins. *Biochim. Biophys. Acta* **1790**:1478-1485; 2009.
10. Rayman, M. P. Food-chain selenium and human health: emphasis on intake. *Brit. J. Nutr.* **100**:254-268; 2008.
11. Tirosh, O.; Levy, E.; Reifen, R. High selenium diet protects against TNBS-induced acute inflammation, mitochondrial dysfunction, and secondary necrosis in rat colon. *Nutrition* **23**:878-886; 2007.
12. Clark, L. C.; Combs, G. F. Jr; Turnbull, B. W.; Slate, E. H.; Chalker, D. K.; Chow, J.; Davis, L. S.; Glover, R. A.; Graham, G. F.; Gross, E. G.; Krongrad, A.; Lesher, J. L. Jr; Park, H. K.; Sanders, B. B. Jr; Smith, C. L.; Taylor, J. R. Effects of selenium supplementation for cancer prevention in patients with carcinoma of the skin. A randomized controlled trial. Nutritional Prevention of Cancer Study Group. *JAMA.* **276**:1957-1963; 1996.
13. Murawaki, Y.; Tsuchiya, H.; Kanbe, T.; Harada, K.; Yashima, K.; Nozaka, K.; Tanida, O.; Kohno, M.; Mukoyama, T.; Nishimuki, E.; Kojo, H.; Matsura, T.; Takahashi, K.; Osaki, M.; Ito, H.; Yodoi, J.; Murawaki, Y.; Shiota, G. Aberrant expression of selenoproteins in the progression of colorectal cancer. *Cancer Letters* **259**:218-230; 2008.

14. Hoffmann, P. R.; Höge, S. C.; Li, P. A.; Hoffmann, F. W.; Hashimoto, A. C.; Berry, M. J. The selenoproteome exhibits widely varying, tissue-specific dependence on selenoprotein P for selenium supply. *Nucleic Acids Res.* **35**:3963-3973; 2007.

15. Al-Taie, O.H.; Uceyler, N.; Eubner, U.; Jakob, F.; Mörk, H.; Scheurlen, M.; Brigelius-Flohe, R.; Schöttker, K.; Abel, J.; Thalheimer, A.; Katzenberger, T.; Illert, B.; Melcher, R.; Köhrle, J. Expression profiling and genetic alterations of the selenoproteins GI-GPx and SePP in colorectal carcinogenesis. *Nutr. Cancer* **48**:6-14; 2004.

16. Schomburg, L.; Schweizer, U.; Holtmann, B.; Flohé, L.; Sendtner, M.; Köhrle, J. Gene disruption discloses role of selenoprotein P in selenium delivery to target tissues. *Biochem. J.* **370**:397-402; 2003.

17. Arteel, G. E.; Mostert, V.; Oubrahim, H.; Briviba, K.; Abel, J.; Sies, H. Protection by selenoprotein P in human plasma against peroxynitrite-mediated oxidation and nitration. *Biol. Chem.* **379**:1201-1205; 1998.

18. Saito, Y.; Hayashi, T.; Tanaka, A.; Watanabe, Y.; Suzuki, M.; Saito, E.; Takahashi, K. Selenoprotein P in human plasma as an extracellular phospholipid hydroperoxide glutathione peroxidase. *J. Biol. Chem.* **274**:2866-2871; 1999.

19. Bosschaerts, T.; Guilliams, M.; Noel, W.; Hérin, M.; Burk, R. F.; Hill, K. E.; Brys, L.; Raes, G.; Ghassabeh, G. H.; De Baetselier, P.; Beschin, A. Alternatively activated myeloid cells limit pathogenicity associated with african trypanosomiasis through the IL-10 inducible gene selenoprotein P. *J. Immunol.* **180**:6168-6175; 2008.

20. Speckmann, B.; Walter, P. L.; Alili, L.; Reinehr, R.; Sies, H.; Klotz, L. O.; Steinbrenner, H. Selenoprotein P expression is controlled through interaction of the coactivator PGC-1α with FoxO1a and hepatocyte nuclear factor 4α transcription factors. *Hepatology* **48**:1998-2006; 2008.

21. Renko, K.; Hofmann, P. J.; Stoedter, M.; Hollenbach, B.; Behrends, T.; Köhrle, J.; Schweizer, U.; Schomburg, L. Down-regulation of the hepatic selenoprotein biosynthesis machinery impairs selenium metabolism during the acute phase response in mice. *FASEB J.* **23**:1758-1765; 2009.

22. Steinbrenner, H.; Alili, L.; Bilgic, E.; Sies, H.; Brenneisen, P. Involvement of selenoprotein P in protection of human astrocytes from oxidative damage. *Free Rad. Biol. Med.* **40**:1513-1523; 2006.

23. Peters, U.; Chatterjee, N.; Hayes, R. B.; Schoen, R. E.; Wang, Y.; Chanock, S. J.; Foster, C.B. Variation in the Selenoenzyme Genes and Risk of Advanced Distal Colorectal Adenoma. *Cancer Epidemiol. Biomarkers Prev.* **17**:1144-1154; 2008.

24. Mostert, V.; Wolff, S.; Dreher, I.; Köhrle, J.; Abel, J. Identification of an element within the promoter of human selenoprotein P responsive to transforming growth factor-beta. *Eur. J. Biochem*. **268**:6176-6181; 2001.

25. Steinbrenner, H.; Alili, L.; Stuhlmann, D.; Sies, H.; Brenneisen, P. Post-translational processing of selenoprotein P: implications of glycosylation for its utilisation by target cells. *Biol. Chem.* **388**:1043-1051; 2007.

26. Rachmilewitz, D.; Karmeli, F.; Takabayashi, K.; Hayashi, T.; Leider-Trejo, L.; Lee, J.; Leoni, L. M.; Raz, E. Immunostimulatory DNA ameliorates experimental and spontaneous murine colitis. *Gastroenterology* **122**:1428-1441; 2002.

27. Engle, M. J.; Goetz, G. S.; Alpers, D. H. Caco-2 cells express a combination of colonocyte and enterocyte phenotypes. *J. Cell. Physiol.* **174**:362-369; 1998.

28. Mariadason, J. M.; Arango, D.; Corner, G. A.; Arañes, M. J.; Hotchkiss, K. A.; Yang, W.; Augenlicht, L. H. A gene expression profile that defines colon cell maturation in vitro. *Cancer Res.* **62**:4791-4804; 2002.

29. Escaffit, F.; Perreault, N.; Jean, D.; Francoeur, C.; Herring, E.; Rancourt, C.; Rivard, N.; Vachon, P. H.; Paré, F.; Boucher, M. P.; Auclair, J.; Beaulieu, J. F. Repressed E-

cadherin expression in the lower crypt of human small intestine: a cell marker of functional relevance. *Exp. Cell. Res.* **302**:206-220; 2005.

30. Mostert, V.; Lombeck, I.; Abel, J. A novel method for the purification of selenoprotein P from human plasma. *Arch. Biochem. Biophys.* **357**:326-330; 1998.
31. Drewes, T.; Senkel, S.; Holewa, B.; Ryffel, G. U. Human hepatocyte nuclear factor 4 isoforms are encoded by distinct and differentially expressed genes. *Mol. Cell. Biol.* **16**:925-931; 1996.
32. Ahn, S. H.; Shah, Y. M.; Inoue, J.; Morimura, K.; Kim, I.; Yim, S.; Lambert, G.; Kurotani, R.; Nagashima, K.; Gonzalez, F. J.; Inoue, Y. Hepatocyte nuclear factor 4alpha in the intestinal epithelial cells protects against inflammatory bowel disease. *Inflamm. Bowel Dis.* **14**:908-920; 2008.
33. Al-Awadi, F. M.; Khan, I.; Dashti, H. M.; Srikumar, T. S. Colitis-induced changes in the level of trace elements in rat colon and other tissues. *Ann. Nutr. Metab.* **42**:304-310; 1998.
34. Squires, J. E.; Stoytchev, I.; Forry, E. P.; Berry, M. J. SBP2 binding affinity is a major determinant in differential selenoprotein mRNA translation and sensitivity to nonsense-mediated decay. *Mol. Cell. Biol.* **27**:7848-7855; 2007.
35. Sääf, A. M.; Halbleib, J. M.; Chen, X.; Yuen, S. T.; Leung, S. Y.; Nelson, W. J.; Brown, P. O. Parallels between global transcriptional programs of polarizing Caco-2 intestinal epithelial cells in vitro and gene expression programs in normal colon and colon cancer. *Mol. Biol. Cell* **18**:4245-4260; 2007.
36. Hu, C.; Perlmutter, D. H. Regulation of alpha1-antitrypsin gene expression in human intestinal epithelial cell line caco-2 by HNF-1alpha and HNF-4. *Am. J. Physiol.* **276**:G1181-1194; 1999.
37. St-Pierre, J.; Drori, S.; Uldry, M.; Silvaggi, J. M.; Rhee, J.; Jäger, S.; Handschin, C.; Zheng, K.; Lin, J.; Yang, W.; Simon, D. K.; Bachoo, R.; Spiegelman, B. M.

Suppression of reactive oxygen species and neurodegeneration by the PGC-1 transcriptional coactivators. *Cell* **127**:397-408; 2006.

38. Olmos, Y.; Valle, I.; Borniquel, S.; Tierrez, A.; Soria, E.; Lamas, S.; Monsalve, M. Mutual dependence of Foxo3a and PGC-1alpha in the induction of oxidative stress genes. *J. Biol. Chem.* **284**:14476-14484; 2009.
39. Grisham, M. B.; MacDermott, R. P.; Deitch, E. A. Oxidant defense mechanisms in the human colon. *Inflammation* **14**:669-680; 1990.
40. Snoeks, L.; Weber, C. R.; Wasland, K.; Turner, J. R.; Vainder, C.; Qi, W.; Savkovic, S. D. Tumor suppressor FOXO3 participates in the regulation of intestinal inflammation. *Lab. Invest.* **89**:1053-1062; 2009.
41. Zhou, W.; Cao, Q.; Peng, Y.; Zhang, Q. J.; Castrillon, D. H.; DePinho, R. A.; Liu, Z. P. FoxO4 inhibits NF-kappaB and protects mice against colonic injury and inflammation. *Gastroenterology* **137**:1403-1414; 2009.
42. Burk, R.F.; Hill, K.E. Selenoprotein P-expression, functions, and roles in mammals. Biochim. Biophys. Acta. **1790**:1441-1447; 2009.
43. Tham, D.M.; Whitin, J.C.; Kim, K.K.; Zhu, S.X.; Cohen, H.J. Expression of extracellular glutathione peroxidase in human and mouse gastrointestinal tract. *Am. J. Physiol.* **275**:G1463-G1471; 1998.
44. Dreher, I.; Jakobs, T. C.; Köhrle, J. Cloning and characterization of the human selenoprotein P promoter. Response of selenoprotein P expression to cytokines in liver cells. *J. Biol. Chem*. **272**:29364-29371; 1997.
45. Yu, Z.; Xia, X.; Kone, B. C. Expression profile of a human inducible nitric oxide synthase promoter reporter in transgenic mice during endotoxemia. *Am. J. Physiol. Renal Physiol.* **288**:F214-F220; 2005.

46. Klotz, T.; Bloch, W.; Volberg, C.; Engelmann, U.; Addicks, K. Selective expression of inducible nitric oxide synthase in human prostate carcinoma. *Cancer* **82**:1897-1903; 1998.

47. Calvo, A.; Xiao, N.; Kang, J.; Best, C. J.; Leiva, I.; Emmert-Buck, M. R.; Jorcyk, C.; Green, J. E. Alterations in gene expression profiles during prostate cancer progression: functional correlations to tumorigenicity and down-regulation of selenoprotein-P in mouse and human tumors. *Cancer Res.* **62**:5325-5335; 2002.

Figure legends

Figure 1. Selenoprotein P is induced in Caco-2 intestinal epithelial cells in the course of differentiation. Caco-2 cells were cultured for the indicated periods of time with respect to the day reaching confluency (day 0), followed by additional 24h of incubation in serum-free medium supplemented with 200nM sodium selenite. (A) SeP mRNA levels were determined by qPCR with normalisation against HPRT1. Data represent means ± SD of four independent experiments. (B) Secretion of SeP was analysed by immunoblotting of cell supernatants. (C) Caco-2 cell differentiation was monitored by detection of E-cadherin and α_1-antitrypsin in cell lysates or supernatants by immunoblotting. Detection of α-tubulin confirmed equal loading. Each blot is representative for three independent experiments. (D) *In vitro* deglycosylation of Caco-2 cell-secreted SeP isoforms. Caco-2 cells were cultured until day 5 post confluency, whereas HepG2 and Huh-7 hepatoma cells were grown until ~90% confluency. SeP was detected in 40-fold concentrated cell supernatants with or without enzymatic cleavage of N-linked glycans by N-glycosidase F treatment prior to immunoblotting.

Figure 2. HNF-4α, FoxO1a and PGC-1α are stimulated concomitantly with selenoprotein P in the course of Caco-2 cell differentiation. (A) Proliferating (day -1) and differentiated (day 6) Caco-2 cells were co-transfected with the reporter gene constructs SeP-luc (wild-type SeP promoter) or SeP-mutant-luc (SeP promoter mutated in the HNF-4α binding site) and the renilla luciferase control plasmid pRL-SV40. 24h post transfection, relative firefly luciferase activity was determined. Data are given as means ± SD of three independent experiments performed in duplicates. (B) Caco-2 cells were cultured as in Figure 1 and assessed for mRNA levels of HNF-4α, FoxO1a and PGC-1α by qPCR. (C) Protein expression of HNF-4α, FoxO1a and PGC-1α was detected by immunoblotting of lysates prepared from Caco-2 cells cultured for the indicated time periods. (D) Nucleic extracts from Caco-2 cells at day -1 and day 6 were subjected to EMSA with a biotin-labelled DNA probe comprising the HNF-4α

binding element of the human SeP promoter. Specificity of binding was tested with excess (25- to 200-fold) non-labelled competitor DNA probe and by addition of 200ng HNF-4α antibody to the binding reactions.

Figure 3. Induction of selenoprotein P mRNA expression in the course of differentiation does not depend on the selenium status of Caco-2 cells. Proliferating (day -1) and differentiated (day 6) Caco-2 cells were cultivated for 24h in serum-free medium with or without supplementation with 200nM sodium selenite. SeP mRNA levels (A) as well as HNF-4α, FoxO1a and PGC-1α mRNA levels (B) were determined by qPCR with normalisation against HPRT1. Data represent means ± SD of three independent experiments. (C) Protein expression of HNF-4α, FoxO1a and PGC-1α was detected by immunoblotting of cell lysates. Representative blots out of three independent experiments are shown.

Figure 4. Selenoprotein P biosynthesis in Caco-2 cells is inhibited by proinflammatory cytokines. Differentiated Caco-2 cells (day 5) were serum-starved for 6h and then incubated for 24h in serum-free medium supplemented with 200nM sodium selenite and TNF-α (1.000 U/ml), IFN-γ (100 U/ml) or IL-1β (1.000 U/ml) or a combination of the three cytokines (cytomix). (A) Relative SeP mRNA levels were determined by qPCR as in Figure 1. (B) SeP in cell supernatants was analysed by immunoblotting. Data are given as means ± SD of three independent experiments (C) Caco-2 cells (day 5) were transfected with SeP-luc and pRL-SV40 plasmids. 18h after transfection, the medium was replaced by serum-free medium ± cytomix and the cells were cultured for additional 24h before determination of SeP promoter activity by dual luciferase assay as in Figure 2. (D) The mRNA expression of four components of the selenoprotein biosynthesis machinery was determined by qPCR with HPRT1 as normalisation control. Data are expressed as means ± SD of four independent

experiments and represent the mRNA levels of SPS-2, Pstk1, SecS and SBP-2 in the cytomix-treated Caco-2 cells in relation to non-treated controls (100%).

Figure 5. Proinflammatory cytokines inhibit SeP biosynthesis in Caco-2 cells via induction of NOS-2. (A) Differentiated Caco-2 cells (day 5) were treated with cytokines (TNF-α, IFN-γ, IL-1β) alone or in combination (cytomix) as in Figure 4. NOS-2 mRNA levels were determined by qPCR and normalised against HPRT1. NOS-2 and α-tubulin protein (loading control) were detected by immunoblotting in lysates of cytokine- and control-treated cells (B) Before addition of cytokines, cells were pre-treated for 1h with the NOS inhibitors L-NIO (500µM) or L-NMMA (1mM), which were present throughout the incubation period of 24h followed by analysis of SeP secretion and SeP mRNA levels. Data of qPCR analyses are given as means ± SD of three independent experiments, and representative immunoblots out of three independent experiments are shown.

Figure 6. Chronic experimental colitis decreases intestinal selenoprotein P mRNA levels in mice. (A) Mice in the +DSS group (n=6) were fed 2% DSS in drinking water at the given time intervals, whereas mice in the -DSS group (n=4) received acidified tap water. Development of colitis was assessed by clinical scoring over the time course and by analysis of colon length and mesenteric lymph node counting at the end of the experiment. (B) SeP and NOS-2 mRNA levels in colons of DSS-treated and control mice were analysed by qPCR and normalised against β-actin. Analysis of statistical differences between samples taken from control and DSS-treated animals was done by Student's t-test.

Table 1

gene	forward primer	reverse primer
huFoxO1a	AAGGGTGACAGCAACAGCTC	TTCTGCACACGAATGAACTTG
huHNF-4α	ACGTCCCCATCAGAAGGCACCAAC	CCAGGGGGAGCTCGCAGAAA
huHPRT1	ATTCTTTGCTGACCTGCTGGATT	CTTAGGCTTTGTATTTTGCTTTTC
huNOS-2	TCGGCAGAATCTACAAAGTCC	CCATCCTCACAGGAG
huPGC-1α	CACCCACCACTCCTCCTCATAAAG	ACAAATCTGCCCCTGCCAATC
huPstk1	GAGTCCAGCATGTGCTTCG	TTTTCCAAAGCAGTGAGCAA
huSBP-2	CGCCCCACTGATGAAGAA	TGCTTTCTCTCTTGCCGTTC
huSecS	CGATGCTTTTTACCAGACAGG	AGTTTGCATGGACCCAAGAG
huSeP	GGAGCTGCCAGAGTAAAGCA	ACATTGCTGGGGTTGTCAC
huSPS-2	GGGGGATATTTGTTCATCACTT	TGGCAAGAGAAAACAGAGGTATT
mβ-actin	TGACAGGATGCAGAAGGAGA	CGCTCAGGAAGGAGCAATG
mNOS-2	GGGCTGTCACGGAGATCA	CCATGATGGTCACATTCTGC
mSeP	GGTGCGGAAACTGCAATC	TTTGTTGTGGTGTTTGTGGTG

Table 1. Primers (5'-3') for qPCR analysis of human (**hu**) or mouse (**m**) mRNAs

Figure 1

Click here to download high resolution image

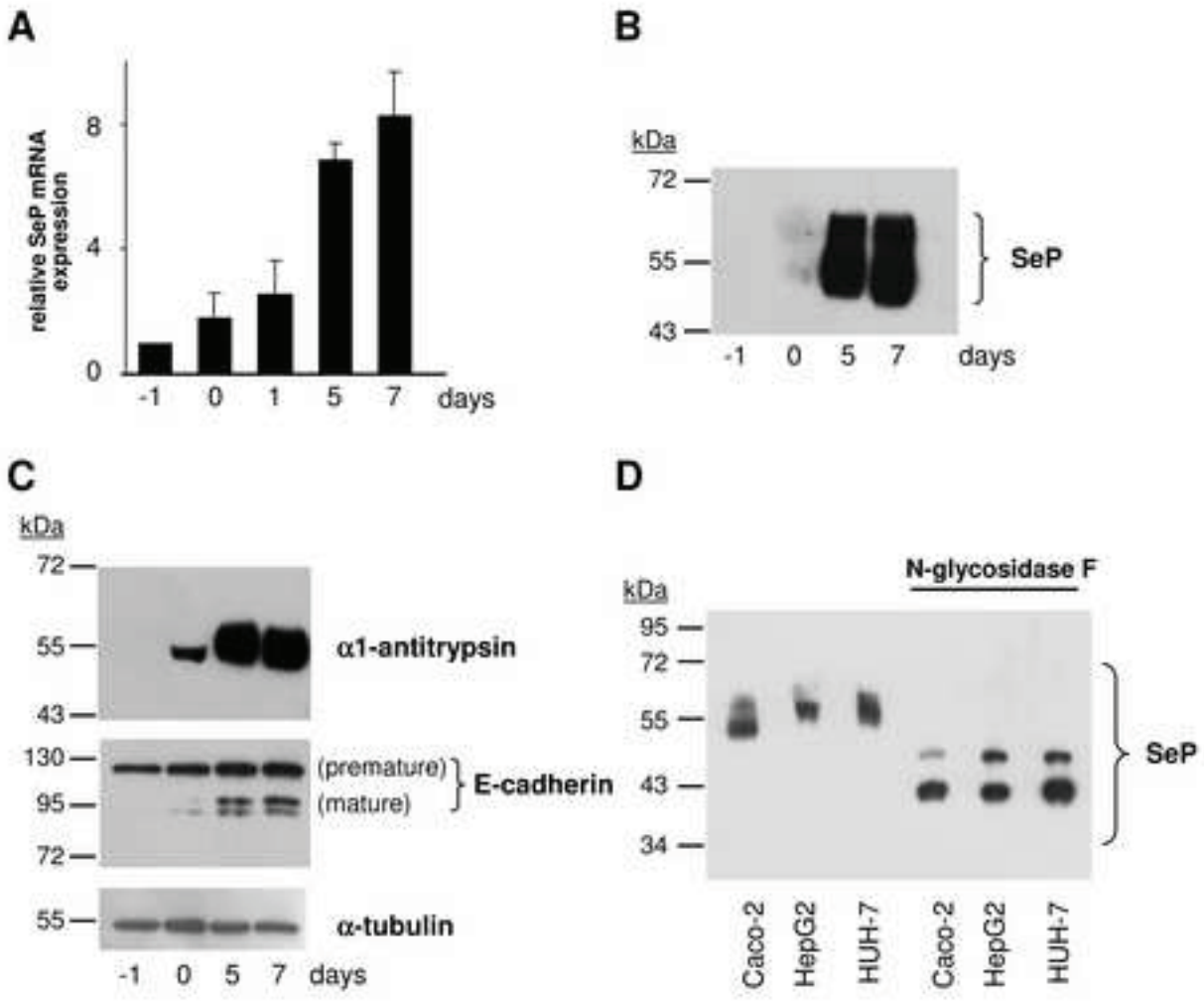

Figure 1

Figure 2
Click here to download high resolution image

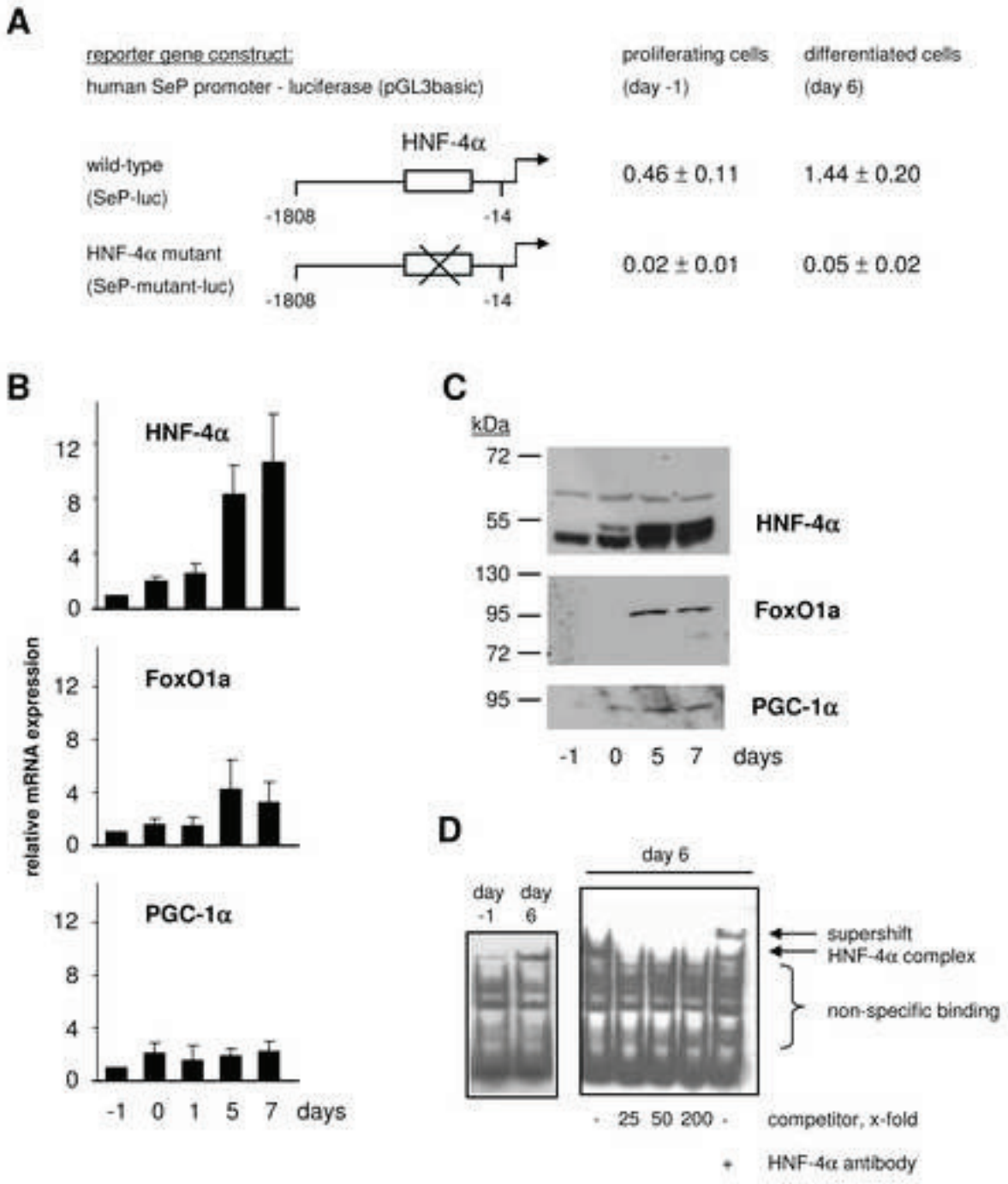

Figure 2

Figure 3 revised

Click here to download high resolution image

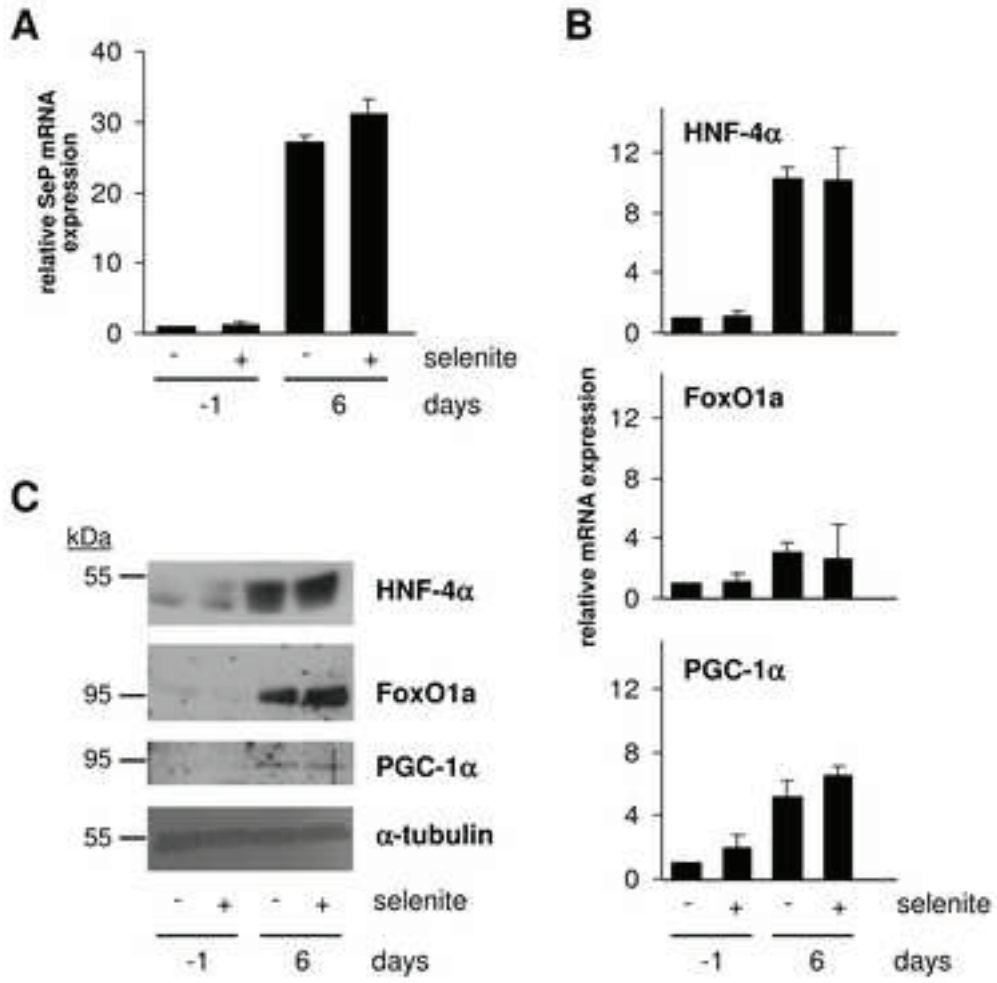

Figure 3

Figure 4 revised
Click here to download high resolution image

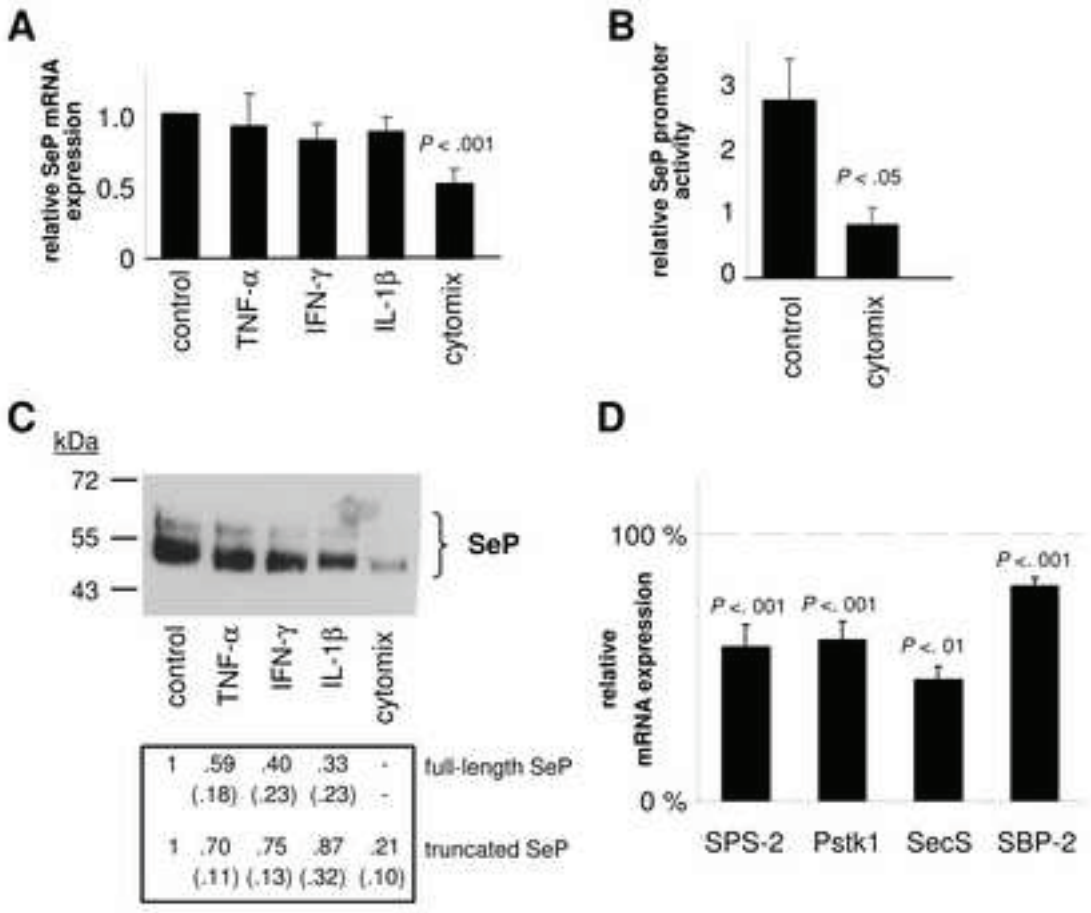

Figure 4

Figure 5 revised

Click here to download high resolution image

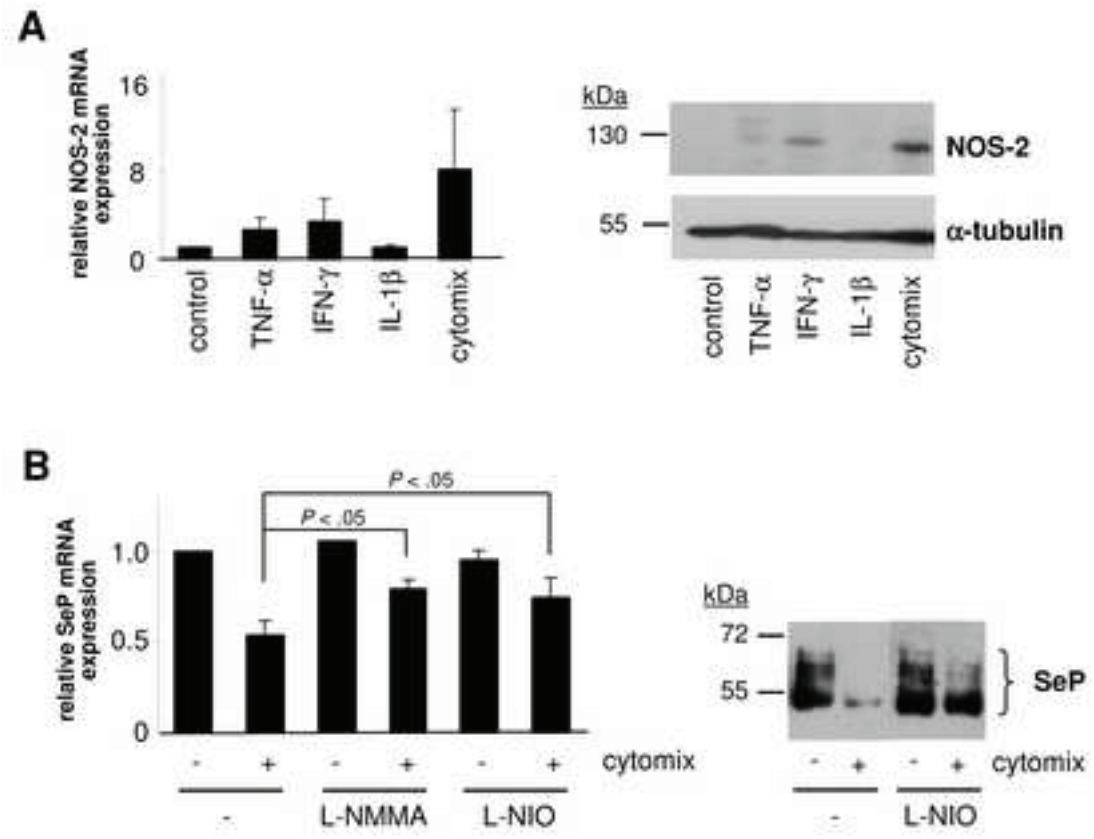

Figure 5

Figure 6 revised

Click here to download high resolution image

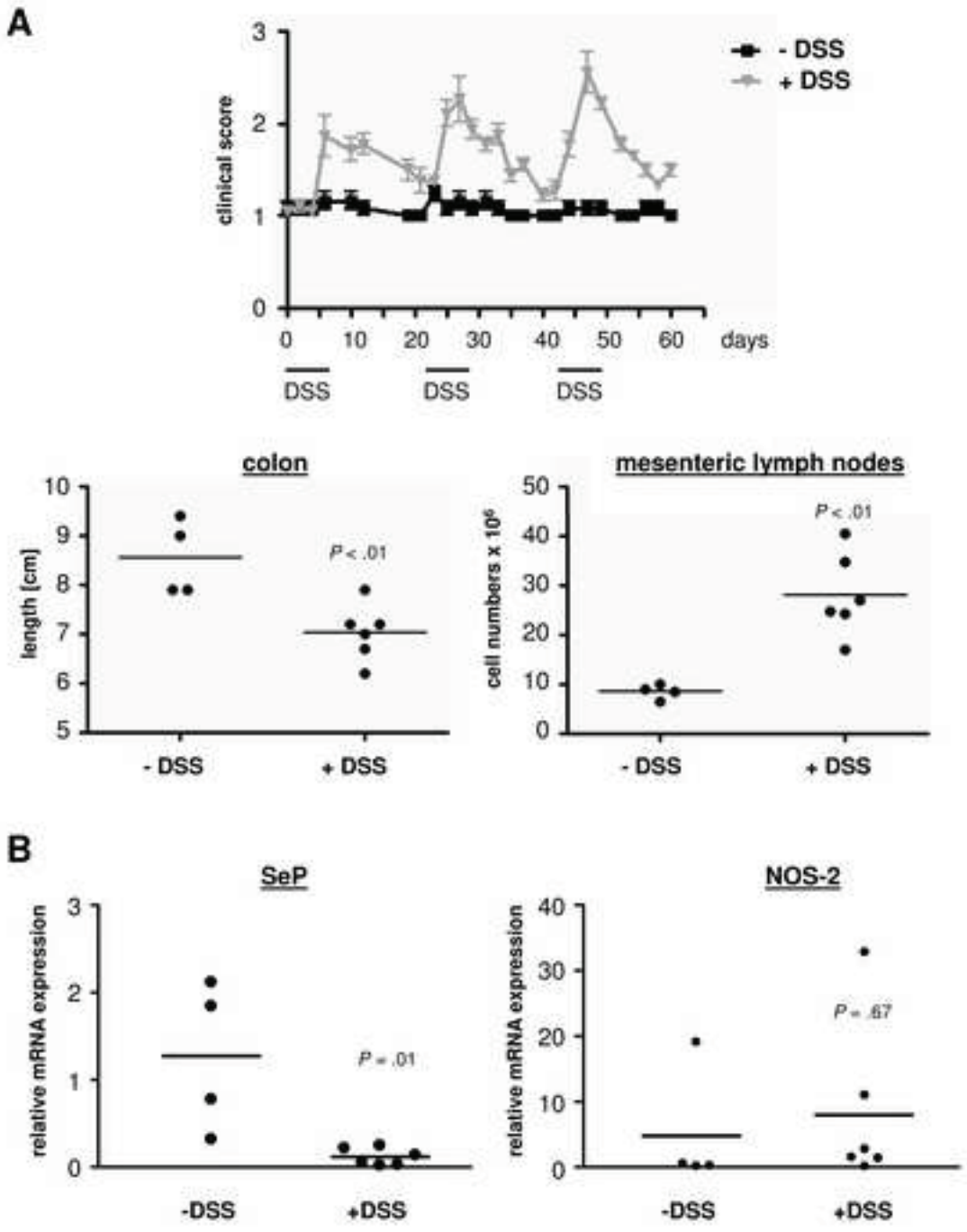

Figure 6

Danksagung

Ich danke allen meinen Kollegen und meiner Familie, die mir meine Promotion erst ermöglicht haben.

Mein besonderer Dank gilt aber Frau Prof. Irmgard Förster für die Bereitstellung des interessanten Themas und die Unterstützung und Förderung in allen Bereichen der Wissenschaft, sowie auf persönlicher Ebene.

Herrn Prof. Klaus Pfeffer danke ich für die Unterstützung, sowie für die Einladung zu so mancher Weihnachtsfeier.

Herrn Prof. Peter Proksch möchte ich für die freundliche Übernahme des Koreferats danken.

Außerdem danke ich Frau Dr. Heike Weighardt, die immer hilfsbereit war und auf alle Fragen eine Antwort wusste.

Meiner Arbeitsgruppe möchte ich für die freundschaftliche und produktive Zusammenarbeit danken!

Mein ganz besonderer Dank gilt meiner Familie, die mich immer unterstützt hat und ohne die meine Promotion wohl nicht möglich gewesen wäre.

Eidesstattliche Erklärung

Die hier vorgelegte Dissertation habe ich eigenständig und ohne unerlaubte Hilfe angefertigt. Die Dissertation wurde in der vorgelegten oder einer ähnlichen Form noch bei keiner anderen Institution eingereicht. Ich habe bisher keine erfolglosen Promotionsversuche unternommen.

Düsseldorf, den 01.06.2010

Meike Winter